REPORT

Scientific publications from 2013 to 2016

Presentazione

Questa pubblicazione presenta, in continuità con la tradizione consolidata del Dipartimento di Fisica dell'Università della Calabria, le attività di ricerca del dipartimento stesso, relative al periodo 2013-2016. L'istituzione del Report annuale, la cui prima stesura risale al 1986, resta una iniziativa lungimirante ed una documentazione di indubbia utilità. Da un lato, i Report hanno anticipato di fatto, almeno come impostazione metodologica, la SUA-RD, un documento oggi richiesto dal MIUR per l'accreditamento dei dipartimenti universitari. Dall'altro, rivisti nel loro insieme, questi resoconti rappresentano una documentazione dettagliata delle dinamiche dipartimentali, ossia di come i ricercatori che si sono avvicendati negli anni nel Dipartimento di Fisica abbiano saputo affermarsi nel panorama nazionale ed internazionale della ricerca e di come il Dipartimento stesso, nel suo insieme, sia cresciuto di conseguenza.

A differenza dell'epoca in cui i primi Report furono redatti, oggi le attività di ricerca sono monitorate e parametrizzate, ed è quindi possibile misurarne la qualità, per esempio con l'esercizio della VQR e della SUA-RD. Ma l'utilità della stesura di un Report annuale permane, anzi, diventa oggi più urgente. Partendo, infatti, da un punto di vista nuovo e di più ampio respiro, dobbiamo e vogliamo fare nostre le due citazioni che compaiono sulla prima pagina del rapporto finale della VQR:

"If you cannot measure it, you cannot improve it" (Lord Kelvin).

"Not everything that can be counted counts, and not everything that counts can be counted" (W.B. Cameron).

Sono sicuro che l'armonizzazione dei due aspetti diventerà, nel nuovo contesto in cui si muove oggi il Dipartimento di Fisica, una delle prerogative dei nuovi Report.

E' necessario innanzitutto evidenziare la qualità e la quantità del lavoro dei ricercatori del Dipartimento, in modo da contribuire al miglioramento continuo delle nostre attività di ricerca. Allo stesso tempo, è opportuno mettere in luce anche tutto quello che non potrà mai apparire nelle tabelle ANVUR, come per esempio il vasto spettro di interessi scientifici, la tenacia nel costruire rapporti con altre sedi per gli interscambi continui, l'opera di coinvolgimento culturale con tutte le aree disciplinari dell'Ateneo e, non ultimo, la passione e la cura per la formazione dei giovani che concorrono, con la loro vivacità e curiosità culturale, alla crescita, all'innovazione ed al miglioramento delle attività del Dipartimento.

Il presente Report nasce quindi nel solco della tradizione, ma i contenuti si amplieranno immediatamente fin dal prossimo numero, perché molte sono le attività che caratterizzano, e caratterizzeranno sempre di più, il Dipartimento di Fisica nei rapporti con l'Ateneo e con il territorio. Queste attività sono in continua crescita, per cui anche queste, a partire dalla prossima pubblicazione, troveranno uno spazio adeguato. In questo modo il Dipartimento potrà mostrare sia la sua valenza nel panorama scientifico nazionale ed internazionale, sia l'impegno costante per lo sviluppo culturale e sociale dell'Ateneo e del territorio.

Arcavacata di Rende, 24 Maggio 2017

Prof. Vincenzo Carbone

Direttore del Dipartimento di Fisica

Il Dipartimento di Fisica

Direttore

Prof. Vincenzo CARBONE

Vicedirettore

Prof. Enrico TASSI

Organi del Dipartimento

Giunta

Prof. Gennaro CHIARELLO

Prof. Antonio DE LUCA

Prof. Vincenzo FORMOSO

Prof. Rita GUZZI

Dr.ssa Anna MASTROBERARDINO

Prof. Alessandro PAPA

Dr. Antonello SINDONA

Dr. Francesco VALENTINI

Commissione Didattica Paritetica Studenti-Docenti

Sig. Giacomo BARRESI

Sig.na Lucia EMANUELE

Sig. Giuseppe Emanuele LIO

Sig. Vincent Ismaele MASIELLO

Dr.ssa Daniela PACILE'

Dr. Marco ROSSI

Prof. Marco SCHIOPPA

Commissione di Riesame

Dr.ssa Anna CUPOLILLO

Dr.ssa Evelin MEONI

Prof. Pasquale PAGLIUSI

Prof. Francesco PLASTINA

Commissioni Didattiche

Prof. Giuseppe ALI'

Dr.ssa Marcella CAPUA

Prof. Gaetano ZIMBARDO

Prof. Gennaro CHIARELLO

Prof.ssa Gabriella CIPPARRONE

Prof. Attilio GOLEMME

Delegati

Orientamento: Dr. Pierfrancesco RICCARDI

Internazionalizzazione: Prof. Lorenzo CAPUTI

Trasferimento tecnologico: Prof. Antonio DE LUCA

La stesura del Report dell'attività scientifica del Dipartimento di Fisica 2013-2016 è stata coordinata dal prof. Alessandro PAPA e curata da Chiara CHIODI e Alessandro SOLE.

1. ASTROPHYSICS, GEOPHYSICS AND PLASMAS

Professors and Researchers

Pierluigi Veltri
Vincenzo Carbone
Sandra Savaglio
Francesco Malara
Gaetano Zimbardo
Leonardo Primavera
Antonella Greco
Fabio Lepreti
Francesco Valentini
Sergio Servidio
Luca Sorriso-Valvo *(CNR-NANOTEC, U.O.S. Rende)*

Research fellows

Giuseppina Nigro
Silvia Perri
Ersilia Leonardis
Claudia Rossi

PhD students

Loris D'Alessi
Gaetano De Vita
Christian Natale Gencarelli
Enrico Maria Trotta
Luca Tiriolo
Francesco Pucci
ChristianVàsconez
Tommaso Alberti
Francesca Di Mare
Oreste Pezzi
Elisa De Giorgio
Gianfranco Brunetti
Filomena Catapano
Federica Chiappetta

Collaborators

R. G. Abraham, *Department of Astronomy and Astrophysics, University of Toronto*
M. Affolter, *University of California, San Diego, USA.*
E. Amato, *INAF-Osservatorio Astrofisico di Arcetri, Italy.*
L. Amati, *INAF-IASF Bologna, Italy*
F. Anderegg, *University of California, San Diego, USA*
M. André, *Swedish Institute of Space Physics, Uppsala, Sweden*
E. Antonucci, *INAF - Astrophysical Observatory of Torino, Italy*
M. Arabsalmani, *European Southern Observatory, Garching by Munich, Germany*
A. Artemyev, *IKI, Russia*
A. Ashourvan, *University of California, San Diego, USA*

S. D. Bale, *Space Sciences Laboratory, University of California, Berkeley, USA*

M. Balikhin, *University of Sheffield, Sheffield, UK*

S. Basa, *Laboratoire d'Astrophysique de Marseille, France*

F. Berrilli, *University of Roma Tor Vergata, Italy*

E. Bevacqua, *Karl-Franzens-Universität Graz, Austria*

R. Bruno, *National Institute for Astrophysics, Roma, Italy*

D. Burgess, *Queen Mary University of London, London, UK*

A. C. Cadavid, *California State University Northridge, CA, USA*

F. Califano, *University of Pisa, Pisa, Italy*

E. Camporeale, *Centrum Wiskunde & Informatica, Amsterdam, Netherlands*

V. Capparelli, *University of Catania, Italy*

D. Caprioli, *Princeton University, Princeton, USA*

P. A. Cassak, *West Virginia University, Morgantown, USA*

F. Cattaneo, *Department of Astronomy and Astrophysics, The University of Chicago, USA*

M. Cavenago, *INFN Laboratori Nazionali di Legnaro, Italy*

S. Chapman, *University of Warwick, Coventry, UK*

C. H. K. Chen, *Imperial College London, London, UK*

D. J. Christian, *California State University Northridge, CA, USA*

E.W. Cliver, *National Solar Observatory, Boulder, USA*

G. Consolini, *INAF, Rome, Italy*

J. Cooke, *Centre for Astrophysics and Supercomputing, Swinburne University of Technology, Hawthorn, Australia*

R. D'Amicis, *IFSI, Institute for Space Astrophysics and Planetology, Roma, Italy*

A. De Cia, *European Southern Observatory, Garching by Munich, Germany*

D. Del Moro, *University of Roma Tor Vergata, Italy*

P. De Michelis, *INGV, Roma, Italy*

S. Dey, *Indian Institute of Technology Kharagpur, India*

P. Dmitruk, *University of Buenos Aires, Buenos Aires, Argentina*

C. F. Driscoll, *University of California, San Diego, USA.*

D. H. E Dubin, *University of California, San Diego, USA.*

J. P. Eastwood, *Imperial College London, London, UK*

F. Effenberger, *Stanford University, Stanford, USA.*

S. Eriksson, *University of Colorado, Boulder, USA*

C. P. Escoubet, *European Space Agency, Noordwijk, Netherlands*

A.N. Fazakerley, *University College London, UK*

H. Fichtner, *Institut fuer Theoretische Physik, Bochum, Germany*

P. Francia, *University of L'Aquila, Italy*

J. P. U. Fynbo, *Dark Cosmology Centre, Niels Bohr Institute, University of Copenhagen, Denmark*

S. P. Gary, *Los Alamos National Laboratory, USA*

K. Glazebrook, *Centre for Astrophysics and Supercomputing, Swinburne Uni. of Technology, Hawthorn, Australia*

D. B. Graham, *Swedish Institute of Space Physics, Uppsala, Sweden*

J. Greiner, *Max Planck Institute for Extraterrestrial Physics, Garching by Munich, Germany*

E. Grigorenko, *IKI, Russia*

M. L. Goldstein, *NASA Goddard, USA*
J. T. Gosling, *University of Colorado, Boulder, USA*
S. L. Guglielmino, *University of Catania, Italy*
C. T. Haynes, *Queen Mary University of London, London, UK*
P. Henri, *CNRS, Orleans, France*
B. Hnat, *University of Warwick, Coventry, UK*
L. K. Hunt, *INAF–Osservatorio Astrofisico di Arcetri, Firenze, Italy*
D. B. Jess, *Queen's University Belfast, UK*
A. Kabantsev, *University of California, San Diego, USA.*
H. Karimabadi, *UCSD, San Diego, USA*
O. Khabarova, *IKI, Russia*
Y. Khotyaintsev, *Swedish Institute of Space Physics, Uppsala, Sweden*
T. Krühler, *Max Planck Institute for Extraterrestrial Physics, Garching by Munich, Germany*
H. Kucharek, *University of New Hampshire, NH, USA*
M. Laurenza, *INAF/IAPS, Rome, Italy*
B. Lavraud, CNRS, *Toulouse, France*
J. K. Lawrence, *California State University Northridge, CA, USA*
D. Le Borgne, *CEA Irfu, SAp, Centre de Saclay, Gif-sur-Yvette, France*
C. Ledoux, *European Southern Observatory, Santiago, Chile*
G. Maero, *University of Milano, Italy*
F. Marcucci, *INAF/IAPS, Rome, Italy*
R. Marino, *École Normale Supérieure de Lyon, Lyon, France.*
B. Maruca, *University of Delaware, Newark, USA*
W. H. Matthaeus, *University of Delaware, Newark, USA*
M. J. Michałowski, *Institute for Astronomy, University of Edinburgh, Edinburgh, UK*
P. Mininni, *University of Buenos Aires, Buenos Aires, Argentina*
P. J. Morrison, *University of Texas, Austin, USA*
R. Nakamura, *Space Research Institute, Graz, Austria*
Y. Narita, *Space Research Institute, Graz, Austria*
Z. Nemecek, *Faculty of Mathematics and Physics, Prague, Czech Republic*
T. M. O'Neil, *University of California, San Diego, USA.*
M. Onofri, *Tri Alpha Energy, Rancho Santa Margarita, California 92688, USA*
K. T. Osman, *University of Warwick, England*
S. Oughton, *University of Waikato, New Zealand.*
T. Parashar, *University of Delaware, Newark, USA*
B. Paroli, *University of Milano, Italy*
E. Palazzi, *INAF-IASF Bologna, Italy*
F. Pegoraro, *University of Pisa, Pisa, Italy*
D. Perrone, *European Space Agency / ESAC, Madrid, Spain*
T. D. Phan, *University of California, Berkeley, USA*
M. Piersanti, *University of L'Aquila, Italy*
E. Pietropaolo, *Dipartimento di Fisica, Università de L'Aquila, Italy*
J.-L. Pinçon, *LPC2E/CNRS, Orléans, France*
A. Pouquet, *NCAR, Boulder, USA*
R. Pozzoli, *University of Milano, Italy*
F. Pucci, *Center for Mathematical Plasma Astrophysics, Universiteit Leuven, Belgium*

P. Schady, *Max Planck Institute for Extraterrestrial Physics, Garching by Munich, Germany*
A. P. Snodin, *Mahidol University, Thailand*
A. Rappazzo, *Advanced Heliophysics, Pasadena, USA*
A. Retinò, *Laboratoire de Physique des Plasmas, CNRS, France*
P. Romano, *INAF - Astrophysical Observatory of Catania, Italy*
M. Romé, *University of Milano, Italy*
A. Rossi, *INAF-IASF Bologna, Italy*
D. Ruffolo, *Mahidol University, Thailand*
F. Sahraoui, *Laboratoire de Physique des Plasmas, CNRS, France*
M. Shay, *University of Delaware, Newark, USA*
J. Soucek, *Czech Academy of Sciences, Praha, Czech Republic*
M. Storini, *INAF/IAPS, Rome, Italy*
D. Telloni, *INAF - Astrophysical Observatory of Torino, Italy*
S. M. Tobias, *Department of Applied Mathematics, University of Leeds, Leeds LS2 9JT, UK*
R. Vainio, *University of Turku, Turku, Finland*
A. Vaivads, *Swedish Institute of Space Physics, Sweden*
C. L. Vasconez, *Escuela Politécnica Nacional, Quito, Ecuador*
A. Vecchio, *LESIA - Observatoire de Paris, France*
S. D. Vergani, *GEPI-Observatoire de Paris Meudon, France*
U. Villante, *University of L'Aquila, Italy*
Z. Vörös, *Space Research Institute, Graz, Austria*
P. M. Vreeswijk, *Department of Particle Physics and Astrophysics, Weizmann Institute of Science, Israel*
M. Wan, *University of Delaware, Newark, USA*
R. F. Wimmer-Schweingruber, *Christian-Albrechts-University, Kiel, Germany*
Y. Yang, *Department of Physics and Astronomy, University of Delaware, USA*
E. Yordanova, *Swedish Institute of Space Physics, Sweden*
G. P. Zank, *University of Alabama, Huntsville, USA*
F. Zuccarello, *University of Catania, Italy*

Introduction

The Universe represents a huge laboratory where a large variety of phenomena takes place, which involve many fields of Physics. The physical conditions of cosmic objects, in terms of temperature, density, particle energy, etc., are in many cases not reproducible in a terrestrial laboratory. Then, the study of cosmic phenomena represents a unique chance to test theories and to improve our understanding of Physics in general.

The research work carried out by the Astrophysics, Geophysics and Plasmas Group is concerned with some aspects of the large multiplicity of cosmic phenomenology, ranging from extremely violent explosions taking place in distant galaxies, to the less energetic dynamics observed in near-Earth objects like the Sun and the Earth environment.

The cosmic matter is in many cases in the state of plasma; thus, plasma physics represents a preeminent component of our investigation. Our research work encompasses different phenomena; in particular, the cosmically ubiquitous turbulence with its peculiar aspects related to energy transfer through different spatial scales and heating; production and diffusion of high-energy particles and radiation; cosmic magnetic field generation. Such phenomena are in many instances inter-dependent and related to one another, thus, a better understanding of one of them improves the knowledge of the others.

For instance, magnetic field generation in the Sun, solar eruptions, production of energetic particles are all correlated aspects influencing the so-called Space-Weather and the Earth's climate, which represents one of the research topic of our group. Our investigation in the plasma physics domain has also applications to Laboratory Plasma Physics with a specific research line devoted to nuclear fusion devices and non-neutral and dusty plasmas.

Our investigation is in part concerned with the formulation of theoretical models, where different methods are employed: large numerical codes, both fluids and kinetics, have bee built up in the last years, and allow us to study phenomena at different space and time scales; other models are used to study particle dynamics or magnetic field generation. Another preeminent aspect is represented by advanced techniques of analysis of data; such data are issued from instruments both ground-based and on board of spacecrafts. In this respect, it is worth mentioning that our group is directly involved in two new space missions: Solar Orbiter, a solar and heliopheric mission which will be launched on 2018; and THOR, a mission dedicated to study turbulence and heating of the interplanetary medium.

In his research work our group collaborate with many researcher of other institutions both in Italy and in other countries, which are listed above. A detailed description of the various research topics is given in the following.

A. Astrophysics

A.1: Stellar explosions, the distant galaxies and the intergalactic medium

Most massive stars are ending their life through a very energetic explosion, called supernova (SN). Among all different types of SNe, the most extreme explosions are producing in a very short time gamma-rays. These are called gamma-ray bursts (GRBs), the most energetic explosions in the universe after the Big Bang. Another class of energetic stellar explosions are the super luminous supernovae (SLSNe). Recently discovered, similarly to GRBs, they are also rare events. Both GRBs and SLSNe are used as probes of the chemical enrichment history of the universe. In particular, they are bright beacons of light which can 'illuminate' the gas in galaxies and among galaxies for our detections and investigations with telescopes on Earth. To study these targets, we have created a public database, called GRB Host Studies (GHostS - www.grbhosts.org), containing information of the properties of the galaxies hosting GRBs. GHostS is the largest and most complete database of its kind.

On a different science topic, we investigate the relation between the mass of galaxies and their chemical enrichment. While this relation in the local universe was known since the 1970s, we have discovered that this is changing with time. These findings support an early formation of massive galaxies, not easily accounted for by most theoretical models.

Additionally, we use absorption lines in bright and distant sources as probes of the intergalactic medium in the distant universe. This medium is made of relatively hot gas which in the past was more abundant than today. The evolution with time is partly due to the expansion of the universe, and partly to the evolution of the ionisation of the gas. The history of the ionisation state of the intergalactic medium is linked to the presence of UV photons, which are produced mainly by young and massive stars in small and medium-size galaxies.

A.2: Space Missions: THOR

The visible Universe is permeated by hot magnetized plasmas which are in most cases in a turbulent state. Turbulent plasmas are found in active galactic nuclei, supernova remnants, the intergalactic and interstellar medium, as well as in the solar corona, the solar wind and the Earth's magnetosphere. They can also be found in laboratory devices such as e.g. Reversed-Field Pinches. Our comprehension of the plasma Universe is largely based on measurements of electromagnetic radiation, such as light or X-rays, which originate from particles that are heated and accelerated as a result of energy dissipation in turbulence. Therefore, it is of key importance to understand how plasma is energized by turbulent fluctuations. Most of the energy dissipation occurs at kinetic scales, where plasma no longer behaves as a fluid and the properties of individual plasma species (electrons, protons and heavier ions) become important.

THOR (Turbulent Heating ObserveR) is a space mission currently in Study Phase as candidate for M-class mission within the Cosmic Vision program of the European Space Agency (Fig. 1). The scientific theme of the THOR mission is turbulent energy dissipation and particle energization in space plasmas, which ties in with ESA's Cosmic Vision science. Specifically, the THOR mission aims to address fundamental questions such as how plasma is heated and particles are accelerated by turbulent fluctuations at kinetic scales, how energy is partitioned among different plasma components and how dissipation operates in different regimes of turbulence. To achieve this goal, THOR will make in situ measurements with unprecedented temporal and phase space resolution in specific regions in near-Earth space: the pristine solar wind, the Earth's bow shock and interplanetary shocks, and the compressed solar wind regions downstream of shocks. These regions are selected because of their different turbulence properties, and reflect similar astrophysical environments. The observational evidences and the science of the THOR mission could have blasting returns in the scientific fields of space, astrophysical and laboratory turbulent plasmas.

Our knowledge about the fundamental processes responsible for turbulent plasma heating and particle acceleration at kinetic scales as of today mainly comes from numerical simulations.

Different simulations studying the kinetic dynamics of main ion species (protons and alpha particles) and electrons, have clearly shown that kinetic physics is different for different species and is an essential ingredient for the description of plasma heating and particle acceleration in turbulent space plasmas at kinetic scales. Therefore, the numerical modelling support for the THOR mission is crucial, both from the science and mission design point of view.

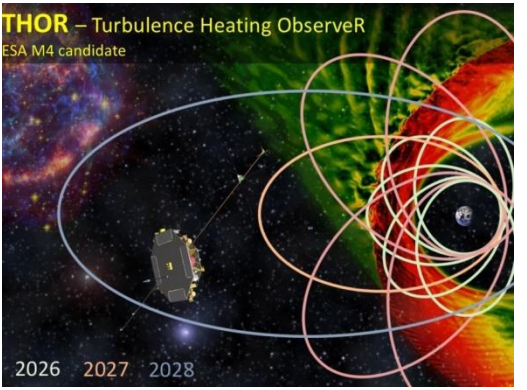

Figure 1: Schematic drawing of the THOR spacecraft (http://thor.irfu.se/) and its orbits during the 3 years of the nominal science mission. During the first year the focus is on the bow shock and magnetosheath, during the second and third years the focus is on the pristine solar wind and foreshock. Courtesy: NASA, OHB-Sweden, FMI and Vlasiator (von Alfthan et al. 2014). *Vaivads et al. J. Plasma Phys. (2016)*

The Astrophysics, Geophysics and Plasma Physics (AGPP) Group at UNICAL is actively involved in the design phase of the THOR spacecraft, having role of Co-I in important instruments that will be mounted on board the spacecraft, in the case of final selection by ESA: the Particle Processing Unit (PPU), the Turbulent Electron Analyzer (TEA), the Cold Solar Wind (CSW) and the Ion Mass Spectrometer (IMS) instruments. Moreover, the AGPP Group coordinates the Numerical Simulation Support Team (NSST) and the Virtual Instrument Team (VIT), which are supporting the THOR science and mission design during the study phase.

The THOR team includes many scientists developing and running different simulation codes (Eulerian-Vlasov, Particle-In-Cell, Gyrokinetics, Two-fluid, MHD, etc.), addressing the physics of plasma turbulence, shocks, magnetic reconnection and so on. Under the coordination of AGPP, these numerical codes are being used during the study phase, mainly with the aim of addressing the main following points:

(i) to simulate the response of real particle instruments on board THOR, by employing an electrostatic analyser simulator which mimics the response of the CSW, IMS and TEA instruments to the particle velocity distributions of protons, alpha particle and electrons, as obtained from kinetic numerical simulations of plasma turbulence.

(ii) to compare multi-spacecraft with single-spacecraft configurations in measuring current density, by making use of both numerical models of synthetic turbulence and real data from MMS spacecraft.

(iii) to investigate the validity of the Taylor hypothesis in different configurations of plasma turbulence.

A.3: Space Missions: Solar Orbiter

The European Space Agency has selected the mission Solar Orbiter for launch in 2018. During the last 7 years, scientists and engineers from the EU and USA have been working on the spacecraft and payload design, which are now close to delivery. The innovative space mission will consist of both in-situ and remote measurements of the interplanetary space and the Sun, with an orbit that will take the spacecraft as close to the Sun as 0.28AU, i.e. right next to Mercury orbit. While solar imagers and coronographers will provide unprecedented data from the solar surface and corona, the dedicated in-situ instruments will measure the solar wind particles and fields in the inner heliosphere, allowing the direct observation of the plasma emitted by regions of the Sun that are actually observed by the spacecraft. The combined action of the two families of instruments will represent a breakthrough in the understanding of the processes occurring in the solar system plasma. With two co-Investigators, our group is directly involved in the preparation of one important component of the payload, i.e. the Data processing Unit (PDU), P.I. being Roberto Bruno of IAPS/INAF. This unit is the hardware responsible for the coordination of the various instruments, collection of data, and management of the data flow. In a payload-packed mission such as Solar Orbiter, this is a component of major importance. Our group is providing the fundamental input to support the observation strategy to be implemented, through the thorough analysis of previous missions measurements (in particular Helios, Wind, Cluster, Messenger, Venus Express, Ulysses), which are used to establish the statistical properties of the fields and particles fluctuations. Furthermore, new data analysis techniques are designed for the maximum return from the expected Solar Orbiter data. Finally, numerical simulations are used to predict the possible in-situ measurement scenario, and to fine-tune the most advanced data analysis techniques.

B. Geophysics

Solar activity and its effects on Space Weather and Earth's climate

The large variability of the physical conditions of the Sun, over a wide range of spatial and temporal scales, represents the primary source which determines global and local changes in the heliosphere, the near Earth space and the Earth's climate. However, due to the extreme complexity of the system, nonlinear interactions among different parts of the Sun-Earth system play a key role, enormously increasing the range of physical processes involved. In fact, fluctuations in the magnetic field within the solar atmosphere act as complex modulation of plasma conditions in the interplanetary space, giving rise to coronal mass ejections (CMEs), sudden enhancements of the fluxes of solar energetic particles (SEP), and solar irradiance changes in several spectral ranges (from the UV to visible and infrared). These events are often associated with the origin of geomagnetic storms, which have important effects on our technological society, and possibly with global changes in the climate conditions through complex interactions with the Earth's atmosphere. The investigation of the physical processes which mainly affect solar and interplanetary space conditions and the observation and understanding of the interactions of the solar wind with the Earth's magnetosphere are crucial to be able to predict and mitigate those phenomena that affect space and ground infrastructures or impair the human health. For this reason, agencies and international panels include, among their activities, the study of Space Weather, like for instance the ESA with the Space Situational Awareness program, or contribute to a better understanding of the effect of the solar radiation on the Earth's climate and its variations, as it is done by the Inter-Governmental Panel on Climate Change. In fact, an interdisciplinary approach and scientific joint ventures, involving expertise in a wide range of different fields, are urgent to face problems related to different areas of solar heliospheric and magnetospheric physics.

The activity of the Group in this field addresses some of the main issues concerning the nature of the variability of solar activity, including the effects on Space Weather and Earth's climate through the analysis of data obtained from ground-based and space observatories as well as through the construction and investigation of theoretical models. Since March 2014 the Group, with the supervision of Prof. V. Carbone, has coordinated the first national scientific project (“The active sun

and its effects on space and Earth climate ") aimed at investigating Space Weather and financed by the Italian Ministry of Education, University and Research in the framework of the PRIN program. The research groups active in this fields and involved in this project are those from the universities of Roma "Tor Vergata", Firenze, Catania, l'Aquila and from the National Institute of Astrophysics. Moreover, the above mentioned research groups together with researchers from other institutes, in particular the National Institute of Geophysics and Volcanology, have established, starting since October 2014, a national research group devoted to Space Weather and named SWICo (Space Weather Italian Community).
The research activities carried out by the Group on the above mentioned topics are summarized below.

B.1: Long term behavior of solar activity

In order to provide a detailed characterization of the long term behavior of solar activity, the revised dataset of sunspot and group numbers (released by the World Data Center - SILSO) and the sunspot number reconstructions based on dendrochronologically dated radiocarbon concentrations were analyzed. The solar activity main periodicities and the role of the Gleissberg and Suess cycles in the grand minima occurrence were investigated by means of the Empirical mode decomposition (EMD) method. A general consistency among the results from all the analyzed datasets confirms the reliability of the EMD approach. The analysis on the revised sunspot data indicates that the highest energy content is associated with the Schwabe 11 year cycle. In correspondence with the grand minima (Maunder and Dalton), the frequency of this cycle changes to longer timescales of ∼14 yr. The Gleissberg and Suess cycles, with timescales of 60−120 yr and ∼200−300 yr, respectively, represent the most energetic contribution to sunspot number reconstruction records and are both found to be characterized by multiple scales of oscillation. The grand minima generation and the origin of the two expected distinct types of grand minima, Maunder and longer Spörer-like, are naturally explained through the EMD approach. It was found that the grand minima sequence is produced by the coupling between Gleissberg and Suess cycles, the latter being responsible for the most intense and longest Spörer-like minima (with typical duration longer than 80 yr). Finally, a non-solar component, characterized by a very long scale oscillation of ∼7000 yr, was identified. The results of this work provided new observational constraints on the properties of the solar cycle periodicities, the grand minima generation, and thus the long-term behavior of the solar dynamo.

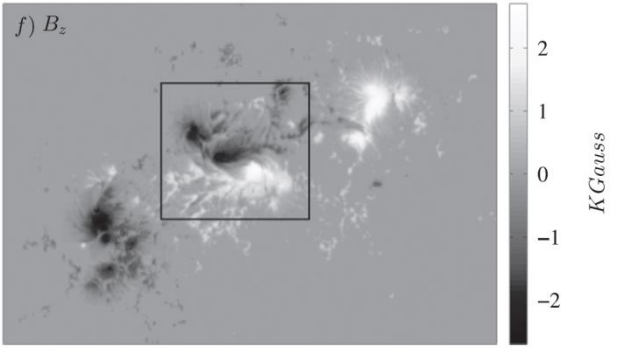

Figure 2: Magnetic field line-of-sight component intensity measured by HMI/SDO for the solar active region NOAA 11158 on February 14 at 03:24 UT. The square box indicates the area selected to perform the cancellation analysis. *Sorriso-Valvo et al., Astrophys. J 2015.*

B.2: Cancellation analysis in solar active regions: a precursor to flares

Solar flares are often associated with changes in the fine magnetic structure of the emitting active region. Such topological modification results in variations of both the scaling properties of the fields' fluctuations, and the fractal dimension of the associated gradients. The use of cancellation analysis of the current density has been attempted for the identification and quantitative estimation of such changes. The characteristics of the magnetic vector as measured by THEMIS telescope for the active region NOAA10019 have been studied, suggesting the presence of disrupted current filaments. The variation of the fractal dimension of the current structures, and in particular their smoothing, shows correlations with occurrence of one flare in the active region.

Solar Active Region NOAA 11158 (Fig. 2) has hosted a number of strong flares, including one X2.2 event. The higher resolution and better time coverage of space-generated data, such as the ones from the NASA spacecraft SDO, allows a more complete description of the evolution of the parameters. Sudden changes of the cancellation exponents at the time of large flares and the presence of correlation with Extreme-Ultra-Violet and X-ray flux clearly suggest that eruption of large flares can be linked to the small-scale properties of the current structures.

B.3: Statistical properties of coronal mass ejections

As already mentioned above, coronal mass ejections (CMEs) are the main solar transient phenomenon which produce effects on Space Weather. A study of the statistical properties of CMEs was performed, revealing that their properties depend on the period of solar activity. In particular, when investigating the origin of the waiting time distribution between CMEs, a significant departure from a Poisson process during periods of high solar activity was found, thus suggesting the existence of at least two physical processes underlying the origin of CMEs. One acts continuously, perhaps related to randomly occurring magnetic reconfigurations of the solar corona at large scales. The other plays a role only during the solar maximum, probably due to the photospheric emergence of magnetic flux as a statistically persistent mechanism, which generates long correlation times among CME events strong enough not to be destroyed by the former random process.

B.4: Alfvén wave propagations in coronal holes and formation of discontinuities.

Solar wind fluctuations are characterized by discontinuities, whose properties have been largely studied and different mechanisms have been proposed to explain their formation. We investigate the evolution of Alfvénic perturbations propagating in the inhomogeneous magnetic field of a coronal open-field region, in order to study both the way that small-scale structures are generated and the possible formation of discontinuities. We constructed a model for the equilibrium magnetic field in a coronal hole, representing a potential field with regions of opposite polarity. The evolution of small-amplitude Alfvén waves in the inhomogeneous structure is studied by employing a WKB approach, finding that small-scale structures form in the perturbation at relatively low altitudes (∼30000 km) above the coronal base. An initially monochromatic perturbation develops a steep power-law spectrum with slope $\alpha \sim 2.3$, which is strongly anisotropic with a predominance of quasi-perpendicular wavevectors. Small-scale structures are localized around separatrices of the magnetic structures. In many cases they contain quasi-perpendicular rotational discontinuities that can propagate to the upper corona, eventually reaching the solar wind. The considered mechanism could be responsible for forming a fraction of the population of discontinuities detected in the solar wind.

B.5: Intermittency of density fluctuations in the solar wind

The radial evolution of the intermittency of density fluctuations in the fast solar wind has been studied by analyzing the plasma density measurements provided by Helios 2 in the inner heliosphere. A complete set of diagnostic tools has been used, including the flatness factor at different timescales to estimate intermittency, the Kolmogorov–Smirnov test to estimate the degree of intermittency, and the Fourier transform to estimate the power spectral densities of these fluctuations. The level of density intermittency and the amplitude of intermittent events decreases with the distance

from the Sun, at odds with the intermittency of both magnetic field and all other plasma parameters. Furthermore, the intermittent events are strongly correlated, exhibiting temporal clustering. This indicates that the mechanism underlying their generation departs from a time-varying Poisson process. A remarkable, qualitative similarity with the behavior of plasma density fluctuations obtained from a numerical study of the nonlinear evolution of parametric instability in the solar wind supports the idea that this mechanism has an important role in governing density fluctuations in the inner heliosphere.

B.6: Analysis of geomagnetic storms

In order to study some of the effects of solar activity on the near Earth magnetic and plasma environment, the time variations of the magnetospheric and ground-based observations of the Earth's magnetic field during both quiet and magnetic storm periods were investigated through the empirical mode decomposition . We found two timescale variations in magnetospheric data which are associated with different magnetospheric current systems and the characteristic diurnal orbital variation, respectively. On the ground we identified three timescale variations related to the solar-wind–magnetosphere high-frequency interactions, the ionospheric processes, and the internal dynamics of the magnetosphere, respectively. This approach is able to identify the different physical processes involved in solar-wind– magnetosphere–ionosphere coupling. In addition, the large-timescale contribution can be used as a local index for the identification of the intensity of a geomagnetic storm on the ground.

B.7: Earth's climate: analysis of paleoclimate datasets and climate modeling

The Earth's climate dynamics and the effects of solar irradiance and variability on it were investigated trough both proxy dataset analysis and simplified climate models.

The climate dynamics over the last glacial period (i.e., 20–120 kyr before present) was investigated through the European Project for Ice Coring in Antarctica Dronning Maud Land (EDML) and North Greenland Ice-Core Project (NGRIP) oxygen isotope delta-18O data sets to study both the time evolution of fast warming events, known as Dansgaard–Oeschger (DO) events, and the dynamics at longer timescales. Empirical mode decomposition (EMD) was used to extract the proper modes of both the data sets. It was shown that EMD allows to separate the time behavior at the typical timescales (about 1500 year timescale) of DO events, from the evolution at longer timescales, characterized by intervals in which DO events happen and intervals when these are not observed. Using EMD signal reconstructions and a simple model based on the one-dimensional Langevin equation, it was argued that the occurrence of a DO event can be described as an excitation of the climate system within the same state, while the longer timescale behavior appears to be due to transitions between different climate states. Finally, on the basis of a cross-correlation analysis performed on EMD reconstructions, evidence that the Antarctic climate changes lead those of Greenland by a lag of ≈ 3.05 kyr was presented.

Concerning Earth's climate modeling, we investigated a modified version of the Daisyworld model, originally introduced by Lovelock and Watson to describe in a simple way the interactions between an Earth-like planet, its biosphere, and the incoming solar radiation. A spatial dependency on latitude was included in the model, and both a variable heat diffusivity along latitudes and a simple greenhouse effect description were introduced. It was found that the spatial interactions between the variables of the system can locally stabilize the coexistence of the two vegetation types and that, at variance with previous results, the system is able to self-regulate even in the presence of values of the incident luminosity which are far from the current Sun-Earth conditions. The diffusion process is able to destabilize the system and plays an important role in setting the symmetry with respect to the equator, while the greenhouse effect, in addition to contributing in self-regulating the planet climate, modifies the stability properties of the system, although does not directly destabilize the system.

C. Plasma Physics

C.1: Plasma turbulence, structures and dynamo

The Universe is permeated by hot, turbulent magnetized plasmas. They are found in active galactic nuclei, supernova remnants, the intergalactic and interstellar medium, the solar corona, the solar wind, and the Earth's magnetosphere, just to mention a few. Our knowledge and understanding of the Universe is largely based on the understanding of the plasma - a highly dynamical medium. Energy dissipation of turbulent fluctuations in plasmas play a key role in plasma heating and energization. Understanding these mechanisms is one of the main goal of our research group. Theory, modeling and observations of these turbulent fluctuations are crucial for the research in space physics and, in general, in physics of matter. The research activity of the group in this field is described in the following.

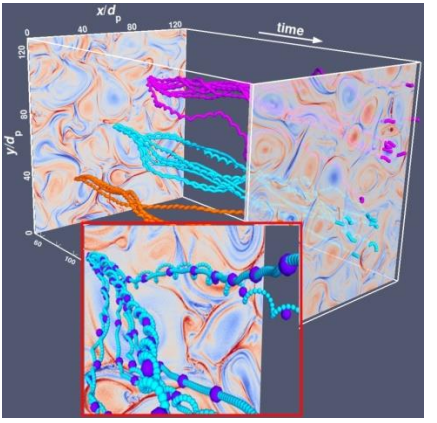

Figure 3: Puffs of particles as a function of time, in a 2D simulation of plasma turbulence. Particles experience a dramatic separation due to plasma turbulence, similarly to passive tracers in classical hydrodynamic turbulence. *Servidio et al., Phys. Rev. Lett. (2016).*

C.1.1: Simulations of plasma turbulence

Plasma dynamics need to be modelled via self-consistent theories and appropriate numerical strategies. The kinetic hybrid Vlasov–Maxwell numerical code, developed by the Group, is a crucial tool to reproduce the turbulent energy cascade down to kinetic scales. Using these simulations, in a turbulent regime, it has been found that kinetic-effects manifest through the deformation of the proton velocity distribution function (DF), with patterns of non-Maxwellian features being concentrated near regions of strong magnetic gradients. Results show an excellent agreement with in situ measurements of satellite data: the comparison between simulations and 10 years of solar wind data reveals that the Vlasov model is capable to describe accurately the dynamics of the heliospheric plasma. These novel results suggest that it is important to adopt self-consistent (and more complex) models of plasma dynamics in order to understand crucial phenomena such as the heating of the plasma in the Universe, as well as unexpected and spectacular events such as solar flares. Following this suggestion, and using a particle-based algorithm, we investigated the role of turbulence on particle energization. Using direct particle in cell (PIC) simulations, we studied the process of particle diffusion and extreme separation in turbulence (Fig. 3). These results are relevant for astrophysical and laboratory plasmas, where turbulence is crucial for heating, mixing, and acceleration processes.

The statistical properties of plasma turbulence have been also investigated. In particular, a classical technique called “signed measure” has been used to characterize the scaling behavior and the topology of sign-oscillating structures in simulations of the above model. Exploring different turbulence regimes, it is observed that plasma turbulence manifests two ranges with different exponents, the transition being observed near the ion skin depth. These results, which may have applications to both laboratory and astrophysical systems, further confirm the singular nature of small scale fluctuations in a plasma, mainly classified as intermittent, narrow, and intense current sheets. Furthermore, the statistical properties of the energy cascade at kinetic scales have been investigated through the high-order moments of the magnetic field fluctuations. The analysis reveals that plasma turbulence is consistent with a scenario where dissipation occurs non-homogeneously in space.

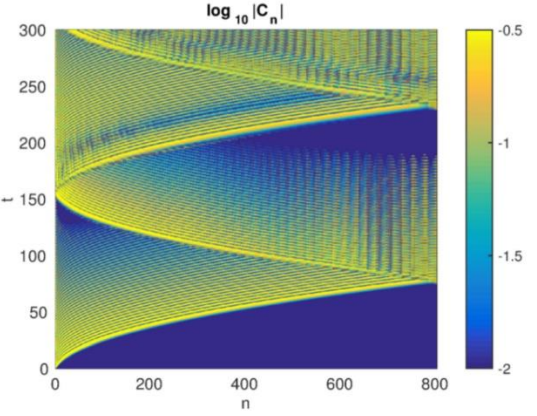

Figure 4: Numerical recurrence of the initial state in a collisionless plasma, pointed out through the evolution of the Hermite coefficients (in logarithm scale) Cn as a function of the Hermite mode n and the time t. *Pezzi et al., Phys. of Plasmas 2016.* ***Cover Image of February 2016 Issue, Volume 23, Number 2***

Collisions are usually neglected in the description of high temperature and low density plasmas. The collisionless assumption is justified by the fact that the particles mean-free-path is comparable with the plasma macroscopic length scales. However, to show that collisions can be neglected, one usually assumes that the plasma is close to the equilibrium - assumption not valid in the solar wind, where kinetic physics strongly distort the particle velocity distribution function. From a thermodynamic point of view, collisions are the unique mechanism able to produce irreversible heating in laboratory and space plasmas (Fig. 4). In this perspective, we showed, by modeling collisions through the fully nonlinear Landau operator in a homogeneous force-free plasma, that the collisionality is effectively enhanced by the presence of strong gradients in the particle distribution function. In fact, fine structures are dissipated much faster than other global quantities as temperature anisotropies. We also compared the full Landau operator, which is demanding from a computational point of view, with the simpler Dougherty operator. We established such a successful comparison, thus presenting a first attempt to describe realistic plasma turbulence.

The solar wind plasma is mainly composed by protons and electrons, with a small percentage of helium nuclei and a significantly lower abundance of heavier ions. Because of the rare collisions, the solar wind is typically far from the thermodynamic equilibrium, and a multicomponent kinetic model is needed. The Vlasov–Maxwell numerical code has been extended to explore the kinetic dynamics of different species. These are mainly protons and alpha particles. From recent numerical results we found that the response of different species to the fluctuating electromagnetic

fields is different. In particular, a significant differential heating of alphas with respect to protons is observed. Interestingly, the preferential heating process occurs in spatial regions nearby the peaks of ion vorticity (intermittent structures), where the strongest deviations from thermodynamic equilibrium are recovered. Both ion species manifest a preferentially perpendicular heating (perpendicular to the mean field), although the anisotropy is more pronounced for the alpha particles, in agreement with observations. The phenomenology is very well recovered in measurements in the turbulent solar wind and supports the idea that future space missions, designed to provide measurements of the particle velocity distribution with unprecedented time and phase space resolutions, will allow a deeper understanding of the Universe.

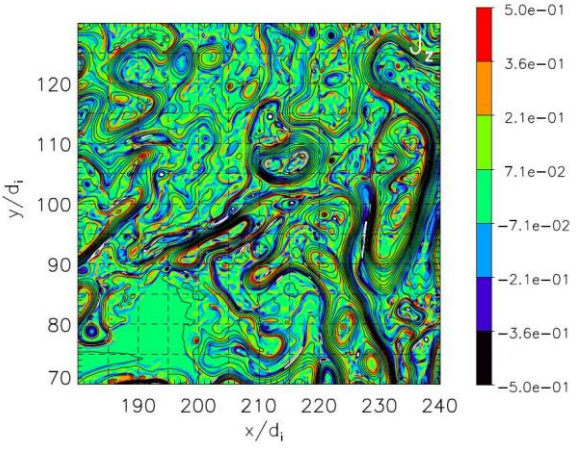

Figure 5: Magnification of out-of-plane current shaded out-of plane current Jz(x,y) together with magnetic potential field lines within a turbulent region inside the Kelvin-Helmoltz vortex in a two-fluid numerical simulation. *Rossi et al., Phys. of Plasmas 2015.* ***Cover Image of December 2015 Issue, Volume 22, Number 12***

C.1.2: Intermittent structures in the solar wind

As suggested by models and simulations, the main characteristic of turbulence is the dynamical involvement of a wide-range of spatial scales. Nonlinear interactions induce cross-scale transfer of energy, called the "turbulent cascade". But this is not the end of the story, because nonlinear cascades also produce coherent structures (Fig. 5) that are responsible for the characteristic burstiness, commonly measured by spacecraft instruments. Interpreting the solar wind as a natural plasma laboratory, it is indeed impressing to see how ubiquitous intermittency is in the interplanetary environment. The most common feature of observations is indeed the frequent appearance of magnetic discontinuities. Discontinuities are embedded into turbulence and, therefore, an efficient methodology is needed in order to "catch" these crucial structures, where dissipation and acceleration processes occur. One such approach is the Partial Variance of Increments (PVI) method - developed by the Group - which consist in an identification algorithm. Since its inception in 2008, the PVI method has expanded rapidly in the past years, used empirically to characterize non-Gaussian dynamical features. The technique is able to identify magnetic reconnection events, where most of the acceleration and explosive plasma processes occur. This topic is intimately related to the heating phenomenon, a puzzling and unsolved issue of space physics. Recent high resolution spacecraft observations provided new insights in cross-scale connection of intermittent discontinuities, going from proton down to electron scales. At these scales, these structures seems to be the sites of turbulent dissipation, where the cascade terminates and energy is finally converted into heat.

Many observational and numerical analyses are devoted to the identification of fluctuation channels along which energy is carried from large to short wavelengths during the development of the turbulent cascade; these fluctuation channels establish the link between macroscopic and microscopic scales. By means of a quantitative comparison between in situ measurements in the solar wind from the STEREO spacecraft and numerical results from kinetic simulations, an electrostatic channel of fluctuations dubbed ion-bulk waves has been identified, which develops along the turbulent cascade in a direction parallel to the ambient magnetic field. This channel appears to be efficient in transferring the energy from large Alfvénic to short electrostatic acoustic-like scales up to a range of wavelengths where it can finally be turned into heat, even when the electron to proton temperature ratio is of the order of unity. These findings suggest that is important to understand the behavior of plasma waves.

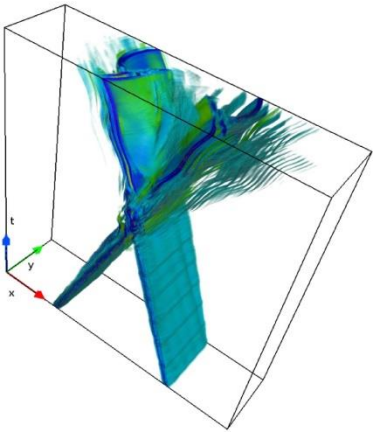

Figure 6: Space-time representation of the Alfvénic wave packets collision, by means of the iso-surfaces of the current density jz, showing that Alfvénic packets are strongly perturbed as a result of the mutual nonlinear interactions which occur during the packets overlap.

C1.3 Waves dynamics in plasmas

Waves are crucial constituents of space and laboratory plasmas and, despite decades of study, their dynamics within turbulent media is still not fully understood. In collaboration with the University of Delaware, we investigated waves-interaction in plasmas. In particular, the interaction of counterpropagating Alfvénic wave packets - known as the "Moffatt & Parker problem" - has been numerically studied. We extended the original model by introducing compressible, dispersive and kinetic effects. When these ingredients are taken into account, the dynamics becomes more complex and, against the prediction of Moffatt & Parker, wave packets are not clearly separated after their collision (Fig. 6). The proton distribution function departs from the Maxwellian shape, similarly to some recent solar wind observations. Finally we have found that, despite the wave-like behavior, several signatures of strong turbulence emerge.

Following the above topic, we studied the dynamics of waves and their interaction with inhomogeneities. The so-called phase-mixing effect takes place when an Alfvén wave propagates in a plasma which is inhomogeneous in the direction perpendicular to the background magnetic field, generating small scales in the transverse direction. We analyzed such a phenomenon using both Hall-MHD and Maxwell-Vlasov numerical simulations. We found that Kinetic Alfvén Waves (KAWs) are generated by the wave-inhomogeneity interaction. These packets leave the inhomogeneous region, propagating outwards. Distortions of the proton distribution function with temperature anisotropy of both signs are associated with these KAWs (Fig. 7). Beams of protons accelerated along the magnetic

field are locally observed, which are compatible with the parallel electric field associated with KAWs. These features are similar to what observed in the proton distribution function of solar wind plasma.

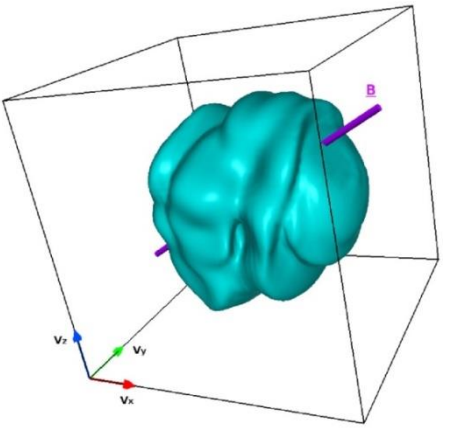

Figure 7: Iso-surface plot of the proton distribution in velocity space from a simulation of Kinetic Alfvèn wave turbulence; the magenta tube in each plot indicates the direction of the local magnetic field. *Valentini et al. Astron. Astrophys. (2017).*

C.1.4: Magnetic field dynamo

Almost all visible objects in our Universe are permeated by magnetic fields. Even though they are generated in an exceptionally turbulent environment, they often display a remarkable degree of order in both space and time. A typical example is the 22 yr solar cycle clearly manifested by the well known butterfly diagram, namely the diagram of the latitude of sunspot occurrence versus time. Parker in 1955 proposed that a latitudinally-travelling "dynamo wave" was at the origin of the observed equatorward drift of sunspot emergences in the course of the cycle. Parker's idea came out from the wave solutions that he found for the linear alpha-Omega dynamo equations. Dynamo waves and sunspots are hence at the base of the idea of large-scale dynamo mechanism, which found its formalization in the Mean Field Electrodynamics (MFE). The idea of a large-scale dynamo mechanism is an extremely idealized concept. The reality is that astrophysical fields do not just have large-scale components, they in fact have structure on multiple scales with indeed the strongest fields often being found at small scales. Hence the problem is to understand how does one get organization on the large scale starting from a chaotic turbulent mess.

In order to address this problem, we made high-resolution simulations of a dynamo that can generate organized fields at large scale in form of dynamo traveling waves at high *Rm* (magnetic Reynolds number). The generation mechanism involves the interaction between helical flows, given by chaotic turbulent eddies at small scales, and velocity shear. We obtain these results both in kinematic regime and in nonlinear regime. In particular in the kinematic regime we used a very large Rm in order to investigate the limit of validation of the Mean Field Electrodynamics and to understand the relationship between dynamo action and large-scale dynamo effect. We find that the all components of the magnetic field, both at large and at small scales, grow at the same rate. The growth rate is determined by the small-scale turbulence, which is removed by the filtering procedure of the MFE and which is the source of both the large-scale dynamo and the small-scale dynamo. The solutions take the form of a time-coherent part (traveling wave) at large scale embedded in incoherent fluctuations at smaller scales. The wave component of the solution is less evident, but still present, for weaker shear. When the shear is particularly weak the overwhelming small-scale turbulent structures hide the large-scale wave component. Since we find that the period of the large-scale component is

compatible with those that emerge from the MFE, we argued that although the growth-rate is determined by small-scale processes, the period of the coherent structures is set by mean-field considerations. Moreover, since the large-scale wave component can only be unambiguously identified from the rest of the structure by its persistent phase coherence, we suggested to draw a new definition of large-scale dynamo action that considers time coherence at large-scale, rather than one that relies on spatial scale alone as it is made in the dynamo literature so far.

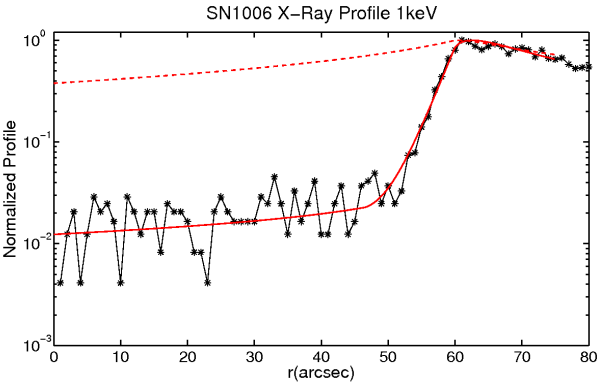

Figure 8: Analysis of the energetic electrons profiles, as obtained from Chandra X-ray observations of SN1006 supernova remnant allow to deduce the superdiffusive transport properties of electrons in the upstream precursor of the shock wave *(Perri et al., Astron. Astrophys. 2016).* Asterisks: Chandra data points; solid red line: fit with superdiffusive profile; dashed red line: fit with the diffusive Bell model.

C.2: Models for energetic particle propagation and acceleration in simulations and in the Heliosphere

The propagation of energetic particles encompasses different transport regimes from diffusive to scatter-free. There are several numerical studies of particle propagation in presence of magnetic turbulence that highlight the possibility of anomalous transport. These evidences have stimulated the study of transport of energetic particles in different astrophysical environments. Indeed, unveiling particle transport properties in presence of magnetic turbulence is an important but unsolved problem of space physics and astrophysics.

An isotropic 3D model of static turbulence, made of a superposition of space-localized fluctuations at different spatial scales, that permits to reproduce a wide turbulent spectrum and to regulate the level of intermittency of the turbulent cascade, has recently been developed. Adjusting the simulation parameters close to solar wind conditions at 1 AU, 1 MeV protons have been injected in the turbulence realization and the parallel and perpendicular diffusion have been investigated. The parallel transport is found to be diffusive and is influenced by intermittency. The distribution of scattering times of particles has a power law decay for more than one decade that needs to be properly interpreted.

Particle transport properties in the Heliosphere can be inferred from the analysis of fluxes of particles accelerated at interplanetary shocks. The frequently observed power-law decay upstream, indeed, implies a superdiffusive transport. Thus, the superdiffusive shock acceleration (SSA) theory has been developed as an extension of the classical diffusive shock acceleration (DSA). A number of interplanetary shocks have been studied and the acceleration times for energetic protons in the framework of SSA have been estimated, in comparison with DSA prediction. The acceleration times due to SSA are found to be much shorter than in DSA, and also shorter than the interplanetary shock lifetimes. Shorter acceleration times are due to the scale-free nature of the particle displacements in

the framework of superdiffusion: a non-negligible probability is associated to very long displacements, so that particles far from the shock can return to it, and short displacements have also a high probability of occurrence, increasing the chances for particles close to the front to cross the shock many times and eventually be accelerated by a first order Fermi mechanism.

Superdiffusion has also allowed to interpret supernova remnant (SNR) X-ray rims. Emission profiles have been derived in presence of synchrotron energy losses, normal diffusion (typically causing an exponential decay), and superdiffusion (causing a power law decay) for a spherically symmetric model. Then the model profiles, projected on the plane of the sky, have been compared with Chandra observations of supernova (SN)1006 and Tycho's SN (Fig. 8). It has been found that downstream of the blast wave the observed profile is exponentially cut-off due to synchrotron energy losses in the amplified magnetic field. Upstream and close to the shock, the observed profile of SN1006 is well reproduced by electron diffusion. However, the long power law X-ray tail far upstream of the shock has been interpreted as a transition to superdiffusion in the electrons' transport regime. Similar results have been obtained for Tycho. These studies suggest that anomalous transport is common in interplanetary space and in the interstellar medium.

Further, spacecraft observations show that energetic ions are found in the Earth's magnetotail, with energies ranging from tens to a few hundreds of keV. The acceleration mechanism that produces such energetic ions is poorly understood. Test particle simulations in which protons and heavier ions are injected in time dependent electromagnetic fields have been run using parameters typical of the Earth's magnetotail. Electromagnetic fields are composed by an unperturbed component and by 3D time-dependent stochastic electromagnetic perturbations. The interaction between time-dependent fields and test particles is second order Fermi-like. The unperturbed component is obtained as solution of a generalized Harris model, which well describes the observed profiles in the magnetotail. Protons reach energies of the order of 100 keV. By changing the ion mass and charge, it is possible to study the acceleration of heavier ions such as He ++ and O + , and it is found that energies of the order of 100–200 keV are reached in a few seconds for He ++ , and about 100 keV for O +, values that compare well with those observed in the Earth's magnetotail.

C.3 Laboratory plasmas.

Laboratory plasmas are often associated with the problem of nuclear fusion, as in the Reversed-Field Pinch devices where the turbulence plays an essential role in keeping the magnetic configuration. Non-neutral plasmas represent a very useful tool to investigate fundamental plasma physics processes, due to their remarkable confinement properties in devices such as the Penning-Malmberg trap. The reseach in this domain has been concerned with aspects like the generation of waves and turbulence in non-neutral plasmas, the study of the dynamics of dusty plasmas by means of particle-in-cell simulations and the role played by resistivity inhomogeneities in RFP machines. A detailed description is given in the following.

C.3.1 Excitation of electrostatic waves in Penning-Malmberg traps

Laboratory experiments with nonneutral plasmas, usually confined in experimental devices called Penning-Malmberg traps, represent an indispensable tool to investigate basic processes in plasma physics, like, the collisionless Landau damping of electrostatic waves, the linear and nonlinear regime of wave-particle interactions and the effects of inter-particle collisions on the plasma dynamics. When a plasma has a finite radial geometry, electrostatic plasma waves can propagate at frequency smaller than the plasma frequency; these waves are usually called Trivelpiece-Gould (TG) waves. However, as the particle velocity distribution function exhibits out of equilibrium features as plateau or beams, other undamped fluctuations like Electron Acoustic Waves (EAW) or Kinetic Electron Electrostatic Nonlinear (KEEN) Waves are also recovered. The kinetic dynamics of a nonneutral plasma column confined in a Penning-Malmberg trap can be described through the drift-kinetic equations. Through a very active collaboration with the nonneutral plasma physics group of the University of California at San Diego, we systematically compared experimental and numerical

results concerning the excitation, the propagation and the stability of the TG modes, both in linear and in the nonlinear regime, and the description of EAWs. We developed numerical codes in different configuration that self-consistently integrate the drift-kinetic equation coupled to Poisson's equation, thus properly describing the kinetic dynamics of pure ion (or pure electron) plasmas. We also introduced collisional effects into the numerical calculation through the implementation of diffusive collisional operators of the Fokker-Planck type. Moreover, we recently focused on the description of the problem of launching of EAWs through an external electric driver, showing that, due to the driver nonlinearity, several secondary fluctuations can be generated at arbitrary phase speeds. However, collisions strongly dissipate these fluctuations, thus inhibiting the observation on such waves in experimental devices. Technical progresses addressed to decrease the collisionality level into laboratory plasma devices may confirm the existence of these waves.

C.3.2 Turbulence in pure electron plasmas

Electron plasmas confined in Penning-Malmberg traps evolve, in a wide range of operational parameters, as near-ideal 2D fluids with a single sign of vorticity. This provides the opportunity to perform experimental studies of 2D fluid dynamical processes such as shear flow instabilities, self-organization, vortex formation, and turbulence. Statistical properties of freely decaying 2D turbulence in pure electron plasmas were studied by analyzing the results of experiments performed in the Penning-Malmberg trap ELTRAP, operated by the Plasma Physics group of the University of Milano. Intermittency phenomena were investigated through scaling properties of the probability density functions and flatness of spatial vorticity increments, computed by analyzing the results of experiments. It was shown that the intermittency properties of the turbulence strongly depends on the initial conditions. While for annular initial conditions the scaling behavior of the increments is basically determined by the initial conditions and the plasma dynamics does not produce intermittency effects, for spiral initial conditions a quite strong development of intermittency is produced by the turbulent dynamics.

C.3.3. Non-neutral complex plasmas

The collective behaviour of dusty plasmas is heavily affected by the presence of a small fraction of micrometric or sub-micrometric dust particles which collect a large surface charge. While dusty plasmas under study are usually quasi-neutral, a magnetized nonneutral plasma (a situation found for example in Penning traps), where a conventional plasma with a single sign of charge (e.g. electrons) is contaminated by a dust population, was investigated. The two-dimensional dynamics of such a plasma was simulated in the plane orthogonal to a homogeneous magnetic field with a tailored Particle-In-Cell code implementing a mass-less fluid (drift-Poisson) approximation for electrons and a kinetic description for the dust component, including gravity effects. Simulations with a range of initial conditions were performed to observe the influence of dust on the diocotron instability developing in the electron plasma. Depending on the density and profile of the dust distribution, a partial damping of the instability at higher mode numbers has been observed, although an asymmetric dust contamination may result in a larger number of active modes. Non-Gaussian PDFs of electron density increments have been observed, and in particular the growth of large tails at small scales as well as the disappearance of peaks related to large structures when dust is added.

C.3.4 Resistivity profiles and helicity structure in Reversed-Field Pinch devices

Simulations of the Reversed-Field Pinch (RFP) plasma configuration, including density and pressure evolution, have shown that a stationary state with a reversed toroidal magnetic field could not be obtained, contrary to the results produced with numerical codes neglecting density and pressure dynamics. In this work new simulations have been performed in which the resistivity is non-uniform, with a radial profile steeply increasing close to the wall. Such resistivity profile is more realistic than a uniform resistivity, since the temperature at the wall is lower than in the plasma core. Moreover, density and pressure evolution are explicitly included in the simulations. The results show

that in such a case a stationary RFP configuration can be obtained, thus stressing the role played by a non-uniform resistivity in the RFP dynamics.

A. PUBLICATIONS ON SCIENTIFIC JOURNALS

A.1 Publications on international journals

A.1.1 Publications on international journals printed in 2013

1. Perrone D., Valentini F., Servidio S., Dalena S., Veltri P.,
   Vlasov simulations of multi-ion plasma turbulence in the solar wind,
   The Astrophysical Journal **762**, 99 (2013).

2. Perrone D., Dendy R. O., Furno I., Sanchez R., Zimbardo G., Bovet A., Fasoli A., Gustafson K., Perri S., Ricci P., Valentini F.,
   Nonclassical Transport and Particle-Field Coupling: from Laboratory Plasmas to the Solar Wind,
   Space Sci Rev **178**, 233 (2013).

3. Valentini F., Perrone D., Califano F., Pegoraro F., Veltri P., Morrison P. J., O'Neil T. M.,
   Response to "Comment on 'Undamped electrostatic plasma waves'" [Phys. Plasmas 20, 034701 (2013)], Physics of Plasmas **20**, 034702 (2013).

4. Pezzi O., Valentini F., Perrone D., Veltri P.,
   Eulerian simulations of collisional effects on electrostatic plasma waves,
   Physics of Plasmas **20**, 092111 (2013).

5. Dudok de Wit T., Alexandrova O., Furno I:, Sorriso-Valvo L., Zimbardo G.,
   Methods for Characterising Microphysical Processes in Plasmas,
   Space Science Reviews **178**, 693 (2013).

6. Alexandrova O., Chen C. H. K., Sorriso-Valvo L., Horbury T. S., Bale, S. D.,
   Solar Wind Turbulence and the Role of Ion Instabilities,
   Space Science Reviews **178**, 101, (2013).

7. Martin L.N., De Vita G., Sorriso-Valvo L., Dmitruk P., Nigro G., Primavera L., Carbone V.,
   Cancellation properties in Hall magnetohydrodynamics with a strong guide magnetic field,
   Physical Review E **88**, 063107 (2013).

8. Maruca B. A., Bale S. D., Sorriso-Valvo L., Kasper J. C., Stevens M. L.,
   Collisional Thermalization of Hydrogen and Helium in Solar-Wind Plasma,
   Physical Review Letters **111**, 241101 (2013).

9. Oughton S., Wan M., Servidio S., Matthaeus W. H.,
   On the origin of anisotropy in magnetohydrodynamic turbulence: the role of higher-order correlations,
   The Astrophysical Journal **768**, 10 (2013)

10. Wan M., Matthaeus W. H., Servidio S., Oughton S.,
    Generation of X-points and secondary islands in 2D magnetohydrodynamic turbulence,
    Physics of Plasmas **20**, 042307 (2013)

11. Snodin A. P., Ruffolo D., Oughton S., Servidio S., Matthaeus W. H.,
Magnetic Field Random Walk Models and Simulations of Reduced Magnetohydrodynamic Turbulence,
The Astrophysical Journal **779**, 56 (2013).

12. Wu P., Perri S., Osman K., Wan M., Matthaeus W. H., Shay M. A., Goldstein M. L., Karimabadi H., Chapman S.,
Intermittent Heating in Solar Wind and Kinetic Simulations,
The Astrophysical Journal Letters **763**, L30 (2013).

13. Gogoberidze G., Perri S., Carbone V.,
The Yaglom law in the expanding solar wind,
The Astrophysical Journal **769**, 111 (2013).

14. Telloni D., Perri S., Bruno R., Carbone V., D'Amicis R.,
An analysis of Magnetohydrodynamic invariants of magnetic fluctuations within interplanetary flux ropes,
The Astrophysical Journal **776**, 3 (2013).

15. Dolgonosov M., Zimbardo G., Perri S., Greco A.,
On the generation of ion beamlets in the magnetotail: resonant acceleration versus stochastic acceleration,
Journal of Geophysical Research **118**, 5445 (2013).

16. Zimbardo G., Perri S.,
From Lèvy walks to superdiffusive shock acceleration,
The Astrophysical Journal **778**, 35 (2013).

17. Malara F.,
Alfvén waves in coronal holes: formation of discontinuities in inhomogeneous magnetic fields ,
Astron. Astrophys. **549**, A54 (2013).

18. Onofri M., Malara F.,
Effects of the resistivity profile on the formation of a reversed configuration and single helicity states in compressible simulations of the Reversed-Field Pinch,
Phys. Plasmas **20**, 102514 (2013).

19. Donato S., Greco A., Matthaeus W. H., Servidio S., Dmitruk P.,
How to identify reconnecting current sheets in Incompressible Hall MHD turbulence,
Journal of Geophysical Research **118**, 4033-4038 (2013).

20. Lepreti F., Romé M., Maero G., Paroli B., Pozzoli R.,
Scaling properties and intermittency of two-dimensional turbulence in pure electron plasmas,
Physical Review E **87**, 063110 (2013).

21. Savaglio S., Grothkopf U.,
Swift Publication Statistics: A Comparison With Other Major Observatories,

Publications of the Astronomical Society of Pacific, **125**, 287 (2013).

22. Sudilovsky V., Greiner J., Rau A., Salvato M., Savaglio S., et al.,
Clustering of galaxies around gamma-ray burst sight-lines,
Astronomy & Astrophysics, **552**, A143 (2013).

23. Hartoog O. E., Wiersema K., Vreeswijk P. M., Kaper L., Tanvir N. R., Savaglio S. et al.,
The host-galaxy response to the afterglow of GRB 100901A,
Monthly Notices of the Royal Astronomical Society, **430**, 2739 (2013).

24. Elliott J., Krühler T., Greiner J., Savaglio S., et al.,
The low-extinction afterglow in the solar-metallicity host galaxy of γ-ray burst 110918A,
Astronomy & Astrophysics, **556**, A23 (2013).

25. Boissier S., Salvaterra R., Le Floc'h E., Basa S., Buat V., Prantzos N., Vergani S. D., Savaglio S.,
A method for quantifying the gamma-ray burst bias. Application in the redshift range of 0-1.1,
Astronomy & Astrophysics, **557**, A34 (2013).

26. De Cia A., Ledoux C., Savaglio S., Schady P., Vreeswijk P. M.,
Dust-to-metal ratios in damped Lyman-α absorbers. Fresh clues to the origins of dust and optical extinction towards γ-ray bursts,
Astronomy & Astrophysics, **560**, A88 (2013).

27. Nigro G., Carbone V., Primavera L.,
Simplified model for an alpha2-omega dynamo fed by dynamical evolution of the zonal shear,
Monthly Notices of the Royal Astronomical Society, **433**, 2206 (2013).

28. Alfonsi G., Lauria A., Primavera L.,
Proper orthogonal flow modes in the viscous-fluid wave-diffraction case,
Journal of flow visualization and Image Processing, **20**, 227 (2013).

29. Alfonsi G., Lauria A., Primavera L.,
On evaluation of wave forces and runups on cylindrical obstacles,
Journal of flow visualization and Image Processing, Vol. **20**, N. 4, pp. 269-291 (2013).

30. Zimbardo G.,
Viewpoint: A Particle Accelerator in the Radiation Belts,
Physics **6**, 131 (2013).

A.1.1 Publications on international journals printed in 2014

31. Servidio S., Osman K. T., Valentini F., Perrone D., Califano F., Chapman S., Matthaeus W. H., Veltri P.,
Proton kinetic effects in Vlasov and solar wind turbulence,
The Astrophysical Journal Letters **781**, L27 (2014).

32. Pezzi O., Valentini F., Perrone D., Veltri P.,

Erratum: "Eulerian simulations of collisional effects on electrostatic plasma waves" [Phys. Plasmas 20, 092111 (2013)],
Physics of Plasmas **21**, 019901 (2014).

33. Perrone D., Bourouaine S., Valentini F., Marsch E., Veltri P.,
Generation of temperature anisotropy for alpha particle velocity distributions in solar wind at 0.3 AU: Vlasov simulations and Helios observations,
J. Geophys. Res., *Space Physics* **119**, 2400 (2014).

34. Pezzi O., Valentini F., Veltri P.,
Kinetic ion-acoustic solitary waves in collisional plasmas,
The European Physical Journal D **68**, 128 (2014).

35. Valentini F., Vecchio A., Donato S., Carbone V., Briand C., Bougeret J., Veltri P.,
The nonlinear and nonlocal link between macroscopic Alfvénic and microscopic electrostatic scales in the solar wind,
Astrophysical Journal Letters **788**, L16 (2014).

36. Perrone D., Valentini F., Servidio S., Dalena S., Veltri P.,
Analysis of intermittent heating in a multi-component turbulent plasma,
European Physical Journal D **68**, 209 (2014).
37. Matthaeus W. H., Oughton S., Osman K. T., Servidio S., Wan M., Gary S. P., Shay M. A., Valentini F., Roytershteyn V., Karimabadi H., Chapman S. C.,
Nonlinear and Linear Timescales near Kinetic Scales in Solar Wind Turbulence,
The Astrophysical Journal **790**, 155 (2014).

38. De Vita G., Sorriso-Valvo L., Valentini F., Servidio S., Primavera L., Carbone V., Veltri P.,
Analysis of Cancellation Exponents in Two-Dimensional Vlasov Turbulence,
Physics of Plasmas **21**, 072315 (2014).

39. Valentini F.,
Editorial. Special issue: Collisions in collisionless plasmas,
Journal of Plasma Physics **80**, 529 (2014).

40. Vecchio A., Valentini F., Donato S., Carbone V., Briand C., Bougeret J., Veltri P.,
Electrostatic fluctuations in the solar wind: An evidence of the link between Alfvénic and electrostatic scales,
J. Geophys. Res., Space Physics, **119**, 7012 (2014).

41. Vasconez C. L., Valentini F., Camporeale E., Veltri P.,
Vlasov simulations of kinetic Alfvén waves at proton kinetic scales,
Physics of Plasmas **21**, 112107 (2014).

42. Valentini F., Servidio S., Perrone D., Califano F., Matthaeus W. H., Veltri P.,
Hybrid Vlasov-Maxwell simulations of two-dimensional turbulence in plasmas,
Physics of Plasmas **21**, 082307 (2014).

43. Bruno R., Telloni D., Primavera L., Pietropaolo E., D'Amicis R., Sorriso-Valvo L., Carbone V., Malara F., Veltri P.,
Radial evolution of intermitency of density fluctuations in the fast solar wind,

The Astrophysical Journal **786**, 53 (2014).

44. Chen C. H. K., Sorriso-Valvo L., Safrankova J., Nemecek Z.,
Intermittency of solar wind density fluctuations from ion to electron scales,
The Astrophysical Journal Letter **789**, L8 (2014).

45. Carbone F. Sorriso-Valvo L.,
Experimental analysis of intermittency in electrohydrodynamic instability,
European Journal of Physics E **37**, 61 (2014).

46. Servidio S., Matthaeus W. H., Wan M., Ruffolo D., Rappazzo A. F., Oughton S.,
Complexity and Diffusion of Magnetic Flux Surfaces in Anisotropic Turbulence,
The Astrophysical Journal **785**, 56 (2014).

47. Servidio S., Gurgiolo C., Carbone V., Goldstein M. L.,
Relaxation Processes in Solar Wind Turbulence,
The Astrophysical Journal Letters **789**, L44 (2014).

48. Wan M., Rappazzo A. F., Matthaeus W. H., Servidio S., Oughton S.,
Dissipation and Reconnection in Boundary-Driven Reduced Magnetohydrodynamics,
The Astrophysical Journal **797**, 63 (2014).

49. Dmitruk P., Mininni P. D., Pouquet A., Servidio S., Matthaeus W. H.,
Magnetic field reversals and long-time memory in conducting flows,
Physical Review E **90**, 043010 (2014).

50. Pucci F., Onofri M., Malara F. ,
Evolution of Magnetohydrodynamic Waves in Low Layers of a Coronal Hole,
Astrophys. J. **796**, 43 (2014).

51. Osman K. T., Matthaeus W. H., Gosling J. T., Greco A., Servidio S., Hnat B., Chapman S. C., Phan T. D.,
Magnetic Reconnection and Intermittent Turbulence in the Solar Wind,
Physical Review Letters **112**, 215002-1 (2014).

52. Greco A., Artemyev A., Zimbardo G.,
Proton acceleration at two-dimensional dipolarization fronts in the magnetotail,
J. Geophys. Res., **119** (2014).

53. Dalena S., Rappazzo A. F., Dmitruk P., Greco A, Matthaeus W. H.,
Test-Particle Acceleration in a Hierarchical Three-dimensional Turbulence Model.
The Astrophysical Journal **783**, 143-153 (2014).

54. Greco A., Perri S.,
Identification of High Shears and Compressive Discontinuities in the Inner Heliosphere,
The Astrophysical Journal **784**, 163-169 (2014).

55. Telloni D., Carbone V., Lepreti F., Antonucci E.,
Stochasticity and Persistence of Solar Coronal Mass Ejections,
The Astrophysical Journal Letters **781**, L1 (2014).

56. Maero G., Romé M., Lepreti F., Cavenago M.,
Numerical study of a dust-contaminated electron plasma,
The European Physical Journal D **68**, 277 (2014).

57. Alberti T., Lepreti F., Vecchio A., Bevacqua E., Capparelli V., Carbone V.,
Natural periodicities and Northern Hemisphere–Southern Hemisphere connection of fast temperature changes during the last glacial period: EPICA and NGRIP revisited,
Climate of the past 1**0**, 1751 (2014).

58. Michałowski, M. J., Hunt, L. K., Palazzi, E., Savaglio, S., et al.,
Spatially-resolved dust properties of the GRB 980425 host galaxy,
Astronomy & Astrophysics, **562**, A70 (2014).

59. D'Elia V., Fynbo J. P. U., Goldoni P. Covino S., de Ugarte Postigo A., Ledoux C., Calura F., Gorosabel J., Malesani D., Matteucci F., Sanchez-Ramirez R., Savaglio S., et al.,
VLT/X-shooter spectroscopy of the GRB 120327A afterglow,
Astronomy & Astrophysics, **564**, A38 (2014).

60. Hunt L. K., Palazzi E., Michałowski M. J., Rossi A., Savaglio S., et al.,
New light on gamma-ray burst host galaxies with Herschel,
Astronomy & Astrophysics, **565**, A112 (2014).

61. Nicuesa Guelbenzu A., Klose S., Michałowski M. J., Savaglio S., Kann D. A., Rossi A., Hunt L. K., Gorosabel J., Greiner J., McKenzie M. R. G., Palazzi E., Schmidl S.,
Another Short-burst Host Galaxy with an Optically Obscured High Star Formation Rate: The Case of GRB 071227,
The Astrophysical Journal, **789**, 45 (2014).

62. Schad, P., Savaglio S., Müller T., et al.,
Herschel observations of gamma-ray burst host galaxies: implications for the topology of the dusty interstellar medium,
Astronomy & Astrophysics, **570**, A52 (2014).

63. Rossi A., Piranomonte S., Savaglio S., et al.,
A quiescent galaxy at the position of the long GRB 050219A,
Astronomy & Astrophysics, **572**, A47 (2014).

64. Vreeswijk P. M., Savaglio S., Gal-Yam A., et al.,
The Hydrogen-poor Superluminous Supernova iPTF 13ajg and its Host Galaxy in Absorption and Emission,
The Astrophysical Journal, **797**, 24 (2014).

65. Restuccia S., Primavera L., Vecchio A., Carbone V.,
Kinematic Numerical Simulations of the Solar Dynamo: Dependence on alpha and Omega Values,
Solar Physics, Vol. **289**, N. 3, pp. 693-706 (2014).

66. Alfonsi G., Ciliberti S. A., Mancini M., Primavera L.,

GPGPU implementation of mixed spectral-finite difference computational code for the numerical integration of the three-dimensional time-dependent incompressible Navier-Stokes equations,
Computers and Fluids, Vol. **102**, pp. 237-249 (2014).

67. Cadavid A.C., Lawrence J.K., Christian D.J., Jess D.B., Nigro G.,
Heating Mechanisms for Intermittent Loops in Active Region Cores from AIA/SDO EUV Observations, Astrophysical Journal, Vol. **795,** Issue 1, 48 (2014).

68. Artemyev A. V., Zimbardo G., Ukhorskiy A. Y., Fujimoto M.,
Preferential acceleration of heavy ions in the reconnection outflow region. Drift and surfatron ion acceleration,
Astron. Astrophys., **562**, A58, (2014).

69. Shklyar D. R., Zimbardo G.,
Particle dynamics in the field of two waves in a magnetoplasma,
Plasma Phys. Control. Fusion 56, 095002 (2014).

70. Aburjania G., Chargazia K., Kharshiladze O., Zimbardo G.,
Self-organization of ULF electromagnetic wave structures in the shear flow driven dissipative ionosphere, Nonlin. Processes Geophys. Discussions, **1**,1431 (2014).

71. Zimbardo G., Shklyar D. R.,
Regular and stochastic electron dynamics in the field of two waves,
LabTalk for Plasma Phys. Control. Fusion, http://iopscience.iop.org/0741-3335/labtalk-article/58471 (2014).

A.1.1 Publications on international journals printed in 2015

72. Servidio S., Valentini F., Perrone D., Greco A., Califano F., Matthaeus W. H., Veltri P.,
A kinetic model of plasma turbulence,
Journal of Plasma Physics **81**, 325810107 (2015).

73. Pezzi O., Valentini F., Veltri P.,
Nonlinear regime of electrostatic waves propagation in presence of electron-electron collisions,
Physics of plasmas **22**, 042112 (2015).

74. Pezzi O., Valentini F., Veltri P.,
Collisional relaxation: Landau versus Dougherty operator,
Journal of Plasma Physics **81**, 305810107 (2015).

75. Veltri P., Valentini F.,
Solar Wind: a space laboratory for plasma turbulence,
Il Nuovo Saggiatore **3-4**, 23 (2015).

76. Rossi C., Califano F., Retino A., Sorriso-Valvo L., Henri P., Servidio S., Valentini F., Chasapis A., Rezeau L.,

Two-fluid numerical simulations of turbulence inside Kelvin-Helmholtz vortices: intermittency and reconnecting current sheets,
Physics of Plasmas **22**, 122303 (2015).

77. Vasconez C., Pucci F., Valentini F., Servidio S., Matthaeus W. H., Malara F.,
Kinetic Alfvén waves generation by large-scale phase-mixing,
The Astrophysical Journal **815**, 7 (2015).

78. Sorriso-Valvo L., G. De Vita, M. Kazachenko, S. Krucker, L. Primavera, S. Servidio, A. Vecchio, B. Welsch, G. Fisher, F. Lepreti, V. Carbone,
Sign singularity and flares in solar active region NOAA 11158,
The Astrophysical Journal **801**, 36 (2015).

79. Yordanova E., Perri S., Sorriso-Valvo L. and Carbone V.,
Multipoint observation of anisotropy and intermittency in solar-wind turbulence,
EPL **110**, 19001 (2015).

80. Chasapis A., Retinò A., Sahraoui F., Vaivads A., Khotyaintsev Y., Sundkvist D., Greco A., Sorriso-Valvo L., Canu P.,
Thin current sheets and associated electron heating in turbulent space plasma,
The Astrophysical Journal Letters **804**, L1 (2015).

81. Sorriso-Valvo L., Marino R., Lijoi L., Perri S. and Carbone V.,
Self-consistent Castaing distribution of solar wind turbulent fluctuations,
The Astrophysical Journal **807**, 86 (2015).

82. De Vita G., Vecchio A., Sorriso-Valvo L., Briand C., Primavera L., Servidio S., Lepreti F., Carbone V.,
Cancellation analysis of current density in solar active region NOAA10019,
Journal of Space Weather and Space Climate **5**, A28 (2015).

83. Carbone F., Ciuchi F., Mazzulla A., Sorriso-Valvo L.,
Anomalous Scaling, *Intermittency and Turbulence in Nematic Liquid Crystals*,
Molecular Crystals and Liquid Crystals **614**, 67 (2015).

84. Goldstein M. L., Escoubet P., Hwang K.-Joo, Wendel D. E., Vinas A.-F., Fung S. F., Perri S., Servidio S., Pickett J. S., Parks G. K., Sahraoui F., Gurgiolo C., Matthaeus W. H., Weygand J. M.,
Multipoint observations of plasma phenomena made in space by Cluster,
Journal of Plasma Physics **81**, 325810301 (2015).

85. Catapano F., Artemyev A.V., Zimbardo G., Vasko I. Y.,
Current sheets with inhomogeneous plasma temperature: Effects of polarization electric field and 2D solutions,
Physics of Plasma **22**, 092905 (2015).

86. Greco A., Artemyev A., Zimbardo G.,
Heavy ion acceleration at dipolarization fronts in planetary magnetotails,
Geophysical Research Letters **42**, 8280-8287 (2015).

87. Matthaeus W. H., Minping W., Servidio S., Greco A., Osman K. T., Oughton S., Dmitruk P., I*ntermittency, nonlinear dynamics and dissipation in the solar wind and astrophysical plasmas*,
Philosophical Transactions - Royal Society. Mathematical, Physical and Engineering Sciences **373**, 20140154 (2015).

88. Goldstein M. L., Wicks R. T., Perri S., Sahraoui F.,
Kinetic scale turbulence and dissipation in the solar wind: key observational results and future outlook,
Philosophical Transaction of the Royal Society A **373**, 20140147 (2015).

89. Perri S., Zimbardo G., Effenberger F., Fichtner H.,
Parameter estimation of superdiffusive motion of energetic particles upstream of heliospheric shocks,
Astronomy and Astrophysics **578**, A2 (2015).

90. Zimbardo G., Amato E., Bovet A., Effenberger F., Fasoli A., Fichtner H., Furno I., Gustafson K., Ricci P., Perri S.,
Superdiffusive transport in laboratory and astrophysical plasmas,
Journal of Plasma Physics **81**, 495810601 (2015).

91. Perri S., Zimbardo G.,
Evidence for superdiffusive shock acceleration at interplanetary shocks,
Journal of Physics: Conference Series **642**, 012020 (2015).

92. Perri S., Zimbardo G.,
Short acceleration times from superdiffusive shock acceleration in the heliosphere,
The Astrophysical Journal **815**, 75 (2015).

93. Del Moro D., Giannattasio F., Berrilli F., Consolini G., Lepreti F., Gosic M.,
Super-diffusion versus competitive advection: a simulation,
Astronomy & Astrophysics **576**, A47 (2015).

94. Alberti T., Primavera L., Vecchio A., Lepreti F., Carbone V.,
Spatial interactions in a modified Daisyworld model: Heat diffusivity and greenhouse effects,
Physical Review E **92**, 052717 (2015).

95. Romano P., Zuccarello F., Guglielmino S.L., Berrilli F., Bruno R., Carbone V., Consolini G., De Lauretis M., Del Moro D., Elmhamdi A., Ermolli I., Fineschi S., Francia P., Kordi A.S., Degl'Innocenti E.L., Laurenza M., Lepreti F., Marcucci M.F., Pallocchia G., Pietropaolo E., Romoli M., Vecchio A., Vellante M., Villante U.,
Recurrent flares in active region NOAA 11283,
Astronomy & Astrophysics **582**, A55 (2015).

96. Nicuesa Guelbenzu A., Klose S., Palazzi E., Greiner J., Michałowski M. J., Kann D. A., Hunt L. K., Malesani D., Rossi A., Savaglio S., et al.,
Identifying the host galaxy of the short GRB 100628A,
Astronomy & Astrophysics, **583**, A88 (2015).

97. Piranomonte S., Japelj J., Vergani S. D., Savaglio S., et al.,
GRB host galaxies with VLT/X-Shooter: properties at 0.8 < z < 1.3,
Monthly Notices of the Royal Astronomical Society, **452**, 3293 (2015).

98. Michałowski M. J., Gentile G., Hjorth J., et al,
Massive stars formed in atomic hydrogen reservoirs: HI observations of gamma-ray burst host galaxies,
Astronomy & Astrophysics, **582**, A78 (2015).

99. Savaglio S.,
Galaxies as seen through the most energetic explosions in the universe,
Journal of High Energy Astrophysics, **7**, 95 (2015).

100. Krühler T., Malesani D., Fynbo J. P. U., et al.,
GRB hosts through cosmic time. VLT/X-Shooter emission-line spectroscopy of 96 γ-ray-burst-selected galaxies at 0.1 <z < 3.6,
Astronomy & Astrophysics, **581**, A125 (2015).

101. Greiner J., Fox D. B., Schady P., Krühler, T., Trenti M., Cikota A., Bolmer J., Elliott J., Delvaux C., Perna R., Afonso P., Kann D. A., Klose S., Savaglio S., Schmidl S., Schweyer T. Tanga M., Varela K.,
Gamma-Ray Bursts Trace UV Metrics of Star Formation over 3 < z < 5,
The Astrophysical Journal, **809**, 76, (2015).

102. Greiner J., Mazzali P. A., Kann D. A., et al.,
A very luminous magnetar-powered supernova associated with an ultra-long γ-ray burst,
Nature, **523**, 7559, 189 (2015).

103. Schady P., Krühler T., Greiner J., Graham J. F., Kann D. A., Bolmer J., Delvaux C., Elliott J., Klose S., Knust F., Nicuesa Guelbenzu A., Rau A., Rossi A. Savaglio S., Schmidl S., Schweyer T., Sudilovsky V., Tanga M., Tanvir N. R., Varela K. Wiseman P.,
Super-solar metallicity at the position of the ultra-long GRB 130925A,
Astronomy & Astrophysics, 579, A126 (2015) .

104. Olivares E. F., Greiner J., Schady P., Klose S. Krühler T., Rau A., Savaglio S., Kann D. A., Pignata G., Elliott J., Rossi A., Nardini M., Afonso P. M. J., Filgas R., Nicuesa Guelbenzu A., Schmidl S., Sudilovsky V.,
Multiwavelength analysis of three supernovae associated with gamma-ray bursts observed by GROND, Astronomy & Astrophysics, **577**, A44 (2015).

105. Arabsalmani M., Møller P., Fynbo J. P. U., Christensen L., Freudling W., Savaglio S., Zafa, T., *On the mass-metallicity relation, velocity dispersion, and gravitational well depth of GRB host galaxies*, Monthly Notices of the Royal Astronomical Society, **446**, 990 (2015).

106. Nigro G, Carbone V.,
Finite-time singularities and flow regularization in a hydromagnetic shell model at extreme magnetic Prandtl numbers,
New Journal of Physics, **17**, 073038 (2015).

107. Trotta R.M., Zimbardo G.,

A numerical study of Lévy random walks: Mean square displacement and power-law propagators,
Journal of Plasma Physics, DOI: http://dx.doi.org/10.1017/S0022377814000592, (2015).

108. Camporeale E., Zimbardo G.,
Wave-particle interactions with parallel whistler waves: Nonlinear and time-dependent effects revealed by particle-in-cell simulations,
Phys. Plasmas, **22**, 092104 (2015).

109. Nistico' G., Zimbardo G., Patsourakos S., Bothmer V., Nakariakov V. M.,
North-south asymmetry in the magnetic deflection of polar coronal hole jets,
Astron. & Astrophys., **583**, A127 (2015).

A.1.1 Publications on international journals printed in 2016

110. Catapano, F. Zimbardo G., Perri S., Greco A., Artemyev A.V.,
Proton and heavy ion acceleration by stochastic fluctuations in the Earth's magnetotail,
Ann. Geophys. **34**, 017-926 (2016).

111. Pezzi O., Camporeale E., Valentini F.,
Collisional effects on the numerical recurrence in Vlasov-Poisson simulations,
Physics of Plasmas **23**, 022103 (2016).

112. Pezzi O., Valentini F., Veltri P.,
Collisional relaxation of fine velocity structures in plasmas,
Physical Review Letters **116**, 145001 (2016).

113. Pucci F., Malara F., Perri S., Zimbardo G., Sorriso-Valvo L., Valentini F.,
Energetic particle transport in the presence of magnetic turbulence: influence of spectral extension and intermittency,
Monthly Notices of the Royal Astronomical Society **459**, 3395 (2016).

114. Leonardis E., Sorriso-Valvo L., Valentini F., Servidio S., Carbone F., Veltri P.,
*Erratum: ``Multifractal Scaling and Intermittency in Hybrid Vlasov-Maxwell Simulations of Plasma Turbulence' [Phys. Plasmas **23**, 022307 (2016)],*
Physics of Plasmas **23**, 059901 (2016).

115. Pucci F., Vasconez C. L., Pezzi O., Servidio S., Valentini F., Matthaeus W. H., Malara F.,
From Alfvén waves to kinetic Alfvén waves in an inhomogeneous equilibrium structure,
Journal of Geophysical Research – Space Physics **121**, 1024 (2016).

116. Leonardis E., Sorriso-Valvo L., Valentini F., Servidio S., Carbone F., Veltri P.,
Multifractal Scaling and Intermittency in Hybrid Vlasov-Maxwell Simulations of Plasma Turbulence,
Physics of Plasmas **23**, 022307 (2016).

117. Rincon F., Califano F., Schekochihin A., Valentini F.,
Turbulent dynamo in a collisionless plasma,

Proceedings of the National Academy of Sciences of the United States of America (PNAS) **114**, 3950 (2016).

118. Valentini F., Perrone D., Stabile S., Pezzi O., Servidio S., De Marco R., Marcucci F., Bruno R., Lavraud B., De Keyser J., Consolini G., Brienza D., Sorriso-Valvo L., Retinò A., Vaivads A., Salatti M.,Veltri P.,
Differential kinetic dynamics and heating of ions in the turbulent solar wind,
New Journal of Physics **18**, 125001 (2016).

119. De Marco R., Marcucci M. F., Bruno R., D'Amicis R., Servidio S., Valentini F., Lavraud B., Louarnc P., Salatti M.,
Importance of energy and angular resolutions in top-hat electrostatic analysers for solar wind proton measurements,
Journal of Instrumentation **11**, C08010 (2016).

120. Califano F., Manfredi G., Valentini F.,
Editorial - Special issue: The Vlasov equation, from space to laboratory plasmas,
Journal of Plasma Physics **82**, 701820603 (2016).

121. Vaivads A., Retinò A., Soucek J., Khotyaintsev Yu. V., Valentini F., Escoubet C. P., Alexandrova O., André M., Bale S. D., Balikhin M., Burgess D., Camporeale E., Caprioli D., Chen C. H. K., Clacey E., Cully C. M., De Keyser J., Eastwood J. P., Fazakerley A. N., Eriksson S., Goldstein M. L., Graham D. B., Haaland S., Hoshino M., Ji H., Karimabadi H., Kucharek H., Lavraud B., Marcucci F., Matthaeus W. H., Moore T. E., Nakamura R., Narita Y., Nemecek Z., Norgren C., Opgenoorth H., Palmroth M., Perrone D., Pinçon J.-L., Rathsman P., Rothkaehl H., Sahraoui F., Servidio S., Sorriso-Valvo L., Vainio R., Vörös Z., Wimmer-Schweingruber R. F.,
Turbulence Heating ObserveR – satellite mission proposal,
J. Plasma Phys. **82**, 905820501 (2016).

122. Malara F., Di Mare F., Nigro G. and Sorriso-Valvo L.,
Fast algorithm for a three-dimensional synthetic model of intermittent turbulence,
Phys. Rev. E **94**, 053109 (2016).

123. Servidio S., Haynes C. T., Matthaeus W. H., Burgess D., Carbone V., Veltri P.,
Explosive Particle Dispersion in Plasma Turbulence,
Physical Review Letters **117**, 095101 (2016).

124. Ferraro D., Servidio S., Carbone V., Dey S., Gaudio R.,
Turbulence laws in natural bed flows,
Journal of Fluid Mechanics **798**, 540 (2016).

125. Greco A., Perri S., Servidio S., Yordanova E., Veltri P.,
The complex structure of magnetic field discontinuities in the turbulent solar wind,
The Astrophysical Journal Letters **823**, L39 (2016).

126. Telloni D., Carbone V., Perri S., Bruno R., Lepreti F., Veltri P.,
Relaxation processes within flux ropes in solar wind,
The Astrophysical Journal **826**, 205 (2016).

127. Perri S., Amato E., Zimbardo G.,
Transport of relativistic electrons at shocks in shell-type supernova remnants: diffusive and superdiffusive regimes,
Astronomy and Astrophysics **596**, A34 (2016).

128. Alberti T., Piersanti M., Vecchio A., De Michelis P., Lepreti F., Carbone V., Primavera L.,
Identification of the different magnetic field contributions during a geomagnetic storm in magnetospheric and ground observations,
Annales Geophysicae **34** , 1069 (2016).

129. Alfonsi G., Ciliberti S. A., Mancini M., Primavera L.,
Direct Numerical Simulation of Turbulent Channel Flow on High-Performance GPU Computing System, COMPUTATION, Vol. **4**, N. 1 (2016).

130. Tanga M., Schady P., Gatto A., Greiner J., Krause M. G. H., Diehl R. Savaglio S., Walch S.,
Soft X-ray absorption excess in gamma-ray burst afterglow spectra: Absorption by turbulent ISM,
Astronomy & Astrophysics, **595**, A24 (2016).

131. Greiner J., Michałowski M. J., Klose S., Hunt L. K., Gentile G., Kamphuis P., Herrero-Illana R., Wieringa M., Krühler T., Schady P., Elliott J., Graham J. F., Ibar E., Knust F., Nicuesa Guelbenzu A., Palazzi E., Rossi A., Savaglio S.,
Probing dust-obscured star formation in the most massive gamma-ray burst host galaxies,
Astronomy & Astrophysics, **593**, A17 (2016).

132. Pongkitiwanichakul P., Nigro G., Cattaneo F., Tobias S.M.,
Shear-Driven Dynamo Waves in Fully Nonlinear Regime,
The Astrophysical Journal, **825**, Issue 1, 23 (2016).

133. Nigro G., Pongkitiwanichakul P., Cattaneo F., Tobias S.M.,
What is a large-scale dynamo?,
Monthly Notices of the Royal Astronomical Society Letters, **464**, L119-L123 (2016).

A.1.2 Publications on international journals accepted in 2016

1. Pezzi O., Parashar T. N., Servidio S., Valentini F., Vasconez C.L., Yang Y., Malara F., Matthaeus W.H., Veltri P.,
Revisiting a classic: the Parker-Moffatt problem,
to appear on The Astrophysical Journal (2017).

2. Pommois K., Valentini F., Pezzi O., Veltri P.,
Slow electrostatic fluctuations generated by beam-plasma interaction,
to appear on Physics of Plasmas (2017).

3. Valentini F., Vasconez C. L., Pezzi O., Servidio S., Malara F., Pucci F.,
Transition to kinetic turbulence at proton scales driven by large-amplitude kinetic Alfvén fluctuations,
to appear on Astronomy and Astrophysics (2017).

4. Sorriso-Valvo L., Carbone F., Leonardis E., Chen C. H., Safrankova J., Nemecek Z., *Multifractal analysis of high resolution solar wind proton density measurements*, to appear on Advances in Space Research (2017).

5. Gingell I., Sorriso-Valvo L., Burgess D., De Vita G: and Matteini L., T*hree-Dimensional Simulations of Sheared Current Sheets: Transition to Non-linear Regimes*, to appear on Journal of Plasma Physics (2017).

6. Pezzi O. Parashar T. N. , Servidio S., Valentini F., Vásconez C. L., Yang Y., Malara F., Matthaeus W. H., P. Veltri, *Colliding Alfvénic wave packets in MHD, Hall and kinetic simulations,* to appear on J. Plasma Phys. (2017).

7. Vecchio A., Lepreti F., Laurenza M., Alberti T., Carbone V., *Connection between solar activity cycles and grand minima generation,* to appear on Astronomy and Astrophysics (2017).

B. PUBLICATIONS ON CONFERENCE PROCEEDINGS

B.1 Publications on international conference proceedings in 2013

1. Perrone D., Valentini F., Servidio S., Dalena S., Veltri P., *Ion temperature anisotropy in the turbulent solar wind: Hybrid-Vlasov simulations,* 40th EPS Conference on Plasma Physics **1**, 121 (2013).

2. Donato S., Servidio S., Dmitruk P., Valentini F., Greco A., Veltri P., Wan M., Shay M. A., Cassak P. A., Matthaeus W. H., *Overview on numerical studies of reconnection and dissipation in the solar wind,* SOLAR WIND 13: Proceedings of the Thirteenth International Solar Wind Conference, AIP Conference Proceedings **1539**, 99 (2013).

3. Oughton S., Wan M., Matthaeus W. H., Servidio S., *Solar Wind Fluctuations and the von Kármán–Howarth Equations: The role of fourth-order correlations*, AIP Conference Proceedings **1539**, 251 (2013).

4. Romé M., Cavaliere F., Cavenago M., Ikram M., Lepreti F., Maero G., Paroli P., Pozzoli R., *Experimental and numerical investigation of non-neutral complex plasmas*,, NON-NEUTRAL PLASMA PHYSICS VIII: 10th International Workshop on Non-Neutral Plasmas, AIP Conference Proceedings **1521**, 273 (2013).

5. Romé M., Lepreti F., Maero G., Pozzoli R., Vecchio A., Carbone V., *Analysis of the two-dimensional turbulence in pure electron plasmas by means of advanced statistical techniques*, NON-NEUTRAL PLASMA PHYSICS VIII: 10th International Workshop on Non-Neutral Plasmas. AIP Conference Proceedings **1521**, 43 (2013).

6. Lepreti F., Maero G., Perrone D., Romé M., Capparelli V., Carbone V., Vecchio A., *Nonlinear dynamics of complex electron plasmas*, 40th EPS Conference on Plasma Physics **37D**, P5.302 (2013).

7. Maero G., Lepreti F., Paroli P., Perrone D., Pozzoli R., Romé M.,
Particle-In-Cell investigation of magnetized non-neutral dusty plasmas,
40th EPS Conference on Plasma Physics **37D**, P5.303 (2013).

8. Savaglio S.,
The Cosmic Evolution of Gamma-Ray Burst Host Galaxies,
Conference on Gamma-ray Bursts: 15 Years of GRB Afterglows, eds. A. J. Castro-Tirado, J. Gorosabel, and I. H. Park, EAS Publications Series, **61**, 381 (2013).

9. Savaglio S., Grothkopf U.,
Swift Publication Statistics and the Comparison with Other Major Observatories,
Conference on Gamma-ray Bursts: 15 Years of GRB Afterglows, eds. A. J. Castro-Tirado, J. Gorosabel, and I. H. Park, EAS Publications Series, **61**, 491 (2013).

10. Trotta E. M., Zimbardo G.,
Non diffusive propagation of solar energetic particles: data analysis and numerical simulations,
EAS Publications Series, **58**, 2013, 99-102 (2013).

B.1 Publications on international conference proceedings in 2014

11. Perrone D., Servidio S., Valentini F., Osman K.T., Alexandrova O., Califano F., Matthaeus W.H., Veltri P.,
Investigation of kinetic effects in turbulence using Vlasov simulations,
41st EPS Conference of Plasma Physics (2014).

B.1 Publications on international conference proceedings in 2015

12. Anderegg F., Affolter M., Ashourvan A., Dubin D. H. E., Valentini F., Driscoll C. F.,
Non-Linear Plasma Wave Decay to Longer Wavelength,
AIP Conference Proceedings **1668**, 020001 (2015).

13. Savaglio, S.,
Gamma-Ray Burst Host Galaxies,
Thirteenth Marcel Grossmann Meeting: On Recent Developments in Theoretical and Experimental General Relativity, Astrophysics and Relativistic Field Theories, 1794 (2015).

14. Savaglio S., Grothkopf U.,
Swift Publication Statistics and the Comparison with Other Major Observatories,
Open Science at the Frontiers of Librarianship, **492**, 133 (2015).

B.1 Publications on international conference proceedings in 2016

15. Telloni D., Perri S., Carbone V., Bruno R.,
Selective decay and dynamic alignment in the MHD turbulence: the role of the rugged invariants, Solar Wind 14: Proceedings of the Fourteenth International Solar Wind Conference. AIP Conference Proceedings **1720**, 040015 (2016).

16. Telloni D., Carbone V., Lepreti F., Antonucci E.,
Statistical properties of solar flares and coronal mass ejections through the solar cycle,

Solar Wind 14: Proceedings of the Fourteenth International Solar Wind Conference. AIP Conference Proceedings **1720**, 4943806 (2016).

D. INVITED PRESENTATIONS

D1. Invited presentations at international conferences in 2013

1. Giuseppina Nigro,
   Shell Models for Astrophysical Phenomena Descriptions,
   Nonlinear Waves and Chaos 9, San Diego, California (USA), 4-8 March 2013.

D1. Invited presentations at international conferences in 2014

2. Veltri P.,
   Kinetic effects in solar wind low frequency turbulence: Vlasov simulations vs Data analysis,
   Dynamical Processes in Space and Astrophysical Plasmas, Dead Sea (Israel) 16-22 March 2014

3. Sorriso-Valvo L.,
   Kinetic scale processes and dissipation in solar wind turbulence: a review,
   SHOCK Workshop on Heliospheric Plasma Kinetics: Simulations vs. Data, Firenze, 12-14/5/2014.

4. Valentini F.,
   How to measure particle velocity distribution in the solar wind,
   THOR Workshop #1: Exploring plasma energization in space turbulence, Paris, France, 9-19 October 2014.

5. Valentini F.,
   Vlasov Plasma Turbulence in the Solar Wind at Proton Kinetic Scales,
   American Geophysical Union Fall Meeting, San Francisco, California (USA), 15-20 December 2014.

6. G. Zimbardo, S. Perri,
   Cosmic Particle Acceleration,
   Symposium Plasma-Astrophysik, 78th Annual Conference of the Deutsche Physikalische Gesellschaft, Humboldt-Universitaet zu Berlin, Berlin, 17-21 March, 2014.

D1. Invited presentations at international conferences in 2015

7. L. Sorriso-Valvo,
   Self-consistent Castaing distribution of the inertial range turbulent fluctuations in the solar wind,
   International Conference on Turbulence and Dissipation in Collisionless Astrophysical Plasmas, Cargèse, France 21-25/9/2015.

8. Pezzi O.,
   Kinetic effects in Vlasov turbulent plasmas,
   Solar Heliospheric and Interplanetary Environment Conference (SHINE), Stowe, Vermont (US), 5-10 July 2015.

9. Valentini F.,
Numerical simulation support to the ESA/THOR mission,
12th International Symposium for Space Simulation (ISSS-12), Prague, Czech Republic, 6-10 July 2015.

10. Valentini F.,
Numerical simulation support to the ESA/THOR mission,
International Conference on Turbulence and dissipation in collisionless astrophysical plasmas, Cargèse, France 21-25/9/2015.

11. Servidio S.,
Magnetic reconnection and kinetic effects in Vlasov turbulence,
European Geosciences Union General Assembly (EGU) 2015, Vienna (Austria), 12-17 April 2015.

12. Servidio S.,
Magnetic Reconnection in Plasma Turbulence:from MHD to Vlasov Models,
Magnetic Reconnection in Plasmas, Stocholm (Sweden), 10-14 August 2015.

13. Greco A., Perri S., Servidio S.,
Characterization of magnetic discontinuities from MHD to subproton scales,
Magnetic Reconnection in Plasmas, Stocholm (Sweden), 10-14 August 2015.

14. Servidio S.,
Simulations for the physics of the Sun-Earth system,
"International School of Space Science", L'Aquila (Italy), 21-25 September 2015.

15. G. Zimbardo,
Particle Transport in the Heliosphere,
"International Space Science School (ISSS) dell'Aquila", Course on Heliospheric physical processes for understanding Solar-Terrestrial Relations, L'Aquila, (Italy) 21-26 September 2015.

D1. Invited presentations at international conferences in 2016

16. Servidio S.,
Vlasov simulations of plasma turbulence,
"5th VLASOVIA Conference", Copanello, Italy, May 30 - June 2 2016.

17. Servidio S.,
Vlasov turbulence in the solar wind,
"THOR Workshop #2: Exploring plasma energization in space turbulence", University of Barcelona, Barcelona (Spain), 27-29 September 2016.

18. Valentini F.,
Kinetic physics at ion scales in the solar wind: Numerical support to the ESA/THOR mission,
International Max-Planck-Princeton Centre for plasma physics workshop, Berlin, Germany, 12-15 January 2016.

19. Alberti T.,

Natural periodicities and Northern Hemisphere.Southern Hemisphere connection of fast temperature changes during the last glacial period: EPICA and NGRIP revisited,
European Geosciences Union General Assembly 2016, Vienna (Austria), April 17-22, 2016.

20. G. Zimbardo,
Superdiffusive transport in space and astrophysical plasmas: theory and observations,
workshop on Cosmic rays, astrophysical turbulence and magnetic reconnection,
International Institute of Physics, Natal (Brazil), December 5-9, 2016.

21. P. Veltri,
Electrostatic Turbulence generated by Solar Wind nonlinear Energy Cascade,
Vlasovia 2016, Copanello (Italy) May 30 - June 2, 2016.

D2. Invited presentations at national conferences in 2015

1. Valentini F.,
L'esplorazione del Sistema Solare: la missione spaziale THOR,
Reggio Scienza – XXV Settimana Nazionale della Cultura Scientifica e Tecnologica, Planetario Astronomico Pythagoras, Reggio Calabria, Italy, 12-18 October 2015.

2. Valentini F.,
Il 5 e la Luce: un excursus scientifico sulle più significative scoperte sulla luce che vennero realizzate in anni che terminano con il numero 5,
Reggio Scienza – XXV Settimana Nazionale della Cultura Scientifica e Tecnologica, Liceo Scientifico "Leonardo da Vinci", Reggio Calabria, Italy, 12-18 October 2015.

D2. Invited presentations at national conferences in 2016

3. L. Sorriso-Valvo,
Turbulence in the solar wind: an observational perspective,
SOHE Meeting, Roma, Italy, 30/05-01/06 2016.

4. Lepreti F.,
Dynamics and diffusion of small scale magnetic elements in the lower solar atmosphere,
"2016 Meeting of the Italian Solar and Heliospheric community", Roma (Italy), May 30 - June 1, 2016.

5. Pezzi O.,
Da Vincenzo Ferraro ai giorni nostri: un viaggio nella complessità (e nella bellezza) della fisica dello spazio,
Premio SIF Vincenzo Ferraro "Una vita per la scienza" VI Edizione, Sorrento (Italy) October 8, 2016.

6. Veltri P.,
Plasma turbulence: a beautiful and complex mathematical problem with a wide spectrum of physical applications,
SIF 102° Congresso Nazionale, Padova, September 26-30, 2016.

7. P. Veltri,

Kinetic effects in solar-wind low-frequency turbulence: Vlasov simulations vs Data analysis, SIF 100° Congresso Nazionale, Pisa, September 22-26, 2016.

E PRESENTATIONS AT CONFERENCES

E1. Presentations at international conferences in 2013

1. Lepreti F., Maero G., Perrone D., Romé M., Capparelli V., Carbone V., Vecchio A., *Nonlinear dynamics of complex electron plasmas*, 40th EPS Conference on Plasma Physics, Espoo (Finland), July 1-5, 2013.

2. Maero G., Lepreti F., Paroli P., Perrone D., Pozzoli R., Romé M., *Particle-In-Cell investigation of magnetized non-neutral dusty plasmas*, 40th EPS Conference on Plasma Physics, Espoo (Finland), July 1-5, 2013.

3. Valentini F., *Kinetic effects in the turbulent solar wind: capturing ion physics with a Vlasov code*, VLASOVIA 2013 - Fourth International Workshop on the theory and Applications of the Vlasov Equation, Nancy (France) 25-28 November 2013.

4. Pezzi O., *Numerical approach to collisional plasmas: collisional effects on electrostatic plasma waves*, Fourth International Workshop on the Theory and Applications of the Vlasov equation (VLASOVIA 2013), Nancy (France), 25-28 November 2013.

5. Chargazia Kh., Zimbardo G., Kharshiladze O., *On the detection of a vortex chain in the Earth's magnetotail,* European Geosciences Union general assembly, Vienna (Austria), 7-12 April, 2013.

6. Zimbardo G., Dolgonosov M., Perri S., Greco A., *On the generation of ion beamlets in the magnetotail: resonant acceleration versus stochastic acceleration,* European Geosciences Union general assembly, Vienna (Austria), 7-12 April, 2013.

E1. Presentations at international conferences in 2014

7. Valentini F., *Electrostatic signals in the solar wind: the link between macroscopic (Alfvénic) and microscopic (electrostatic) scales*, Arcetri 2014 International Workshop on Plasma Astrophysics, Arcetri (Italy), 27-30 October 2014.

8. Greco A., *Magnetic discontinuities from MHD to subproton scales: their role in space plasma physics*, Arcetri 2014 International Workshop on Plasma Astrophysics, Arcetri (Italy), 27-30 October 2014.

9. Alberti T., Lepreti F., Vecchio A., Carbone V., De Lauretis M., Francia P., Regi M., Villante U., Berrilli F., Bruno R., Consolini G., Del Moro D., Ermolli I., Fineschi S., Landi Degl'Innocenti E., Laurenza M., Marcucci M.F., Pallocchia G., Piersanti M., Pietropaolo E., Romano P., Romoli M., Vellante M., Zuccarello F.,

The main Periodicities of the ULF Geomagnetic Power and their Relationship with the Solar wind and Magnetospheric Electron Fluxes,
"11th of the European Space Weather Week", Liege (Belgium), November 17-21 2014.

10. Malara F.,
A fast algorithm for a synthetic turbulence model ,
Arcetri 2014 International Workshop on Plasma Astrophysics, Arcetri (Italy), 27-30 October 2014.

11. Pezzi O.,
Collisional relaxation: Landau versus Dougherty operator,
Arcetri 2014 International Workshop on Plasma Astrophysics, Florence, (Italy), 27-30 October 2014.

12. Pezzi O.,
Collisional effects on ion-acoustic solitary waves propagation,
International Conference on Plasma Physics (ICPP), Lisbon (Portugal), 15-19 September 2014.

E1. Presentations at international conferences in 2015

13. Greco A.,
The Complex Structure of Magnetic Field Discontinuities in the Turbulent Solar Wind,
Arcetri 2015 International Workshop on Plasma Astrophysics, Arcetri (Italy), 9-12 November 2015.

14. Servidio S.,
Double Averaging Method and Turbulence Statistics for a Rough-Bed Flow,
International conference on turbulence and interactions in Marine Systems "TURBINTERMARS", Trieste (Italy), 23-25 February, 2015.

15. Alberti T., Lepreti F., Vecchio A., Bevacqua E., Capparelli V., Carbone V.,
Natural periodicities and Northern Hemisphere - Southern Hemisphere connection of fast temperature changes during the last glacial period: EPICA and NGRIP revisited,
European Geosciences Union General Assembly 2015, Vienna (Austria), April 12-17, 2015.

16. Alberti T., Primavera L., Lepreti F., Vecchio A., Carbone V.,
Pattern formation throught spatial interactions in a modified Daisyworld model,
European Geosciences Union General Assembly 2015, Vienna (Austria), April 12-17, 2015.

17. Alberti T., Piersanti M., Vecchio A., Lepreti F., Carbone V., Villante U., Francia P., De Lauretis M., Regi M.,
The main periodicities of the geomagnetic Pc5 wave power and their relationship with solar wind flow pressure and electron flux,
European Geosciences Union General Assembly 2015, Vienna (Austria), April 12-17, 2015.

18. Alberti T., Lepreti F., Vecchio A., Bevacqua E., Capparelli V., Carbone V.,
Natural periodicities and Northern-Hemisphere – Southern-Hemisphere connection of temperature changes during the last glacial period: EDML and NGRIP revisited,
"26th General Assembly of the International Union of Geodesy and Geophysics (IUGG)", Prague (Czech Republic), June 23-28, 2015.

19. Piersanti M., Alberti T., Lepreti F., Vecchio A., Villante U., Carbone V.,
The modulated baseline and anomalies of geomagnetic field during geomagnetic storms,
"26th General Assembly of the International Union of Geodesy and Geophysics (IUGG)",
Prague (Czech Republic), June 23-28, 2015.

20. Alberti T., Piersanti M., Lepreti F., Vecchio A., Carbone V., Villante U., Francia P., De Lauretis M., Regi M.,
The main periodicities of the geomagnetic pc5 wave power and relationship with solar wind dynamic pressure,magnetospheric field and electron fluxes,
"26th General Assembly of the International Union of Geodesy and Geophysics (IUGG)",
Prague (Czech Republic), June 23-28, 2015.

21. Servidio S.,
Kinetic effects in the turbulent solar wind: Vlasov simulations and observations,
"First Joint Solar Probe Plus-Solar Orbiter Workshop", Florence, Italy, 2-4 September, 2015.

22. Alberti T., Piersanti M., Lepreti F., Vecchio A., Villante U., Carbone V.,
Identification of the different magnetic field contributions during a geomagnetic storm in magnetosphere and at ground,
International School of Space Science, L'Aquila (Italy), September 21-26, 2015.

23. Perri S.,
Evidence for Superdiffusive shock acceleration at interplanetary shock waves,
14th Annual International Astrophysics Conference, Tampa Bay, (USA), April 20, 2015.

24. Perri S.,
Superdiffusive Shock Acceleration at Interplanetary Shock Waves: Exploring the Heliosphere,
First joint Solar Probe Plus- Solar Orbiter workshop, Artimino (Italy), September 2-4, 2015.

25. Malara F.,
Generation of Kinetic Alfvén Waves during phase-mixing of large-scale Alfvén waves,
First joint Solar Probe Plus- Solar Orbiter workshop, Artimino (Italy), September 2-4, 2015.

26. Valentini F.,
Turbulent heating and dissipation of the solar-wind plasma: Vlasov simulations at proton kinetic scales,
Complex Plasma Phenomena in the Laboratory and in the Universe, Accademia Nazionale dei Lincei, Roma. Italy, 19-20 January 2015.

27. Pezzi O.,
Collisions of two Alfvénic wave packets in a kinetic plasma,
Arcetri 2015 International Workshop on Plasma Astrophysics, Florence, Italy, 9-12 November 2015.

E1. Presentations at international conferences in 2016

28. Valentini F.,
Numerical simulation support to the ESA/THOR mission,

American Geophysical Union Fall Meeting, San Francisco, California (USA), 12-16 December 2016.

29. Valentini F.,
Numerical simulation support to the ESA/THOR Mission,
THOR Workshop #2: Exploring plasma energization in space turbulence, Barcelona, Spain, 27-29 September 2016.

30. Alberti T., Laurenza M., Storini M., Lepreti F., Cliver E.W.,
Characterization of X-ray and Type III radio bursts during solar cycle 24 for short-term warning of solar energetic particle events,
European Geosciences Union General Assembly 2016, Vienna (Austria), April 17-22, 2016.

31. Alberti T., Lepreti F., Vecchio A., Carbone V.,
Paleoclimate changes: a stochastic resonance model based on ice-core data analysis,
European Geosciences Union General Assembly 2016, Vienna (Austria), April 17-22, 2016.

32. Alberti T., Consolini G., Lepreti F., Vecchio A., Carbone V.,
A statistical study on the timescales involved into the solar wind-magnetosphere interaction during the March 17, 2015 storm,
European Geosciences Union General Assembly 2016, Vienna (Austria), April 17-22, 2016.

33. Alberti T., Lepreti F., Vecchio A., Carbone V.,
The response of the ozone layer to the solar UV input: analysis of nonlinear trends,
European Geosciences Union General Assembly 2016, Vienna (Austria), April 17-22, 2016.

34. Alberti T., Piersanti M., Lepreti F., Vecchio A., de Michelis P., Villante U., Carbone V.,
The latitudinal distribution of the baseline geomagnetic field during the March 17, 2015 geomagnetic storm,
European Geosciences Union General Assembly 2016, Vienna (Austria), April 17-22, 2016.

35. Greco A., Artemyev A., Zimbardo G.,
Heavy Ion Acceleration at Jet Fronts,
European Geosciences Union General Assembly 2010, Vienna (Austria), April 17-22, 2016.

36. Greco A., Perri S., Servidio S., Yordanova, E., P. Veltri,
The Complex Structure of Magnetic Field Discontinuities in the Turbulent Solar Wind,
European Geosciences Union General Assembly 2010, Vienna (Austria), April 17-22, 2016.

37. Alberti T., Consolini G., Lepreti F., Laurenza M., Vecchio A., Carbone V.,
A statistical study on the timescales involved into the solar wind-magnetosphere interaction during the March 17, 2015 storm,
International School of Space Science, L'Aquila (Italy), June 6-10, 2016.

38. Greco A.,
PVI (Partial Variance of Increments) method in solar wind observations and plasma simulations,
2016 Arcetri International Workshop on Plasma Astrophysics, Arcetri (Italy), October 17-20, 2016.

39. Malara F.,

Diffusion of energetic protons in MHD turbulence; effects of spectral width, fluctuation amplitude and intermittency,
Arcetri 2016 International Workshop on Plasma Astrophysics, Arcetri (Italy), October 17-20, 2016.

40. Perri S.,
Estimation of the current density via single and multi-spacecraft analysis and study of the validity of the Taylor hypothesis,
THOR Workshop #2, Barcelona, Spain, 27-29 September 2016.

41. Pezzi O.,
Alfvénic wave packet collisions in a kinetic plasma,
Arcetri 2016 International Workshop on Plasma Astrophysics, Florence (Italy), 17-20 October 2016.

42. Pezzi O.,
Collisions of two Alfvénic wave packets: beyond the Moffatt-Parker problem,
Fifth International Workshop on the Theory and Applications of the Vlasov equation (VLASOVIA 2016), Copanello, (Italy), May 30 - June 2, 2016.

43. Pezzi O.,
Fine velocity structures collisional dissipation in plasmas,
EGU 2016, Vienna (Austria) 17-22 April 2016.

E1. Presentations at national conferences in 2013

1. Malara F.,
Turbulence and kinetic effects in heliospheric plasmas,
"2013 Meeting of the Italian Community in Solar and Heliospheric Physics", Catania (Italy), September 4-6, 2013.

2. Lepreti F., Carbone V., Abramenko V.I., Yurchyshyn V., Goode P.R., Capparelli V., Vecchio A.,
Turbulent Diffusion and Pair Dispersion of Photospheric Bright Points,
"2013 Meeting of the Italian Community in Solar and Heliospheric Physics", Catania (Italy), September 4-6 2013.

3. Maero G., Lepreti F., Paroli B., Perrone D., PozzolI R., Romé M., Capparelli V., Carbone V., Vecchio A.,
Numerical simulations of magnetized non-neutral complex plasmas,
"Italian National Conference on Condensed Matter Physics (FisMat2013)", Milano (Italy), September 9-13 2013.

4. Romé M., Cavaliere F., Cavenago M., Ikram M., Lepreti F., Maero G., Paroli B., Pozzoli R.,
Investigation of non-neutral complex plasmas,
"Italian National Conference on Condensed Matter Physics (FisMat2013)", Milano (Italy), September 9-13 2013.

5. G. Zimbardo,
Superdiffusive transport in space and laboratory plasmas,

FisMat2013, Italian National Conference on Condensed Matter Physics, Milano, 09-13 September 2013.

6. G. Zimbardo, Dolgonosov, M., Perri, S., Greco, A.,
Ion beamlets in the plasma sheet boundary layer of the Earth's magnetotail: resonant acceleration versus stochastic acceleration,
FisMat2013, Italian National Conference on Condensed Matter Physics, Milano, 09-13 September 2013.

E1. Presentations at national conferences in 2016

7. Alberti T., Consolini G., Lepreti F., Laurenza M., Vecchio A., Carbone V.,
A statistical study on the timescales involved into the solar wind-magnetosphere interaction during the March 17, 2015 storm,
2016 Meeting of the Italian Solar and Heliospheric community, Roma (Italy), May 30 – June 1, 2016.

8. Alberti T., Laurenza M., Storini M., Consolini G., Lepreti F., Cliver E.W.,
Characterization of X-ray and Type III radio bursts during solar cycle 24 for short-term warning of solar energetic particle events,
2016 Meeting of the Italian Solar and Heliospheric community, Roma (Italy), May 30 – June 1, 2016.

9. Alberti T., Piersanti M., Lepreti F., Vecchio A., De Michelis P., Villante U., Carbone V.,
The latitudinal distribution of the baseline geomagnetic field during the March 17, 2015 geomagnetic storm, 102° Congresso Nazionale Società Italiana di Fisica, Padova (Italy), September 26-30, 2016.

10. Alberti T., Consolini G., Lepreti F., Laurenza M., Vecchio A., Carbone V.,
A statistical study on the timescales involved into the solar wind-magnetosphere interaction during the March 17, 2015 storm,
102° Congresso Nazionale Società Italiana di Fisica, Padova (Italy), September 26-30, 2016.

11. Pezzi O.,
Collisional relaxation of fine velocity structures in plasmas,
102° Congresso Nazionale Società Italiana di Fisica, Padova (Italy), September 26-30, 2016.

2. BIOMEDICAL PHYSICS

Professors and researchers: L. Sportelli *(Molecular Biophysics Group, University of Calabria)*
A. Santaniello (*Biomedical Physics, University of Calabria)*

Collaborators: E. Marsich *(Life Science Department, University of Trieste)*
L. Strigari *(Laboratory of Medical Physics and Expert Systems, Regina Elena National Cancer Institute, Roma)*
C. Pace *(NexusLab, DIMES, University of Calabria)*
I. Løvik, M. Licandro, G. Scalzo, C. Scalzo *(Pugliese- Ciaccio Hospital, AO-CZ Italy)*
E. Pikhay, Y. Nemirovsky, Y. Roizin *(Technion, IIT, Haifa, Israel,*
and TowerJazz, Migdal Haemek, Israel).

Research subjects:
2.1. Study of radiation effects in biomolecules of dosimetric interest by EPR
2.2. Dosimetry with innovative materials
2.3. Dosimetric characterisation of radiation beams and sensor devices

Introduction

Physical Dosimetry has to face the challenges of innovative radiotherapeutic methods. These include, besides innovative conformal radiotherapy with megavoltage beams (tomotherapy, intensity modulated radiotherapy), the novel applications of kilovoltage beams based on brilliant synchrotron radiation (microbeam radiation therapy, synchrotron stereotactic radiotherapy). The new methods, by spatially or energy modulating the beam intensity, or by reducing beam size and increasing beam intensity, deliver a higher therapeutic dose to the tumor while sparing the surrounding healthy tissues. This, at the same time, improves tumor control and reduces toxicity, thus limiting tumor recurrence and improving quality of life of the patient. In order to obtain an effective treatment, it is crucial to match the accurate positioning of the patient, nowadays improved by radiological, image-controlled specialized software, to dose determinations affording lower detection limit, higher dynamic range and better spatial resolution. This carries on the need of improved or new dosimetric materials and approaches.

2.1 . STUDY OF RADIATION EFFECTS IN BIOMOLECULES OF DOSIMETRIC INTEREST

2.1.1 New materials: HAp-Alginate

Hydroxyapatite alginate (HApA) is a low-density, biocompatible composite material of recent synthesis. It was studied because of possible applications for osteoimplants. We investigated the radiation-induced effects in samples of different density. We showed the presence of stable radioinduced radicals of interest for medical Dosimetry (radiation doses below 100 Gy). Figure 1 shows typical HApA scaffolds and the porous microstructure of HApA.

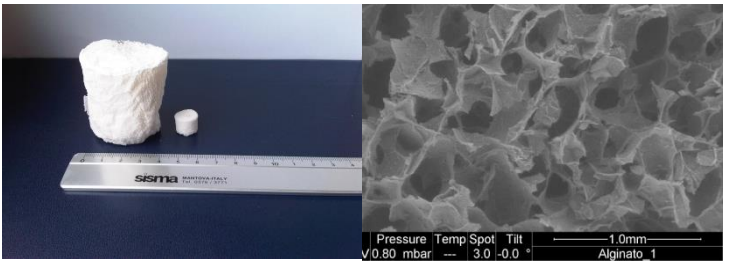

Fig. 1 Photo of the HApA scaffolds and SEM image of the porous microstructure.

The use of HAp-Alginate for EPR dosimetry was patented, in collaboration with Dr. E. Marsich of the Life Science Department of the University of Trieste (ITUB20150449, 23.02.2015). European Patent extension has been applied.

2.1.1 Modified materials: Li-formate doped with metal impurities

Li formate ($HCO_2Li{\cdot}H_2O$) is an innovative electron paramagnetic resonance (EPR) radiosensitive material which, unlike conventional EPR materials like alanine, allows the measurement of the small fractionated dose values delivered in a radiotherapeutic treatment (of the order of a few Gy) with the low uncertanties required by medical protocols (within 5%). Doping with metal impurities is intended to extend the measuring interval towards the lower dose levels delivered in Radiology. However, ambient humidity affects the intensity of the EPR signal. We studied the dosimetric behaviour of pure and Zn- and Cd-doped Li-formate powders kept at selected equilibrium values of the relative humidity Hr in the interval Hr = 33% to 75%. The study indicates that the EPR signal depends on the value of both Hr and doping concentration. We relate the observed effects to the presence of absorbed water at the grain surfaces of the LiFo powder, which is favoured by the addition of metal impurities upon doping. The EPR signal is depressed by water induced dielectric loss within the EPR cavity.

2.2 DOSIMETRY WITH INNOVATIVE MATERIALS

2.2.1 Characterisation of the dosimetric behaviour of new EPR-sensitive materials

Li formate dosimeter pellets (0.1 cm^3) prepared by using an ordinary mechanical press (die size of the order of 1 cm) without binding material are used for the purpose of the dose determination during irradiation sessions of samples of various interest at the Molecular Biophysics Laboratory. Irradiation is performed in-house with kilovoltage beams from the X-ray irradiator Faxitron RX-650. The Li formate pellet dosimeters are point calibrated by comparison with the dose response curve which was obtained for a set of dosimers irradiated with clinical megavoltage beams (6 MeV). The calibration procedure was performed in the dose interval 0.5-80 Gy as measured by ionimetry (Farmer-type ionization chamber Scdx-Wellhöfer FC65-P), with 6 MV and 18 MV photons from a linear accelerator (Elekta Sli-Plus, Pugliese-Ciaccio Hospital of CZ, Italy) in reference conditions in a water equivalent slab phantom (IAEA TRS 398 protocol). At least three pellets were irradiated in identical conditions at each dose value. A total of 54 dosimeters was exposed in the interval 0.5-10 Gy. The value of the standard deviation of the distribution of the relative EPR dosimeter readings per dose (3-4%) was comparable to literature results obtained for similar beam energy and dose intervals. The dose detection limit was 0.5 Gy. The results have been presented at the VIII National Meeting of the Italian Association of Medical Physics.

2.2.2 Study of the dosimetric response of EBT3 gafchromic films at kilovoltage energies

The present space resolution of EPR dosimetry with the salts of the formic acid (formates) is, by EPR Imaging (EPRI), of the order of a few tenths of mm. Our conventional EPR spectrometer allows, instead, a space resolution of the order of a few mm, linear size, by using pellet Li-formate

dosimeters. Gafchromic films, offering superior space resolution (0.1 mm), are used to determine beam profiles and doses at megavoltage energies. However, since the energy response of gafchromic films is not flat, the determination of the dose requires correction factors which depend on the gafchromic film type, and may be particularly large at kilovoltage energies. More important, the energy response is batch dependent, which implies that correction factors have to be determined for each film batch. We studied by EPR dosimetry the energy response of EBT3 films which, according to the manufacturer, present improved features. Li formate correction factors are well known and weakly dependent on energy (less than 10% within the full energy range of medical interest). The EBT3 films, calibrated at 6 MeV (Ospedale Regina Elena, Roma), were irradiated with 70 and 100 kVp photon beams from the Faxitron RX-650 irradiator of the Molecular Biophysics Laboratory. The dose values, as determined by the film dosimeter and the EPR pellet, coincide within the experimental error at 100 kVp, while the gafchromic film overestimates the dose by more than 20% at 70 kVp (see Figure 2).

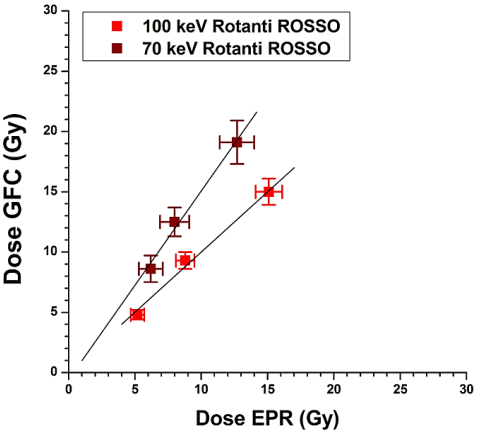

Fig. 2 Absorbed dose, as determined by gafchromic film dosimetry, as a function of the point calibrated dose obtained by EPR dosimetry, showing dose overestimation at lower energies (70 kVp).

2.3 DOSIMETRIC CHARACTERISATION OF RADIATION BEAMS AND SENSOR DEVICES

2.3.1 Beam profiles and doses from kilovoltage beams

We used EPR Li-formate pellet and gafchromic film dosimetry to determine the beam profiles and doses of the Faxitron RX-650 irradiator present in our laboratory. The technical sheets of the irradiator only include exposure rates, and values of the beam size as a function of the source-sample distance. We measured almost flat beam profiles, with small peaks in the central region, which we related to secondary electron scattering from high-Z metallic parts (screws and rotating shaft) of the sample holder, which are directly exposed to the beam. Dose differences are within a few %. The results have been presented at the IX National Meeting of the Italian Association of Medical Physics.

2.3.2 Determination of the dose delivered to radiation sensor devices

The reduced size of Li-formate dosimeters, the absence of cables and housings, their dose integrating character and weak photon energy dependence make pellet EPR dosimetry well-suited to the determination of the radiation dose for the calibration of sensor devices. We studied by EPR pellet dosimetry the energy and dose response of TowerJazz C-Flash based FG single sensors and array-

type devices exposed to X-ray radiation of different energy (from 40 to 130kVp) in a dose interval of therapeutic interest (1-50 Gy), with high accuracy (a few %). CMOS sensors based on the discharge of the floating gate structure allow building compact and low-cost dosimeters, implemented in standard VLSI technologies. Previous studies on FG-sensors were carried out at 6 MeV. The dependence of the FG sensors response on beam quality, which is a significant issue in medical dosimetry where total dose uncertainties as low as a few % are required, is determined by comparing to that of the LiFo dosimeters, which is well known and weakly modulated over a wide interval of beam qualities. We demonstrated higher sensitivity of the FG sensors to X-rays in the superficial and orthovoltage ranges compared with the previous data obtained for irradiation at 6 MeV. A linear dose response of about 0.5 V/Gy was observed up to about 4 Gy. No remarkable energy dependence of the C-sensor response was registered.

PUBLICATIONS and PRESENTATIONS

Patents

A. Santaniello, E. Marsich, L. Sportelli, Patent ITUB20150449, 23.02.2015.
A. Santaniello, E. Marsich, L. Sportelli, European patent extension in progress.

Meeting contributions

A. Santaniello, F.V. Quaranta, L. Strigari, L. Sportelli, *Dose profiles of low energy beams for dosimeter calibration,* IX National Meeting of the Italian Association of Medical Physics, February 25-28, 2016, Perugia-Italy.

A. Santaniello, I. Løvik, L. Sportelli, M. Licandro, G. Scalzo, C. Scalzo, *Medical EPR dosimetry at low doses,* VIII National Meeting of the Italian Association of Medical Physics, November 16-19, 2013, Turin-Italy.

Submitted papers

31. E. Pikhay, C. Pace, A. Santaniello, L. Sportelli, Y. Nemirovsky, Y. Roizin, *Calibration of floating gate X-ray radiation sensors using LiFo electron paramagnetic resonance dosimeters*, Physics in Medicine and Biology, 2016.
32. A. Santaniello, E. Marsich, L. Sportelli, *A novel low-density Electron Paramagnetic Resonance dosimetric material*, Radiation Research, 2016.

3. ELECTRON SPECTROSCOPIES OF TWO-DIMENSIONAL MATERIALS

Professor	Gennaro Chiarello
Post-doc fellow	Antonio Politano
Technicians	Vito Fabio
	Eugenio Li Preti
Collaborators	D. Farías (*Universidad Autonoma de Madrid, Spain)*
	D. Boukhvalov (*Hanyang University, Seoul, South Korea*)
	M. S. Vitiello (*Scuola Normale Superiore, Pisa*)
	R. Larciprete (*CNR-ISC, Roma*)
	D. Campi (*EPFL, Lausanne, Switzerland*)
	G. Nicotra (*CNR-IMM, Catania*)
	H. A. Arafat (*Masdar Center, Abu Dhabi, United Arab Emirates*)
	R. Roldan (*CSIC-ICMM, Madrid, Spain*)
	S. Yuan, M. I. Katsnelson (*Radboud University, Nijmegen, the Netherland*)
	E. Drioli (*CNR-ITM, Rende*)
	G. Granozzi (*University of Padova*)
	Z. Mišković (*University of Waterloo, Canada*)
	D. Borka, I. Radović (*VINCA Institute, Belgrade, Serbia*)
	G. Liu, A. Balandin (*University of California, Riverside, USA*)
	E.V. Chulkov (*Donostia International Physics Center, San Sebastian, Spain*)
	Z. Aliev (*ANAS, Baku, Azerbaijan*)
	V. Pellegrini (*Graphene Labs, Italian Institute of Technology, Genova*)
	S. Jaziri (*Université de Carthage, Tunisia*)
	S. Duman (*Atatürk University, Erzurum,Turkey*)

Introduction

Our research focuses on the synthesis, modification (by means of functionalization, intercalation and adsorption of chemical species), characterization and technological exploitation of innovative nanomaterials. We study (i) nanomaterials as graphene and materials beyond graphene (phosphorene, indium selenide, tin selenide) and (ii) the novel topological phases of matter (topological insulators and Dirac/Weyl semimetals) by means of different spectroscopic and microscopic tools. We are interested in fundamental properties (plasmons, phonons, elasticity, chemical reactivity, band structure, geometric structure) of these materials, as well as to their potential applications in the fields of nano-plasmonics, photodetection of Terahertz light, energy storage and production, and, moreover, membrane technology for seawater desalination.

Our research activities are quite broad and interdisciplinary. In order to address the various research lines, we have activated different collaborations with researchers and industries from different countries.

Our group has reached in 2015-2016 a leading position at international scale in surface science with two-dimensional materials and with the novel topological phases of matter, as certified by a large number of publications on top journals (*Advanced Materials, Nano Letters*, *Physical Review Letters*, *ACS Nano*, *Nano Research*, *2D Materials*, *Nanoscale*), invited talks at international conferences and the invitation to take part to the Italian delegation in formal meetings organized by Ministry of Foreign Affairs with delegations from both China and South Korea. In the latter case, we have

organized with the Embassy of Italy in Seoul the first meeting on science and technology of two-dimensional materials between Italian and Korean scientists and technologists.
Our leading position is confirmed by the numerous invitations to write review or Perspective papers on different topics: surface chemistry with alkali metals (*Surface Science Reports*), physical chemistry of 2D materials (*Flatchem*), quantum size effects and electron confinement (*Progress in Surface Science*), energy-filtered transmission electron microscopy on 2D semiconductors (*Materials Science in Semiconductor Processing*), lattice dynamics and electron-phonon in graphene (*Critical Reviews in Solid State and Materials Science*), plasmonics with graphene (*Nanoscale* and *New Journal of Physics*), plasma-wave Terahertz photodetection with topological insulators and phosphorene (*APL Materials*), thermoplasmonics (*Journal of Physics: Condensed Matter*) and, moreover, recent invitations for activities in photothermal membrane distillation (*Desalination*) and the applications of nanocomposites with 2D materials in membrane technology (*Current Opinion in Chemical Engineering*). The productivity of our group is growing each year and we are expected to consolidate our results in next years, with novel investigations on fundamental properties and applications of novel materials.
RESEARCH SUBJECTS:

1. *SPATIALLY-RESOLVED ELECTRON ENERGY LOSS SPECTROSCOPY WITH TRANSMISSION ELECTRON MICROSCOPY (EELS-TEM): APPLICATION TO TWO-DIMENSIONAL MATERIALS*
2. *SCANNING TUNNELING MICROSCOPY (STM) OF GRAPHENE/METAL INTERFACES AND TOPOLOGICAL INSULATORS*
3. *REAL-TIME GROWTH OF GRAPHENE ON COPPER FOILS, NICKEL AND METAL ALLOYS*
4. *HYDROGEN STORAGE AND PRODUCTION WITH GRAPHENE-BASED MATERIALS*
5. *SURFACE CHEMISTRY WITH GRAPHENE/METAL INTERFACES AND BIMETALLIC SURFACES*
6. *ELECTRON CONFINEMENT AND QUANTUM SIZE EFFECTS IN NOBLE-METAL FILMS*
7. *PHYSICOCHEMICAL INVESTIGATIONS ON ACTIVE CHANNELS OF FIELD-EFFECT TRANSISTORS BASED ON TOPOLOGICAL INSULATORS AND OTHER MATERIALS BEYOND GRAPHENE*
8. *PLASMON MODES AT GRAPHENE/METAL CONTACTS*
9. *PLASMONIC EXCITATIONS IN TOPOLOGICAL INSULATORS*
10. *LATTICE DYNAMICS AND ELECTRON-PHONON COUPLING IN GRAPHENE METAL/INTERFACES*
11. *ELASTIC PROPERTIES OF TWO-DIMENSIONAL MATERIALS AND TOPOLOGICAL PHASES OF MATTER*
12. *PLASMA-WAVE TERAHERTZ PHOTODETECTION WITH NANODEVICES BASED ON TOPOLOGICAL INSULATORS, BLACK PHOSPHORUS AND TWO-DIMENSIONAL HETEROSTRUCTURES*
13. *APPLICATIONS OF THERMOPLASMONICS IN MEMBRANE TECHNOLOGY FOR SEAWATER DESALINATION*

In the following, we will mention the most important milestones of our scientific production.

1. SPATIALLY-RESOLVED ELECTRON ENERGY LOSS SPECTROSCOPY WITH TRANSMISSION ELECTRON MICROSCOPY (EELS-TEM): APPLICATION TO TWO-DIMENSIONAL MATERIALS

We have carried out experiments at Beyond Nano Laboratory of the CNR-IMM Institute in Catania. We imaged for the first time the anisotropic lattice of phosphorene (monolayer of black phosphorus) with sub-Å resolution. Moreover, we were able to probe the anisotropy in the plasmon dispersion. Thus, we introduced the concept of nanoplasmonics through EELS-TEM experiments for the first time.

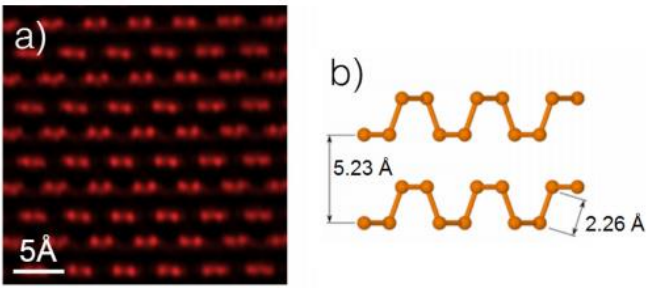

(a) Cross-sectional view (HAADF-STEM image) of bulk black phosphorus, in which, as shown in panel (b), P atoms are arranged in puckered honeycomb layers, bound together by Van der Waals forces

Moreover, we have studied the excited states of black phosphorus through the analysis of *K* and *L* absorption edges of black phosphorus with energy-filtered TEM. Energy-loss spectra exhibit several peaks reflecting features in the density of conduction-band states at corresponding energies above the vacuum level. We have reproduced the experimental electron energy-loss near-edge structures by means of ab initio self-consistent real-space multiple-scattering theory.

2. SCANNING TUNNELING MICROSCOPY OF GRAPHENE/METAL INTERFACES AND TOPOLOGICAL INSULATORS

We have used the scanning tunneling microscope (STM) at the CNR-ISM institute in Rome to study the morphological changes occurring during the implantation of argon in graphene/metal interfaces [Nano Letters 16 (2016) 1808]. The nanoblisters contain Ar aggregates compressed at high pressure arranged below the graphene monolayer skin, that is decoupled from the Ni substrate and sealed only at the periphery through stable C–Ni bonds. Their in-plane truncated triangular shapes are driven by the crystallographic directions of the Ni surface. The nonuniform strain revealed along the blister profile is explained by the inhomogeneous expansion of the flexible graphene lattice that adjusts to envelop the Ar-atom stacks.

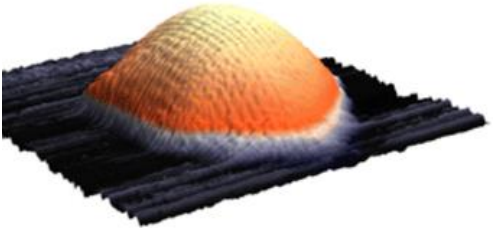

Nanoblister in Ar aggregates compressed at high pressure below monolayer graphene on Ni(111)

Concerning topological insulators, using the STM apparatus at the CNR-IOM institute at Elettra, Trieste, we have studied a novel interface formed by organic molecules Co-phtalocyanines with Bi_2Se_3 topological insulators [Nano Letters 16 (2016) 3409]. The hybrid interface can act on the topological protection of the surface and bury the Dirac cone below the first quintuple layer.

3. REAL-TIME GROWTH OF GRAPHENE ON COPPER FOILS, NICKEL AND METAL ALLOYS

By means of time-resolved X-ray photoelectron spectroscopy (with synchrotron radiation) on the C 1s core level, we have followed in real time the growth of graphene on copper foils, nickel single crystals and metal alloys during (i) the exposure to ethylene or (ii) upon heating the sample. This procedure also allows to probe the onset of the graphene phase and the occurrence of intermediates formed during the thermal decomposition of hydrocarbons.

4. HYDROGEN STORAGE AND PRODUCTION WITH GRAPHENE-BASED MATERIALS

By means of a combination of surface-science spectroscopies and theory, we have investigated the mechanisms ruling the catalytic role of epitaxial graphene (Gr) grown on transition-metal substrates for the production of hydrogen from water. Water decomposition at the Gr/metal interface at room temperature provides a hydrogenated Gr sheet, which is buckled and decoupled from the metal substrate. We have evaluated the performance of Gr/metal interface as a hydrogen storage medium, with a storage density in the Gr sheet comparable with state-of-the-art materials (1.42 wt %). Moreover, thermal programmed reaction experiments have shown that molecular hydrogen can be released upon heating the water-exposed Gr/metal interface above 400 K. The Gr hydro/dehydrogenation process might be exploited for an effective and eco-friendly device to produce (and store) hydrogen from water, i.e., starting from an almost unlimited source.
For the first time the same material has been used for both storing and producing hydrogen.

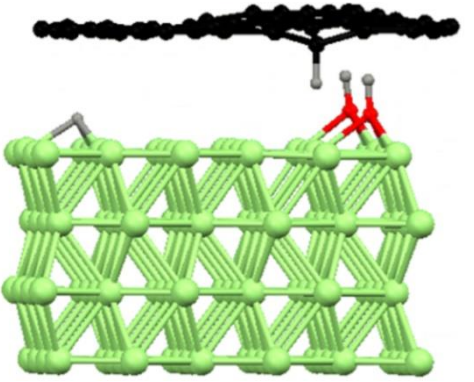

Hydrogen storage at graphene/Ni interfaces

5. SURFACE CHEMISTRY WITH GRAPHENE/METAL INTERFACES AND BIMETALLIC SURFACES

5.1.Alkali adsorption and co-adsorption on metal surfaces and graphene: vibrational spectroscopy and theory

Alkali-metal (AM) atoms adsorbed on single-crystal surfaces are a model system for understanding the properties of adsorption. AM adsorption, besides introducing new overlayer vibrational states, induces significant modifications in the surface vibrational structure of the metal substrate. The adsorbed phase is characterized by a stretch (S) vibrational mode, with a polarization normal to the surface, and by other two modes polarized in the surface plane, known as frustrated translation (T) modes. The frequencies and intensities of these modes depend on the coverage, thus providing a spectroscopic signature for the characterization of the adsorbed phases. The vibrational spectroscopy joined to an ab-initio theoretical analysis can provide useful information about surface charge re-distribution and the nature of the adatom-surface bond, establishing, e.g., its partial ionicity and

polarization. Gaining this information implies a significant advancement in our knowledge on surface chemical bonds and on catalytic reactions occurring in AM co-adsorption with other chemical species. Hence, systematic studies of co-adsorption systems are essential for a more complete understanding of heterogeneous catalysis. The two principal experimental techniques for studying the vibrations of AM adsorbed phases are high-resolution electron energy loss spectroscopy (HREELS) and inelastic helium atom scattering (HAS), the former being better suited to the analysis of the higher part of the vibrational spectrum, while the latter exploits its better resolution in the study of slower dynamics, e.g., T modes, surface acoustic phonons and diffusive phenomena. We have studied AM adsorption and co-adsorption on many systems, including graphene, transition-metal surfaces and bimetallic alloys.

5.2 Segregation and selective oxidation of Ni atoms in $Pt_3Ni(111)$ in oxygen environment

Understanding the microscopic mechanism of oxygen interaction with the surfaces of Pt-based alloys is an important issue for applications in various fields, such as corrosion and oxygen reaction reduction in fuel cells, for which Pt-based alloys are more efficient catalysts with respect to platinum. We have studied the interaction of oxygen with $Pt_3Ni(111)$ by X-ray photoemission, X-ray absorption, and HREELS spectroscopies. We have found that the oxidation of $Pt_3Ni(111)$ at 600 K leads to the segregation of Ni atoms to the surface region. The presence of Ni atoms at the $Pt_3Ni(111)$ surface allows O_2 to dissociate to form NiO*x* surface species. Vibrational measurements performed on Pt(111), Ni(111), and $Pt_3Ni(111)$ have directly shown that, on the $Pt_3Ni(111)$ surface, oxygen binds selectively on Ni sites and, moreover, that the O–Ni bond formed on Pt_3Ni is weaker than the O–Pt bond formed on Pt(111).

5.3 On the intercalation of CO molecules in ultra-high vacuum conditions underneath graphene epitaxially grown on metal substrates

We have studied the interaction of CO with epitaxial graphene on Pt(111) and Ru(0001) by means of HREELS measurements. Our experiments unambiguously demonstrate that in ultra-high vacuum conditions CO does not intercalate underneath the graphene monolayer supported on Pt(111) and Ru(0001). For submonolayer coverages of graphene on Pt(111), CO adsorption occurs only in Pt on-top sites while bridge sites, usually populated on the clean Pt(111) surface, are inhibited. Instead, we find that epitaxial graphene is rather reactive toward water molecules.

6. ELECTRON CONFINEMENT AND QUANTUM SIZE EFFECTS IN NOBLE-METAL FILMS

The influence of electron confinement, quantum size effects, and film morphology on the dispersion and the damping of plasmonic modes in Ag and Au thin films has been studied by HREELS.

Loss measurements for Ag/Cu(111), characterized by a Stranski-Krastanow growth mode, reveal plasmon confinement within islands in as-deposited Ag layers. Annealing causes an enhanced free-electron density of states of the Ag quantum well states (QWS), which makes negative the linear coefficient of the dispersion relation of the surface plasmon of Ag. The increased value of the line-width in plasmons in Ag films compared with Ag single-crystal surfaces suggests the occurrence of enhanced damping mechanism, due to the opening of new decay channels in systems with QWS.

The loss spectrum of Au thin films on Cu(111) presents both single-particle and collective excitations.

7. PHYSICOCHEMICAL INVESTIGATIONS ON ACTIVE CHANNELS OF FIELD-EFFECT TRANSISTORS BASED ON TOPOLOGICAL INSULATORS AND OTHER MATERIALS BEYOND GRAPHENE

We have demonstrated that, in contrast to most two-dimensional materials (including phosphorene), ultrathin flakes of InSe are stable under ambient conditions. Despite their ambient stability, InSe-based nanodevices show an environmental p-type doping, suppressed by capping InSe with hexagonal boron nitride. By means of transport experiments, density functional theory and vibrational spectroscopy, we attribute the p-type doping assumed by uncapped InSe under an ambient atmosphere to the decomposition of water at Se vacancies. We have estimated the site-dependent adsorption energy of O_2, N_2, H_2O, CO and CO_2 on InSe. A stable adsorption is found only for the case of H_2O, with a charge transfer of only 0.01 electrons per water molecule.
Moreover, the chemical inertness of bismuth selenide, proven by our vibrational experiments, has been crucial for the nanofabrication of nanodevices with superb performances in detection of Terahertz light.

8. PLASMON MODES AT GRAPHENE/METAL CONTACTS

Plasmons in graphene have unusual properties and offer promising prospects for plasmonic applications covering a wide frequency range, ranging from terahertz up to the visible. We studied plasmon modes in both free-standing and supported graphene, in order to shed light on the influence of the underlying substrate on the screening processes. Plasmon in graphene can be tuned by chemical doping and gating potentials. We have shown that the adsorbates can be used to tune the plasmon frequency and, consequently, the dispersion relation. In particular, we have studied plasmonic modes in graphene/metal contacts for plasmonic devices before and after interaction with ambient air humidity. Graphene/metal contacts are omnipresent and inevitable components in each graphene-based device and, thus, experiments on graphene/metal contacts in ambient conditions are crucial in order to assess the suitability of the technological exploitation of plasmonics with graphene. We have found remarkable differences in the ambient stability of different graphene/metal contacts, related to the presence of the underlying metal substrate. Finally, we have also reported intriguing effects due to many-body interaction, such as the excitations generated by electron–electron coupling and the composite modes arising from the coupling of plasmons with phonons and with charge carriers.

9. PLASMONIC EXCITATIONS IN TOPOLOGICAL INSULATORS

We have investigated plasmonic excitations at the surface of Bi_2Se_3 via HREELS. For low parallel momentum transfer $q_{||}$, the loss spectrum shows a distinctive feature peaked at 104 meV. This mode varies weakly with $q_{||}$. The behavior of its intensity as a function of primary energy and scattering angle indicates that it is a surface plasmon. At larger momenta, an additional peak, attributed to the Dirac plasmon, becomes clearly defined in the loss spectrum. Momentum-resolved loss spectra provide evidence of the mutual interaction between the surface plasmon and the Dirac plasmon of Bi_2Se_3. The proposed theoretical model accounting for the coexistence of three-dimensional doping electrons and two-dimensional Dirac fermions accurately represents the experimental observations. The results reveal novel routes for engineering plasmonic devices based on topological insulators.

10. LATTICE DYNAMICS AND ELECTRON-PHONON COUPLING IN GRAPHENE METAL/INTERFACES

Kohn anomalies are the most evident manifestation of electron-phonon coupling (EPC). In neutral graphene, two prominent cusps known as Kohn anomalies are found in the phonon dispersion of the highest optical phonon at q=Γ (LO branch) and q=K (TO branch), reflecting a significant EPC to undoped Dirac electrons. We used HREELS to measure the phonon dispersion around the Γ point in quasifreestanding graphene epitaxially grown on Pt(111). The Kohn anomaly for the LO phonon is observed at finite momentum $q \sim 2k_F$ from Γ, with a shape in excellent agreement with the theory and consistent with known values of the EPC and the Fermi level. More strikingly, we also observe a Kohn anomaly at the same momentum for the out-of-plane optical phonon (ZO) branch. This observation is the first direct evidence of the coupling of the ZO mode with Dirac electrons, which is forbidden for freestanding graphene but becomes allowed in the presence of a substrate. Moreover, we estimate the EPC to be even greater than that of the LO mode, making graphene on Pt(111) an optimal system to explore the effects of this new coupling in the electronic properties.

11. ELASTIC PROPERTIES OF TWO-DIMENSIONAL MATERIALS AND TOPOLOGICAL PHASES OF MATTER

By analyzing phonon dispersion, we have evaluated the average Young's modulus and Poisson's ratio in graphite and in graphene grown on Ru(0001), Pt(111), Ir(111), Ni(111), and BC_3/NbB_2(0001). In both flat and corrugated graphene sheets and in graphite, we find a Poisson's ratio of 0.19 and a Young's modulus of 342 N/m. The unique exception is graphene/Ni(111), for which we find different values because of the stretching of C-C bonds occurring in the commensurate overstructure (0.36 and 310 N/m for the Poisson's ratio and Young's modulus, respectively). Such findings are in excellent agreement with calculations performed for a free-standing graphene membrane. The high crystalline quality of graphene grown on metal substrates leads to macroscopic samples with high tensile strength and bending flexibility for use in technological applications such as electromechanical devices and carbon-fiber reinforcements.

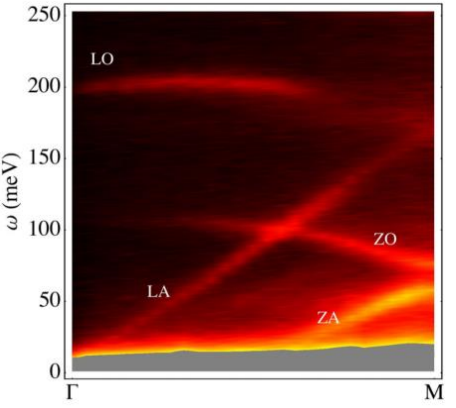

HREELS Intensity plot for phonon dispersion of graphene/Pt(111). Phonon modes have been recorded in HREELS spectra acquired in off- specular geometry along the Γ − M direction. To put in evidence only inelastic losses due to phonons, the tail of the elastic peak is grayed out for clarity.

We have also evaluated the mechanical properties of topological insulators though depth-sensing nanoindentation experiments, performed along the directions parallel and perpendicular to the cleavage plane of Bi_2Te_3. Moreover, we investigated for the first time the fracture toughness of bulk single crystals of Bi_2Te_3 topological insulators, grown using the Bridgman-Stockbarger method.

Our results have highlighted one of the possible pitfalls of the technology based on topological insulators.

12. PLASMA-WAVE TERAHERTZ PHOTODETECTION WITH TOPOLOGICAL MATERIALS AND PHOSPHORENE

New advances in different technologies have made the previously unused terahertz (THz) frequency band accessible for imaging systems. The 'terahertz gap' has a frequency ranges from ~0.3 THz to ~10 THz in the electromagnetic spectrum which in between microwave and infrared. The terahertz radiations are invisible to naked eye and in comparison with X-ray they are intrinsically safe, non-destructive and non-invasive. THz imaging has number of applications ranging from product inspection (industry), spectroscopy (chemistry, astronomy), material characterization (physics), weapons concealed under clothing (body scanner at airports), early detection of cancer and caries. In the pharmaceutical industries it enables nondestructive, internal, chemical analysis of tablets, capsules and other dosage forms.
The most promising application of THz plasmonics is related to the rectification of THz radiation via the excitation of plasma waves in the active channel of antenna-coupled field-effect transistors (FETs). This photodetection mechanism is based on the fact that a FET hosting a two-dimensional electron gas (2DEG) can act as a cavity for plasma waves, which are launched at the source by means of a modulation of the potential difference between gate and source. Plasma waves propagating in the active channel of FETs cannot be merely recognized with the plasmonic resonance of a 2DEG (2D plasmon) because of the presence of a metal gate.
For the case of topological insulators, we find that the predominant photodetection mechanism is that associated with the excitation of plasma waves, which are over-damped in the transistor channel.
We have also devised the first room-temperature nanodetector in the THz range exploiting a 10 nm thick flake of exfoliated crystalline black phosphorus as an active channel of a FET. By engineering and embedding planar THz antennas for efficient light harvesting, the first technological demonstration of a phosphorus-based active THz device has been reported. We also used hBN-phosphorene-hBN heterostructures for novel nanodetectors with superb values of the signal-to-noise ratio.
We used our nanodetectors for imaging experiments in transmission with THz light, with excellent results.

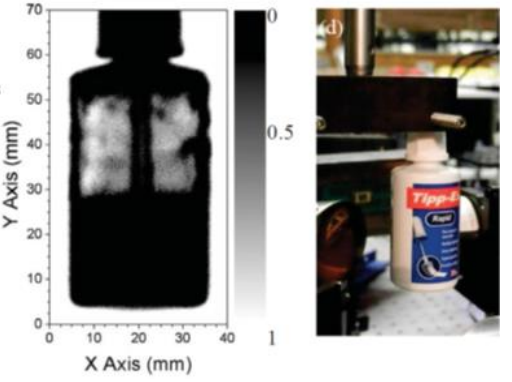

Imaging the content of a glue jar filled up to one half by means of radiation at 0.3 THz

13. APPLICATIONS OF THERMOPLASMONICS IN MEMBRANE TECHNOLOGY FOR SEAWATER DESALINATION

The technological applications related to the excitation of localized surface plasmon modes in noble-metal nanoparticles (NPs) have originated the emerging field of plasmonics. Among the various technological capabilities of plasmonics, those related to thermoplasmonics are particularly promising. Thermoplasmonics, i.e. the Joule heating associated to optically resonant plasmonic excitations in metal NPs, is based on the control by means of light source of nanoscale thermal hotspots. The use of thermoplasmonics has been proposed in different fields. However, most applications are only at an initial state of development.
We find that thermoplasmonic effects notably improve the efficiency of vacuum membrane distillation, an economically sustainable tool for high-quality seawater desalination. Poly(vinylidene fluoride) (PVDF) membranes filled with spherical silver nanoparticles have been used, whose size is tuned for the aim. With the addition of plasmonic nanoparticles in the membrane, the transmembrane flux increases by 11 times, and, moreover, the temperature at the membrane interface is higher than bulk temperature.

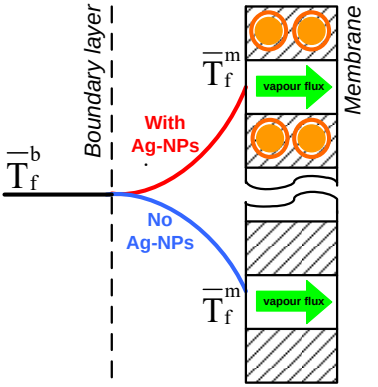

Energy balance within the boundary layer adjacent to the membrane at the feed side: the temperature profile falls for an unloaded membrane, and raises due to the thermoplasmonic effects activated by Ag NPs inside the polymeric membranes

A PUBLICATIONS ON SCIENTIFIC JOURNALS
A.1 Publications on international journals
A.1.1 Publications on international journals printed in 2013-2016

1. Politano A., Chiarello G.,
Alkali-induced hydrogenation of epitaxial graphene by water splitting at 100 K
The Journal of Chemical Physics, **138**, 044703-044704 (2013).

2. Politano A.,
Low-Energy Collective Electronic Mode at a Noble Metal Interface
Plasmonics, **8**, 357-360 (2013).

3. Politano A., Caputo M., Goldoni A., Torelli P., Chiarello G.,
Segregation and Selective Oxidation of Ni Atoms in $Pt_3Ni(111)$ in Low-Pressure Oxygen Environment
The Journal of Physical Chemistry C, **117**, 27007 (2013).

4. Politano A., Campi D., Formoso V., Chiarello G.,
Evidence of confinement of the π plasmon in periodically rippled graphene on Ru(0001)
Physical Chemistry Chemical Physics, **15**, 11356-11361 (2013).

5. Cazzanelli E., Caruso T., Castriota M., Marino A. R., Politano A., Chiarello G., Giarola M., Mariotto G.,
Spectroscopic characterization of graphene films grown on Pt(111) surface by chemical vapor deposition of ethylene
Journal of Raman Spectroscopy, **44**, 1393-1397 (2013).

6. Politano A., Chiarello G.,
Quenching of plasmons modes in air-exposed graphene-Ru contacts for plasmonic devices
Applied Physics Letters, **102**, 201608-201604 (2013).

7. Politano A, Chiarello G.,
Unravelling suitable graphene-metal contacts for graphene-based plasmonic devices
Nanoscale, **5**, 8215-8220 (2013).

8. Politano A., Chiarello G.,
On the intercalation of CO molecules in ultra-high vacuum conditions underneath graphene epitaxially grown on metal substrates
Carbon, **62**, 263-269 (2013).

9. Politano A., Chiarello G.,
The nature of free O-H stretching in water adsorbed on carbon nanosystems
The Journal of Chemical Physics, **139**, 064704-064704 (2013).

10. Politano A., Chiarello G.,
Periodically rippled graphene on Ru(0001): A template for site-selective adsorption of hydrogen dimers via water splitting and hydrogen-spillover at room temperature
Carbon, **61**, 412-417 (2013).

11. Politano A., Chiarello G., Benedek G., Chulkov E. V., Echenique P. M.,
Vibrational measurements on alkali coadsorption systems: experiments and theory
Surface Science Reports, **68**, 305–389 (2013).

12. Politano A., Formoso V., Chiarello G.,
Interplay between single-particle and plasmonic excitations in the electronic response of thin Ag films
Journal of Physics: Condensed Matter, **25**, 305001 (2013).

13. Politano A., Formoso V., Chiarello G.,
Evidence of composite plasmon–phonon modes in the electronic response of epitaxial graphene
Journal of Physics: Condensed Matter, **25**, 345303 (2013).

14. Politano A., Formoso V., Chiarello G.,
Collective Electronic Excitations in Thin Ag Films on Ni(111)
Plasmonics, **8**, 1683-1690 (2013).

15. Alzari V., Sanna V., Biccai S., Caruso T., Politano A., Scaramuzza N., Sechi M., Nuvoli D., Sanna R., Mariani A.,
Tailoring the physical properties of nanocomposite films by the insertion of graphene and other nanoparticles
Composites Part B: Engineering, **60**, 29-35 (2014).

16. Fladischer K., Politano A., Ernst W. E., Farías D. Miranda R.,
A helium atom scattering study of well-ordered TCNQ adlayers on Cu(100)
Surface Science, **620**, 65-69 (2014).

17. Politano A., Caputo M., Nappini S., Bondino F., Magnano E., Aliev Z. S., Babanly M. B., Goldoni A., Chiarello G. Chulkov E. V.,
Exploring the Surface Chemical Reactivity of Single Crystals of Binary and Ternary Bismuth Chalcogenides
The Journal of Physical Chemistry C, **118**, 21517–21522 (2014).

18. Politano A, Chiarello G.,
Emergence of a nonlinear plasmon in the electronic response of doped graphene
Carbon, **71**, 176–180 (2014).

19. Politano A, Chiarello G.,
Plasmonic modes in thin films: quo vadis?
Frontiers in Materials, **1**, doi: 10.3389/fmats.2014.00009 (2014).

20. Politano A, Chiarello G.,
Plasmon modes in graphene: status and prospect
Nanoscale, **6**, 10927-10940 (2014).

21. Politano A, Chiarello G.,
The formation of HOCO in the coadsorption of water and carbon monoxide on $Pt_3Ni(111)$
RSC Advances, **4**, 45641-45646 (2014).

22. Cupolillo A., Politano A., Ligato N., Cid D., Chiarello G., Caputi L. S.,
Substrate-dependent plasmonic properties of supported graphene
Surface Science, **634**, 76–80 (2015).

23. de Juan F., Politano A., Chiarello G., and Fertig H. A.,
Symmetries and selection rules in the measurement of the phonon spectrum of graphene and related materials
Carbon, **85**, 225–232 (2015).

24. Nechaev I. A., Aguilera I., De Renzi V., di Bona A., Lodi Rizzini A., Mio A. M., Nicotra G., Politano A., Scalese S., Aliev Z. S., Babanly M. B., Friedrich C., Blügel S., and Chulkov E. V.,
Quasiparticle spectrum and plasmonic excitations in the topological insulator Sb_2Te_3
Physical Review B, **91**, 245123 (2015).

25. Nicotra G., Mio A. M., Cupolillo A., Hu J., Wei J., Mao Z., Deretzis I., Politano A., and Spinella C.,
STEM and EELS Investigation on Black Phosphorus at Atomic Resolution
Microscopy and Microanalysis, **21**, 427-428 (2015).

26. Politano A.,
Probing growth dynamics of graphene/Ru(0001) and the effects of air exposure by means of helium atom scattering
Surface Science, **634**, 44-48 (2015).

27. Politano A, Chiarello G.,
The influence of electron confinement, quantum size effects, and film morphology on the dispersion and the damping of plasmonic modes in Ag and Au thin films
Progress in Surface Science, **90**, 144-193 (2015).

28. Politano A, Chiarello G.,
Probing Young's modulus and Poisson's ratio in graphene/metal interfaces and graphite: A comparative study
Nano Research, **8**, 1847-1856 (2015).

29. Politano A, Chiarello G.,
Ice formation on clean and alkali-doped quasi-freestanding graphene: A vibrational investigation
Carbon, **93**, 242-249 (2015).

30. Politano A., Chiarello G., and Cupolillo A.,
Toward a novel theoretical approach for determining the nature of electronic excitations in quasi-two-dimensional systems
New Journal of Physics, **17**, 081002 (2015).

31. Politano A., de Juan F., Chiarello G., and Fertig H. A.,
Emergence of an Out-of-Plane Optical Phonon (ZO) Kohn Anomaly in Quasifreestanding Epitaxial Graphene
Physical Review Letters, **115**, 075504 (2015).

32. Politano A., Silkin V. M., Nechaev I. A., Vitiello M. S., Viti L., Aliev Z. S., Babanly M. B., Chiarello G., Echenique P. M., and Chulkov E. V.,
Interplay of Surface and Dirac Plasmons in Topological Insulators: The Case of Bi_2Se_3
Physical Review Letters, **115**, 216802 (2015).

33. Viti L., Hu J., Coquillat D., Knap W., Tredicucci A., Politano A., Vitiello M. S.,
Black Phosphorus Terahertz Photodetectors
Advanced Materials, **27**, 5567–5572 (2015).

34. Aliev Z. S., Zúñiga F. J., Koroteev Y. M., Breczewski T., Babanly N. B., Amiraslanov I. R., Politano A., Madariaga G., Babanly M. B., Chulkov E. V.,
Insight on a novel layered semiconductors: CuTlS and CuTlSe
Journal of Solid State Chemistry, **242, Part 1**, 1-7 (2016).

35. Caputo M., Panighel M., Lisi S., Khalil L., Santo G. D., Papalazarou E., Hruban A., Konczykowski M., Krusin-Elbaum L., Aliev Z. S., Babanly M. B., Otrokov M. M., Politano A., Chulkov E. V., Arnau A., Marinova V., Das P. K., Fujii J., Vobornik I., Perfetti L., Mugarza A., Goldoni A., Marsi M.,
Manipulating the Topological Interface by Molecular Adsorbates: Adsorption of Co-Phthalocyanine on Bi_2Se_3
Nano Letters, **16**, 3409–3414 (2016).

36. Lamuta C., Campi D., Cupolillo A., Aliev Z. S., Babanly M. B., Chulkov E. V., Politano A., Pagnotta L.,
Mechanical properties of Bi_2Te_3 topological insulator investigated by density functional theory and nanoindentation
Scripta Materialia, **121**, 50-55 (2016).

37. Lamuta C., Cupolillo A., Politano A., Aliev Z. S., Babanly M. B., Chulkov E. V., Alfano M., Pagnotta L.,
Nanoindentation of single-crystal Bi_2Te_3 topological insulators grown with the Bridgman–Stockbarger method
physica status solidi (b), **253**, 1082–1086 (2016).

38. Lamuta C., Cupolillo A., Politano A., Aliev Z. S., Babanly M. B., Chulkov E. V., Pagnotta L.,
Indentation fracture toughness of single-crystal Bi_2Te_3 topological insulator
Nano Research, **9**, 1032-1042 (2016).

39. Larciprete R., Colonna S., Ronci F., Flammini R., Lacovig P., Apostol N. G., Politano A., Feulner P., Menzel D., Lizzit S.,
Self-assembly of graphene nanoblisters sealed to a bare metal surface
Nano Letters, **16**, 1808–1817 (2016).

40. Politano A.,
Spectroscopic investigations of phonons in epitaxial graphene
Critical Reviews in Solid State and Materials Sciences, **42**, 99-128 (2016).

41. Politano A.,
Quasi-freestanding graphene on Ni(110): A graphene/metal contact with suppressed interface states
Nano Research, **9**, 1795-1800 (2016).

42. Politano A., Cattelan M., Boukhvalov D. W., Campi D., Cupolillo A., Agnoli S., Apostol N. G., Lacovig P., Lizzit S., Farías D., Chiarello G., Granozzi G., Larciprete R.,
Unveiling the Mechanisms Leading to H_2 Production Promoted by Water Decomposition on Epitaxial Graphene at Room Temperature
ACS Nano, **10**, 4543–4549 (2016).

43. Politano A, Chiarello G.,
Unveiling the Oxidation Processes of $Pt_3Ni(111)$ by Real-Time Surface Core-Level Spectroscopy
ChemCatChem, **8**, 713–718 (2016).

44. Politano A., Chiarello G., Samnakay R., Liu G., Gurbulak B., Duman S., Balandin A. A., Boukhvalov D. W.,
The influence of chemical reactivity of surface defects on ambient-stable InSe-based nanodevices
Nanoscale, **8**, 8474-8479 (2016).

45. Politano A., Chiarello G., Spinella C.,
Plasmon spectroscopy of graphene and other two-dimensional materials with transmission electron microscopy

Materials Science in Semiconductor Processing, doi:10.1016/j.mssp.2016.1005.1002 (2016).

46. Politano A., Cupolillo A., Di Profio G., Arafat H., Chiarello G., Curcio E., *When plasmonics meets membrane technology* Journal of Physics: Condensed Matter, **28**, 363003 (2016).

47. Politano A., Radović I., Borka D., Mišković Z. L., Chiarello G., *Interband plasmons in supported graphene on metal substrates: Theory and experiments* Carbon, **96**, 91-97 (2016).

48. Politano A., Vitiello M. S., Viti L., Hu J., Mao Z., Wei J., Chiarello G., Boukhvalov D. W., *Unusually strong lateral interaction in the CO overlayer in phosphorene-based systems* Nano Research, **9**, 2598–2605 (2016).

49. Viti L., Coquillat D., Politano A., Kokh K. A., Aliev Z. S., Babanly M. B., Tereshchenko O. E., Knap W., Chulkov E. V., Vitiello M. S., *Plasma-Wave Terahertz Detection Mediated by Topological Insulators Surface States* Nano Letters, **16**, 80–87 (2016).

50. Viti L., Hu J., Coquillat D., Politano A., Consejo C., Knap W., Vitiello M. S., *Heterostructured hBN-BP-hBN Nanodetectors at Terahertz Frequencies* Advanced Materials, **28**, 7390–7396 (2016).

51. Viti L., Hu J., Coquillat D., Politano A., Knap W., Vitiello M. S., *Efficient Terahertz detection in black-phosphorus nano-transistors with selective and controllable plasma-wave, bolometric and thermoelectric response* Scientific Reports, **6**, 20474 (2016).

A.1.2 Publications on international journals accepted in 2016

1. Politano A., Argurio P., Di Profio G., Sanna V., Cupolillo A., Chakaraborthy S., Arafat H. A., Curcio E., *Photothermal membrane distillation for seawater desalination* to appear on Advanced Materials (2017).

2. Politano A., Radović I., Borka D., Mišković Z. L., Yu H. K., Farías D., Chiarello G., *Dispersion and damping of the interband π plasmon in graphene grown on Cu(111) foils* to appear on Carbon (2017).

3. Farrell E., Hassan M. I., Tufa R. A., Tuomiranta A., Avci A. H., Politano A., Curcio E., Arafat H. A., *Reverse electrodialysis powered greenhouse concept for water- and energy-self-sufficient agriculture* to appear on Applied Energy (2017).

4. Politano A., Slotman G. J., Roldán R., Chiarello G., Campi D., Katsnelson M. I., Yuan S., *Effect of moiré superlattice reconstruction in the electronic excitation spectrum of graphene-metal heterostructures* to appear on 2D Materials (2017).

5. Politano A., Vitiello M. S., Viti L., Boukhvalov D. W., Chiarello G.,

The role of surface chemical reactivity in the stability of electronic nanodevices based on two-dimensional materials "beyond graphene" and topological insulators
to appear on FlatChem (2017).

6. Politano A., Viti L., Vitiello M. S.,
Optoelectronic devices, plasmonics and photonics with topological insulators
to appear on APL Materials (2017).

7. Verre S., Politano A., Ombres L.,
Evaluation of the free-vibration frequency and the variation of the bending rigidity of graphene nanoplates: the role of the shape geometry and boundary conditions
to appear on Journal of Nanoscience and Nanotechnology (2017).

8. Mitrofanov O., Viti L., Dardanis E., Giordano M., Ercolani D., Politano A., Sorba L., Vitiello M.S.,
Near-field terahertz probes with room-temperature nanodetectors for subwavelength resolution imaging
to appear on Scientific Reports (2017).

9. Politano A., Campi D., Cattelan M., Ben Amara I., Jaziri S., Mazzotti A., Barinov A., Gürbulak B., Duman S., Agnoli S., Caputi L., Granozzi G., Cupolillo A.,
Indium selenide: an insight on electronic band structure and surface excitations
to appear on Scientific Reports (2017).

B PUBLICATIONS ON CONFERENCE PROCEEDINGS

B.1 Publications on international conference proceedings in 2013-2016

1. Viti L., Hu J., Coquillat D., Politano A., Consejo C., Knap W., Vitiello M. S.,
Black phosphorus and hybrid van der Waals heterostructured terahertz photodetectors
Proceedings of the 41st International Conference on Infrared, Millimeter, and Terahertz waves (IRMMW-THz), doi: 10.1109/IRMMW-THz.2016.7758894

2. Alfano M., Lamuta C., Chiarello G., Politano A.
Elastic properties and electron-phonon coupling of graphene/metal interfaces probed by phonon dispersion
Proceedings of GraphITA 2015, Springer, 2016

C BOOK CHAPTERS

1. Politano A., Chiarello G.
Collective modes in graphene/metal interfaces probed by electron energy loss spectroscopy, in "*Innovative Graphene Technologies: Developments, Characterization and Evaluation*", 2013, Smithers Rapra Technology Ltd, Shawbury (UK).

2. Politano A., Chiarello G.
Probing collective excitations in graphene/metal interfaces by high-resolution electron energy loss spectroscopy measurements, in "*Graphene Science Handbook: Electrical and Optical Properties*", 2013, CRC Press, Taylor&Francis (USA).

3. Politano A., Chiarello G.
Collective excitations in monolayer graphene on metals: Phonons and plasmons, in "*Exotic*

properties of carbon nanomatter", Springer (2015).

4. Politano A., Chiarello G.
Electron scattering studies on the growth of monolayer graphene coating on metal surfaces, in "*Comprehensive guide for nanocoatings technology, 2: Characterization and reliability*" Novapublisher (2015).

5. Horing N.J.M., Iurov A., Gumbs G., Politano A., Chiarello G.
Recent Progress on non local graphene Surface Plasmons, in "*Low-dimensional and nanostructured materials and devices*" Springer (2016)

6. Gugliuzza A., Politano A., Drioli E.
Two-dimensional materials for laminar membranes, in "Nanostructured Materials Membranes"- Pan Stanford Publishing (2016).

D INVITED PRESENTATIONS

D1. Invited presentations at international conferences in 2013-2016

1. Politano A.
   Carbon Topology Workshop, Erice, Italy, June, 21th 2013

2. Politano A.
   Italy-China Workshop on graphene, Dalian, China, September, 19th 2014

3. Politano A.
   Surface plasmons and plasmonics Workshop, Santa Margherita Ligure, Italy, June, 10th 2015

4. Politano A.
   New Trends in Topological Insulators Workshop, San Sebastian, Spain, July, 10th 2015

5. Politano A.
   GraphITA- A Multidisciplinary and Intersectorial European Workshop on Synthesis, Characterization and Technological Exploitation of Graphene and 2D Materials Beyond Graphene, Bologna, Italy, September, 14th 2015

6. Politano A.
   II edition of the Italy-China Workshop on graphene, Genova, Italy, April, 24th 2016

7. Politano A.
   Italy-Republic of Korea workshop on science and technology of materials "beyond graphene"Seoul, Republic of Korea, May 2016

8. Politano A.
   Third international conference on scattering of atoms and molecules from surfaces, Bergen, Norway, August 2016

9. Politano A.
   Materials 2016 Conference, Catania, Italy, December, 16th 2016

D2. Invited seminars at national institutions in 2013-2016

1. Politano A.
Seminar at CNR-S3, Modena, November, 27th 2013

2. Politano A.
Seminar at Department of Physics, University of L'Aquila, December, 2nd 2013

3. Politano A.
Seminar at Department of Physics, University of Genova, April, 21th 2016

4. Politano A.
Seminar at Department of Physics and Chemistry, University of L'Aquila, November, 15th 2016

E PRESENTATIONS AT CONFERENCES

E1. Presentations at international conferences in 2013-2016

1. Politano A., Chiarello G.
Angle-resolved Energy Loss Spectroscopy Experiments on Epitaxial Graphene on Pt(111): a Powerful Tool for Investigating Vibrational, Elastic and Electronic Properties.
FisMat 2013, Milan, Italy

2. Nicotra G., Mio AM, Cupolillo A, Hu J, Wei J, Mao ZQ, Deretsis I, Politano A, Spinella C
STEM and EELS Investigation on Black Phosphorus at Atomic Resolution
Microscopy and microanalysis 2015, Portland, USA

3. Samnakay R., Liu G., Rumyantsev S., Politano A., Gürbulak B., Duman S, Shur M., Balandin A.A.
Sweep-Dependent Electrical Switching in InSe Thin-Film FETs
MRS Spring Meeting 2016, Phoenix, USA

4. Viti L., Coquillat D., Politano A, Kokh KA, Aliev ZS, Babanly MB, Tereschchenko OE, Knap W, Chulkov EV, Vitiello MS
Probing topological insulators surface states via plasma-wave terahertz detection
Quantum Sensing and Nano Electronics and Photonics XIII, San Francisco, USA, 2016

5. Nicotra G, Politano A, Capitani M, Ienco A, Mio AM, Mao ZQ, Molle A, Peruzzini M, Spinella C
Atomic structure and electronic properties of phosphorene
E-MRS 2016 Spring Meeting, Symposium Z: Two-dimensional crystals and van der Waals heterostructures for nanoelectronics, Lille, France

6. Larciprete R, Colonna S, Ronci F, Flammini R, Lacovig P, Apostol NG, Politano A, Feulner P, Menzel D, Lizzit S
Self-assembly of graphene nanoblisters sealed to a bare metal surface
European Conference on Nanofilms (ECNF 2016), Bilbao, Spain

7. Larciprete R, Colonna S, Ronci F, Flammini R, Lacovig P, Apostol NG, Politano A, Feulner P, Menzel D, Lizzit S
Self-assembly of graphene nanoblisters sealed to a bare metal surface
Materials 2016, Aci Castello (CT), Italy

E2. Presentations at national conferences in 2013-2016

1. Nicotra G., Mio AM, Cupolillo A, Hu J, Wei J, Mao ZQ, Deretsis I, Politano A, Spinella C
STEM and EELS Investigation on Black Phosphorus at Atomic Resolution
Fosforene day, Firenze, Italy, 2015

2. Viti L, Hu J, Coquillat D, Knap W, Tredicucci A, Politano A, Vitiello MS
Black Phosphorus Terahertz Photodetectors
Fosforene day, Firenze, Italy, 2015

F. ORGANIZATION OF INTERNATIONAL WORKSHOPS

First Korea-Italy workshop on science and technology of two-dimensional materials "beyond graphene", Seoul (2016). Funded by Embassy of Italy, Ministry of Foreign Affairs, Hanyang University, University of Calabria

G. PARTICIPATION TO INTERNATIONAL AND NATIONAL PROJECTS

1. COST Action CA1507 MultiCOMP **"**Multi-Functional Nano-Carbon Composite Materials".
   Dr. Antonio Politano has been nominated by MIUR Substitute MC member for Italy

2. COST Action MP1306 "Modern Tools for Spectroscopy on Advanced Materials: a European Modelling Platform"

3. PRIN 2010-2011 *"Membrane nanocomposite avanzate ed elettrocatalizzatori innovativi per celle a combustibile ad elettrolita polimerico a lunga durata, NAMED-PEM*

4. MaTeRiA *(materials, technologies and advanced research)*

4. EXPERIMENTAL PARTICLE PHYSICS

Professors and Researchers	M. Capua G. Crosetti L. La Rotonda E. Tassi
Postdoc fellows	V. Lavorini
PhD students	V. Scarfone S. Palazzo G. Callea F. La Ruffa M. Scornajenghi D. Micieli
Engineers:	A. Tarasio
Technicians:	F. Pellegrino, V. Romano, P. Turco

Experimental particle physics studies the fundamental constituents of matter and their mutual interactions, as described by the *Standard Model*, by means of particles accelerators and detectors. A particles accelerator is a device that uses electromagnetic fields to propel charged particles to high energy (in the most powerful accelerator, the Large Hadron Collider (LHC), the centre of mass energy reaches 13 TeV). There are two ways to exploit particle accelerators: sending the accelerated particles towards a fixed target, accelerating two beams of particles directed one against the other. A particle detector is a device used to detect, track and identify high energy particles produced by the reactions in a particle accelerator. The innovative technologies used for these studies have wide implications in many fields of science (medicine, biology, informatics, etc.).

The researchers of the Experimental Particle Physics group of the University of Calabria are active in the following areas:

33. Study of the proton structure and the theory of the strong interactions in deep inelastic scattering processes with
    the ZEUS experiment at the lepton-proton accelerator HERA of the DESY Laboratory (Hamburg, Germany).
34. 333 Study of proton-proton interactions and tests of the Standard Model with the ATLAS experiment at the LHC
    accelerator of the CERN Laboratory (Geneva, Switzerland).
35. ATLAS Detector Upgrade: Micromegas Chambers.
36. Hadronic Calorimetry
37. High Performance Computing with the ReCaS Data Center
38. Proposal for a low energy γ-γ collider
39. Applied Physics: Research on the gas Radon

4.1 THE ZEUS EXPERIMENT AT THE HERA *ep* COLLIDER (DESY, HAMBURG-GERMANY)

Physicists: M. Capua
E. Tassi

International collaboration

The ZEUS experiment was an international collaboration running a large particle detector that operated on the HERA electron-proton collider at the DESY laboratory in Hamburg. The experiment began running together with HERA in 1992 and was functional until HERA was decommissioned in June 2007. The final analyses of the rich data sample collected with the ZEUS detector in its 15 years of operation are still underway. The ZEUS experiment studies the internal structure of the proton and the theory of the strong interactions, Quantum Chromodynamics (QCD), through measurements of deep inelastic scattering by colliding leptons (electrons or positrons) of 27.6 GeV with protons of 920 GeV. The large centre of mass energy of the machine (320 GeV) allows to probe the proton's structure down to distance scales as low as
10^{-18} m which is a factor 1000 smaller than the proton radius. At large momentum transfers (the kinematical limit at HERA is 10^5 GeV^2/c^2) there is a direct interaction of the electron with one of the quarks in the proton. For this reason HERA is often addressed as the world's first and only lepton-quark collider. In the period 2013-2016 our group has been mostly involved in:

72. the analysis of the final combination of the ZEUS and H1 inclusive cross sections results ("HERA Legacy Data") and the determination of the proton's parton distribution functions (see Fig.1);
1. studies of diffractive processes with the complete HERA data set (e.g. Deeply Virtual Compton Scattering).

The precise determination of the proton's parton distribution functions is of fundamental importantece in itself and to fully realize the physics programme at the LHC.

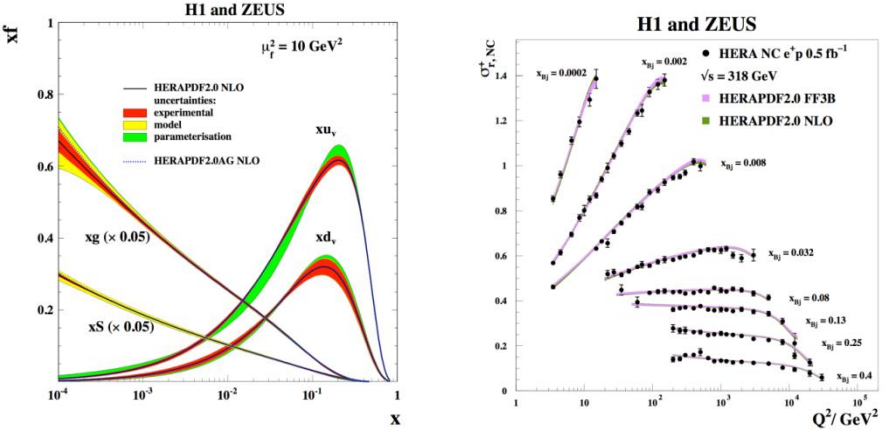

Fig.1 (*Left*) *The proton parton distribution functions determined from the final combination of the H1 and ZEUS cross section measurements. (Right) The reduced neutral current cross sections as function of Q^2 for eight representative values of x-Biorken.*

4.2 ATLAS EXPERIMENT AT THE LHC PROTON-PROTON COLLIDER (Geneva – Switzerland)

Physicists: M. Capua
G. Crosetti
L. La Rotonda
E. Tassi

Postdoc fellows V. Lavorini
PhD students: G. Callea, F. La Ruffa, S. Palazzo, V. Scarfone, M. Scornajenghi
Technicians: F. Pellegrino, V. Romano, P. Turco

International collaboration

Nature has given us more than one elementary particle (6 leptons, 6 quarks and the carriers of the four fundamental interactions), whose masses range in a wide interval of values from the massless photon to the top quark mass, m_t=170 GeV/c^2. The mechanism that determines the particle masses is still unknown and many experiments with particle accelerator have been undertaken to give an insight into it and explain the mass origin.

In 1964 Peter Higgs first proposed a clever solution to this puzzle: an undetectable field, similar to the electromagnetic one, permeates the whole space. As particles move in space they travel through this field, and interaction with this field allows them to acquire their masses. This is similar to the action of viscous forces felt by particles moving through any thick liquid: the stronger the interaction of the particles with the field, the bigger the mass they seem to have. We know from quantum theory that fields have particles associated with them, so a Higgs boson should be associated to the Higgs field. Up to 2012 no one had ever observed the Higgs boson in an experiment to confirm the theory. Finding this particle would give an insight into why particles have certain mass, and help to develop subsequent physics. The technical problem is that we do not know the mass of the Higgs boson itself, which makes it more difficult to identify. Physicists have to look for it by systematically searching a range of mass within which it is predicted to exist. The yet unexplored range has become accessible using the Large Hadron Collider.

On 4 July 2012 the ATLAS and CMS Collaborations jointly announced the independent discovery of a previously unknown neutral boson, compatible with the Higgs Boson, with a mass in the range 125-127 GeV/c^2. In the last four years the ATLAS and CMS collaborations have continued the study of the properties of the discovered boson confirming that its properties are indeed the ones characterizing the Standard Model Higgs boson.

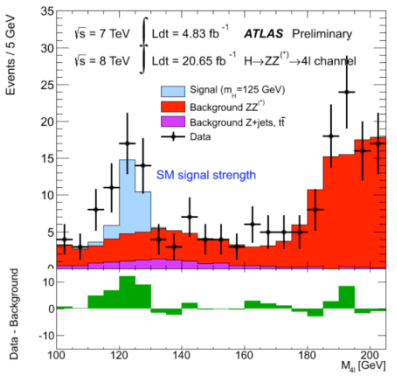

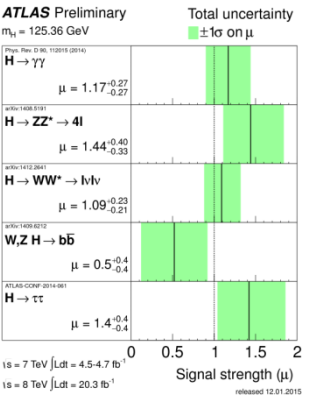

Fig. 2 *(Left) Higgs to four leptons invariant mass spectrum (using 2011 and 2012 data samples) (Right) The measured production strengths for a Higgs boson of mass m_H =125.36 GeV, normalised to the SM expectations, for the f=H→γγ, H→ZZ*→llll, H→WW*→lνlν, H→ττ, and H→bb; final states. The best-fit values are shown by the solid vertical lines. The total ±1σ uncertainty is indicated by the shaded band.*

This collider provides 10 times higher center of mass energy and 100 times higher p-p collision rates than the Tevatron collider and is fully operational since November 2009. This opens up a new frontier of physics and the LHC experiments, ATLAS, CMS, ALICE and LHCb, are ready to explore this great potential.

ATLAS is a general-purpose experiment. Designed to see a wide range of particles and phenomena produced in LHC collisions, it involves approximately 2500 physicists and engineers from some 35 countries. These scientists use the data collected from the complex detectors to search for new phenomena, including the Higgs boson, super-symmetry and extra dimensions. They also measure the properties of previously-discovered quarks and bosons with unprecedented precision, and are on the lookout for completely new, unpredicted phenomena. The basic design concept to achieve these goals includes three detector systems (Fig. 3):

8. the *inner tracker***,** with semiconductor pixel and strip detectors for very high accuracy measurements of the charged particle trajectories, followed by straw tube detectors giving independent electron identification. The tracker is confined to a cylinder 6.8 m long and with a radius of 1.1 m in a 2 T magnetic field, provided by a superconductive solenoid;
9. the *calorimeter***,** with an inner cylinder in highly granular liquid argon technology with Pb absorber, followed at large radius by an iron-tile scintillator calorimeter providing good resolution in a very cost-effective manner;
10. the high precision standalone *muon spectrometer*. Its conceptual layout is based on the magnetic deflection of muon track in a system of three large superconducting air-core toroid magnets instrumented with separate-function trigger and high-precision tracking chambers.

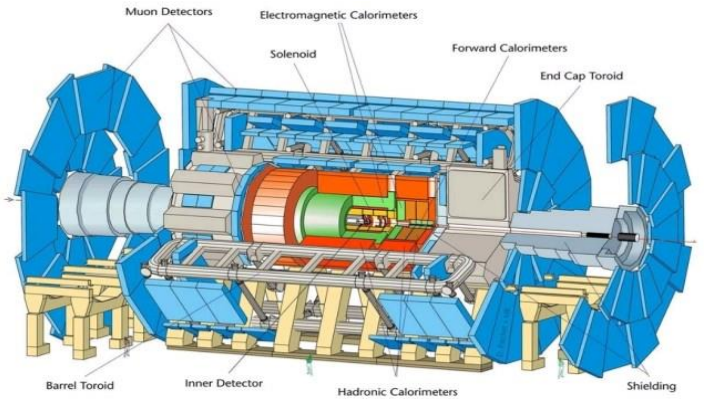

Fig. 3 *Overview of the ATLAS detector.*

The researchers of the experimental particle physics group of UNICAL have been strongly involved in various aspects of the design, construction, installation and test of the muon spectrometer since 1994. During this period the contribution from many undergraduate, graduate and PhD students and postdoc researchers has been substantial to this end.

In the period 2013-2016 our group has contributed to the following analyses:

11. Measurement of the top-antitop single differential cross sections in the lepton plus jet channel at the center of mass
    energies of 8 and 13 TeV.
12. Measurement of the differential cros sections for the production of a prompt-photon in association with hadronic
    jets at the center of mass energies of 8 and 13 TeV.
13. Measurement of the production of the W and Z gauge bosons: inclusive and in association with jets

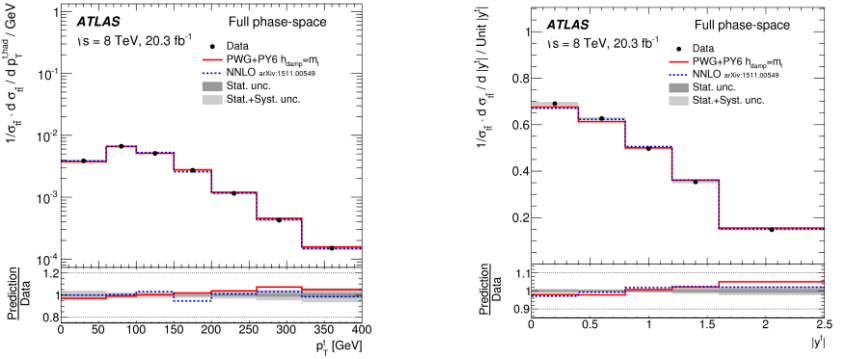

Fig. 4 *Full phase-space normalized differential cross-section as a function of the (Left) transverse momentum (p_T^t) and (Right) absolute value of the rapidity of the top quark ($|y^t|$) compared to NNLO theoretical calculations.*

These studies constitute an important part of the ATLAS physics program at the LHC. They allow to perform very precise tests of the predictions of the Standard Model at the next-to-leading order (NLO) and next-to-next-to-leading order (NNLO) and to improve the determination of the proton's parton distribution functions.

4.3 ATLAS DETECTOR UPGRADE: MICROMEGAS CHAMBERS

Physicists: L. La Rotonda

PhD Students: S. Palazzo

After the second long shutdown (LS2) in 2019-2020, the LHC luminosity will be increased up to 2-3 10^{34} cm^{-2} s^{-1} in Phase-1 and eventually, in the High Luminosity LHC eperiod, to ~7 10^{34} cm^{-2} s^{-1} in . While high luminosity will provide more data, it is essential that the ATLAS detectors are still able to operate in the higher background environment maintaining their performances as good as that at lower luminosities. To obtain this, some of the detectors that are located nearest to the beam pipe have to be replaced. For the upgrade of the ATLAS Muon Spectrometer the present Small Wheel equipped with CSC, MDT and TGC chambers will be replaced by the New Small Wheel. This will contain two new detector types: the MicroMegas (MM) and the small-stripTGC (sTGC). The New Small Wheels will be equipped with eight layers of MM
chambers arranged in multilayers of two quadruplets. Each MM quadruplet will provide 4 detection layers, and will consist of 5 panels made of aluminum honeycomb core sandwiched by printed circuit boards (PCBs) and 4 micro-meshes. The New Small Wheels detector technologies will provide both trigger and tracking capabilities: 15% transverse-momentum resolution for 1 TeV muons and a

spatial resolution corresponding to ~100 μm resolution per plane on a multilayer station. The first Module-0 of a MM quadruplet has been built by a consortium of several INFN groups in Italy and tested with high energy π on beam at the H8 SPS Test Beam experimental area at CERN in June 2016 and now it is under test at the LNF-INFN cosmic ray stand. The researchers of this group have been involved in the setup of the cosmic ray stand at LNF and in the preliminary data taking using small MM prototypes, in the Module-0 quality control, in the data analysis, and have developed a reconstruction code for the data collected at the CERN-Test Beam.

Fig. 5 (*Left*) *Exploded view of a MM chamber including read-out electrodes with strips, pillar, mesh and drift chatode.(Rigth) Principle of operation of a MM*

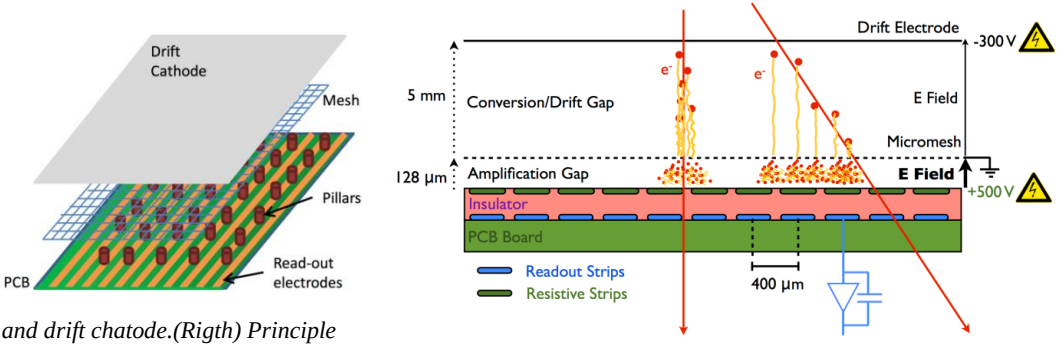

4.4 HADRONIC CALORIMETRY

Physicists: L. La Rotonda
Technicians: F. Pellegrino, V. Romano

International collaboration

High-precision measurements of hadrons and hadron jets have become increasingly important in experimental particle physics. The energy resolution of a hadron calorimeter is in general much worse than what can be achieved for e.m. shower detection. The wide variety of possible interaction processes and the effects associated with excitation of the absorber nuclei are considered responsible for this. In compensating hadron calorimeters a dominant source of fluctuations that comes from π^0 production in the shower is eliminated by equalising the calorimeter response to e.m. and purely hadronic shower component. In recent years, R. Wigmans (Texas Tech) in collaboration with other groups have developed an alternative technique: the Dual Readout Method (DREAM). DREAM calorimeters are based on a simultaneous measurement of different types of signals which provide complementary information about details of the shower development. The DREAM prototype, that has been successfully tested at CERN, is a copper absorber structure, equipped with two types of active media. Scintillating fibres measure the total energy deposited by the shower particles, while Quartz fibres measure the Cerenkov light that is only produced by the charged, relativistic shower particles. Since the latter are almost exclusively found in the e.m. shower component (dominated by π^0 s produced in hadronic showers), a comparison of the two signals makes it possible to measure the energy fraction carried by this component, fem, event by event. Once the effects of the dominant source of fluctuations, *i.e.,* fluctuations in the e.m. energy fraction fem, are eliminated, the performance characteristics are determined (and limited) by other types of fluctuations. In the described detector, a prominent role is played by the small number of Cerenkov

photoelectrons constituting the signals (8 p.e./GeV) due to the small sampling fraction used in the prototype. Moreover, for the measurement of electromagnetic showers and photons, it could be convenient to place in front to a DREAM-like calorimeter a high resolution electromagnetic homogenous calorimeter. In such a calorimeter it would be important to preserve the possibility of dual readout in order to correct the energy measurement of the fraction of hadrons developing electromagnetic showers already in this detector.

To the DREAM project, an Italian collaboration (Bologna, Cagliari, Cosenza, Roma1, Pavia) together with U.S. Researchers is working since 2006. MIUR has considered this project as a PRIN (Progetto di Ricerca di Interesse Nazionale) and has funded it in the period 2010-2012. In the summer of 2011 the same project has also been accepted as an official CERN R&D experiment. A new fiber calorimeter has been produced and tested. In this calorimeter the sampling fraction was increased, to increase the light collected. The new results obtained show a better energy resolution and linearity respect to the original DREAM calorimeter. The Cosenza researchers participated to the Test Beam and data analysis.

4.5 HIGH PERFORMANCE COMPUTING WITH THE RECAS DATA CENTER

Physicists: E. Tassi
Postdoc Fellow: V. Lavorini
Engineers and Technicians: A. Tarasio, N. Guarracino

The ReCaS Cosenza Data Center represents a unique IT infrastructure in the Calabria region. A medium-sized Data Center, funded with a total budget of 1.3 M€, is characterized by an efficient, scalable and state-of-the-art support infrastructure that guarantees very high operational standards. Its present computing and storage resources (more than 1.2 PB raw storage capacity and 3500 cores) contribute in a substantial way, jointly with the other ReCaS Data Centers, to the computing needs of all the experiments at the LHC as well as in supporting the needs (in the field of high performance computing) of diverse scientific and non-scientific communities. A detailed technical description of the ReCaS Data Centers, as well as of the scientific results achieved within the adopted grid- and cloud-based open software solutions, will soon become available in the monographic volume accepted for publication by World Scientific in 2016.

Fig. 6 (Left) *The two-Chiller sytem (with integrated free cooling) installed at the ReCaS Cosenza Site. (Right) The white space and the racks (with LCPs) hosting part of the IT equipment.*

4.6 PROPOSAL FOR A LOW ENERGY γ-γ COLLIDER

Physicists: E. Tassi
PhD Students: D. Micieli

The scattering of light by light (γγ -> γγ), a process that is precluded in classical electrodynamics *in vacuo*, is one of the most elusive and interesting effects foreseen by quantum electrodynamics; this process has never been observed for real photons. In a study performed in collaboration with colleagues of the Universities and INFN units of Milan and Trieste we presented the design of a γγ collider based on conventional Compton gamma sources. Two symmetric electron beams, generated by photocathodes and accelerated in linacs, produce two primary gamma rays through Compton backscattering with two high energy lasers. The two primary gamma pulses cross and scatter. Tuning the gamma energies to the energy corresponding to the maximum of the photon-photon cross section, a significant amount of γγ -> γγ events can be generated. Using state-of-the-art MC simulations of the Compton backscattering and γγ -> γγ processes, as well as a detailed simulation of the characteristics of the electron and photon beams, we could estimate the γγ event rate as a function of the distance L between the Compton and γγ interaction points (see Fig. 7). With a repetition rate of 100 Hz one event per hour is achieved for L between 1 and 1.5 mm. The same machine may be used to study the equally interesting Breit-Wheeler process ($\gamma\gamma \rightarrow e^+e^-$) still unobserved to this date.

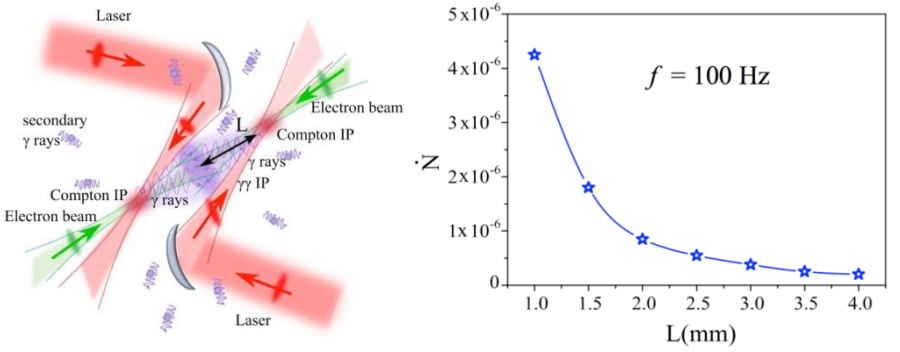

Fig. 7 (*Left*) *Scheme of the γγ interaction. Two lasers (in red) impinge on two electron beams (in green) in two interaction points (Compton IP), generating primary gamma rays (in violet). (Right) The γγ event rate as a function of the distance L between the Compton and γγ interaction points*

4.7 APPLIED PHYSICS: RESEARCH ON THE GAS RADON

Our group is also active in the field of physics applied to the environment, particularly radon radio protection. Radon is a natural noble gas present everywhere in the environment, it is a very dangerous intake alfa emitter. The World Health Organization, placed it in the higher class of physically hazardous substances in terms of risk of lung cancer. The gas is present in a non-homogeneous manner across the earth's crust and therefore in spring water, building materials and soil; all three environmental matrices can lead to significant accumulation of this gas in homes and workplaces. In 2013, EURATOM issued two directives: the directive n.51 (already in force in Italy D.L. 28/2016) and n.59 that will become law before the end of 2018, both including control obligations and if necessary action, in closed environments, including private homes, building materials and spring water for human use.

The group's research activity is focused on:
1)radon gas concentration sampling and measurement protocols in spring water with emanometric technique and gamma spectrometry, for a screening of Calabrian spring waters and techniques comparison;
2)exhalation rate measurement techniques in building materials. The measurements were made with materials of volcanic origin widely used as building materials in central Italy. To perform the measurement, a radon closed chamber in 78alabria78 was built;
3)measurements of radon transfer velocity at the water/air interface using the closed chamber. The chamber, in fact, has the unique peculiarity of being able to be used also with spring water samples providing original results of great interest. Research is under way to allow the use of the chamber also for gas concentration measurements in water samples with a new technique.
The activity is carried out mainly in the environmental laboratory of the Department of Physics, the laboratory is equipped with appropriate instrumentation for concentrations of radionuclides in environmental matrices (such as food or waste) and has adequate instrumentation for radon gas concentration measurements in water, air and materials. The activity started in 2012 and external collaborations with colleagues from the Earth Science Department, CNR and ArpaCAL led to the production of a regional law proposal for protection against radon gas hazards (http://www .consiglioregionale.calabria.it/pl9/347.htm).

A. PUBLICATIONS ON SCIENTIFIC JOURNALS

A.1 Publications on international scientific journals

A.1.1 Publications on international scientific journals published in 2013-2016

ZEUS Collaboration

15. Capua M., Tassi E., Zeus Collaboration
Measurement of $D^{\pm}$ Production in Deep Inelastic ep Scattering with the ZEUS detector.
JHEP 05 (2013) 023

16. Capua M., Tassi E., Zeus Collaboration
Measurement of $D^{*\pm}$Production in Deep Inelastic Scattering at HERA.
JHEP 05 (2013) 097 and Erratum JHEP 02 (2014) 106

1. Capua M., Tassi E., Zeus Collaboration
Measurement of Charm Fragmentation Fractions in Photoproduction at HERA.
JHEP 09 (2013) 058

7. Capua M., Tassi E., Zeus Collaboration
Photoproduction of Isolated Photons, Inclusively and with a jet, at HERA.
Phys. Lett. B 730 (2014) 293-301

8. Capua M., Tassi E., Zeus Collaboration
Measurament of Neutral Current $e^{\pm}p$ Cross Sections at High Bjorken x with the ZEUS Detector.
Phys. Rev. D 89 (2014) 072007

9. Capua M., Tassi E., Zeus Collaboration
Deep inelastic cross-section measurements at large y with the ZEUS detector at HERA.
Phys. Rev. D 90 (2014) 072002

10. Capua M., Tassi E., Zeus Collaboration
Measurement of D^{*} photoproduction at three different centre-of-mass energies at HERA.
JHEP 10 (2014) 003

11. Capua M., Tassi E., Zeus Collaboration
Measurement of beauty and charm production in deep inelastic scattering at HERA and measurement of the beauty-quark mass.
JHEP 09 (2014) 127

12. Capua M., Tassi E., Zeus Collaboration
Further studies of the photoproduction of isolated photons with a jet at HERA.
JHEP 08 (2014) 023

13. Capua M., Tassi E., H1 and Zeus Collaboration
Combination of Differential $D^{*\pm}$ Cross-Section Measurements in Deep-Inelastic ep Scattering at HERA.
JHEP 09 (2015) 149

14. Capua M., Tassi E., H1 and Zeus Collaboration
Combination of Measurements of Inclusive Deep Inelastic e+p Scattering Cross sections and QCD Analysis of HERA Data.

Eur. Phys. J. C 75 (2015) 580

15. Capua M., Tassi E., Zeus Collaboration
Production of exclusive dijets in diffractive deep inelastic scattering at HERA.
Eur. Phys. J. C 76 (2016) 1

16. Capua M., Tassi E., Zeus Collaboration
Measurement of the cross-section ratio $\sigma_{\psi(2S)}/\sigma_{J/\psi(1S)}$ in deep inelastic exclusive ep scattering at HERA.
Nucl. Phys. B 909 (2016) 934

17. Capua M., Tassi E., Zeus Collaboration
Limits on the effective quark radius from inclusive ep scattering at HERA.
Phys. Lett. B 757 (2016) 468

18. Capua M., Tassi E., Zeus Collaboration
Combined QCD and electroweak analysis of HERA data.
Phys. Rev. D 93 (2016) 092002

19. Capua M., Tassi E., Zeus Collaboration
Search for a narrow baryonic state decaying to pK^0_S and $p(bar)K^0_S$ in deep inelastic scattering at HERA.
Phys. Lett. B 759 (2016) 446

ATLAS Collaboration

1. Capua M., Crosetti G., La Rotonda L., Tassi E., Atlas Collaboration
Measurement of the cross-section for producing a W boson in association with a single top quark in pp collisions at $\sqrt{s}$=13 TeV with ATLAS.
arXiv:1612.07231 [hep-ex]

2. Capua M., Crosetti G., La Rotonda L., Tassi E., Atlas Collaboration
Measurements of top-quark pair differential cross-sections in the eμ channel in pp collisions at $\sqrt{s}$ =13 TeV using the
ATLAS detector.
arXiv:1612.05220 [hep-ex]

3. Capua M., Crosetti G., La Rotonda L., Tassi E., Atlas Collaboration
Precision measurement and interpretation of inclusive W^+, W^- and Z/γ production cross sections with the ATLAS*
detector
arXiv:1612.03016 [hep-ex]

4. Capua M., Crosetti G., La Rotonda L., Tassi E., Atlas Collaboration
Measurement of the W boson polarisation in t\bar{t} events from pp collisions at $\sqrt{s}$ =8 TeV in the lepton+jets channel with ATLAS
arXiv:1612.02577 [hep-ex]

5. Capua M., Crosetti G., La Rotonda L., Tassi E., Atlas Collaboration
Reconstruction of primary vertices at the ATLAS experiment in Run 1 proton-proton collisions at the LHC

arXiv:1611.10235 [physics.ins-det]

6. Capua M., Crosetti G., La Rotonda L., Tassi E., Atlas Collaboration
Performance of the ATLAS Trigger System in 2015
arXiv:1611.09661 [hep-ex].

7. Capua M., Crosetti G., La Rotonda L., Tassi E., Atlas Collaboration
Measurement of W^+W^- vector-boson scattering and limits on anomalous quartic gauge couplings with the ATLAS detector.
arXiv:1611.02428 [hep-ex]

8. Capua M., Crosetti G., La Rotonda L., Tassi E., Atlas Collaboration
Measurements of long-range azimuthal anisotropies and associated Fourier coefficients for pp collisions at √s =5.02 and 13 TeV and p+Pb collisions at √s{NN}=5.02 TeV with the ATLAS detector
arXiv:1609.06213 [nucl-ex]

9. Capua M., Crosetti G., La Rotonda L., Tassi E., Atlas Collaboration
A measurement of material in the ATLAS tracker using secondary hadronic interactions in 7 TeV pp collisions
JINST 11 (2016) no.11, P11020

10. Capua M., Crosetti G., La Rotonda L., Tassi E., Atlas Collaboration
Measurement of the inclusive cross-sections of single top-quark and top-antiquark t-channel production in pp collisions at √s =13 TeV with the ATLAS detector
arXiv:1609.03920 [hep-ex]

11. Capua M., Crosetti G., La Rotonda L., Tassi E., Atlas Collaboration
Luminosity determination in pp collisions at √s =8 TeV using the ATLAS detector at the LHC
Eur.Phys.J. C76 (2016) no.12, 653

12. Capua M., Crosetti G., La Rotonda L., Tassi E., Atlas Collaboration
Measurement of W^+W^- production in association with one jet in proton--proton collisions at √s =8 TeV with the ATLAS detector
Capua M., Crosetti G., La Rotonda L., Tassi E., Atlas Collaboration
Phys.Lett. B763 (2016) 114-133

13. Capua M., Crosetti G., La Rotonda L., Tassi E., Atlas Collaboration
Search for dark matter produced in association with a hadronically decaying vector boson in pp collisions at √s =13 TeV with the ATLAS detector
Phys.Lett. B763 (2016) 251-268

14. Capua M., Crosetti G., La Rotonda L., Tassi E., Atlas Collaboration
Study of hard double-parton scattering in four-jet events in pp collisions at √s =7 TeV with the ATLAS experiment
JHEP 1611 (2016) 110.

15. Capua M., Crosetti G., La Rotonda L., Tassi E., Atlas Collaboration
Search for Minimal Supersymmetric Standard Model Higgs bosons H/A and for a Z' boson in the ττ final state
produced in pp collisions at √s =13 TeV with the ATLAS Detector.
Eur.Phys.J. C76 (2016) no.11, 585

16. Capua M., Crosetti G., La Rotonda L., Tassi E., Atlas Collaboration
Dark matter interpretations of ATLAS searches for the electroweak production of supersymmetric particles in √s =8 TeV proton-proton collisions
JHEP 1609 (2016) 175

17. Capua M., Crosetti G., La Rotonda L., Tassi E., Atlas Collaboration
Measurement of the b\overline{b} dijet cross section in pp collisions √s =7 TeV with the ATLAS detector
Eur.Phys.J. C76 (2016) no.12, 670

18. Capua M., Crosetti G., La Rotonda L., Tassi E., Atlas Collaboration
Search for new phenomena in different-flavour high-mass dilepton final states in pp collisions at √s =13 TeV with the ATLAS detector
Eur.Phys.J. C76 (2016) no.10, 541

19. Capua M., Crosetti G., La Rotonda L., Tassi E., Atlas Collaboration
Measurement of top quark pair differential cross-sections in the dilepton channel in pp collisions at √s = 7 and 8 TeV with ATLAS
Phys.Rev. D94 (2016) no.9, 092003

20. Capua M., Crosetti G., La Rotonda L., Tassi E., Atlas Collaboration
Measurement of the total cross section from elastic scattering in pp collisions at √s =8 TeV with the ATLAS detector
Phys.Lett. B761 (2016) 158-178

21. Capua M., Crosetti G., La Rotonda L., Tassi E., Atlas Collaboration
Search for squarks and gluinos in events with hadronically decaying tau leptons, jets and missing transverse momentum in proton–proton collisions at √s =13 TeV recorded with the ATLAS detector
Eur.Phys.J. C76 (2016) no.12, 683

22. Capua M., Crosetti G., La Rotonda L., Tassi E., Atlas Collaboration
Measurement of exclusive γτ→W^+W^- production and search for exclusive Higgs boson production in pp collisions at √s =8 TeV using the ATLAS detector
Phys.Rev. D94 (2016) no.3, 032011

23. Capua M., Crosetti G., La Rotonda L., Tassi E., Atlas Collaboration
Search for high-mass new phenomena in the dilepton final state using proton-proton collisions at √s =13 TeV with the ATLAS detector
Phys.Lett. B761 (2016) 372-392

24. Capua M., Crosetti G., La Rotonda L., Tassi E., Atlas Collaboration
Search for Higgs and Z Boson Decays to ϕγ with the ATLAS Detector
Phys.Rev.Lett. 117 (2016) no.11, 111802

25. Capua M., Crosetti G., La Rotonda L., Tassi E., Atlas Collaboration
Measurement of jet activity in top quark events using the eμ final state with two b-tagged jets in pp collisions at √s =8 TeV with the ATLAS detector
JHEP 1609 (2016) 074

26. Capua M., Crosetti G., La Rotonda L., Tassi E., Atlas Collaboration
Search for supersymmetry in a final state containing two photons and missing transverse momentum in √s =13 TeV pp collisions at the LHC using the ATLAS detector
Eur.Phys.J. C76 (2016) no.9, 517

27. Capua M., Crosetti G., La Rotonda L., Tassi E., Atlas Collaboration
Search for bottom squark pair production in proton–proton collisions at √s =13 TeV with the ATLAS detector
Eur.Phys.J. C76 (2016) no.10, 547

28. Capua M., Crosetti G., La Rotonda L., Tassi E., Atlas Collaboration
Search for the Higgs boson produced in association with a W boson and decaying to four b-quarks via two spin-zero particles in pp collisions at 13 TeV with the ATLAS detector
Eur.Phys.J. C76 (2016) no.11, 605

29. Capua M., Crosetti G., La Rotonda L., Tassi E., Atlas Collaboration
Measurement of forward-backward multiplicity correlations in lead-lead, proton-lead and proton-proton collisions with the ATLAS detector
arXiv:1606.08170 [hep-ex]

30. Capua M., Crosetti G., La Rotonda L., Tassi E., Atlas Collaboration
The performance of the jet trigger for the ATLAS detector during 2011 data taking
Eur.Phys.J. C76 (2016) no.10, 526

31. Capua M., Crosetti G., La Rotonda L., Tassi E., Atlas Collaboration
Search for heavy long-lived charged R-hadrons with the ATLAS detector in 3.2 fb^{-1} of proton--proton collision data at √s =13 TeV
Phys.Lett. B760 (2016) 647-665

32. Capua M., Crosetti G., La Rotonda L., Tassi E., Atlas Collaboration
Searches *for heavy diboson resonances in pp collisions at √s =13 TeV with the ATLAS detector*
JHEP 1609 (2016) 173

33. Capua M., Crosetti G., La Rotonda L., Tassi E., Atlas Collaboration
Search *for pair production of Higgs bosons in the b\bar{b}b\bar{b} final state using proton--proton collisions at √s =13 TeV with the ATLAS detector*
Phys.Rev. D94 (2016) no.5, 052002

34. Capua M., Crosetti G., La Rotonda L., Tassi E., Atlas Collaboration
Measurement of the $W^{\pm}Z$ boson pair-production cross section in pp collisions at √s =13 TeV with the ATLAS Detector
Phys.Lett. B762 (2016) 1-22
35. Capua M., Crosetti G., La Rotonda L., Tassi E., Atlas Collaboration
Search for new resonances in events with one lepton and missing transverse momentum in pp collisions at √s =13 TeV with the ATLAS detector
Phys.Lett. B762 (2016) 334-352

36. Capua M., Crosetti G., La Rotonda L., Tassi E., Atlas Collaboration
Search for top squarks in final states with one isolated lepton, jets, and missing transverse momentum in √s =13 TeV pp collisions with the ATLAS detector
Phys.Rev. D94 (2016) no.5, 052009

37. Capua M., Crosetti G., La Rotonda L., Tassi E., Atlas Collaboration
Search for resonances in diphoton events at √s =13 TeV with the ATLAS detector
JHEP 1609 (2016) 001

38. Capua M., Crosetti G., La Rotonda L., Tassi E., Atlas Collaboration
Measurement of the t\bar{t} production cross-section using eμ events with b-tagged jets in pp collisions at √s =13 TeV with the ATLAS detector
Phys.Lett. B761 (2016) 136-157

39. Capua M., Crosetti G., La Rotonda L., Tassi E., Atlas Collaboration
Measurement of the Inelastic Proton-Proton Cross Section at √s =13 TeV TeV with the ATLAS Detector at the LHC
Phys.Rev.Lett. 117 (2016) no.18, 182002

40. Capua M., Crosetti G., La Rotonda L., Tassi E., Atlas Collaboration
Measurements of the Higgs boson production and decay rates and constraints on its couplings from a combined ATLAS and CMS analysis of the LHC pp collision data at √s =7 and 8 TeV
JHEP 1608 (2016) 045

41. Capua M., Crosetti G., La Rotonda L., Tassi E., Atlas Collaboration
Search for TeV-scale gravity signatures in high-mass final states with leptons and jets with the ATLAS detector at √s =13 TeV
Phys.Lett. B760 (2016) 520-537

42. Capua M., Crosetti G., La Rotonda L., Tassi E., Atlas Collaboration
Search for the Standard Model Higgs boson produced by vector-boson fusion and decaying to bottom quarks in √s =8 TeV pp collisions with the ATLAS detector
JHEP 1611 (2016) 112

43. Capua M., Crosetti G., La Rotonda L., Tassi E., Atlas Collaboration
Measurement of the top quark mass in the t\bar{t}→ dilepton channel from √s =8 TeV ATLAS data
Phys.Lett. B761 (2016) 350-371

44. Capua M., Crosetti G., La Rotonda L., Tassi E., Atlas Collaboration
Measurement *of the photon identification efficiencies with the ATLAS detector using LHC Run-1 data*
Eur.Phys.J. C76 (2016) no.12, 666

45. Capua M., Crosetti G., La Rotonda L., Tassi E., Atlas Collaboration
Measurement of the double-differential high-mass Drell-Yan cross section in pp collisions at √s =8 TeV with the ATLAS detector
JHEP 1608 (2016) 009

46. Capua M., Crosetti G., La Rotonda L., Tassi E., Atlas Collaboration
Charged-particle distributions at low transverse momentum in √s =13 TeV pp interactions measured with the ATLAS detector at the LHC
Eur.Phys.J. C76 (2016) no.9, 502

47. Capua M., Crosetti G., La Rotonda L., Tassi E., Atlas Collaboration

Measurement of the angular coefficients in -boson events using electron and muon pairs from data taken at √s =8 TeV with the ATLAS detector
JHEP 1608 (2016) 159

48. Capua M., Crosetti G., La Rotonda L., Tassi E., Atlas Collaboration
Search for pair production of gluinos decaying via stop and sbottom in events with b-jets and large missing transverse momentum in pp collisions at √s =13 TeV with the ATLAS detector
Phys.Rev. D94 (2016) no.3, 032003

49. Capua M., Crosetti G., La Rotonda L., Tassi E., Atlas Collaboration
Measurement of the relative width difference of the B^0-\bar B^0 system with the ATLAS detector
JHEP 1606 (2016) 081

50. Capua M., Crosetti G., La Rotonda L., Tassi E., Atlas Collaboration
Transverse momentum, rapidity, and centrality dependence of inclusive charged-particle production in √s{NN} = 5.02 TeV p+Pb collisions measured by the ATLAS experiment
Phys.Lett. B763 (2016) 313-336

51. Capua M., Crosetti G., La Rotonda L., Tassi E., Atlas Collaboration
Search *for scalar leptoquarks in pp collisions at √s =13 TeV with the ATLAS experiment*
New J.Phys. 18 (2016) no.9, 093016

52. Capua M., Crosetti G., La Rotonda L., Tassi E., Atlas Collaboration
Search for gluinos in events with an isolated lepton, jets and missing transverse momentum at √s =13 TeV with the ATLAS detector
Eur.Phys.J. C76 (2016) no.10, 565

53. Capua M., Crosetti G., La Rotonda L., Tassi E., Atlas Collaboration
Search for squarks and gluinos in final states with jets and missing transverse momentum at √s =13 TeV with the ATLAS detector
Eur.Phys.J. C76 (2016) no.7, 392

54. Capua M., Crosetti G., La Rotonda L., Tassi E., Atlas Collaboration
Measurement of the inclusive isolated prompt photon cross section in pp collisions at √s =8 TeV with the ATLAS detector
JHEP 1608 (2016) 005

55. Capua M., Crosetti G., La Rotonda L., Tassi E., Atlas Collaboration
Search for new phenomena in final states with an energetic jet and large missing transverse momentum in pp collisions at √s =13 TeV using the ATLAS detector
Phys.Rev. D94 (2016) no.3, 032005

56. Capua M., Crosetti G., La Rotonda L., Tassi E., Atlas Collaboration
Measurements of the charge asymmetry in top-quark pair production in the dilepton final state at √s =8 TeV with the ATLAS detector
Phys.Rev. D94 (2016) no.3, 032006

57. Capua M., Crosetti G., La Rotonda L., Tassi E., Atlas Collaboration
Measurements of Zγ and Zγγ production in pp collisions at √s =8 TeV with the ATLAS detector
Phys.Rev. D93 (2016) no.11, 112002

58. Capua M., Crosetti G., La Rotonda L., Tassi E., Atlas Collaboration
Search for metastable heavy charged particles with large ionization energy loss in pp collisions at √s =13 TeV using the ATLAS experiment
Phys.Rev. D93 (2016) no.11, 112015

59. Capua M., Crosetti G., La Rotonda L., Tassi E., Atlas Collaboration
Study of the rare decays of B^0_s and B^0 into muon pairs from data collected during the LHC Run 1 with the ATLAS detector
Eur.Phys.J. C76 (2016) no.9, 513

60. Capua M., Crosetti G., La Rotonda L., Tassi E., Atlas Collaboration
Search for the Standard Model Higgs boson decaying into b\overline{b} produced in association with top quarks decaying hadronically in pp collisions at √s =8 TeV with the ATLAS detector
JHEP 1605 (2016) 160

61. Capua M., Crosetti G., La Rotonda L., Tassi E., Atlas Collaboration
Measurement of fiducial differential cross sections of gluon-fusion production of Higgs bosons decaying to WW→evμv with the ATLAS detector at √s =8 TeV*
JHEP 1608 (2016) 104

62. Capua M., Crosetti G., La Rotonda L., Tassi E., Atlas Collaboration
Search for new phenomena in events with a photon and missing transverse momentum in pp collisions at √s =13 TeV with the ATLAS detector
JHEP 1606 (2016) 059

63. Capua M., Crosetti G., La Rotonda L., Tassi E., Atlas Collaboration
Measurement of $W^{\pm}$ and Z-boson production cross sections in pp collisions at √s =13 TeV with the ATLAS detector
Phys.Lett. B759 (2016) 601-621

64. Capua M., Crosetti G., La Rotonda L., Tassi E., Atlas Collaboration
Search for charged Higgs bosons produced in association with a top quark and decaying via $H^{\pm}$→τv using pp collision data recorded at √s =13 TeV by the ATLAS detector
Phys.Lett. B759 (2016) 555-574

65. Capua M., Crosetti G., La Rotonda L., Tassi E., Atlas Collaboration
Beam-induced and cosmic-ray backgrounds observed in the ATLAS detector during the LHC 2012 proton-proton running period
JINST 11 (2016) no.05, P05013

66. Capua M., Crosetti G., La Rotonda L., Tassi E., Atlas Collaboration
Search for resonances in the mass distribution of jet pairs with one or two jets identified as b-jets in proton--proton collisions at √s =13 TeV with the ATLAS detector
Phys.Lett. B759 (2016) 229-246

67. Capua M., Crosetti G., La Rotonda L., Tassi E., Atlas Collaboration
Muon reconstruction performance of the ATLAS detector in proton–proton collision data at √s =13 TeV
Eur.Phys.J. C76 (2016) no.5, 292

68. Capua M., Crosetti G., La Rotonda L., Tassi E., Atlas Collaboration
Identification of high transverse momentum top quarks in pp collisions at $\sqrt{s}$ =8 TeV with the ATLAS detector
JHEP 1606 (2016) 093

69. Capua M., Crosetti G., La Rotonda L., Tassi E., Atlas Collaboration
Topological cell clustering in the ATLAS calorimeters and its performance in LHC Run 1
arXiv:1603.02934 [hep-ex]

70. Capua M., Crosetti G., La Rotonda L., Tassi E., Atlas Collaboration
Charged-particle distributions in pp interactions at $\sqrt{s}$ =8 TeV measured with the ATLAS detector
Eur.Phys.J. C76 (2016) no.7, 403.

71. Capua M., Crosetti G., La Rotonda L., Tassi E., Atlas Collaboration
Measurements of $W^{\pm}Z$ production cross sections in pp collisions at $\sqrt{s}$ =8 TeV with the ATLAS detector and limits on anomalous gauge boson self-couplings
Phys.Rev. D93 (2016) no.9, 092004

72. Capua M., Crosetti G., La Rotonda L., Tassi E., Atlas Collaboration
Measurement of total and differential $W^{+}W^{-}$ production cross sections in proton-proton collisions at $\sqrt{s}$ =8 TeV with the ATLAS detector and limits on anomalous triple-gauge-boson couplings
JHEP 1609 (2016) 029

73. Capua M., Crosetti G., La Rotonda L., Tassi E., Atlas Collaboration
Search for supersymmetry at $\sqrt{s}$ =13 TeV in final states with jets and two same-sign leptons or three leptons with the ATLAS detector
Eur.Phys.J. C76 (2016) no.5, 259

74. Capua M., Crosetti G., La Rotonda L., Tassi E., Atlas Collaboration
Measurement of event-shape observables in $Z \rightarrow l^{+}l^{-}$ events in pp collisions at $\sqrt{s}$ =7 TeV with the ATLAS detector at the LHC
Eur.Phys.J. C76 (2016) no.7, 375

75. Capua M., Crosetti G., La Rotonda L., Tassi E., Atlas Collaboration
Search for new phenomena in final states with large jet multiplicities and missing transverse momentum with ATLAS using $\sqrt{s}$ =13 TeV proton-proton collisions
Phys.Lett. B757 (2016) 334-355

76. Capua M., Crosetti G., La Rotonda L., Tassi E., Atlas Collaboration
Search for single production of a vector-like quark via a heavy gluon in the 4b final state with the ATLAS detector in pp collisions at $\sqrt{s}$ =8 TeV
Phys.Lett. B758 (2016) 249-268

77. Capua M., Crosetti G., La Rotonda L., Tassi E., Atlas Collaboration
Search for single production of vector-like quarks decaying into Wb in pp collisions at $\sqrt{s}$ =8 TeV with the ATLAS detector
Eur.Phys.J. C76 (2016) no.8, 442

78. Capua M., Crosetti G., La Rotonda L., Tassi E., Atlas Collaboration

Test of CP Invariance in vector-boson fusion production of the Higgs boson using the Optimal Observable method in the ditau decay channel with the ATLAS detector
Eur.Phys.J. C76 (2016) no.12, 658

79. Capua M., Crosetti G., La Rotonda L., Tassi E., Atlas Collaboration
arged-particle distributions in \√s =13 TeV pp interactions measured with the ATLAS detector at the LHC
Phys.Lett. B758 (2016) 67-88

80. Capua M., Crosetti G., La Rotonda L., Tassi E., Atlas Collaboration
Measurement of the charged-particle multiplicity inside jets from √s =8 TeV pp collisions with the ATLAS detector
Eur.Phys.J. C76 (2016) no.6, 322

81. Capua M., Crosetti G., La Rotonda L., Tassi E., Atlas Collaboration
A search for top squarks with R-parity-violating decays to all-hadronic final states with the ATLAS detector in √s =8 TeV proton-proton collisions
JHEP 1606 (2016) 067

82. Capua M., Crosetti G., La Rotonda L., Tassi E., Atlas Collaboration
A search for an excited muon decaying to a muon and two jets in pp collisions at √s =8 TeV with the ATLAS detector
New J.Phys. 18 (2016) no.7, 073021

83. Capua M., Crosetti G., La Rotonda L., Tassi E., Atlas Collaboration
Probing lepton flavour violation via neutrinoless $\tau \rightarrow 3\mu$ decays with the ATLAS detector
Eur.Phys.J. C76 (2016) no.5, 232

84. Capua M., Crosetti G., La Rotonda L., Tassi E., Atlas Collaboration
Measurement of the CP-violating phase ϕ_s and the B^0_s meson decay width difference with $B^0_s \rightarrow J/\psi\phi$ decays in ATLAS
JHEP 1608 (2016) 147

85. Capua M., Crosetti G., La Rotonda L., Tassi E., Atlas Collaboration
Measurement of the charge asymmetry in highly boosted top-quark pair production in √s =8 TeV pp collision data collected by the ATLAS experiment
Phys.Lett. B756 (2016) 52-71

86. Capua M., Crosetti G., La Rotonda L., Tassi E., Atlas Collaboration
Reconstruction of hadronic decay products of tau leptons with the ATLAS experiment
Eur.Phys.J. C76 (2016) no.5, 295

87. Capua M., Crosetti G., La Rotonda L., Tassi E., Atlas Collaboration
Search for new phenomena with photon+jet events in proton-proton collisions at √s =13 TeV with the ATLAS detector
JHEP 1603 (2016) 041

88. Capua M., Crosetti G., La Rotonda L., Tassi E., Atlas Collaboration
Measurement of the ZZ Production Cross Section in pp Collisions at √s =13 TeV with the ATLAS Detector
Phys.Rev.Lett. 116 (2016) no.10, 101801

89. Capua M., Crosetti G., La Rotonda L., Tassi E., Atlas Collaboration
Combination of searches for WW, WZ, and ZZ resonances in pp collisions at √s =8 TeV with the ATLAS detector
Phys.Lett. B755 (2016) 285-305.

90. Capua M., Crosetti G., La Rotonda L., Tassi E., Atlas Collaboration
Search for charged Higgs bosons in the $H^{\pm} \rightarrow tb$ decay channel in pp collisions at √s =8 TeV using the ATLAS detector
JHEP 1603 (2016) 127

91. Capua M., Crosetti G., La Rotonda L., Tassi E., Atlas Collaboration
Measurement of the differential cross-sections of prompt and non-prompt production of J/ψ and φ(2S) in pp collisions at √s =7 and 8 TeV with the ATLAS detector
Eur.Phys.J. C76 (2016) no.5, 283

92. Capua M., Crosetti G., La Rotonda L., Tassi E., Atlas Collaboration
Measurement of $D^{*\pm}$, $D^{\pm}$ and $D_s^{\pm}$ meson production cross sections in pp collisions at √s =7 TeV with the ATLAS detector
Nucl.Phys. B907 (2016) 717-763

93. Capua M., Crosetti G., La Rotonda L., Tassi E., Atlas Collaboration
Search for strong gravity in multijet final states produced in pp collisions at √s =13 TeV using the ATLAS detector at the LHC
JHEP 1603 (2016) 026

94. Capua M., Crosetti G., La Rotonda L., Tassi E., Atlas Collaboration
Measurement of the transverse momentum and φ^*_η distributions of Drell–Yan lepton pairs in proton–proton collisions at √s =8 TeV with the ATLAS detector
Eur.Phys.J. C76 (2016) no.5, 291

95. Capua M., Crosetti G., La Rotonda L., Tassi E., Atlas Collaboration
Search for new phenomena in dijet mass and angular distributions from pp collisions at √s =13 TeV with the ATLAS detector
Phys.Lett. B754 (2016) 302-322

96. Capua M., Crosetti G., La Rotonda L., Tassi E., Atlas Collaboration
Performance of b-Jet Identification in the ATLAS Experiment
JINST 11 (2016) no.04, P04008

97. Capua M., Crosetti G., La Rotonda L., Tassi E., Atlas Collaboration
Top quark studies with the ATLAS detector
By ATLAS Collaboration (Marcella Capua for the collaboration).
Int.J.Mod.Phys.Conf.Ser. 39 (2015) 1560092.

98. Capua M., Crosetti G., La Rotonda L., Tassi E., Atlas Collaboration
Measurement of the dependence of transverse energy production at large pseudorapidity on the hard-scattering kinematics of proton-proton collisions at √s = 2.76 TeV with ATLAS
Phys.Lett. B756 (2016) 10-28

99. Capua M., Crosetti G., La Rotonda L., Tassi E., Atlas Collaboration

Search for the Standard Model Higgs boson produced in association with a vector boson and decaying into a tau pair in pp collisions at √s =8 TeV TeV with the ATLAS detector
Phys.Rev. D93 (2016) no.9, 092005

100. Capua M., Crosetti G., La Rotonda L., Tassi E., Atlas Collaboration
Evidence for single top-quark production in the s-channel in proton-proton collisions at √s =8 TeV with the ATLAS detector using the Matrix Element Method
Phys.Lett. B756 (2016) 228-246

101. Capua M., Crosetti G., La Rotonda L., Tassi E., Atlas Collaboration
A search for prompt lepton-jets in pp collisions at √s =8 TeV with the ATLAS detector
JHEP 1602 (2016) 062

102. Capua M., Crosetti G., La Rotonda L., Tassi E., Atlas Collaboration
Measurements of top-quark pair differential cross-sections in the lepton+jets channel in pp collisions at √s =8 TeV using the ATLAS detector
Eur.Phys.J. C76 (2016) no.10, 538

103. Capua M., Crosetti G., La Rotonda L., Tassi E., Atlas Collaboration
Dijet production in √s =7 TeV pp collisions with large rapidity gaps at the ATLAS experiment
Phys.Lett. B754 (2016) 214-234

104. Capua M., Crosetti G., La Rotonda L., Tassi E., Atlas Collaboration
Measurement of the correlations between the polar angles of leptons from top quark decays in the helicity basis at √s =7 TeV using the ATLAS detector
Phys.Rev. D93 (2016) no.1, 012002

105. Capua M., Crosetti G., La Rotonda L., Tassi E., Atlas Collaboration
Search for dark matter produced in association with a Higgs boson decaying to two bottom quarks in pp collisions at √s =8 TeV with the ATLAS detector
Phys.Rev. D93 (2016) no.7, 072007

106. Capua M., Crosetti G., La Rotonda L., Tassi E., Atlas Collaboration
Identification of boosted, hadronically decaying W bosons and comparisons with ATLAS data taken at √s =8 TeV
Eur.Phys.J. C76 (2016) no.3, 154

107. Capua M., Crosetti G., La Rotonda L., Tassi E., Atlas Collaboration
Performance of pile-up mitigation techniques for jets in pp collisions at √s =8 TeV using the ATLAS detector
Eur.Phys.J. C76 (2016) no.11, 581

108. Capua M., Crosetti G., La Rotonda L., Tassi E., Atlas Collaboration
Measurement of the differential cross-section of highly boosted top quarks as a function of their transverse momentum in √s =8 TeV proton-proton collisions using the ATLAS detector
Phys.Rev. D93 (2016) no.3, 032009

109. Capua M., Crosetti G., La Rotonda L., Tassi E., Atlas Collaboration
Search for anomalous couplings in the Wtb vertex from the measurement of double differential angular decay rates of single top quarks produced in the t-channel with the ATLAS detector
JHEP 1604 (2016) 023

110. Capua M., Crosetti G., La Rotonda L., Tassi E., Atlas Collaboration
Measurement of the production cross-section of a single top quark in association with a W boson at 8 TeV with the ATLAS experiment
JHEP 1601 (2016) 064

111. Capua M., Crosetti G., La Rotonda L., Tassi E., Atlas Collaboration
Search for the production of single vector-like and excited quarks in the Wt final state in pp collisions at √s =8 TeV with the ATLAS detector
JHEP 1602 (2016) 110

112. Capua M., Crosetti G., La Rotonda L., Tassi E., Atlas Collaboration
Search for magnetic monopoles and stable particles with high electric charges in 8 TeV pp collisions with the ATLAS detector
Phys.Rev. D93 (2016) no.5, 052009

113. Capua M., Crosetti G., La Rotonda L., Tassi E., Atlas Collaboration
Measurements of four-lepton production in pp collisions at √s =8 TeV with the ATLAS detector
Phys.Lett. B753 (2016) 552-572

114. Capua M., Crosetti G., La Rotonda L., Tassi E., Atlas Collaboration
Measurement of four-jet differential cross sections in √s =8 TeV proton-proton collisions using the ATLAS detector
JHEP 1512 (2015) 105

115. Capua M., Crosetti G., La Rotonda L., Tassi E., Atlas Collaboration
Search for the electroweak production of supersymmetric particles in √s =8 TeV pp collisions with the ATLAS detector
Phys.Rev. D93 (2016) no.5, 052002

116. Capua M., Crosetti G., La Rotonda L., Tassi E., Atlas Collaboration
Search for flavour-changing neutral current top quark decays t-> Hq in pp collisions at √s =8 TeV with the ATLAS detector
JHEP 1512 (2015) 061

117. Capua M., Crosetti G., La Rotonda L., Tassi E., Atlas Collaboration
Measurement of the t\overline{t}W and t\overline{t}Z production cross sections in pp collisions at √s =8 TeV with the ATLAS detector
JHEP 1511 (2015) 172

118. Capua M., Crosetti G., La Rotonda L., Tassi E., Atlas Collaboration
Measurement of jet charge in dijet events from √s =8 TeV pp collisions with the ATLAS detector
Phys.Rev. D93 (2016) no.5, 052003

119. Capua M., Crosetti G., La Rotonda L., Tassi E., Atlas Collaboration
Search for new phenomena in events with at least three photons collected in pp collisions at √s =8 TeV with the ATLAS detector
Eur.Phys.J. C76 (2016) no.4, 210

120. Capua M., Crosetti G., La Rotonda L., Tassi E., Atlas Collaboration

Search for direct top squark pair production in final states with two tau leptons in pp collisions at √s =8 TeV with the ATLAS detector
Eur.Phys.J. C76 (2016) no.2, 81

121. Capua M., Crosetti G., La Rotonda L., Tassi E., Atlas Collaboration
A new method to distinguish hadronically decaying boosted Z bosons from W bosons using the ATLAS detector
Eur.Phys.J. C76 (2016) no.5, 238

122. Capua M., Crosetti G., La Rotonda L., Tassi E., Atlas Collaboration
Observation of Long-Range Elliptic Azimuthal Anisotropies in √s =13 and 2.76 TeV pp Collisions with the ATLAS Detector
Phys.Rev.Lett. 116 (2016) no.17, 172301

123. Capua M., Crosetti G., La Rotonda L., Tassi E., Atlas Collaboration
Searches for Higgs boson pair production in the hh→ bbττ, γγWW, γγbb, bbbb channels with the ATLAS detector*
Phys.Rev. D92 (2015) 092004

124. Capua M., Crosetti G., La Rotonda L., Tassi E., Atlas Collaboration
Search for pair production of a new heavy quark that decays into a W boson and a light quark in pp collisions at √s =8 TeV with the ATLAS detector
Phys.Rev. D92 (2015) no.11, 112007

125. Capua M., Crosetti G., La Rotonda L., Tassi E., Atlas Collaboration
Measurement of the charge asymmetry in top-quark pair production in the lepton-plus-jets final state in pp collision data at √s =8 TeV with the ATLAS detector
Eur.Phys.J. C76 (2016) no.2, 87

126. Capua M., Crosetti G., La Rotonda L., Tassi E., Atlas Collaboration
Constraints on new phenomena via Higgs boson couplings and invisible decays with the ATLAS detector
JHEP 1511 (2015) 206

127. Capua M., Crosetti G., La Rotonda L., Tassi E., Atlas Collaboration
Search for a high-mass Higgs boson decaying to a W boson pair in pp collisions at √s =8 TeV with the ATLAS detector
JHEP 1601 (2016) 032

128. Capua M., Crosetti G., La Rotonda L., Tassi E., Atlas Collaboration
Search for single top-quark production via flavour-changing neutral currents at 8 TeV with the ATLAS detector
Eur.Phys.J. C76 (2016) no.2, 55

129. Capua M., Crosetti G., La Rotonda L., Tassi E., Atlas Collaboration
Search for invisible decays of a Higgs boson using vector-boson fusion in pp collisions at √s =8 TeV with the ATLAS detector
JHEP 1601 (2016) 172

130. Capua M., Crosetti G., La Rotonda L., Tassi E., Atlas Collaboration

Measurements of fiducial cross-sections for t\bar{t} production with one or two additional b-jets in pp collisions at √s =8 TeV using the ATLAS detector
Eur.Phys.J. C76 (2016) no.1, 11

131. Capua M., Crosetti G., La Rotonda L., Tassi E., Atlas Collaboration
Summary of the ATLAS experiment's sensitivity to supersymmetry after LHC Run 1 — interpreted in the phenomenological MSSM
JHEP 1510 (2015) 134

132. Capua M., Crosetti G., La Rotonda L., Tassi E., Atlas Collaboration
Search for flavour-changing neutral current top-quark decays to qZ in pp collision data collected with the ATLAS detector at √s =8 TeV
Eur.Phys.J. C76 (2016) no.1, 12

133. Capua M., Crosetti G., La Rotonda L., Tassi E., Atlas Collaboration
Searches for scalar leptoquarks in pp collisions at √s =8 TeV with the ATLAS detector
Eur.Phys.J. C76 (2016) no.1, 5

134. Capua M., Crosetti G., La Rotonda L., Tassi E., Atlas Collaboration
Search for lepton-flavour-violating $H \rightarrow \mu\tau$ decays of the Higgs boson with the ATLAS detector
JHEP 1511 (2015) 211

135. Capua M., Crosetti G., La Rotonda L., Tassi E., Atlas Collaboration
Constraints on non-Standard Model Higgs boson interactions in an effective Lagrangian using differential cross sections measured in the H → γγ decay channel at √s =8 TeV with the ATLAS detector
Phys.Lett. B753 (2016) 69-85

136. Capua M., Crosetti G., La Rotonda L., Tassi E., Atlas Collaboration
Measurement of transverse energy-energy correlations in multi-jet events in pp collisions at √s =7 TeV using the ATLAS detector and determination of the strong coupling constant $\alpha_s(m_Z)$
Phys.Lett. B750 (2015) 427-447

137. Capua M., Crosetti G., La Rotonda L., Tassi E., Atlas Collaboration
Measurement of the centrality dependence of the charged-particle pseudorapidity distribution in proton–lead collisions at √s{NN} = 5.02 TeV with the ATLAS detector
Eur.Phys.J. C76 (2016) no.4, 199

138. Capua M., Crosetti G., La Rotonda L., Tassi E., Atlas Collaboration
Determination of the ratio of b-quark fragmentation fractions f_s/f_d in pp collisions at √s =7 TeV with the ATLAS detector
Phys.Rev.Lett. 115 (2015) no.26, 262001

139. Capua M., Crosetti G., La Rotonda L., Tassi E., Atlas Collaboration
Measurement of the branching ratio $\Gamma(\Lambda_b^0 \rightarrow \varphi(2S)\Lambda^0)/\gamma(\Lambda b^0$ \rightarrow J/\psi\Lambda^0$ with the ATLAS detector
Phys.Lett. B751 (2015) 63-80

140. Capua M., Crosetti G., La Rotonda L., Tassi E., Atlas Collaboration
Study of the $B_c^+ \rightarrow J/\psi\, D_s^+$ and $B_c^+ \rightarrow J/\psi\, D_s^{*+}$ decays with the ATLAS detector
Eur.Phys.J. C76 (2016) no.1, 4

141. Capua M., Crosetti G., La Rotonda L., Tassi E., Atlas Collaboration
Z boson production in p+Pb collisions at √s{NN}=5.02 TeV measured with the ATLAS detector
Phys.Rev. C92 (2015) no.4, 044915
142. Capua M., Crosetti G., La Rotonda L., Tassi E., Atlas Collaboration
Search for an additional, heavy Higgs boson in the H→ZZ decay channel at √s =8 TeV in pp collision data with the ATLAS detector
Eur.Phys.J. C76 (2016) no.1, 45

143. Capua M., Crosetti G., La Rotonda L., Tassi E., Atlas Collaboration
Summary of the searches for squarks and gluinos using √s =8 TeV pp collisions with the ATLAS experiment at the LHC
JHEP 1510 (2015) 054

144. Capua M., Crosetti G., La Rotonda L., Tassi E., Atlas Collaboration
Search for photonic signatures of gauge-mediated supersymmetry in 8 TeV pp collisions with the ATLAS detector
Phys.Rev. D92 (2015) no.7, 072001

145. Capua M., Crosetti G., La Rotonda L., Tassi E., Atlas Collaboration
Measurements of the Higgs boson production and decay rates and coupling strengths using pp collision data at √s =7 and 8 TeV in the ATLAS experiment
Eur.Phys.J. C76 (2016) no.1, 6

146. Capua M., Crosetti G., La Rotonda L., Tassi E., Atlas Collaboration
Determination of the top-quark pole mass using t\bar{t} + 1-jet events collected with the ATLAS experiment in 7 TeV pp collisions
JHEP 1510 (2015) 121

147. Capua M., Crosetti G., La Rotonda L., Tassi E., Atlas Collaboration
Measurement of the production of neighbouring jets in lead–lead collisions at √s{NN} = 2.76 TeV with the ATLAS detector
Phys.Lett. B751 (2015) 376-395

148. Capua M., Crosetti G., La Rotonda L., Tassi E., Atlas Collaboration
ATLAS Run 1 searches for direct pair production of third-generation squarks at the Large Hadron Collider
Eur.Phys.J. C75 (2015) no.10, 510, Erratum: Eur.Phys.J. C76 (2016) no.3, 153

149. Capua M., Crosetti G., La Rotonda L., Tassi E., Atlas Collaboration
Centrality, rapidity and transverse momentum dependence of isolated prompt photon production in lead-lead collisions at √s{NN} = 2.76 TeV measured with the ATLAS detector
Phys.Rev. C93 (2016) no.3, 034914

150. Capua M., Crosetti G., La Rotonda L., Tassi E., Atlas Collaboration
Measurement of exclusive γγ→l^+l^- production in proton-proton collisions at √s =7 TeV with the ATLAS detector
Phys.Lett. B749 (2015) 242-261

151. Capua M., Crosetti G., La Rotonda L., Tassi E., Atlas Collaboration

Study of (W/Z)H production and Higgs boson couplings using $H \rightarrow WW^{*}$ decays with the ATLAS detector
JHEP 1508 (2015) 137

152. Capua M., Crosetti G., La Rotonda L., Tassi E., Atlas Collaboration
Search for heavy Majorana neutrinos with the ATLAS detector in pp collisions at √s =8 TeV
JHEP 1507 (2015) 162

153. Capua M., Crosetti G., La Rotonda L., Tassi E., Atlas Collaboration
Search for the associated production of the Higgs boson with a top quark pair in multilepton final states with the ATLAS detector
Phys.Lett. B749 (2015) 519-541

154. Capua M., Crosetti G., La Rotonda L., Tassi E., Atlas Collaboration
Study of the spin and parity of the Higgs boson in diboson decays with the ATLAS detector
Eur.Phys.J. C75 (2015) no.10, 476, Erratum: Eur.Phys.J. C76 (2016) no.3, 152

155. Capua M., Crosetti G., La Rotonda L., Tassi E., Atlas Collaboration
Measurement of colour flow with the jet pull angle in t\bar{t} events using the ATLAS detector at √s =8 TeV
Phys.Lett. B750 (2015) 475-493

156. Capua M., Crosetti G., La Rotonda L., Tassi E., Atlas Collaboration
Modelling $Z \rightarrow \tau\tau$ processes in ATLAS with τ-embedded $Z \rightarrow \mu\mu$ data
JINST 10 (2015) no.09, P09018

157. Capua M., Crosetti G., La Rotonda L., Tassi E., Atlas Collaboration
Search for metastable heavy charged particles with large ionisation energy loss in pp collisions at √s =8 TeV using the ATLAS experiment
Eur.Phys.J. C75 (2015) no.9, 407

158. Capua M., Crosetti G., La Rotonda L., Tassi E., Atlas Collaboration
Measurements of the top quark branching ratios into channels with leptons and quarks with the ATLAS detector
Phys.Rev. D92 (2015) no.7, 072005

159. Capua M., Crosetti G., La Rotonda L., Tassi E., Atlas Collaboration
Search for type-III Seesaw heavy leptons in pp collisions at √s =8 TeV with the ATLAS Detector
Phys.Rev. D92 (2015) no.3, 032001

160. Capua M., Crosetti G., La Rotonda L., Tassi E., Atlas Collaboration
Search for heavy lepton resonances decaying to a Z boson and a lepton in pp collisions at √s =8 TeV with the ATLAS detector
JHEP 1509 (2015) 108

161. Capua M., Crosetti G., La Rotonda L., Tassi E., Atlas Collaboration
Search for Dark Matter in Events with Missing Transverse Momentum and a Higgs Boson Decaying to Two Photons in pp Collisions at √s =8 TeV with the ATLAS Detector
Phys.Rev.Lett. 115 (2015) no.13, 131801

162. Capua M., Crosetti G., La Rotonda L., Tassi E., Atlas Collaboration

Search for high-mass diboson resonances with boson-tagged jets in proton-proton collisions at √s =8 TeV with the ATLAS detector
JHEP 1512 (2015) 055

163. Capua M., Crosetti G., La Rotonda L., Tassi E., Atlas Collaboration
Search for Higgs boson pair production in the b\bar{b}b\bar{b} final state from pp collisions at √s =8 TeV with the ATLAS detector
Eur.Phys.J. C75 (2015) no.9, 412

164. Capua M., Crosetti G., La Rotonda L., Tassi E., Atlas Collaboration
Measurement of differential J/Ψ production cross sections and forward-backward ratios in p + Pb collisions with the ATLAS detector
Phys.Rev. C92 (2015) no.3, 034904

165. Capua M., Crosetti G., La Rotonda L., Tassi E., Atlas Collaboration
Search for new light gauge bosons in Higgs boson decays to four-lepton final states in pp collisions at √s =8 TeV with the ATLAS detector at the LHC
Phys.Rev. D92 (2015) no.9, 092001

166. Capua M., Crosetti G., La Rotonda L., Tassi E., Atlas Collaboration
A search for t\overline{t} resonances using lepton-plus-jets events in proton-proton collisions at √s =8 TeV with the ATLAS detector
JHEP 1508 (2015) 148

167. Capua M., Crosetti G., La Rotonda L., Tassi E., Atlas Collaboration
Search for production of vector-like quark pairs and of four top quarks in the lepton-plus-jets final state in pp collisions at √s =8 TeV with the ATLAS detector
JHEP 1508 (2015) 105

168. Capua M., Crosetti G., La Rotonda L., Tassi E., Atlas Collaboration
Search for Higgs bosons decaying to aa in the μμττ final state in pp collisions at √s =8 TeV with the ATLAS experiment
Phys.Rev. D92 (2015) no.5, 052002

169. Capua M., Crosetti G., La Rotonda L., Tassi E., Atlas Collaboration
Measurements of the Total and Differential Higgs Boson Production Cross Sections Combining the H→γγ and H→ZZ→4ℓ Decay Channels at √s =8 TeV with the ATLAS Detector*
Phys.Rev.Lett. 115 (2015) no.9, 091801

170. Capua M., Crosetti G., La Rotonda L., Tassi E., Atlas Collaboration
Search for high-mass diphoton resonances in pp collisions at √s =8 TeV with the ATLAS detector
Phys.Rev. D92 (2015) no.3, 032004

171. Capua M., Crosetti G., La Rotonda L., Tassi E., Atlas Collaboration
Search for massive, long-lived particles using multitrack displaced vertices or displaced lepton pairs in pp collisions at √s =8 TeV with the ATLAS detector
Phys.Rev. D92 (2015) no.7, 072004

172. Capua M., Crosetti G., La Rotonda L., Tassi E., Atlas Collaboration

Analysis of events with b-jets and a pair of leptons of the same charge in pp collisions at √s =8 TeV with the ATLAS detector
JHEP 1510 (2015) 150

173. Capua M., Crosetti G., La Rotonda L., Tassi E., Atlas Collaboration
Measurement of charged-particle spectra in Pb+Pb collisions at √s{NN} = 2.76 TeV with the ATLAS detector at the LHC
JHEP 1509 (2015) 050

174. Capua M., Crosetti G., La Rotonda L., Tassi E., Atlas Collaboration
Search for invisible decays of the Higgs boson produced in association with a hadronically decaying vector boson in pp collisions at √s =8 TeV with the ATLAS detector
Eur.Phys.J. C75 (2015) no.7, 337

175. Capua M., Crosetti G., La Rotonda L., Tassi E., Atlas Collaboration
Measurement of the top pair production cross section in 8 TeV proton-proton collisions using kinematic information in the lepton+jets final state with ATLAS
Phys.Rev. D91 (2015) no.11, 112013

176. Capua M., Crosetti G., La Rotonda L., Tassi E., Atlas Collaboration
Search for heavy long-lived multi-charged particles in pp collisions at √s =8 TeV using the ATLAS detector
Eur.Phys.J. C75 (2015) 362

177. Capua M., Crosetti G., La Rotonda L., Tassi E., Atlas Collaboration
Search for long-lived, weakly interacting particles that decay to displaced hadronic jets in proton-proton collisions at √s =8 TeV with the ATLAS detector
Phys.Rev. D92 (2015) no.1, 012010

178. Capua M., Crosetti G., La Rotonda L., Tassi E., Atlas Collaboration
Measurement of the correlation between flow harmonics of different order in lead-lead collisions at √s{NN}=2.76 TeV with the ATLAS detector
Phys.Rev. C92 (2015) no.3, 034903

179. Capua M., Crosetti G., La Rotonda L., Tassi E., Atlas Collaboration
Search for New Phenomena in Dijet Angular Distributions in Proton-Proton Collisions at √s =8 TeV Measured with the ATLAS Detector
Phys.Rev.Lett. 114 (2015) no.22, 221802

180. Capua M., Crosetti G., La Rotonda L., Tassi E., Atlas Collaboration
Search *for low-scale gravity signatures in multi-jet final states with the ATLAS detector at √s =8 TeV*
JHEP 1507 (2015) 032

181. Capua M., Crosetti G., La Rotonda L., Tassi E., Atlas Collaboration
Search for a new resonance decaying to a W or Z boson and a Higgs boson in the ll/lv/vv + b \bar{b} final states with the ATLAS detector
Eur.Phys.J. C75 (2015) no.6, 263

182. Capua M., Crosetti G., La Rotonda L., Tassi E., Atlas Collaboration

Combined Measurement of the Higgs Boson Mass in pp Collisions at √s =7 and 8 TeV with the ATLAS and CMS Experiments
Phys.Rev.Lett. 114 (2015) 191803

183. Capua M., Crosetti G., La Rotonda L., Tassi E., Atlas Collaboration
Measurement of the top quark mass in the t\bar{t}→{ lepton+jets } and t\bar{t}→ { dilepton } channels using √s =7 TeV ATLAS data
Eur.Phys.J. C75 (2015) no.7, 330

184. Capua M., Crosetti G., La Rotonda L., Tassi E., Atlas Collaboration
Search for vector-like B quarks in events with one isolated lepton, missing transverse momentum and jets at √s =8 TeV with the ATLAS detector
Phys.Rev. D91 (2015) no.11, 112011

185. Capua M., Crosetti G., La Rotonda L., Tassi E., Atlas Collaboration
Search for the Standard Model Higgs boson produced in association with top quarks and decaying into b\bar{b} in pp collisions at √s =8 TeV with the ATLAS detector
Eur.Phys.J. C75 (2015) no.7, 349

186. Capua M., Crosetti G., La Rotonda L., Tassi E., Atlas Collaboration
Search for production of WW/WZ resonances decaying to a lepton, neutrino and jets in pp collisions at √s =8 TeV with the ATLAS detector
Eur.Phys.J. C75 (2015) no.5, 209, Erratum: Eur.Phys.J. C75 (2015) 370

187. Capua M., Crosetti G., La Rotonda L., Tassi E., Atlas Collaboration
Search for a Heavy Neutral Particle Decaying to eμ, eτ, or μτ in pp Collisions at √s =8 TeV with the ATLAS Detector
Phys.Rev.Lett. 115 (2015) no.3, 031801

188. Capua M., Crosetti G., La Rotonda L., Tassi E., Atlas Collaboration
Search for a Charged Higgs Boson Produced in the Vector-Boson Fusion Mode with Decay $H^{\pm}$→\to $W^{\pm}Z$ using pp Collisions at √s =8 TeV with the ATLAS Experiment
Phys.Rev.Lett. 114 (2015) no.23, 231801

189. Capua M., Crosetti G., La Rotonda L., Tassi E., Atlas Collaboration
Measurement of the forward-backward asymmetry of electron and muon pair-production in pp collisions at √s =78 TeV with the ATLAS detector
JHEP 1509 (2015) 049

190. Capua M., Crosetti G., La Rotonda L., Tassi E., Atlas Collaboration
Determination of spin and parity of the Higgs boson in the WW^{*}→ evμν decay channel with the ATLAS detector
Eur.Phys.J. C75 (2015) no.5, 231

191. Capua M., Crosetti G., La Rotonda L., Tassi E., Atlas Collaboration
Search for supersymmetry in events containing a same-flavour opposite-sign dilepton pair, jets, and large missing transverse momentum in √s =8 TeV pp collisions with the ATLAS detector
Eur.Phys.J. C75 (2015) no.7, 318, Erratum: Eur.Phys.J. C75 (2015) no.10, 463

192. Capua M., Crosetti G., La Rotonda L., Tassi E., Atlas Collaboration

Evidence of Wγγ Production in pp Collisions at s=8 TeV and Limits on Anomalous Quartic Gauge Couplings with the ATLAS Detector
Phys.Rev.Lett. 115 (2015) no.3, 031802

193. Capua M., Crosetti G., La Rotonda L., Tassi E., Atlas Collaboration
Constraints on the off-shell Higgs boson signal strength in the high-mass ZZ and WW final states with the ATLAS detector
Eur.Phys.J. C75 (2015) no.7, 335
194. Capua M., Crosetti G., La Rotonda L., Tassi E., Atlas Collaboration
Two-particle Bose–Einstein correlations in pp collisions at √s =0.9 and 7 TeV measured with the ATLAS detector
Eur.Phys.J. C75 (2015) no.10, 466

195. Capua M., Crosetti G., La Rotonda L., Tassi E., Atlas Collaboration
A search for high-mass resonances decaying to $\tau^+\tau^-$ in pp collisions at √s =8 TeV with the ATLAS detector
JHEP 1507 (2015) 157

196. Capua M., Crosetti G., La Rotonda L., Tassi E., Atlas Collaboration
Differential top-antitop cross-section measurements as a function of observables constructed from final-state particles using pp collisions at √s =7 TeV in the ATLAS detector
JHEP 1506 (2015) 100

197. Capua M., Crosetti G., La Rotonda L., Tassi E., Atlas Collaboration
Search for massive supersymmetric particles decaying to many jets using the ATLAS detector in pp collisions at √s =8 TeV
Phys.Rev. D91 (2015) no.11, 112016, Erratum: Phys.Rev. D93 (2016) no.3, 039901

198. Capua M., Crosetti G., La Rotonda L., Tassi E., Atlas Collaboration
Search for a CP-odd Higgs boson decaying to Zh in pp collisions at √s =8 TeV with the ATLAS detector
Phys.Lett. B744 (2015) 163-183

199. Capua M., Crosetti G., La Rotonda L., Tassi E., Atlas Collaboration
Search for new phenomena in final states with an energetic jet and large missing transverse momentum in pp collisions at √s =8 TeV with the ATLAS detector
Eur.Phys.J. C75 (2015) no.7, 299, Erratum: Eur.Phys.J. C75 (2015) no.9, 408

200. Capua M., Crosetti G., La Rotonda L., Tassi E., Atlas Collaboration
Observation *of top-quark pair production in association with a photon and measurement of the t\bar{t}γ production cross section in pp collisions at √s =7 TeV using the ATLAS detector*
Phys.Rev. D91 (2015) no.7, 072007

201. Capua M., Crosetti G., La Rotonda L., Tassi E., Atlas Collaboration
Measurement of the charge asymmetry in dileptonic decays of top quark pairs in pp collisions at √s =7 TeV using the ATLAS detector
JHEP 1505 (2015) 061

202. Capua M., Crosetti G., La Rotonda L., Tassi E., Atlas Collaboration

Search for direct pair production of a chargino and a neutralino decaying to the 125 GeV Higgs boson in √s =8 TeV pp collisions with the ATLAS detector
Eur.Phys.J. C75 (2015) no.5, 208

203. Capua M., Crosetti G., La Rotonda L., Tassi E., Atlas Collaboration
Evidence for the Higgs-boson Yukawa coupling to tau leptons with the ATLAS detector
JHEP 1504 (2015) 117

204. Capua M., Crosetti G., La Rotonda L., Tassi E., Atlas Collaboration
Search for pair-produced long-lived neutral particles decaying in the ATLAS hadronic calorimeter in pp collisions at √s =8 TeV
Phys.Lett. B743 (2015) 15-34

205. Capua M., Crosetti G., La Rotonda L., Tassi E., Atlas Collaboration
Search for squarks and gluinos in events with isolated leptons, jets and missing transverse momentum at √s =8 TeV with the ATLAS detector
JHEP 1504 (2015) 116

206. Capua M., Crosetti G., La Rotonda L., Tassi E., Atlas Collaboration
Search for Higgs and Z Boson Decays to J/ψγ and ϒ(nS)γ with the ATLAS Detector
Phys.Rev.Lett. 114 (2015) no.12, 121801

207. Capua M., Crosetti G., La Rotonda L., Tassi E., Atlas Collaboration
Search for Scalar Charm Quark Pair Production in pp Collisions at √s =8 TeV with the ATLAS Detector
Phys.Rev.Lett. 114 (2015) no.16, 161801

208. Capua M., Crosetti G., La Rotonda L., Tassi E., Atlas Collaboration
Identification and energy calibration of hadronically decaying tau leptons with the ATLAS experiment in pp collisions at √s =8 TeV
Eur.Phys.J. C75 (2015) no.7, 303

209. Capua M., Crosetti G., La Rotonda L., Tassi E., Atlas Collaboration
Search for charged Higgs bosons decaying via $H^{\pm}\rightarrow\tau^{\pm}\nu$ in fully hadronic final states using pp collision data at √s =8 TeV with the ATLAS detector
JHEP 1503 (2015) 088

210. Capua M., Crosetti G., La Rotonda L., Tassi E., Atlas Collaboration
Observation and measurements of the production of prompt and non-prompt J/Ψ mesons in association with a Z boson in pp collisions at √s =8 TeV with the ATLAS detector
Eur.Phys.J. C75 (2015) no.5, 229

211. Capua M., Crosetti G., La Rotonda L., Tassi E., Atlas Collaboration
Measurement of Spin Correlation in Top-Antitop Quark Events and Search for Top Squark Pair Production in pp Collisions at √s =8 TeV Using the ATLAS Detector
Phys.Rev.Lett. 114 (2015) no.14, 142001

212. Capua M., Crosetti G., La Rotonda L., Tassi E., Atlas Collaboration
Centrality and rapidity dependence of inclusive jet production in √s{NN} = 5.02 TeV proton-lead collisions with the ATLAS detector
Phys.Lett. B748 (2015) 392-413

213. Capua M., Crosetti G., La Rotonda L., Tassi E., Atlas Collaboration
Observation and measurement of Higgs boson decays to WW with the ATLAS detector*
Phys.Rev. D92 (2015) no.1, 012006

214. Capua M., Crosetti G., La Rotonda L., Tassi E., Atlas Collaboration
Measurement of the transverse polarization of Λ and \bar{Λ} hyperons produced in proton-proton collisions at √s =7 TeV using the ATLAS detector
Phys.Rev. D91 (2015) no.3, 032004

215. Capua M., Crosetti G., La Rotonda L., Tassi E., Atlas Collaboration
Search for anomalous production of prompt same-sign lepton pairs and pair-produced doubly charged Higgs bosons with √s =8 TeV pp collisions using the ATLAS detector
JHEP 1503 (2015) 041

216. Capua M., Crosetti G., La Rotonda L., Tassi E., Atlas Collaboration
Searches for heavy long-lived charged particles with the ATLAS detector in proton-proton collisions at √s =8 TeV
JHEP 1501 (2015) 068

217. Capua M., Crosetti G., La Rotonda L., Tassi E., Atlas Collaboration
Search for new phenomena in events with three or more charged leptons in pp collisions at √s =8 TeV with the ATLAS detector
JHEP 1508 (2015) 138

218. Capua M., Crosetti G., La Rotonda L., Tassi E., Atlas Collaboration
Measurements of the Nuclear Modification Factor for Jets in Pb+Pb Collisions at √s{NN}=2.76 TeV with the ATLAS Detector
Phys.Rev.Lett. 114 (2015) no.7, 072302

219. Capua M., Crosetti G., La Rotonda L., Tassi E., Atlas Collaboration
Measurement of three-jet production cross-sections in pp collisions at 7 TeV centre-of-mass energy using the ATLAS detector
Eur.Phys.J. C75 (2015) no.5, 228

220. Capua M., Crosetti G., La Rotonda L., Tassi E., Atlas Collaboration
Search for new phenomena in events with a photon and missing transverse momentum in pp collisions at √s =8 TeV with the ATLAS detector
Phys.Rev. D91 (2015) no.1, 012008, Erratum: Phys.Rev. D92 (2015) no.5, 059903

221. Capua M., Crosetti G., La Rotonda L., Tassi E., Atlas Collaboration
Measurement of the inclusive jet cross-section in proton-proton collisions at √s =7 TeV using 4.5 fb^{-1} of data with the ATLAS detector
JHEP 1502 (2015) 153, Erratum: JHEP 1509 (2015) 141

222. Capua M., Crosetti G., La Rotonda L., Tassi E., Atlas Collaboration
Measurement of the WW+WZ cross section and limits on anomalous triple gauge couplings using final states with one lepton, missing transverse momentum, and two jets with the ATLAS detector at √s =7 TeV
JHEP 1501 (2015) 049

223. Capua M., Crosetti G., La Rotonda L., Tassi E., Atlas Collaboration

Search for invisible particles produced in association with single-top-quarks in proton-proton collisions at √s =8 TeV with the ATLAS detector
Eur.Phys.J. C75 (2015) no.2, 79

224. Capua M., Crosetti G., La Rotonda L., Tassi E., Atlas Collaboration
Search for the X_b and other hidden-beauty states in the $\pi^+\pi^-$ \Upsilon(1S) channel at ATLAS
Phys.Lett. B740 (2015) 199-217

225. Capua M., Crosetti G., La Rotonda L., Tassi E., Atlas Collaboration
Search for W′ →t\bar{b} in the lepton plus jets final state in proton-proton collisions at a centre-of-mass energy of √s =8 TeV with the ATLAS detector
Phys.Lett. B743 (2015) 235-255

226. Capua M., Crosetti G., La Rotonda L., Tassi E., Atlas Collaboration
Search for dark matter in events with heavy quarks and missing transverse momentum in pp collisions with the ATLAS detector
Eur.Phys.J. C75 (2015) no.2, 92

227. Capua M., Crosetti G., La Rotonda L., Tassi E., Atlas Collaboration
Search for s-channel single top-quark production in proton–proton collisions at √s =8 TeV with the ATLAS detector
Phys.Lett. B740 (2015) 118-136

228. Capua M., Crosetti G., La Rotonda L., Tassi E., Atlas Collaboration
Measurements of the W production cross sections in association with jets with the ATLAS detector
Eur.Phys.J. C75 (2015) no.2, 82

229. Capua M., Crosetti G., La Rotonda L., Tassi E., Atlas Collaboration
Search for the b\bar{b} decay of the Standard Model Higgs boson in associated (W/Z)H production with the ATLAS detector
JHEP 1501 (2015) 069

230. Capua M., Crosetti G., La Rotonda L., Tassi E., Atlas Collaboration
Search for resonant diboson production in the llq\bar{q} final state in pp collisions at √s =8 TeV with the ATLAS detector
Eur.Phys.J. C75 (2015) 69

231. Capua M., Crosetti G., La Rotonda L., Tassi E., Atlas Collaboration
Search for neutral Higgs bosons of the minimal supersymmetric standard model in pp collisions at √s =8 TeV with the ATLAS detector
JHEP 1411 (2014) 056

232. Capua M., Crosetti G., La Rotonda L., Tassi E., Atlas Collaboration
Search for nonpointing and delayed photons in the diphoton and missing transverse momentum final state in 8 TeV pp collisions at the LHC using the ATLAS detector
Phys.Rev. D90 (2014) no.11, 112005

233. Capua M., Crosetti G., La Rotonda L., Tassi E., Atlas Collaboration

Search for pair and single production of new heavy quarks that decay to a Z boson and a third-generation quark in pp collisions at √s =8 TeV with the ATLAS detector
JHEP 1411 (2014) 104

234. Capua M., Crosetti G., La Rotonda L., Tassi E., Atlas Collaboration
Measurement of distributions sensitive to the underlying event in inclusive Z-boson production in pp collisions at √s =7 TeV with the ATLAS detector
Eur.Phys.J. C74 (2014) no.12, 3195

235. Capua M., Crosetti G., La Rotonda L., Tassi E., Atlas Collaboration
Search for H →γγ produced in association with top quarks and constraints on the Yukawa coupling between the top quark and the Higgs boson using data taken at 7 TeV and 8 TeV with the ATLAS detector
Phys.Lett. B740 (2015) 222-242

236. Capua M., Crosetti G., La Rotonda L., Tassi E., Atlas Collaboration
Measurement of long-range pseudorapidity correlations and azimuthal harmonics in √s{NN}=5.02 TeV proton-lead collisions with the ATLAS detector
Phys.Rev. C90 (2014) no.4, 044906

237. Capua M., Crosetti G., La Rotonda L., Tassi E., Atlas Collaboration
Measurement of the top-quark mass in the fully hadronic decay channel from ATLAS data at √s =7 TeV
Eur.Phys.J. C75 (2015) no.4, 158

238. Capua M., Crosetti G., La Rotonda L., Tassi E., Atlas Collaboration
Search for long-lived neutral particles decaying into lepton jets in proton-proton collisions at √s =8 TeV with the ATLAS detector
JHEP 1411 (2014) 088

239. Capua M., Crosetti G., La Rotonda L., Tassi E., Atlas Collaboration
Measurement of Higgs boson production in the diphoton decay channel in pp collisions at center-of-mass energies of 7 and 8 TeV with the ATLAS detector
Phys.Rev. D90 (2014) no.11, 112015

240. Capua M., Crosetti G., La Rotonda L., Tassi E., Atlas Collaboration
A measurement of the ratio of the production cross sections for W and Z bosons in association with jets with the ATLAS detector
Eur.Phys.J. C74 (2014) no.12, 3168

241. Capua M., Crosetti G., La Rotonda L., Tassi E., Atlas Collaboration
Measurement of the total cross section from elastic scattering in pp collisions at √s =7 TeV with the ATLAS detector
Nucl.Phys. B889 (2014) 486-548

242. Capua M., Crosetti G., La Rotonda L., Tassi E., Atlas Collaboration
Search for the lepton flavor violating decay Z→eμ in pp collisions at √s TeV with the ATLAS detector
Phys.Rev. D90 (2014) no.7, 072010

243. Capua M., Crosetti G., La Rotonda L., Tassi E., Atlas Collaboration

Measurements of Higgs boson production and couplings in the four-lepton channel in pp collisions at center-of-mass energies of 7 and 8 TeV with the ATLAS detector
Phys.Rev. D91 (2015) no.1, 012006

244. Capua M., Crosetti G., La Rotonda L., Tassi E., Atlas Collaboration
Measurement of the production and lepton charge asymmetry of W bosons in Pb+Pb collisions at √s{NN}=2.76 TeV with the ATLAS detector
Eur.Phys.J. C75 (2015) no.1, 23

245. Capua M., Crosetti G., La Rotonda L., Tassi E., Atlas Collaboration
Measurement of flow harmonics with multi-particle cumulants in Pb+Pb collisions at √s{NN}=2.76 TeV with the ATLAS detector
Eur.Phys.J. C74 (2014) no.11, 3157

246. Capua M., Crosetti G., La Rotonda L., Tassi E., Atlas Collaboration
Fiducial and differential cross sections of Higgs boson production measured in the four-lepton decay channel in pp collisions at √s =8 TeV with the ATLAS detector
Phys.Lett. B738 (2014) 234-253

247. Capua M., Crosetti G., La Rotonda L., Tassi E., Atlas Collaboration
Performance of the ATLAS muon trigger in pp collisions at √s =8 TeV
Eur.Phys.J. C75 (2015) 120

248. Capua M., Crosetti G., La Rotonda L., Tassi E., Atlas Collaboration
Search for W′ →tb →qqbb decays in pp collisions at √s =8 TeV with the ATLAS detector
Eur.Phys.J. C75 (2015) no.4, 165

249. Capua M., Crosetti G., La Rotonda L., Tassi E., Atlas Collaboration
Search for new resonances in Wγ and Zγ final states in pp collisions at √s =8 TeV with the ATLAS detector
Phys.Lett. B738 (2014) 428-447

250. Capua M., Crosetti G., La Rotonda L., Tassi E., Atlas Collaboration
Search for new particles in events with one lepton and missing transverse momentum in pp collisions at √s =8 TeV with the ATLAS detector
JHEP 1409 (2014) 037

251. Capua M., Crosetti G., La Rotonda L., Tassi E., Atlas Collaboration
Search for Scalar Diphoton Resonances in the Mass Range 65-600 GeV with the ATLAS Detector in pp Collision Data at √s =8 TeV
Phys.Rev.Lett. 113 (2014) no.17, 171801

252. Capua M., Crosetti G., La Rotonda L., Tassi E., Atlas Collaboration
Measurements of jet vetoes and azimuthal decorrelations in dijet events produced in pp collisions at √s =7 TeV using the ATLAS detector
Eur.Phys.J. C74 (2014) no.11, 3117

253. Capua M., Crosetti G., La Rotonda L., Tassi E., Atlas Collaboration
Measurement of the production cross-section of ψ(2S) \to J/ψ(→$\mu^+\mu^-$) $\pi^+\pi^-$ in pp collisions at √s =7 TeV at ATLAS
JHEP 1409 (2014) 079

254. Capua M., Crosetti G., La Rotonda L., Tassi E., Atlas Collaboration
Electron and photon energy calibration with the ATLAS detector using LHC Run 1 data
Eur.Phys.J. C74 (2014) no.10, 3071

255. Capua M., Crosetti G., La Rotonda L., Tassi E., Atlas Collaboration
Measurements of spin correlation in top-antitop quark events from proton-proton collisions at $\sqrt{s}$ =7 TeV using the ATLAS detector
Phys.Rev. D90 (2014) no.11, 112016

256. Capua M., Crosetti G., La Rotonda L., Tassi E., Atlas Collaboration
Measurements of fiducial and differential cross sections for Higgs boson production in the diphoton decay channel at $\sqrt{s}$ =8 TeV with ATLAS
JHEP 1409 (2014) 112

257. Capua M., Crosetti G., La Rotonda L., Tassi E., Atlas Collaboration
Measurement of the muon reconstruction performance of the ATLAS detector using 2011 and 2012 LHC proton–proton collision data
Eur.Phys.J. C74 (2014) no.11, 3130

258. Capua M., Crosetti G., La Rotonda L., Tassi E., Atlas Collaboration
Measurement of differential production cross-sections for a Z boson in association with b-jets in 7 TeV proton-proton collisions with the ATLAS detector
JHEP 1410 (2014) 141

259. Capua M., Crosetti G., La Rotonda L., Tassi E., Atlas Collaboration
Search for contact interactions and large extra dimensions in the dilepton channel using proton-proton collisions at $\sqrt{s}$ =8 TeV with the ATLAS detector
Eur.Phys.J. C74 (2014) no.12, 3134

260. Capua M., Crosetti G., La Rotonda L., Tassi E., Atlas Collaboration
Flavor tagged time-dependent angular analysis of the $B_s \rightarrow J/\psi\phi$ decay and extraction of $\Delta\Gamma s$ and the weak phase ϕ_s in ATLAS
Phys.Rev. D90 (2014) no.5, 052007

261. Capua M., Crosetti G., La Rotonda L., Tassi E., Atlas Collaboration
Search for new phenomena in the dijet mass distribution using p-p collision data at $\sqrt{s}$ =8 TeV with the ATLAS detector
Phys.Rev. D91 (2015) no.5, 052007

262. Capua M., Crosetti G., La Rotonda L., Tassi E., Atlas Collaboration
Observation *of an Excited $B_c^{\pm}$ Meson State with the ATLAS Detector*
Phys.Rev.Lett. 113 (2014) no.21, 212004

263. Capua M., Crosetti G., La Rotonda L., Tassi E., Atlas Collaboration
Measurement of the t\overline{t} production cross-section as a function of jet multiplicity and jet transverse momentum in 7 TeV proton-proton collisions with the ATLAS detector
JHEP 1501 (2015) 020

264. Capua M., Crosetti G., La Rotonda L., Tassi E., Atlas Collaboration

Measurement of the cross-section of high transverse momentum vector bosons reconstructed as single jets and studies of jet substructure in pp collisions at $\sqrt{s}$ =7 TeV with the ATLAS detector
New J.Phys. 16 (2014) no.11, 113013

265. Capua M., Crosetti G., La Rotonda L., Tassi E., Atlas Collaboration
Search for pair-produced third-generation squarks decaying via charm quarks or in compressed supersymmetric scenarios in pp collisions at $\sqrt{s}$ =8 TeV with the ATLAS detector
Phys.Rev. D90 (2014) no.5, 052008

266. Capua M., Crosetti G., La Rotonda L., Tassi E., Atlas Collaboration
Search for supersymmetry in events with large missing transverse momentum, jets, and at least one tau lepton in 20 fb^{-1} of $\sqrt{s}$ =8 TeV proton-proton collision data with the ATLAS detector
JHEP 1409 (2014) 103

267. Capua M., Crosetti G., La Rotonda L., Tassi E., Atlas Collaboration
Search for strong production of supersymmetric particles in final states with missing transverse momentum and at least three b-jets at $\sqrt{s}$ =8 TeV proton-proton collisions with the ATLAS detector
JHEP 1410 (2014) 024

268. Capua M., Crosetti G., La Rotonda L., Tassi E., Atlas Collaboration
Search for top squark pair production in final states with one isolated lepton, jets, and missing transverse momentum in $\sqrt{s}$ =8 TeV pp collisions with the ATLAS detector
JHEP 1411 (2014) 118

269. Capua M., Crosetti G., La Rotonda L., Tassi E., Atlas Collaboration
Simultaneous measurements of the t\bar{t}, W^+W^-, and $Z/\gamma^* \rightarrow \tau\tau$ production cross-sections in pp collisions at $\sqrt{s}$ =7 TeV with the ATLAS detector
Phys.Rev. D91 (2015) no.5, 052005

270. Capua M., Crosetti G., La Rotonda L., Tassi E., Atlas Collaboration
Measurements of normalized differential cross sections for t\bar{t production in pp collisions at $\sqrt{s}$ =7 TeV using the ATLAS detector
Phys.Rev. D90 (2014) no.7, 072004

271. Capua M., Crosetti G., La Rotonda L., Tassi E., Atlas Collaboration
Search for the direct production of charginos, neutralinos and staus in final states with at least two hadronically decaying taus and missing transverse momentum in pp collisions at $\sqrt{s}$ =8 TeV with the ATLAS detector
JHEP 1410 (2014) 096

272. Capua M., Crosetti G., La Rotonda L., Tassi E., Atlas Collaboration
Comprehensive measurements of t-channel single top-quark production cross sections at $\sqrt{s}$ =7 TeV with the ATLAS detector
Phys.Rev. D90 (2014) no.11, 112006

273. Capua M., Crosetti G., La Rotonda L., Tassi E., Atlas Collaboration
A neural network clustering algorithm for the ATLAS silicon pixel detector
JINST 9 (2014) P09009

274. Capua M., Crosetti G., La Rotonda L., Tassi E., Atlas Collaboration

Search for the Standard Model Higgs boson decay to $\mu^+\mu^-$ with the ATLAS detector
Phys.Lett. B738 (2014) 68-86

275. Capua M., Crosetti G., La Rotonda L., Tassi E., Atlas Collaboration
Measurement of the t\bar{t} production cross-section using eμ events with b-tagged jets in pp collisions at $\sqrt{s}$ = 7 and 8 TeV with the ATLAS detector
Eur.Phys.J. C74 (2014) no.10, 3109, Addendum: Eur.Phys.J. C76 (2016) no.11, 642

276. Capua M., Crosetti G., La Rotonda L., Tassi E., Atlas Collaboration
Search For Higgs Boson Pair Production in the γγb\bar{b} Final State using pp Collision Data at $\sqrt{s}$ =8 TeV from the ATLAS Detector
Phys.Rev.Lett. 114 (2015) no.8, 081802
277. Capua M., Crosetti G., La Rotonda L., Tassi E., Atlas Collaboration
Search for WZ resonances in the fully leptonic channel using pp collisions at $\sqrt{s}$ =8 TeV with the ATLAS detector
Phys.Lett. B737 (2014) 223-243

278. Capua M., Crosetti G., La Rotonda L., Tassi E., Atlas Collaboration
Measurement of the Higgs boson mass from the H→γγ and H → ZZ→ 4l channels with the ATLAS detector using 25 fb^{-1} of pp collision data*
Phys.Rev. D90 (2014) no.5, 052004

279. Capua M., Crosetti G., La Rotonda L., Tassi E., Atlas Collaboration
Measurement of the Zγ boson transverse momentum distribution in pp collisions at $\sqrt{s}$ =7 TeV with the ATLAS detector*
JHEP 1409 (2014) 145

280. Capua M., Crosetti G., La Rotonda L., Tassi E., Atlas Collaboration
Measurement of inclusive jet charged-particle fragmentation functions in Pb+Pb collisions at $\sqrt{s}$\{NN\} = 2.76 TeV with the ATLAS detector
Phys.Lett. B739 (2014) 320-342

281. Capua M., Crosetti G., La Rotonda L., Tassi E., Atlas Collaboration
Search for direct pair production of the top squark in all-hadronic final states in proton-proton collisions at $\sqrt{s}$ =8 TeV with the ATLAS detector
JHEP 1409 (2014) 015

282. Capua M., Crosetti G., La Rotonda L., Tassi E., Atlas Collaboration
Measurement of the underlying event in jet events from 7 TeV proton-proton collisions with the ATLAS detector
Eur.Phys.J. C74 (2014) no.8, 2965

283. Capua M., Crosetti G., La Rotonda L., Tassi E., Atlas Collaboration
Jet energy measurement and its systematic uncertainty in proton-proton collisions at $\sqrt{s}$ =7 TeV with the ATLAS detector
Eur.Phys.J. C75 (2015) 17

284. Capua M., Crosetti G., La Rotonda L., Tassi E., Atlas Collaboration
Search for squarks and gluinos with the ATLAS detector in final states with jets and missing transverse momentum using $\sqrt{s}$ =8 TeV proton--proton collision data
JHEP 1409 (2014) 176

285. Capua M., Crosetti G., La Rotonda L., Tassi E., Atlas Collaboration
Light-quark and gluon jet discrimination in pp collisions at √s =7 TeV with the ATLAS detector
Eur.Phys.J. C74 (2014) no.8, 3023

286. Capua M., Crosetti G., La Rotonda L., Tassi E., Atlas Collaboration
Evidence for Electroweak Production of $W^{\pm}W^{\pm}$jj in pp Collisions at √s =8 TeV with the ATLAS Detector
Phys.Rev.Lett. 113 (2014) no.14, 141803

287. Capua M., Crosetti G., La Rotonda L., Tassi E., Atlas Collaboration
Search for supersymmetry in events with four or more leptons in √s =8 TeV pp collisions with the ATLAS detector
Phys.Rev. D90 (2014) no.5, 052001

288. Capua M., Crosetti G., La Rotonda L., Tassi E., Atlas Collaboration
Search for microscopic black holes and string balls in final states with leptons and jets with the ATLAS detector at sqrt(s) = 8 TeV
JHEP 1408 (2014) 103

289. Capua M., Crosetti G., La Rotonda L., Tassi E., Atlas Collaboration
Search for high-mass dilepton resonances in pp collisions at √s =8 TeV with the ATLAS detector
Phys.Rev. D90 (2014) no.5, 052005

290. Capua M., Crosetti G., La Rotonda L., Tassi E., Atlas Collaboration
Measurement of the centrality and pseudorapidity dependence of the integrated elliptic flow in lead-lead collisions at √s{NN} =2.76 TeV with the ATLAS detector
Eur.Phys.J. C74 (2014) no.8, 2982

291. Capua M., Crosetti G., La Rotonda L., Tassi E., Atlas Collaboration
Monitoring and data quality assessment of the ATLAS liquid argon calorimeter
JINST 9 (2014) P07024

292. Capua M., Crosetti G., La Rotonda L., Tassi E., Atlas Collaboration
Operation and performance of the ATLAS semiconductor tracker
Capua M., Crosetti G., La Rotonda L., Tassi E., Atlas Collaboration
JINST 9 (2014) P08009

293. Capua M., Crosetti G., La Rotonda L., Tassi E., Atlas Collaboration
Measurement of the cross section of high transverse momentum Z⟶ b\bar{b} production in proton--proton collisions at √s =8 TeV with the ATLAS Detector
Phys.Lett. B738 (2014) 25-43

294. Capua M., Crosetti G., La Rotonda L., Tassi E., Atlas Collaboration
Measurement of χ_{c1} and χ_{c2} production with √s =7 TeV pp collisions at ATLAS
JHEP 1407 (2014) 154

295. Capua M., Crosetti G., La Rotonda L., Tassi E., Atlas Collaboration
Muon reconstruction efficiency and momentum resolution of the ATLAS experiment in proton-proton collisions at √s =7 TeV in 2010
Eur.Phys.J. C74 (2014) no.9, 3034

296. Capua M., Crosetti G., La Rotonda L., Tassi E., Atlas Collaboration
Search for supersymmetry at √s =8 TeV in final states with jets and two same-sign leptons or three leptons with the ATLAS detector
JHEP 1406 (2014) 035

297. Capua M., Crosetti G., La Rotonda L., Tassi E., Atlas Collaboration
Electron reconstruction and identification efficiency measurements with the ATLAS detector using the 2011 LHC proton-proton collision data
Eur.Phys.J. C74 (2014) no.7, 2941

298. Capua M., Crosetti G., La Rotonda L., Tassi E., Atlas Collaboration
Measurement of the low-mass Drell-Yan differential cross section at √s =7 TeV using the ATLAS detector
JHEP 1406 (2014) 112

299. Capua M., Crosetti G., La Rotonda L., Tassi E., Atlas Collaboration
Measurement of the parity-violating asymmetry parameter α_b and the helicity amplitudes for the decay $\Lambda_b^0 \rightarrow J/\psi+\Lambda^0$ with the ATLAS detector
Phys.Rev. D89 (2014) no.9, 092009

300. Capua M., Crosetti G., La Rotonda L., Tassi E., Atlas Collaboration
Search for dark matter in events with a Z boson and missing transverse momentum in pp collisions at √s =8 TeV with the ATLAS detector
Phys.Rev. D90 (2014) no.1, 012004

301. Capua M., Crosetti G., La Rotonda L., Tassi E., Atlas Collaboration
Search for top quark decays $t \rightarrow qH$ with $H \rightarrow \gamma\gamma$ using the ATLAS detector
JHEP 1406 (2014) 008

302. Capua M., Crosetti G., La Rotonda L., Tassi E., Atlas Collaboration
Measurements of Four-Lepton Production at the Z Resonance in pp Collisions at √s =7 and 8 TeV with ATLAS
Phys.Rev.Lett. 112 (2014) no.23, 231806

303. Capua M., Crosetti G., La Rotonda L., Tassi E., Atlas Collaboration
Search for direct production of charginos, neutralinos and sleptons in final states with two leptons and missing transverse momentum in pp collisions at √s =8 TeV with the ATLAS detector
JHEP 1405 (2014) 071

304. Capua M., Crosetti G., La Rotonda L., Tassi E., Atlas Collaboration
Search for direct top squark pair production in events with a Z boson, b-jets and missing transverse momentum in sqrt(s)=8 TeV pp collisions with the ATLAS detector
Eur.Phys.J. C74 (2014) no.6, 2883

305. Capua M., Crosetti G., La Rotonda L., Tassi E., Atlas Collaboration
Search for direct top-squark pair production in final states with two leptons in pp collisions at √s =8 TeV with the ATLAS detector
JHEP 1406 (2014) 124

306. Capua M., Crosetti G., La Rotonda L., Tassi E., Atlas Collaboration

Measurement of event-plane correlations in √s{NN} = 2.76 TeV lead-lead collisions with the ATLAS detector
Phys.Rev. C90 (2014) no.2, 024905

307. Capua M., Crosetti G., La Rotonda L., Tassi E., Atlas Collaboration
Search for direct production of charginos and neutralinos in events with three leptons and missing transverse momentum in √s =8 TeV pp collisions with the ATLAS detector
JHEP 1404 (2014) 169

308. Capua M., Crosetti G., La Rotonda L., Tassi E., Atlas Collaboration
Measurement of the production of a W boson in association with a charm quark in pp collisions at √s =7 TeV with the ATLAS detector JHEP 1405 (2014) 068

309. Capua M., Crosetti G., La Rotonda L., Tassi E., Atlas Collaboration
The differential production cross section of the ϕ(1020) meson in √s =7 TeV pp collisions measured with the ATLAS detector
Eur.Phys.J. C74 (2014) no.7, 2895

310. Capua M., Crosetti G., La Rotonda L., Tassi E., Atlas Collaboration
Search for Invisible Decays of a Higgs Boson Produced in Association with a Z Boson in ATLAS
Phys.Rev.Lett. 112 (2014) 201802

311. Capua M., Crosetti G., La Rotonda L., Tassi E., Atlas Collaboration
Search for Higgs boson decays to a photon and a Z boson in pp collisions at √s =7 and 8 TeV with the ATLAS detector
Phys.Lett. B732 (2014) 8-27

312. Capua M., Crosetti G., La Rotonda L., Tassi E., Atlas Collaboration
Measurement of the electroweak production of dijets in association with a Z-boson and distributions sensitive to vector boson fusion in proton-proton collisions at √s =8 TeV using the ATLAS detector
JHEP 1404 (2014) 031

313. Capua M., Crosetti G., La Rotonda L., Tassi E., Atlas Collaboration
Measurement of the production cross section of prompt J/ψ mesons in association with a $W^{\pm}$ boson in pp collisions at √s =7 TeV with the ATLAS detector
JHEP 1404 (2014) 172

314. Capua M., Crosetti G., La Rotonda L., Tassi E., Atlas Collaboration
Measurement of dijet cross sections in pp collisions at 7 TeV centre-of-mass energy using the ATLAS detector
JHEP 1405 (2014) 059

315. Capua M., Crosetti G., La Rotonda L., Tassi E., Atlas Collaboration
Search for a multi-Higgs-boson cascade in $W^{+}W^{-}b\bar{b}$ events with the ATLAS detector in pp collisions at √s =8 TeV
Phys.Rev. D89 (2014) no.3, 032002

316. Capua M., Crosetti G., La Rotonda L., Tassi E., Atlas Collaboration

Standalone vertex finding in the ATLAS muon spectrometer
Capua M., Crosetti G., La Rotonda L., Tassi E., Atlas Collaboration
JINST 9 (2014) P02001

317. Capua M., Crosetti G., La Rotonda L., Tassi E., Atlas Collaboration
Measurement of the top quark pair production charge asymmetry in proton-proton collisions at $\sqrt{s}$ =7 TeV using the ATLAS detector
JHEP 1402 (2014) 107.

318. Capua M., Crosetti G., La Rotonda L., Tassi E., Atlas Collaboration
Search for Quantum Black Hole Production in High-Invariant-Mass Lepton+Jet Final States Using pp Collisions at $\sqrt{s}$ =8 TeV and the ATLAS Detector
Phys.Rev.Lett. 112 (2014) no.9, 091804.
319. Capua M., Crosetti G., La Rotonda L., Tassi E., Atlas Collaboration
Measurement of the inclusive isolated prompt photons cross section in pp collisions at $\sqrt{s}$ =7 TeV with the ATLAS detector using 4.6 fb^{-1}
Phys.Rev. D89 (2014) no.5, 052004.

320. Capua M., Crosetti G., La Rotonda L., Tassi E., Atlas Collaboration
Search for long-lived stopped R-hadrons decaying out-of-time with pp collisions using the ATLAS detector
Phys.Rev. D88 (2013) no.11, 112003.

321. Capua M., Crosetti G., La Rotonda L., Tassi E., Atlas Collaboration
Measurement of the mass difference between top and anti-top quarks in pp collisions at $\sqrt{s}$ =7 TeV using the ATLAS detector
Phys.Lett. B728 (2014) 363-379.

322. Capua M., Crosetti G., La Rotonda L., Tassi E., Atlas Collaboration
Search for charginos nearly mass degenerate with the lightest neutralino based on a disappearing-track signature in pp collisions at $\sqrt{s}$ =8 TeV with the ATLAS detector
Phys.Rev. D88 (2013) no.11, 112006.

323. Capua M., Crosetti G., La Rotonda L., Tassi E., Atlas Collaboration
Search for dark matter in events with a hadronically decaying W or Z boson and missing transverse momentum in pp collisions at $\sqrt{s}$ =8 TeV with the ATLAS detector
Phys.Rev.Lett. 112 (2014) no.4, 041802.

324. Capua M., Crosetti G., La Rotonda L., Tassi E., Atlas Collaboration
Search for new phenomena in photon+jet events collected in proton--proton collisions at sqrt(s) = 8 TeV with the ATLAS detector
Phys.Lett. B728 (2014) 562-578.

325. Capua M., Crosetti G., La Rotonda L., Tassi E., Atlas Collaboration
Search for microscopic black holes in a like-sign dimuon final state using large track multiplicity with the ATLAS detector
Phys.Rev. D88 (2013) no.7, 072001.

326. Capua M., Crosetti G., La Rotonda L., Tassi E., Atlas Collaboration

Search for direct third-generation squark pair production in final states with missing transverse momentum and two b-jets in √s =8 TeV pp collisions with the ATLAS detector
JHEP 1310 (2013) 189.

327. Capua M., Crosetti G., La Rotonda L., Tassi E., Atlas Collaboration
Search for new phenomena in final states with large jet multiplicities and missing transverse momentum at √s =8 TeV proton-proton collisions using the ATLAS experiment
JHEP 1310 (2013) 130, Erratum: JHEP 1401 (2014) 109.

328. Capua M., Crosetti G., La Rotonda L., Tassi E., Atlas Collaboration
Search *for excited electrons and muons in √s =8 TeV proton-proton collisions with the ATLAS detector*
New J.Phys. 15 (2013) 093011.

329. Capua M., Crosetti G., La Rotonda L., Tassi E., Atlas Collaboration
Dynamics of isolated-photon plus jet production in pp collisions at √s =7 TeV with the ATLAS detector
Nucl.Phys. B875 (2013) 483-535.

330. Capua M., Crosetti G., La Rotonda L., Tassi E., Atlas Collaboration
Measurement of Top Quark Polarization in Top-Antitop Events from Proton-Proton Collisions at √s =7 TeV Using the ATLAS Detector
Phys.Rev.Lett. 111 (2013) no.23, 232002.

331. Capua M., Crosetti G., La Rotonda L., Tassi E., Atlas Collaboration
Measurement of jet shapes in top-quark pair events at √s =7 TeV using the ATLAS detector
Eur.Phys.J. C73 (2013) no.12, 2676.

332. Capua M., Crosetti G., La Rotonda L., Tassi E., Atlas Collaboration
Measurement of the top quark charge in pp collisions at √s =7 TeV with the ATLAS detector
JHEP 1311 (2013) 031.

333. Capua M., Crosetti G., La Rotonda L., Tassi E., Atlas Collaboration
Evidence for the spin-0 nature of the Higgs boson using ATLAS data
Phys.Lett. B726 (2013) 120-144.

334. Capua M., Crosetti G., La Rotonda L., Tassi E., Atlas Collaboration
Measurements of Higgs boson production and couplings in diboson final states with the ATLAS detector at the LHC
Phys.Lett. B726 (2013) 88-119, Erratum: Phys.Lett. B734 (2014) 406-406.

335. Capua M., Crosetti G., La Rotonda L., Tassi E., Atlas Collaboration
Measurement of the differential cross-section of B^+ meson production in pp collisions at √s =7 TeV at ATLAS
JHEP 1310 (2013) 042.

336. Capua M., Crosetti G., La Rotonda L., Tassi E., Atlas Collaboration
Measurement of the Azimuthal Angle Dependence of Inclusive Jet Yields in Pb+Pb Collisions at √s{NN} = 2.76 TeV with the ATLAS detector
Phys.Rev.Lett. 111 (2013) no.15, 152301.

337. Capua M., Crosetti G., La Rotonda L., Tassi E., Atlas Collaboration
Performance of jet substructure techniques for large-R jets in proton-proton collisions at $\sqrt{s}$ =7TeV using the ATLAS detector
JHEP 1309 (2013) 076.

338. Capua M., Crosetti G., La Rotonda L., Tassi E., Atlas Collaboration
Measurement of the high-mass Drell--Yan differential cross-section in pp collisions at $\sqrt{s}$ =7 TeV with the ATLAS detector
Phys.Lett. B725 (2013) 223-242

339. Capua M., Crosetti G., La Rotonda L., Tassi E., Atlas Collaboration
Measurement of the distributions of event-by-event flow harmonics in lead-lead collisions at = 2.76 TeV with the ATLAS detector at the LHC
JHEP 1311 (2013) 183.

340. Capua M., Crosetti G., La Rotonda L., Tassi E., Atlas Collaboration
Search for t\bar t resonances in the lepton plus jets final state with ATLAS using 4.7 fb^{-1} of pp collisions at $\sqrt{s}$ =7 TeV
Phys.Rev. D88 (2013) no.1, 012004

341. Capua M., Crosetti G., La Rotonda L., Tassi E., Atlas Collaboration
Triggers for displaced decays of long-lived neutral particles in the ATLAS detector
JINST 8 (2013) P07015

342. Capua M., Crosetti G., La Rotonda L., Tassi E., Atlas Collaboration
Search for resonant diboson production in the WW/WZ→ℓνjj decay channels with the ATLAS detector at $\sqrt{s}$ =7 TeV
Phys.Rev. D87 (2013) no.11, 112006

343. Capua M., Crosetti G., La Rotonda L., Tassi E., Atlas Collaboration
Measurement of the production cross section of jets in association with a Z boson in pp collisions at $\sqrt{s}$ =7 TeV with the ATLAS detector
JHEP 1307 (2013) 032

344. Capua M., Crosetti G., La Rotonda L., Tassi E., Atlas Collaboration
Study of heavy-flavor quarks produced in association with top-quark pairs at $\sqrt{s}$ =7 TeV using the ATLAS detector
Phys.Rev. D89 (2014) no.7, 072012

345. Capua M., Crosetti G., La Rotonda L., Tassi E., Atlas Collaboration
Search for nonpointing photons in the diphoton and E_T{miss} final state in $\sqrt{s}$ =7 TeV proton-proton collisions using the ATLAS detector
Phys.Rev. D88 (2013) no.1, 012001

346. Capua M., Crosetti G., La Rotonda L., Tassi E., Atlas Collaboration
Measurement of the inclusive jet cross section in pp collisions at $\sqrt{s}$=2.76 TeV and comparison to the inclusive jet cross section at $\sqrt{s}$ =7TeV using the ATLAS detector
Eur.Phys.J. C73 (2013) no.8, 2509

347. Capua M., Crosetti G., La Rotonda L., Tassi E., Atlas Collaboration

Measurement with the ATLAS detector of multi-particle azimuthal correlations in p+Pb collisions at √s{NN} = 5.02 TeV
Phys.Lett. B725 (2013) 60-78

348. Capua M., Crosetti G., La Rotonda L., Tassi E., Atlas Collaboration
Search for third generation scalar leptoquarks in pp collisions at √s =7TeV with the ATLAS detector
JHEP 1306 (2013) 033

349. Capua M., Crosetti G., La Rotonda L., Tassi E., Atlas Collaboration
Characterisation and mitigation of beam-induced backgrounds observed in the ATLAS detector during the 2011 proton-proton run
JINST 8 (2013) P07004

350. Capua M., Crosetti G., La Rotonda L., Tassi E., Atlas Collaboration
Search for WH production with a light Higgs boson decaying to prompt electron-jets in proton-proton collisions at √s =7 TeV with the ATLAS detector
New J.Phys. 15 (2013) 043009

351. Capua M., Crosetti G., La Rotonda L., Tassi E., Atlas Collaboration
Improved luminosity determination in pp collisions at √s =7 TeV using the ATLAS detector at the LHC
Eur.Phys.J. C73 (2013) no.8, 2518

352. Capua M., Crosetti G., La Rotonda L., Tassi E., Atlas Collaboration
Search for a light charged Higgs boson in the decay channel $H^+ \to c\bar{s}$ in $t\bar{t}$ events using pp collisions at √s =7 TeV with the ATLAS detector
Eur.Phys.J. C73 (2013) no.6, 2465

353. Capua M., Crosetti G., La Rotonda L., Tassi E., Atlas Collaboration
Measurement of the cross-section for W boson production in association with b-jets in pp collisions at √s =7 TeV with the ATLAS detector
JHEP 1306 (2013) 084

354. Capua M., Crosetti G., La Rotonda L., Tassi E., Atlas Collaboration
Measurement of kT splitting scales in W->lv events at √s =7 TeV with the ATLAS detector
Eur.Phys.J. C73 (2013) no.5, 2432

355. Capua M., Crosetti G., La Rotonda L., Tassi E., Atlas Collaboration
Measurements of W γ and Z γ production in pp collisions at √s =7 TeV with the ATLAS detector at the LHC
Phys.Rev. D87 (2013) no.11, 112003, Erratum: Phys.Rev. D91 (2015) no.11, 119901

356. Capua M., Crosetti G., La Rotonda L., Tassi E., Atlas Collaboration
Measurement of hard double-parton interactions in W(→lv)+ 2 jet events at √s =7 TeV with the ATLAS detector
New J.Phys. 15 (2013) 033038

357. Capua M., Crosetti G., La Rotonda L., Tassi E., Atlas Collaboration

Search for long-lived, multi-charged particles in pp collisions at √s =7 TeV using the ATLAS detector
Phys.Lett. B722 (2013) 305-323

358. Capua M., Crosetti G., La Rotonda L., Tassi E., Atlas Collaboration
Search for single b-quark production with the ATLAS detector at √s =7 TeV*
Phys.Lett. B721 (2013) 171-189

359. Capua M., Crosetti G., La Rotonda L., Tassi E., Atlas Collaboration
Jet energy measurement with the ATLAS detector in proton-proton collisions at √s =7 TeV
Eur.Phys.J. C73 (2013) no.3, 2304

360. Capua M., Crosetti G., La Rotonda L., Tassi E., Atlas Collaboration
Search for the Standard Model Higgs boson in the decay channel $H \to ZZ^{(*)} \to 4\ell$ with the ATLAS detector
Phys.Lett. B705 (2011) 435-451

361. Capua M., Crosetti G., La Rotonda L., Tassi E., Atlas Collaboration
Search for the Standard Model Higgs boson in the two photon decay channel with the ATLAS detector at the LHC
Phys.Lett. B705 (2011) 452-470

362. Capua M., Crosetti G., La Rotonda L., Tassi E., Atlas Collaboration
Search for a heavy gauge boson decaying to a charged lepton and a neutrino in 1 fb^{-1} of pp collisions at √s =7 TeV using the ATLAS detector
Phys.Lett. B705 (2011) 28-46

363. Capua M., Crosetti G., La Rotonda L., Tassi E., Atlas Collaboration
Measurement of the inclusive isolated prompt photon cross-section in pp collisions at √s =7 TeV using 35 pb^{-1} of ATLAS data
Phys.Lett. B706 (2011) 150-167

364. Capua M., Crosetti G., La Rotonda L., Tassi E., Atlas Collaboration
Search for neutral MSSM Higgs bosons decaying to $\tau^+\tau^-$ pairs in proton-proton collisions at √s =7 TeV with the ATLAS detector
Phys.Lett. B705 (2011) 174-192.

365. Capua M., Crosetti G., La Rotonda L., Tassi E., Atlas Collaboration
Measurement of the transverse momentum distribution of $Z/\gamma*$ bosons in proton–proton collisions at √s =7 TeV with the ATLAS detector
Phys.Lett. B705 (2011) 415-434

366. Capua M., Crosetti G., La Rotonda L., Tassi E., Atlas Collaboration
Measurement of the Upsilon(1S) production cross-section in pp collisions at √s =7 TeV in ATLAS
Phys.Lett. B705 (2011) 9-27

367. Capua M., Crosetti G., La Rotonda L., Tassi E., Atlas Collaboration
Search for new phenomena with the monojet and missing transverse momentum signature using the ATLAS detector in √s =7 TeV proton-proton collisions
Phys.Lett. B705 (2011) 294-312

368. Capua M., Crosetti G., La Rotonda L., Tassi E., Atlas Collaboration
Search for heavy long-lived charged particles with the ATLAS detector in pp collisions at √s =7 TeV
Phys.Lett. B703 (2011) 428-446

369. Capua M., Crosetti G., La Rotonda L., Tassi E., Atlas Collaboration
Search for high mass dilepton resonances in pp collisions at √s =7 TeV with the ATLAS experiment
Phys.Lett. B700 (2011) 163-180

370. Capua M., Crosetti G., La Rotonda L., Tassi E., Atlas Collaboration
Search for supersymmetry in pp collisions at √s =7 TeV in final states with missing transverse momentum and b-jets
Phys.Lett. B701 (2011) 398-416

371. Capua M., Crosetti G., La Rotonda L., Tassi E., Atlas Collaboration
Measurement of the W charge asymmetry in the W →μν decay mode in pp collisions at √s =7 TeV with the ATLAS detector
Phys.Lett. B701 (2011) 31-49

372. Capua M., Crosetti G., La Rotonda L., Tassi E., Atlas Collaboration
Search for high-mass states with one lepton plus missing transverse momentum in proton-proton collisions at √s =7 TeV with the ATLAS detector
Phys.Lett. B701 (2011) 50-69.

373. Capua M., Crosetti G., La Rotonda L., Tassi E., Atlas Collaboration
Search for squarks and gluinos using final states with jets and missing transverse momentum with the ATLAS detector in √s =7 TeV proton-proton collisions
Phys.Lett. B701 (2011) 186-203

374. Capua M., Crosetti G., La Rotonda L., Tassi E., Atlas Collaboration
Search for Massive Long-lived Highly Ionising Particles with the ATLAS Detector at the LHC
Phys.Lett. B698 (2011) 353-370

375. Capua M., Crosetti G., La Rotonda L., Tassi E., Atlas Collaboration
Measurement of the production cross section for W-bosons in association with jets in pp collisions at √s =7 TeV with the ATLAS detector
Phys.Lett. B698 (2011) 325-345

376. Capua M., Crosetti G., La Rotonda L., Tassi E., Atlas Collaboration
Measurement of the centrality dependence of J/ψ yields and observation of Z production in lead–lead collisions with the ATLAS detector at the LHC
Phys.Lett. B697 (2011) 294-312

377. Capua M., Crosetti G., La Rotonda L., Tassi E., Atlas Collaboration
Search for quark contact interactions in dijet angular distributions in pp collisions at √s =7 TeV measured with the ATLAS detector
Phys.Lett. B694 (2011) 327-345

Hadronic Calorimetry

1. La Rotonda L. et al.,
   The small-angle performance of a dual-readout fiber calorimeter
   Nucl.Instrum.Meth. A808 (2016) 41-53.

2. La Rotonda L. et al.,
   The electromagnetic performance of the RD52 fiber calorimeter
   Nucl.Instrum.Meth. A735 (2014) 130-144.

3. La Rotonda L. et al.,
   Particle identification in the longitudinally unsegmented RD52 calorimeter
   Nucl.Instrum.Meth. A735 (2014) 120-129.

4. La Rotonda L. eta al.,
   Dual-readout Calorimetry
   arXiv:1307.5538 [physics.ins-det].

Proposal for a low energy γ-γ collider

1. Micieli D., Tassi E., et al.
   Compton sources for the observation of elastic photon-photon scattering events
   Phys.Rev.Accel.Beams 19 (2016) no.9, 093401.

Other publications

1. Crosetti G., BaBar and Belle Collaborations
   The Physics of the B Factories
   Eur.Phys.J. C74 (2014), 3026.

2. Crosetti G., BaBar Collaboration
   The BABAR Detector: Upgrades, Operation and Performance
   Nucl.Instrum.Meth. A729 (2013) 615-701.

3. La Rotonda L., NOMAD Collaboration
   A Precision Measurement of Charm Dimuon Production in Neutrino Interactions from the NOMAD Experiment
   Nucl.Phys. B876 (2013) 339-375.

B. PUBLICATIONS ON CONFERENCE PROCEEDINGS

B.1 Publications on international conference proceedings

B.1.1 Publications on international conference proceedings published in 2013-2016

1. *Top quark studies with the ATLAS detector*
   By ATLAS Collaboration (Marcella Capua for the collaboration).
   Int.J.Mod.Phys.Conf.Ser. 39 (2015) 1560092.

2. M. Capua, R Fiore, K Kumerički, A Papa, K Passek-Kumerički, E Tassi, GP Vacca., Proceedings, 8th International Workshop on Diffraction in High Energy Physics (Diffraction 2014), Primosten, Croatia, September 10-16, 2014, AIP Conf.Proc. 1654 (2015).

3. M. Capua, R Fiore, A Papa, Agustin Sabio Vera, E Tassi, GP Vacca., Proceedings, 7th International Workshop on Diffraction in High Energy Physics (Diffraction 2012) : Puerto del Carmen, Lanzarote, Canary Islands, Spain, September 10-15, 201210.1063/1.4802102,AIP Conf.Proc. 1523 (2013) pp.1-347.

C. BOOKS AND BOOK CHAPTERS

C.1 Book and Book chapters accepted for publication in 2016

ReCaS Collaboration

1. Tassi E., et al. (Editor) - ReCaS Collaboration
   High Performance Scientific Computing Using Distributed Infrastructures - Results and Scientific Applications Derived from the Italian PON ReCaS Project
   ISBN 9789814759700 – World Scientific 2016
2. Guarracino N., Lavorini V., Tarasio A., Tassi E.
   High Performance Scientific Computing Using Distributed Infrastructures - Results and Scientific Applications Derived from the Italian PON ReCaS Project
   Chapter 5: The ReCaS project Cosenza Infrastructure
   ISBN 9789814759700 – World Scientific 2016, pag. 43.

3. Tarasio A., et al.,
   High Performance Scientific Computing Using Distributed Infrastructures - Results and Scientific Applications Derived from the Italian PON ReCaS Project
   Chapter 8: Monitoring the ReCaS Project Resources
   ISBN 9789814759700 – World Scientific 2016, pag. 91.

4. Tarasio A., et al.,
   High Performance Scientific Computing Using Distributed Infrastructures – Results and Scientific Applications Derived from the Italian PON ReCaS Project
   Chapter 12: Applications on the ReCaS Project Infrastructure
   ISBN 9789814759700 – World Scientific 2016, pag. 129

5. Guarracino N., Lavorini V., Tarasio A., Tassi E.
   High Performance Scientific Computing Using Distributed Infrastructures – Results and Scientific Applications Derived from the Italian PON ReCaS Project
   Chapter 34: An Integrated Monitoring System, with Ganglia and Nagios, for the Cosenza ReCaS Site
   ISBN 9789814759700 – World Scientific 2016, pag. 417

D. PRESENTATIONS AT SCHOOLS AND CONFERENCES

D.1 Invited presentations at international conferences and schools in 2013

1. M. Capua,
   Deeply Virtual Compton scattering at HERA
   LOWX2013 - The International Workshop on Low x Physics, 30/5. – 4/6/2013, Rehovot, Israel.

2. E. Tassi,
   Proton structure at high Q^2
   LOWX2013 The International Workshop on Low x Physics, 30/5. – 4/6/2013, Rehovot, Israel.

3. E. Tassi for the ATLAS Collaboration,
   Recent QCD results from ATLAS
   QCD@WORK2014 - 7th International Workshop on QCD, Theory and Experiment, 16-19 June 2014, Giovinazzo
   (Bari - Italy)

4. E. Tassi for the ZEUS Collaboration,
   Measurement of the structure of the proton at HERA,
   QFTHEP2015 - XXII International Workshop High Energy Physics and Quantum Field Theory, 24.6 - 1.7.2015,
   Samara, Russia.

5. E. Tassi for the ATLAS Collaboration,
   Latest results on top production from the CMS and ATLAS collaborations: inclusive and differential measurements
   ISMD2015 - XLV International Symposium on Multiparticle Dynamics, 4-9 October 2015, Wildbad Kreuth, Germany.

6. M. Capua for the ATLAS Collaboration,
   Top quark studies with the ATLAS detector
   HS2015 - Hadron Structure 2015, 29 June-3 July 2015, Horný Smokovec, Slovak Republic

7. T. Tene, M. Capua,
   Radon concentrations studies on old building materials
   2nd International Conference Radon in the Environment 2015, 25-29 May 2015, Krakow, Poland.

8. E. Tassi for the ZEUS Collaboration,
   Latest results on QCD at HERA,
   QCD@WORK2016 - 8th International on QCD, Theory and Experiment, 27-30 June 2016, Martina Franca, Italy

9. S. Palazzo,
   Prestazioni delle camere MicroMegas di piccole dimensioni studiate con un fascio di elettroni di 500 MeV
   SIF2016 - 102° Congresso Nazionale della Società Italiana di Fisica, 26-30 Settembre 2016, Padova.

10. D. Micieli, E. Tassi et al.,

Compton sources for the observation of elastic photon-photon scattering events
SIF2016 - 102° Congresso Nazionale della Società Italiana di Fisica, 26-30 Settembre 2016, Padova.

11. G. Callea,
Studio della produzione di fotoni prompt in associazione a jet adronici con il rivelatore ATLAS
SIF2016 - 102° Congresso Nazionale della Società Italiana di Fisica, 26-30 Settembre 2016, Padova.

12. S. Palazzo,
Top precision measurements
XII Workshop ATLAS-Italia: Fisica e Upgrade, 23- 25 Novembre 2016, Napoli.

13. V. Scarfone et al.,
Top SM and BSM
XI ATLAS-Italia Workshop on Run 2 First Results, 4-6 Novembre 2015, Cosenza

14. T. Tene, M. Capua,
Radon assessment of volcanic tuff of the Lazio region, Italy
V Terrestrial Radioisotopes in Environment – International Conference on Environmental Protection, 17–20 May,
2016, Veszprém, Hungary

5. MODELLING OF CLASSICAL AND QUANTUM COMPLEX SYSTEMS

Professors and Researchers	Eleonora Bilotta Pietro Pantano Giuseppe Alì Roberto Beneduci
Postdoc fellows	Lorella Gabriele Francesco Chiaravalloti Tommaso Gentile Assunta Tavernise
PhD students	Notaro Patrizia (XXIX *cycle*) Vigna Mara (XXIX cycle) Altomari Natalia (XXIX *cycle*) Giglio Simona (XXXII *cycle*) Rizzo Rossella (XXXII *cycle*) De Pietro Michela (XXXII *cycle*)
Collaborators	L. Chua *(University of Berkeley, USA)* M. Sammartino *(University of Palermo, Italy)* W.H.A. Schilders (*TU Eindhoven, The Nederlands*) N. Banagaaya (*Max Planck Institute, Germany*). A. Jungel (*TU Wien, Austria*) M. Guenther (*University of Wuppertal, Germany)* I. Torcicollo, (*CNR, Napoli*)

O. Morandi (*Institut de Physique et Chimie des Matériaux de Strasbourg*)
V. Romano (*University of Catania, Italy*)
R. Lucente (*Università della Calabria*)
S. Nigro (*CNR, Catanzaro*)
A. Cerasa (*CNR, Catanzaro*)
F.E. Schroeck *(University of Denver, USA)*
L. Molnar (*Bolyai* Institute, University of Szeged, Hungary)
P. Busch *(Department of Mathematics, University of York, UK)*
S. Pulmannova *(Slovak Academy of Science, SK)*
S.T. Ali *(Department of Mathematics and Statistics, Concordia University, Canada)*
J.J. Slawianowski *(Polish Academy of Science, Poland)*
J. Brooke (*Department of Mathematics and Statistics, University of Saskatchewan, Canada)*

European and National Research projects:

ENIAC SCIENAR
ENIAC LAST POWER (2010-2013)
ENIAC ERG (2011-2014)
ENIAC E2SG (2012-2015)

Organization of International Conferences:

WASCOM 2015 (International conference on Waves and Stability in Continuous Media)

Summary

The research activity in the Academic Years 2013-16 included the following subjects:

- Complex Systems:
  Chua oscillators and Synchronization
  Cellular Neural networks (CNN)
  Mathematical modeling for brain imaging
  Reaction-Diffusion chemotaxis models for multiple sclerosis
- Educational technologies and human computer interaction
- Industrial Mathematics:
  Mathematical Models for Compound Semiconductors
  Quantum models for semiconductors
  Coupled models of PDAEs (partial differential algebraic equations)
  Modeling of heat transport phenomena in integrated circuits
  Model Order Reduction (MOR)

- Foundations of Quantum Mechanics:
  Quantum Mechanics on Phase Space
  Mathematical structure and physical meaning of Unsharp quantum observables
  Interpretations of quantum mechanics
  Applications of functional analysis to quantum mechanics

In the following, we give some details for any of the topics listed above.

5.1 Complex systems

5.1.1 Chua oscillators and Synchronization

Large ensembles of coupled nonlinear oscillators represent a focal research topic in nonlinear dynamics researches. Such systems can display various kinds of spontaneous collective behavior, like synchronization, waves and emergence of self-organized patterns. For this reason, clusters of interacting nonlinear oscillators are a useful model for studying the behavior of real complex systems in many branches of science and technology with a wide variety of significant applications.
We studied an ensemble of Chua oscillators bidirectionally coupled in a ring geometry where locally coupled circuits form a closed loop of signal transmission. The spontaneous dynamics of this system has been studied numerically for different coupling strengths. A transition from periodic to chaotic regimes has been observed when the coupling decreases. In the former situation, characterized by high coupling, all the circuits oscillate with pseudo-sinusoidal dynamics on periodic attractors; in the latter they evolve on the same-type of chaotic attractor with a progression of the dynamics from the Chua's spiral to the double scroll as the coupling decreases. Synchronization and traveling waves moving along the ring have been identified in the non-chaotic regime. Complex patterns formation appears at the “edge of chaos”, for a small couplings interval after the transition between these two regimes.

5.1.2 Cellular Neural networks (CNN)

In 1988, Chua and Yang invented the CNN, a mathematical model in which a set of cells interact with neighboring cells in a nonlinear way. A CNN is a large-scale nonlinear analog circuit that processes signals in real time. It is made of a massive aggregate of regularly spaced circuit clones, called cells, which communicate with each other through their nearest neighbors. Each cell is made of a linear capacitor, a nonlinear voltage-controlled current source, and a few resistive linear circuit elements. The CNNs have the important characteristic of being a metamodel for discrete and continuous systems and they are particularly suitable for image processing tasks.
We proposed a modification of standard CNN when a memristor in a basic cell is introduced. This simple modification with ordinary parameters values allows the improvement of the system performances, in comparison with the standard CNN, without varying the templates.

We also developed a distributed computing system based on CNN and called DCMARK, aimed at solving partial differential equations at the basis of many investigation fields such as Solid State Physics, Nuclear Physics and Plasma Physics. In order to test the computing platform, we implemented a 200 cells, Korteweg de Vries (KdV) equation solver. Since our distributed architecture takes a constant computing time to solve the equation system, independently of the number of dynamical elements (cells) of the CNN array, it allows to reduce the elaboration time more than other similar systems in the literature.

5.1.3 Mathematical modeling for brain imaging

We introduced a novel method to automatically segment the human brainstem into midbrain and pons, called LABS: *Landmark-based Automated Brainstem Segmentation*. LABS processes high-resolution structural magnetic resonance images (MRIs) according to a revised landmark-based approach integrated with a thresholding method, without manual interaction. The comparison between the quantitative measurements provided by LABS against manual segmentations revealed excellent results in healthy controls when considering either the midbrain (percent volume overlap measures higher that 0.9; Volume ratio around 1 and Hausdorff distance around 3) or the pons (percent volume overlap measures around 0.93; Volume ratio ranging 1.024–1.05 and Hausdorff distance around 2).

5.1.4 Reaction-Diffusion chemotaxis models for multiple sclerosis

We derived a reaction-diffusion-chemotaxis model for the dynamics of multiple sclerosis focusing on the early inflammatory phase of the disease characterized by activated local microglia, with the recruitment of a systemically activated immune response, and by oligodendrocyte apoptosis. The model consists of three equations describing the evolution of macrophages, cytokine and apoptotic oligodendrocytes. The main driving mechanism is the chemotactic motion of macrophages in response to a chemical gradient provided by the cytokines.
We also studied the wavefront propagation for a chemotaxis reaction-diffusion system describing the demyelination in Multiple Sclerosis. In particular, through a weakly non linear analysis we obtained the Ginzburg–Landau equation governing the evolution of the amplitude of the pattern.

5.1.5 Educational technologies and human computer interaction

Some recent researches affirm that students' perception of lessons is highly positive when various multimedia teaching tools are integrated. Topics seems more interesting, learners are motivated and feel that media provide them an advantage over the students in a traditional setting. However, in Italy, pre-service teachers' training does not involve a laboratorial approach to the Information and Communication Technologies (ICT) to use in classroom. We proposed a case study on the integration of different technologies involving a new advanced setting by which teachers can interact with diverse specific technologies. In particular, in this technology-enhanced environment, pedagogical agents in a virtual world, touch-screen technologies and robotics can be combined in order to make enjoyable the acquisition of technological skills. Pre-service teachers' reports have shown an overwhelmingly positive response.
We also designed a first experience of coding with Scratch, a simple programming language for pre-service teachers. In particular, the aim of this study has been the investigation of the Scratch programming setting for 58 pre-service teachers, enrolled in a Motor Science course, Degree of Science of Primary Training, at University of Calabria (Italy). The experience has had a duration of 2 months and 4 mentors for instructional interventions have been involved.
Then, we illustrated how Information and Communication Technologies (ICT) could be used to exploit and disseminate Cultural Heritage, providing learning experiences for different targets of users, especially young people. The objective was also to promote and diffuse Calabrian cultural heritage of the ancient Magna Graecia period in a global perspective. The case study of Calabrian Magna Graecia (Italy) has been presented with

particular reference to the projects “Virtual Museum Net of Magna Graecia” and “NETConnect”.
In connection with our studies on complex systems, we analyzed the merging of Chaos with art, including such forms as digital images, sounds and music, based on dynamic systems derived from Chua's Circuit and using appropriate coding methods.

5.2 Mathematical models for semiconductors and industrial mathematics:

5.2.1 Mathematical models for compound semiconductors

We built the first macroscopical model for charge transport in compound semiconductors to make use of analytic ellipsoidal approximations for the energy dispersion relationships in the neighbours of the lowest minima of the conduction bands. The model considers the main scattering mechanisms charges undergo in polar semiconductors, that is the acoustic, polar optical, intervalley non-polar optical phonon interactions and the ionized impurity scattering. Simulations for the cases of bulk 4H and 6H-SiC have been shown.

5.2.2 Quantum models for semiconductors

By the technological progress made in the last decade on the fabrication of microelectronics devices, the active regions of integrated transistors is nowadays downscaled to the submicrometer dimensions. Under such extremal conditions, mathematical models for particle transport in semiconductor devices cannot discard quantum effects.
We derived a quantum-corrected hydrodynamic and drift-diffusion model for the out-of-equilibrium particle dynamics in the presence of particle collisions, modeled by a BGK collision term. The quantum mechanical corrections are obtained within the Liouville formalism and are expressed by an effective nonlinear force. The Boltzmann and Fermi-Dirac statistics have been included.

5.2.3 Coupled models of PDAEs (partial differential algebraic equations):

We analyzed an elliptic partial differential-algebraic model which arises in the modeling of an electric network that contains semiconductor devices. In this context, the electric network is described by linear differential-algebraic equations, while the semiconductor devices are described by nonlinear elliptic partial differential equations. The coupling takes place through the source term for the network equations and the boundary conditions for the device equations. Under the assumption that the fully coupled model has tractability index 2, we prove an existence result for this system. The notion of tractability index has been extended to a specific class of coupled systems.

We also proved the global existence and uniqueness of smooth solutions to a nonlinear system of parabolic–elliptic equations, which describes the chemical aggression of a permeable material, like calcium carbonate rocks, in the presence of acid atmosphere. This model applies when convective flows are not negligible, due to the high permeability of the material. The global (in time) result is proven by using a weak continuation principle for the local solutions.

5.2.4 Modeling of heat transport phenomena in integrated circuits:

An existence and uniqueness result for a two-temperature energy-transport model is proved, in the one-dimensional steady-state case, considering a bounded domain and physically appropriate boundary conditions. The model arises in the description of heat effects in semiconductors, the two temperatures account for the electron and the lattice temperature.

5.2.5 Model Order Reduction (MOR):

The index-aware model order reduction (IMOR) method for differential algebraic equations (DAEs) is based on the decomposition of a DAE into differential and algebraic parts, depending on its tractability index. Then, the differential part is reduced by using existing MOR methods for ODE, and this reduction induces a reduction on the algebraic part, which can be further enhanced. However the IMOR method involves matrix inversions which may limit its practicability in some real-life examples. We presented a modified IMOR method which does not involve matrix inversion.

We also introduces a model order reduction method for index-2 differential-algebraic equations (DAEs) which is based on the intrinsic differential equations and on the remaining algebraic constraints. This extends the method introduced previously for index-1 DAEs. This procedure is implemented numerically and the results show numerical evidence of its robustness over the traditional methods.

5.3 Foundations of Quantum Mechanics

A physical theory can be ideally divided into two parts: the mathematical formalism and the correspondence rules. Correspondence rules are necessary to give a physical content to the formalism. The formalism without the correspondence rules is indeed a mathematical theory avoid of any physical meaning. Vice versa, without a well developed mathematical formalism, the theory remains at the primitive stage of an empirical theory. On the other hand, the correspondence rules must be well clarified in the theory in order to make the theory well formulated. They should also be able to maximize the physical content of the formalism. Unfortunately, the standard formulation of quantum mechanics is lacking concerning both the formalism and the correspondence rules. The main objective of our research group was to contribute to the development of an improved formalism of quantum mechanics that can be coupled to a more precise, clear and complete set of correspondence rules (‘‘physical meaning”). That has been done in the framework of the so called “operational approach” [Ludwig, Davies, Holevo, Ali, Busch, Schroeck, Brooke] and can be divided into the following four topics.

5.3.1 Quantum Mechanics on Phase Space and Classical Mechanics in Hilbert Spaces

The Phase Space formulation of quantum mechanics developed by E. Prugovecki, S.T.Ali, F.E. Schroeck, J. Brooke, P. Busch et al., is a geometric formulation of quantum mechanics that, at variance with the Wigner formulation, describes the states of a system as positive semidefinite distribution functions on the phase space. That is a relevant conceptual advantage. We have shown that the phase space formalism can be used to obtain a representation of classical mechanics in Hilbert spaces. In particular, we considered the Hamilton formulation as well as the Hamiltonian flows on a symplectic (phase) space Γ (both are derivable from the Lie group of symmetries of the physical system considered) and derived the Hamiltonian formalism in the Hilbert spaces of square integrable functions

on Γ. It is worth remarking that the formalism we used to provide a formulation of classical mechanics in Hilbert spaces is the same formalism we used to formulate quantum mechanics on phase space. We also outlined possible applications of the previous results to the description of the quantum transport of electrons in a semiconductor.

5.3.2 Mathematical structure and physical meaning of Unsharp quantum observables

In the standard formulation of quantum mechanics, observables are described by self-adjoint operators (or equivalently by Projection Valued Measures, for short PVMs). It can be shown that self-adjoint operators describe only a very limited class of observables and furthermore they are not able to give a clear mathematical representation of the joint measurability of two observables. For example, the non-commutativity of the position and momentum operators Q, P forbids a mathematical description of their joint measurement. That is instead possible (by respecting the Heisenberg inequality) if we represent the position and the momentum observables by two compatible normalized commutative Positive Operator Valued Measures F^Q, F^P that are noisy versions of Q and P respectively [Davies,Prugovecki,Schroeck]. Positive Operator Valued Measures (for short POVMs) are then relevant from the physical viewpoint and indeed the phase space formulation of quantum mechanics we briefly outlined in the previous section is based on the concept of POVM. They are interesting also from the mathematical viewpoint since the spectral theorem for PVMs can be generalized to POVMs. Commutative POVMs are the most similar to PVMs and are relevant in many physical problems. Our research group has worked at the mathematical characterization of commutative POVMs and at their physical interpretation. In particular, we have shown that any commutative POVM is the randomization of a PVM and that the randomization can be realized by a Feller Markov kernel. We have also shown the connection between the previous characterization and Naimark's dilation theorem.

The problem of localization of the photon provides another example of the usefulness of POVMs in quantum mechanics. Indeed, it is well known that it is not possible to define a localization observable for the photon by means of projection-valued measures while it is possible by means of positive operator-valued measures. Generally speaking, PVMs imply a kind of localization which is stronger than that implied by positive operator-valued measures. It has been claimed that the norm-1 property would in some sense reduce the gap between the two kinds of localizations. We have proved a necessary condition for the norm-1 property and have shown that it is not satisfied by several important localization observables.

5.3.3 Interpretations of quantum mechanics

There is a great confusion on what the interpretation of a physical theory should be. Someone claims that quantum mechanics does not need an interpretation and that it is scandalous that physicists still work on the interpretation of quantum mechanics. Others says that quantum mechanics finds a clear and natural interpretation in quantum filed theory. It is our opinion that before we start speaking about the interpretations of quantum mechanics we first need to clarify what an interpretation is. That can be easily done once we have divided our theory into a formalism and a set of correspondence rules. In some way the correspondence rules provide an "interpretation'' of the formalism. We have shown that once the concept of ''interpretation" has been clarified under this guidelines, any time we speak of quantum mechanics we are implicitly assuming

a particular interpretation, the interpretations we usually assume are often contradictory and the particular interpretation which is coupled to quantum field theory is in no way clear or complete.

5.3.4 Applications of functional analysis to quantum mechanics

C*-algebras are mathematical structures that provide powerful tools in quantum theory. They are powerful tools in the modern formulation of functional analysis and, as a consequence, also in quantum mechanics whose mathematical structure is based on functional analysis.
C*-algebras are particularly relevant in quantum field theory and quantum measurement theory.
We investigated the algebraic properties of the operation $a \circ b = \sqrt{A}\, B \sqrt{A}$ on the set of all positive invertible elements of a C∗-algebra *A*. The operation $\sqrt{A}\, B \sqrt{A}$ is called sequential product in the literature and is relevant in quantum measurement theory where it represents the sequential measurement in which A is performed first and B second. It is also relevant in special relativity where it is connected to Einstein's velocity addition. We have shown that commutativity, associativity and distributivity of the positive invertible elements are equivalent to the commutativity of *A*.

By means of C*-algebraic technics we have proved some mathematical connections among the different characterizations of commutative POVMs.

A. PUBLICATIONS ON SCIENTIFIC JOURNALS

A.1 Publications on international journals in 2013-2016

F. Bertacchini,E.Bilotta, P. Pantano, *Shopping with a robotic companion*, to appear on Computers in Human Behavior (2017).

M Abdechiri, K Faez, H Amindavar, E Bilotta, *Chaotic target representation for robust object tracking*, to appear on Signal Processing: Image Communication (2017).

D Olmedo-Vizueta, J Hernandez-Ambato, D Ávila-Pesantez, E Bilotta, P Pantano, *VALE-Emotions: Aplicación móvil de enseñanza para individuos con Desordenes del Espectro Autista,* to appear on Enfoque UTE (2017).

R. Beneduci, *Joint measurability through Naimark's dilation theorem,* to appear on Reports on Mathematical Physics (2017).

MC Lombardo, R Barresi, E Bilotta, F Gargano, P Pantano, M Sammartino, Journal of Mathematical Biology, 145
(2016) 1-45.

R Barresi, E Bilotta, F Gargano, MC Lombardo, P Pantano, M Sammartino, *Wavefront invasion for a chemotaxis model of Multiple Sclerosis,* Ricerche di Matematica, 65 (2) (2016) 423-434.

B Swaid, E Bilotta, P Pantano, R Lucente, *Bio-Inspired Design Tool to Emerge Multifractal Forms,* International Journal of Academic Scientific Research, 19 (2016) 1-9.

L. VacaCárdenas, A Tavernise, F Bertacchini, L Gabriele, A Valenti, *An Educational Coding Laboratory for Elementary Preservice Teachers: A Qualitative Approach,* International Journal of Engineering Pedagogy, 6 (2016) 11-17.

E Bilotta, P Pantano, S Vena, *Speeding Up Cellular Neural Network Processing Ability by Embodying*
Memristors, IEEE Transactions on Neural Networks and Learning Systems, 99 (2016) 1-5.

E Bilotta, F Chiaravalloti, P Pantano, *Complexity and emergence of wave dynamics in a chain of sequentially*
interconnected Chua circuits, Mechanics Research Communications, 68 (2015) 9-17.

A Piscioneri, S Morelli, M Mele, M Canonaco, E Bilotta, P Pantano, *Neuroprotective effect of human mesenchymal stem cells in a compartmentalized neuronal membrane system,* Acta biomaterialia, 24 (2015) 297-308.

A Tavernise, F Bertacchini, PS Pantano, E Bilotta, *Implementing a New ClassLab: Guidelines for Integrating Innovative Devices in PreService Teachers' Practice*, International Journal of Digital Literacy and Digital Competence (IJDLDC) 6
(2015) 33-49
.
G Borgese, S Vena, P Pantano, C Pace, E Bilotta, *Simulation, modeling, and analysis of soliton waves interaction and propagation in CNN transmission lines for innovative data communication and processing,* Discrete Dynamics in Nature and Society, vol. 2015 (2015) Article ID 139238, 13 pages.
E Bilotta, F Chiaravalloti, P Pantano, *Synchronization and waves in a ring of diffusively coupled memristor based*
Chua's circuits, Acta applicandae mathematicae, 132 (2014) 83-94.

E Bilotta, F Chiaravalloti, P Pantano, *Spontaneous Synchronization in Two Mutually Coupled MemristorBased Chua's Circuits: Numerical Investigations,* Mathematical Problems in Engineering, Volume 2014 (2014) Article ID 594962, 15 pages.

S Nigro, A Cerasa, G Zito, P Perrotta, F Chiaravalloti, G Donzuso, F Fera, *Fully automated segmentation of the pons and midbrain using human T1 MR brain images,* PloS one, 9 (2014) e85618.

G Borgese, C Pace, P Pantano, E Bilotta, *Reconfigurable implementation of a CNNUM platform for fast dynamical systems simulation,* Applications in Electronics Pervading Industry, Environment and Society, 2 (2014) 85-101.

F Bertacchini, E Bilotta, L Gabriele, P Pantano, A Tavernise, *Toward the use of Chua's Circuit in education, art and interdisciplinary research: Some implementation and opportunities*, Leonardo, 46 (2013) 456-463.

G Borgese, C Pace, P Pantano, E Bilotta, *FPGA based distributed computing microarchitecture for complex physical dynamics investigation*, IEEE transactions on neural networks and learning systems 24 (2013) 1390-1399

E Bilotta, P Pantano, *An Advanced Tool for Authoring Multimedia,* Progress in Industrial Mathematics at ECMI 2000, 1 (2013) 118.

G Borgese, C Pace, P Pantano, E Bilotta, *FPGA based calculator using a CNN-UM approach for dynamical systems investigation*, Numerical Computations: Theory and Algorithms, 51 (2013)

F Bertacchini, E Bilotta, P Pantano, G Laria, *The genesis of Chua's circuit: connecting science, art and creativity,*Chaos, CNN, Memristors and Beyond, 4 (2013) 108-123.

P Pantano, E Bilotta, *Cellular nonlinear networks meet KdV equation: a new paradigm*, International Journal of Bifurcation and Chaos 23 (2013) 619-645.

G. Alì, V Romano *Existence and uniqueness for a two temperature energy transport model for semiconductors,* Journal of Mathematical Analysis and Applications, 449 (2016) 1248-1264.

G Alì, A Bartel, N Rotundo, *Index2 elliptic partial differential alalgebraic models for circuits and devices,* Journal of Mathematical Analysis and Applications, 423 (2015) 1348-1369

G Alì, R Natalini, I Torcicollo, *Global existence for a 1D parabolic–elliptic model for chemical aggression in permeable materials,* Nonlinear Analysis: Real World Applications, 21 (2015) 1-12.

G Alì, O Morandi, *Hydrodynamic models with quantum corrections,* Acta applicandae mathematicae, 132 (2014) 3-14.

G Alì, N Banagaaya, WHA Schilders, C Tischendorf, *Index aware model order reduction for differentialalgebraic equations,* Mathematical and Computer Modelling of Dynamical Systems, 20 (2014) 345- 373.

N Banagaaya, WHA Schilders, G Alì, C Tischendorf, *Indexaware model order reduction: LTI DAEs in electric networks,* COMPEL, 33 (2014) 1123-1144.

G Ali, G Mascali, V Romano, RC Torcasio, *A hydrodynamical model for covalent semiconductors with a generalized energy dispersion relation,* European Journal of Applied Mathematics, 25 (2014) 255-276.

G Alì, F Butera, N Rotundo, *Geometrical and physical optimization of a photovoltaic cell by means of a genetic algorithm,* Journal of Computational Electronics, 13 (2014) 323-328

N Banagaaya, G Ali, WHA Schilders, *Implicit-IMOR method for index1 and index2 linear constant DAEs,* Numerical Algebra, Control and Optimization (NACO) (2014)

G Alì, N Banagaaya, WHA Schilders, C Tischendorf, *Indexaware model order reduction for linear index2 DAEs with constant coefficients,* SIAM Journal on Scientific Computing, 35 (2013) A1487-A1510.

R. Beneduci, *Positive Operator Valued Measures and Feller Markov Kernels*, Journal of Mathematical Analysis and Applications, 442 (2016) 50-71.

R. Beneduci, L. Molnar, *On the standard K-loop structure of positive invertible elements in a C*-algebra*, Journal of Mathematical Analysis and Applications 420 (2014) 551-562.

R. Beneduci, F.E. Schroeck, *On the unavoidability of the interpretations of quantum mechanics*, American Journal of Physics, 82 (2014) 80-82.

R. Beneduci, T. Bullock, P. Busch, C. Carmeli, T. Heinosaari, A. Toigo, *Operational link between mutually unbiased bases and symmetric informationally complete positive operator-valued measures*, Phys. Rev. A, 88 (2013) 032312-1-15.

R. Beneduci, F.E. Schroeck, Jr., *A note on the relationship between localization and the norm-1 property,* J. Phys. A: Math. Theor., 46 (2013) 305303-1-13.

R. Beneduci, Uniform continuity of POVMs, *Int. J. Theor. Phys.*, 53 (2014) 3531-3545.

G. Alì, R. Beneduci, G. Mascali, F.E. Schroeck, J.J. Slawianowski, *Some Mathematical Considerations on Solid State Physics in the Framework of the Phase Space Formulation of Quantum Mechanics,* Int. J. Theor. Phys. 53 (2014) 3546-3574.

B. PUBLICATIONS ON CONFERENCE PROCEEDINGS

B.1 Publications on international conference proceedings in 2013-2016

F Bertacchini, E Bilotta, F Caldarola, P Pantano, LR Bustamante, *Emergence of linguistic like structures in one dimensional*
cellular automata, AIP Conference Proceedings, 1776 (1) (2016) 090044.
L.A.V. Cárdenas, F Bertacchini, A Tavernise, L Gabriele, A Valenti, *Coding with Scratch: The design of an educational setting for Elementary preservice teachers,* Interactive Collaborative Learning (ICL), 2015 International Conference, 1171-1177 (2015).

L.A. V. Cárdenas, F Bertacchini, L Gabriele, A Tavernise, DEO Vizueta, *Surfing virtual environment in the Galápagos Islands,* 12th International Conference on Remote Engineering and Virtual Instrumentation (REV), (2015) 192-198.

B Swaid, E Bilotta, P Pantano, R Lucente, *Thresholding Urban Connectivity by Local Connected Fractal Dimensions and*
Lacunarity Analyses, Late Breaking Proceedings of the European Conference on Artificial Life 2015.

S Giglio, L Gabriele, A Tavernise, P Pantano, E Bilotta, F Bertacchini, *Virtual museums and Calabrian Cultural Heritage: projects and challenges,* Digital Heritage, 2 (2015) 703-708.

L.A.V. Cárdenas, F. Bertacchini, L. Gabriele, A. Tavernise, D.E.O. Vizueta, P. Pantano, E. Bilotta, *Surfing virtual environment in the Galápagos Islands*, 12th International Conference on Remote Engineering and Virtual Instrumentation (REV), 2015.

D.E.O. Vizueta, F. Bertacchini, L.V. Cárdenas, L. Gabriele, A. Tavernise, P. Pantano, E. Bilotta, *A video-modeling system for improving social skills and lexicon in autistic spectrum disorder children*, EDULEARN14 Proceedings, 5 (2014) 6081-6087.

L.A.V. Cárdenas, D.E.O. Vizueta, A Tavernise, L Gabriele, F Bertacchini, P Pantano, E Bilotta, *Darwin has come back to the Galápagos Islands: An educational journey to discover biological evolution*, EDULEARN14 Proceedings, 6 (2014) 6088-6095.

N Banagaaya, G Alì, WHA Schilders, C Tischendorf, *Implicit index-aware model order reduction for RLC/RC networks,* Design, Automation and Test in Europe Conference and Exhibition (DATE) (2014).

F Bertacchini, E Bilotta, L Gabriele, DEO Vizueta, P Pantano, F Rosa, *An emotional learning environment for subjects with Autism Spectrum Disorder*, International Conference on Interactive Collaborative Learning (ICL), 2013 653-659.

F Bertacchini, A Tavernise, L Gabriele, E Bilotta, P Pantano, F Rosa, *Musical Lab role in developing creativity and cognitive skills,* EDULEARN13 Proceedings, 3 (2013) 5784-5792.

L Gabriele, E Bilotta, *Robot for thinking: cognitive strategies to experiment the use of educational robotics in classroom*,
EDULEARN13 Proceedings, (2013) 5801-5810

6. MOLECULAR BIOPHYSICS

Professors and Researchers: Luigi Sportelli
Rosa Bartucci
Rita Guzzi
Bruno Rizzuti *(Lab. LiCryL, CNR-NANOTEC, UOS Cosenza)*

Post-Doc: Manuela Pantusa (01/09/2011-31/08/2014)
Andrea Stirpe (02/11/2013-30/04/2015)

PhD Student: Stefania Evoli (XXVII ciclo, 2012-2014)

Technical staff: Massimo Sposato

Collaborators: D. Marsh (*MPI for Biophysical Chemistry, Goettingen, Germany*)
M. Esmann (*Aarhus University, Dept. of Biochemistry, Denmark*)
V. Daggett (*Washington University, Dept. of Bioengineering*)
D. E. Otzen (*Aarhus University, Dept Mol Biol and i-Nano Centre)*
D.L. Mobley (*University of California, Dept of Pharm. Sci and Chem., Irvine, USA*)
J.L. Neira (*Universidad Miguel Hernández, Instituto de Biol. Mol. Cel., Elche, Spain*)
R. Mezzenga (*ETH, Zurigo, Laboratory of Food & Soft Materials*)
M.P. De Santo *(Univ. Calabria, Dept. of Physics, Lab. LiCryL, CNR-NANOTEC, UOS Cosenza)*
B. Zappone *(Lab. LicryL, CNR-NANOTEC, UOS Cosenza)*
F. Ciuchi (*Lab. LicryL, CNR-NANOTEC, UOS Cosenza)*

Introduction

The research activity of the Molecular Biophysics Group in the period 2013-2016 has concerned biophysical studies of the structure, dynamics and function of cell membrane components, namely lipids and proteins. In particular, the research activity focused on the

following topics: i) interaction of lipid bilayers and transport proteins with ligands; ii) folding, stability and aggregation of proteins; iii) lipid/protein interface in membranes.
As regards the first research line, ligands of biological and biomedical interest have been considered such as resveratrol, fatty acids and ibuprofen. Resveratrol is a natural polyphenol that has positive effects (anti-oxidant, anti-inflammatory, cardioprotective and anti-tumoral) on human health. Fatty acids regulate a broad spectrum of metabolic activities and are involved in many physiological processes in cells. Finally, ibuprofen is a nonsteroidal anti-inflammatory drug widely used as a therapeutic agents worldwide for pain treatment. From a biophysical standpoint, it is therefore crucial to characterize the effects of these ligands on lipid bilayers and proteins. To this end, membrane model systems made up of phosphatidylcholine molecules, which are the most abundant phospholipid in eukaryotic cells, and the transport proteins human serum albumin (HSA) and β-lactoglobulin (β-LG) have been considered. The research activity has been carried out by combining an array of appropriate experimental and computational approaches. In particular, these techniques include continuous wave EPR, fluorescence, optical absorption, infrared spectroscopy, high-sensitivity differential scanning calorimetry, molecular dynamics simulations and docking.
The second research line regards some of the most complex systems in protein biophysics. Studies of intrinsically disordered proteins (IDPs) and fibrillation-prone proteins are relevant not only in basic research, but also in the biomedical field and for other practical applications. IDPs are often associated with a number of severe diseases in humans, and insoluble fibrillar aggregates of proteins are found in the brain of patients affected by neurodegenerative/neurological disorders. In addition, the self-assembly of proteins and polypeptides in amyloid fibrillar aggregates is rapidly emerging as a promising route towards the fabrication of nano-objects with controlled morphologies and properties. Another relevant aspect that has been studied is the glassy-behavior shown by proteins at around 200 K, when they are cryogenically frozen at low temperature. This behavior is driven by complex motions that include protein librations. Within this context, key features of proteins have been addressed by spectroscopic, calorimetric and microscopic approaches, as well as with computing methods.
Finally, the molecular interaction of the lipid/protein interface has been studied by considering Na,K-ATPase membranes, a large integral enzyme that is responsible for maintaining the ionic balance in animal cells. By using advanced methods of pulsed, Fourier transform electron spin echo spectroscopy in the time and frequency domain, the lipid/protein interface has been characterized for the first time by studying both the protein component and the bilayer region, and also including the investigation of bilayers formed by extracted lipids.

In the following, the main research results are briefly presented in the form of abstracts.

6.1 INTERACTION OF LIPID BILAYERS AND TRANSPORT PROTEINS WITH LIGANDS

6.1.1 Interaction of membrane model systems with resveratrol

EPR of chain labeled lipids, calorimetry, X-ray diffraction and molecular docking have been used to study the interaction of resveratrol with membrane model systems of dipalmitoylphosphatidylcholine (DPPC) as a function of resveratrol concentration (0–30 mol% of the lipid) and temperature (10–50 °C). Resveratrol incorporated in DPPC bilayers induces considerable motional restriction at the lipid tail termini, removing the gradient of increasing mobility along the chain found in DPPC bilayers in the gel phase. In contrast, it leaves unperturbed the DPPC chain flexibility profile in the liquid-crystalline phase. At low concentration, resveratrol progressively reduces the pre-transition temperature and eliminates the pre-transition for content ≥5 mol%. A reduced cooperativity and a

downshift of the main transition temperature are observed, especially at high content. The typical diffraction pattern of DPPC multibilayers in the $L_{\beta'}$ phase is converted to a lamellar pattern with reduced *d*-spacing of untilted lipid chain in a hexagonal packing at 30 mol% of resveratrol. Molecular docking indicates that the energetically favoured anchoring site is the polar headgroup region, where resveratrol acts as a spacer. The overall results are consistent with the formation in DPPC of an interdigitated $L_{\beta i}$ gel phase induced by 30 mol% resveratrol.

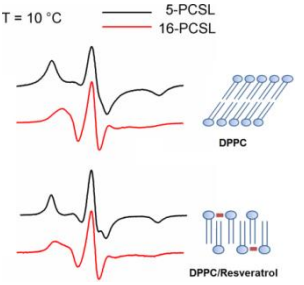

EPR spectra of model membrane of DPPC in the gel phase with and without resveratrol and schematic representation of resveratrol-induced acyl chain interdigitation in

6.1.2 Interaction of transport proteins with resveratrol

Two aspects of this topic have been addressed: the stability of trans-resveratrol associated with the transport proteins, HSA and β-LG, and the ability of resveratrol to interfere with the aggregation process upon binding to HSA.

Spectrophotometry and fluorescence combined with docking and molecular dynamics simulations were used to study the effect of β-lactoglobulin and human serum albumin on the degradative *trans*-to-*cis* conversion of resveratrol. The spectroscopic measurements quantified the concentration of resveratrol isoforms after 2 h of irradiation with light at 340 nm, showing that their ratio depends linearly on temperature between 20 and 50 °C and obeys an Arrhenius law with activation energies of photoisomerization of 7.8 and 11.2 kcal/mol for β-lactoglobulin and albumin, respectively, compared to 5.1 kcal/mol in solution. Thus, both proteins protect *trans*-resveratrol from degradation, with albumin being more effective than β-lactoglobulin. The computational techniques clarified details of the binding of *trans*-resveratrol to the proteins and showed that the stabilizing effect correlates with an increase of the dihedral order parameter of the ligand. These findings suggest that transport proteins are viable carriers to stabilize and deliver resveratrol *in vivo* in the biologically effective *trans* form.

The impact of resveratrol on the stability and heat induced aggregation of HSA were investigated by differential scanning calorimetry, attenuated total reflectance Fourier transform infrared, UV–vis absorbance, ThT fluorescence, atomic force microscopy and molecular modeling. The binding of resveratrol to HSA improved the stability of the protein to thermal unfolding, particularly for the energetic domain containing the ligand binding site, as modeled by computational techniques. The thermal unfolding is irreversible and after the melting the protein aggregated, either with or without the ligand. The kinetics of HSA aggregation between 70 and 80 °C showed an exponential growth of the absorbance change and it slowed down when resveratrol was added. The aggregates had fibril-like morphology and resveratrol attenuated the formation of β-structured species. The overall results suggest that resveratrol stabilizes the protein structure and modulates the formation of fibrils along the initial stage of the HSA aggregation pathway.

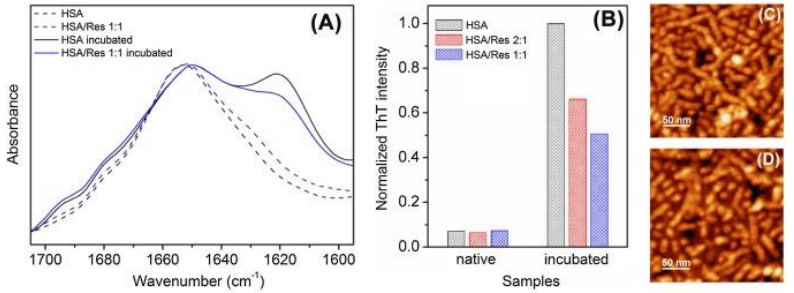

Characterization of human serum albumin with and without resveratrol, before and after incubation at 80 °C for 180 min. (A) ATR-FTIR spectra in the amide I region, (B) ThT fluorescence and AFM images of incubated protein samples (C) without and (D) with resveratrol.

6.1.3 Molecular dynamics and docking of HSA and β-LG complexed with fatty acids

Multiple molecular dynamics simulations were performed to investigate the association of stearic acid into the highest affinity binding site of human serum albumin. All binding events ended with a rapid (<10 ps) lock-in of the fatty acid due to formation of a hydrogen bond with Tyr401. The kinetics and energetics of the penetration process both depended linearly on the positional shift of the fatty acid, with an average insertion time and free energy reduction of, respectively, 32 ± 20 ps and 0.70 ± 0.15 kcal/mol per methylene group absorbed. Binding events of longer duration ($t_{bind} > 1$ ns) were characterized by a slow exploration of the pocket entry and, frequently, of a nearby protein crevice corresponding to a metastable state along the route to the binding site. Taken all together, these findings reconstructed the following pathway for the binding process of stearic acid: (i) contact with the protein surface, possibly facilitated by the presence of an intermediate location, (ii) probing of the site entry, (iii) insertion into the protein, and (iv) lock-in at the final position. This general description may also apply to other long-chain fatty acids binding into any of the high-affinity sites of albumin, or to specific sites of other lipid-binding proteins.
The interaction of saturated fatty acids of different length (C8:0 to C18:0) with β-LG was investigated by molecular dynamics simulation and docking approaches. The results showed that the presence of such ligands in the hydrophobic central cavity of β-LG, known as the protein calyx, determines an enhancement of atomic fluctuations compared with the unliganded form, especially for loops at the entrance of the binding site. Concerted motions were evidenced for protein regions that could favor the binding of ligands. The mechanism of anchoring of fatty acids of different length was similar for the carboxylate head-group, through electrostatic interactions with the side chains of Lys60/Lys69. The key protein residues to secure the hydrocarbon chain are Phe105/Met107, which adapt their conformation upon ligand binding. In particular, Phe105 provides an additional hydrophobic clamp only for the tail of the two fatty acids with the longest chains, palmitic, and stearic acid, which are known to bind βLG with a high affinity. The search of additional external binding sites for fatty acids, distinct from the calyx, was also carried out for palmitic acid. Two external sites with a lower affinity were identified as secondary sites, one consisting in a hydrophobic cavity allowing two distinct binding modes for the fatty acid, and the other corresponding to a surface crevice close to the protein α-helix. The overall results provide a comprehensive picture of the dynamical behavior of βLG in complex with fatty acids, and elucidate the structural basis of the binding of these physiological ligands.

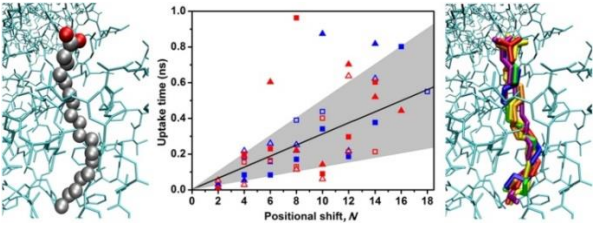

Binding dynamics of stearic acid in the highest affinity site of HSA derived by molecular dynamics simulation.

6.1.4 Binding free energy calculations of ibuprofen in human serum albumin

A complete map of the binding sites of ibuprofen in albumin is difficult to obtain in traditional experiments, because of the structural adaptability of this protein in accommodating small ligands. We provided a set of predictions covering the geometry, affinity of binding and protonation state for the pharmaceutically most active form (*S*-isomer) of ibuprofen to albumin, by using absolute binding free energy calculations in combination with classical molecular dynamics simulations and molecular docking. The most favorable binding modes correctly reproduced several experimentally identified binding locations, which include the two Sudlow's drug sites and the fatty acid binding sites 6 and 2. Previously unknown details of the binding conformations were revealed for some of them, and formerly undetected binding modes were found in other protein sites. The calculated binding affinities exhibited trends which seem to agree with the available experimental data, and drastically degrade when the ligand was modeled in a protonated (neutral) state, indicating that ibuprofen associates with albumin preferentially in its charged form. These findings provide a detailed description of the binding of ibuprofen, help to explain a wide range of results reported in the literature in the last decades, and demonstrate the possibility of using simulation methods to predict ligand binding to albumin.

6.2 FOLDING, STABILITY AND AGGREGATION OF PROTEINS

6.2.1 Intrinsically disordered and highly flexibile proteins: solution properties

The assembly of the protein complex of cytochrome *c* oxidase (COX), which participates in the mitochondrial respiratory chain, requires a large number of accessory proteins (the so-called assembly factors). Human COX assembly factor 3 (hCOA3) interacts with the first subunit protein of COX to form its catalytic core and promotes its assemblage with the other units. Therefore, hCOA3 is involved in COX biogenesis in humans and can be exploited as a drug target in patients with mitochondrial dysfunctions. However, to be considered a molecular target, its structure and conformational stability must first be elucidated. We have embarked on the description of such features by using spectroscopic and hydrodynamic techniques, in aqueous solution and in the presence of detergents, together with computational methods. Our results show that hCOA3 is an oligomeric protein, forming aggregates of different molecular masses in aqueous solution. Moreover, on the basis of fluorescence and circular dichroism results, the protein has (i) its unique tryptophan partially shielded from solvent and (ii) a relatively high percentage of secondary structure. However, this structure is highly flexible and does not involve hydrogen bonding. Experiments in the presence of detergents suggest a slightly higher content of nonrigid helical structure. Theoretical results, based on studies of the primary structure of the protein, further support the idea that hCOA3 is a disordered protein. We suggest that the flexibility of hCOA3 is crucial for its interaction with other proteins to favor mitochondrial protein translocation and assembly of proteins involved in the respiratory chain.

Another protein of great interest is NUPR1, a multifunctional IDP involved in the development and progression of pancreatic cancer. In an effort to contribute to the understanding of the conformational features of NUPR1 and to provide clues on amino acid interactions in disordered states of proteins, we measured the pK_a values of all its acidic groups (aspartic and glutamic residues, and backbone C terminus) by using NMR spectroscopy at low (100 mM) and high (500 mM) NaCl concentration. At low ionic strength, the pK_a values were similar to those reported for random-coil models, except for Glu18 and Asp19, suggesting electrostatic interactions around these residues. Molecular modelling and simulation indicate an additional, significant role of nearby proline residues in determining the polypeptide conformational features and water accessibility in the region around Glu18, modulating the titration properties of these amino acids. In the other acidic residues of NUPR1, the small deviations of pK_a values (compared to those expected for a random-coil) are likely due to electrostatic interactions with charged adjacent residues, which should be reduced at high NaCl concentrations. In fact, at high ionic strength, the pK_a values of the aspartic residues were similar to those in a random coil, but there were still small differences for those of glutamic acids, probably due to hydrogen-bond formation. The overall findings suggest that local interactions and hydrophobic effects play a major role in determining the electrostatic features of NUPR1, whereas long-range charge contributions appear to be of lesser importance.

6.2.2 Alpha-synuclein and familial variants fold-in and affect lipid bilayers

Alpha-synuclein (aSN) is a presynaptic protein with a pathological role in Parkinson's disease (PD). The mutants A30P, E46K and A53T are involved in PD early-onset forms. aSN is natively unfolded but can self-assemble to oligomers and fibrils and binds anionic membranes in a helical conformation. We have studied the influence of wild-type (wt) aSN and familial variants on the chain order and thermotropic phase behavior of anionic dimyristoylphosphatidylglycerol (DMPG) bilayers by using electron spin resonance and calorimetry, respectively. The alpha-helical conformation of the proteins in the membrane-bound state was assessed by circular dichroism thermal scans. wt and mutated aSN upon binding to fluid DMPG vesicles progressively increase chain order. Lipid:protein molar binding stoichiometries corresponded to 50 for A30P, 35–36 for aSN and A53T, 30 for E46K. The temperature range over which the variants assumed the α-helical fold correlates directly with the density of proteins on vesicle surfaces. All variants preserved the characteristic chain flexibility gradient and impart motional restriction in the lipid chain. This was evident at the first CH_2 segments and was markedly reduced at the chain termini, disappearing completely for A30P. The proteins slightly reduce DMPG main transition temperature, revealing preferential affinity for the fluid phase, and broaden the transition, promoting gel-fluid phase coexistence. The overall results are consistent with protein surface association in which the degree of binding correlates with the degree of folding and perturbation of the membrane bilayer. However, the degree of binding of monomer to membrane does not correlate directly with aSN toxicity *in vivo*.

6.2.3 β-LG fibrillation and role of transition metal ions

Transition metal ions are known to play an important but elusive role in the amyloid fibrillation associated with neurodegenerative diseases such as Alzheimer's and Parkinson's diseases. We have considered the effect of transition metal ions on fibrillation of β-LG, a model protein not related to amyloid diseases, which denatures and self-assembles in nanofibrils upon heating at low pH and ionic strength. The energetics of amyloid fibrillar aggregation of β-LG following incubation at high temperature and acid pH was studied by differential scanning calorimetry in the presence of Cu^{2+} or Fe^{3+} cations, and without any metal. Cu^{2+} and metal-free protein solutions showed a distinct exothermic response that disappeared almost completely when the Fe^{3+} molar concentration was ten times greater than the βLG concentration. Thioflavin T fluorescence studies in solution and atomic force microscopy analysis of the deposit left on flat mica substrates by heat-incubated β-LG solutions correlated the absence of exothermic response of Fe^{3+}-βLG solutions with a lack of fibril production. In contrast, abundant fibril deposits were observed for Cu^{2+}/β-LG solutions, with a rich

polymorphism of multistrand fibrillar structures. Electron paramagnetic resonance revealed that Fe^{3+} permanently binds to β-LG in the aggregate state whereas Cu^{2+} plays a catalytic role without binding to the protein. We propose that Fe^{3+} inhibits fibril production after binding to a key region of the protein sequence, possibly interfering with the nucleation step of the fibrillation process and opening a nonfibrillar aggregation pathway. These findings suggest that transition metal ions can be utilized to effectively modulate protein self-assembly into a variety of structures with distinct morphologies at the nanoscale level.
In addition, we have considered the effect of copper ions Cu^{2+} on the nanoscale morphology and fibrillation kinetics of β-LG. We found that an increasing level of Cu^{2+} decreases the enthalpy of denaturation and significantly increases the rate of fibril nucleation, also producing a small increase of the fibril elongation rate. Cu^{2+} acts as a catalytic agent during protein denaturation and fibrillation, without binding to βLG before or after heating, and produces only minor changes in fibril morphology. Beside possible implications for amyloid pathologies *in vivo*, our results suggest that transition metal ions can be used to control the self-assembly of protein-based nano-objects *in vitro*.

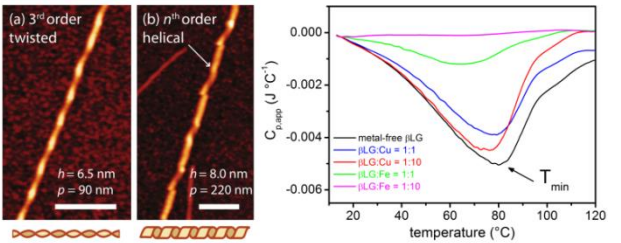

Models of fibril topology formed by high temperature incubation of βLG at pH 2 and the calorimetric exotermic response of fibrils solution in the absence and in the presence of metal ions.

6.2.4 Conformational substates and glassy behavior of proteins

The energy landscape of proteins is characterized by a hierarchy of substates, which give rise to conformational heterogeneity at low temperatures. In multiply spin-labeled membranous Na,K-ATPase, this heterogeneous population of conformations is manifest by strong inhomogeneous broadening of the electron paramagnetic resonance line shapes and nonexponential spin-echo decays, which undergo a transition to homogeneous broadening and exponential relaxation at higher temperatures. We also investigated small water-soluble proteins, of the type for which the existence of conformational substates is well established. Both α-helical and β-sheet aqueous proteins that are spin-labeled on a single cysteine residue display spin-echo decays with a single phase-memory time T_{2M} and conventional EPR line shapes with predominantly homogeneous broadening, over a broad range of temperatures from 77 K to ~ 250 K or higher. Above ~ 200 K, the residual inhomogeneous broadening is reduced almost to zero. In contrast, both the proteins and the spin label alone, when in a glycerol-water mixture below the glass transition, display heterogeneity in spin-echo phase-memory time and a stronger inhomogeneous broadening of the conventional line shapes, similar to multiply spin-labeled membranous Na,K-ATPase below 200 K. Above 200 K (or the glass transition), a single phase-memory time and predominantly homogeneous broadening are found in both spin-label systems. The results were examined in terms of solvent-mediated protein transitions, the ability of single spin-label sites to detect conformational heterogeneity, and the desirability of exploring multiple sites for proteins with the size and complexity of the Na,K-ATPase.
The librational motions in the region of the protein "glass" (or dynamic) transition were analyzed for spin-labelled haemoglobin, serum albumin and β-lactoglobulin by EPR spectroscopy. A discontinuity in the temperature dependence of the mean-square librational amplitude, $\langle\alpha^2\rangle$, occurs in the region of 200 K as found for the mean-square atomic displacement, $\langle r^2\rangle$, at the protein dynamic transition by Mössbauer spectroscopy and neutron scattering. The discontinuity in $\langle\alpha^2\rangle$ vs. T can be described by the Vogel–Tammann–Fulcher equation, implying a finite glass transition temperature. Above the

dynamic transition, $<\alpha^2>$ vs. $1/T$ can be approximated by the Arrhenius law with activation energies similar to those usually found for $<r^2>$, and relaxation processes in glass-forming media and the hydration shells of proteins. Similar results are found for librational fluctuations of membranous Na,K-ATPase spin-labelled either on superficial -SH groups or on those essential to activity.

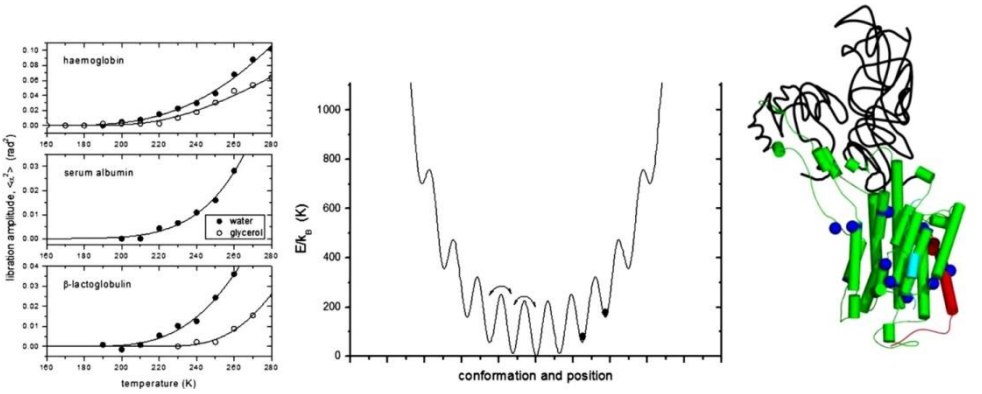

Librational amplitude (left) and energy landscape of proteins with librational fluctuations within the conformational substates (centre). Schematic representation of Na,K-ATPase enzyme (right).

6.3 MOLECULAR INTERACTION at the LIPID/PROTEIN INTERFACE

6.3.1 Lipid librations at the interface with Na,K.ATPase

Transitions between conformational substates of membrane proteins can be driven by torsional librations in the protein that may be coupled to librational fluctuations of the lipid chains. Librational motion of spin-labeled lipid chains in membranous Na,K-ATPase was investigated by spin-echo electron paramagnetic resonance. Lipids at the protein interface were targeted by using negatively charged spin-labeled fatty acids that display selectivity of interaction with the Na,K-ATPase. Echo-detected electron paramagnetic resonance spectra from native membranes were corrected for the contribution from the bilayer regions of the membrane by using spectra from dispersions of the extracted membrane lipids. Lipid librations at the protein interface have a flat profile with chain position, whereas librational fluctuations of the bilayer lipids increased pronouncedly from C-9 onward, then flatten off toward the terminal methyl end of the chains. This difference is accounted for by increased torsional amplitude at the chain ends in bilayers, while the amplitude remains restricted throughout the chain at the protein interface with a limited lengthening in correlation time. The temperature dependence of chain librations at the protein interface strongly resembles that of the spin-labeled protein side chains, suggesting solvent-mediated transitions in the protein are driven by fluctuations in the lipid environment.

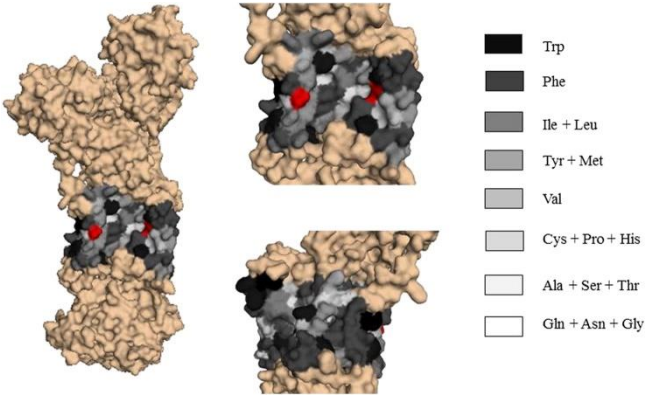

Hydrophobicity profile of residues at the protein membrane interface in Na,K-ATPase.

6.3.2 Water penetration profile at the protein-lipid interface in Na,K-ATPase membranes

The affinity of ionized fatty acids for the Na,K-ATPase has been used to determine the transmembrane profile of water penetration at the protein-lipid interface. The standardized intensity of the electron spin echo envelope modulation from ^{2}H-hyperfine interaction with D_2O was determined for stearic acid, *n*-SASL, spin-labelled systematically at the C-*n* atoms throughout the chain. In both native Na,K-ATPase membranes from shark salt gland and bilayers of the extracted membrane lipids, the D_2O-ESEEM intensities of fully charged n-SASL decreased progressively with position down the fatty acid chain towards the terminal methyl group. Whereas the D_2O intensities decreased sharply at the n=9 position in the lipid bilayers, a much broader transition region in the range n=6 to 10 was found with Na,K-ATPase membranes. Correction for the bilayer population in the membranes yielded the D_2O-intensity profile at the protein-lipid interface. For each chain position, the D_2O concentrations at the interface were greater than in the lipid bilayer, and the positional profile was much broader. In particular, there was a significant water concentration at the membrane mid-plane adjacent to the protein, unlike the situation in the bilayer regions of this cholesterol-containing membrane. Experiments with protonated fatty acid and phosphatidylcholine spin labels, both of which have a considerably lower affinity for the Na,K-ATPase, confirmed these results.

A PUBLICATIONS ON SCIENTIFIC JOURNALS

A.1 Publications on international journals printed in 2013-2016

1. S. Evoli, R. Guzzi, B. Rizzuti
Dynamics and unfolding pathway of chimeric azurin variants: insights from molecular dynamics simulation
J. Biol. Inorg. Chem. 18 (2013) 739-749.

2. D. Marsh, R. Bartucci, R. Guzzi, L. Sportelli, M. Esmann
Librational fluctuations in protein glasses
Biochim. Biophys. Acta – Proteins and Proteomics 1834 (2013) 1591-1595.

3. B. Rizzuti and V. Daggett
Using simulations to provide the framework for experimental protein folding studies

Arch. Biochem. Biophys. 531 (2013) 128-135.

4. B. Zappone, M.P. De Santo, C. Labate, B. Rizzuti, R. Guzzi
Catalytic activity of copper ions in the amyloid fibrillation of ß-lactoglobulin;
Soft Matter 9 (2013) 2412-2419.

5. R. Guzzi, R. Bartucci, D. Marsh
Heterogeneity of protein substates visualised by spin-label EPR
Biophys. J. 106 (2014) 716-722.

6. M. Pantusa, R. Bartucci, B. Rizzuti
Stability of trans-resveratrol associated with transport proteins
J. Agric. Food Chem. 62 (2014) 4384-4391.

7. A. Stirpe, M. Pantusa, R. Guzzi, R. Bartucci, L. Sportelli
Chain interdigitation in DPPC bilayers induced by $HgCl_2$: Evidences from continuous wave and pulsed EPR Chem. Phys. Lipids 183 (2014) 176-183.

8. R. Bartucci, R. Guzzi, L. Sportelli, M. Esmann D. Marsh
Water penetration profiles at the protein-lipid interface in Na,K-ATPase membranes
Biophys. J. 107 (2014) 1375-1382.

9. S. Evoli, R. Guzzi, B. Rizzuti
Molecular simulations of ß-lactoglobulin complexed with fatty acids reveal the structural basis of ligand affinity to internal and possible external binding sites
Proteins: Structure, Function, and Bioinformatics 82 (2014) 2609-2619.

10. R. Guzzi and R. Bartucci
Electron Spin Resonance of spin-labelled lipid assemblies and proteins
Arch. Biochem. Biophys. 580 (2015) 102-111.

11. R. Guzzi, R. Bartucci, M. Esmann, D. Marsh
Lipid librations at the interface with the Na,K-ATPase
Biophys. J. 108 (2015) 2825-2832.

12. B. Rizzuti, R. Bartucci, L. Sportelli, R. Guzzi
Fatty acid binding into the highest affinity site of human serum albumin observed in molecular dynamics simulation
Arch. Biochem. Biophys. 579 (2015) 18-25.

13. R. Guzzi, B. Rizzuti, C. Labate, B. Zappone, M.P. De Santo
Ferric ions inhibit the amyloid fibrillation of ß-lactoglobulin at high temperature
Biomacromolecules 16 (2015) 1794-1801.

14. S. Evoli, D.L. Mobley, R. Guzzi, B. Rizzuti
Multiple binding modes of ibuprofen in human serum albumin identified by absolute binding free energy calculations
Phys. Chem. Chem. Phys. 18 (2016) 32358-32368.

15. J.L. Neira, S. Martínez-Rodríguez, J.G. Hernández-Cifre, A. Cámara-Artigas, P. Clemente, S. Peralta, M.A. Fernández-Moreno, R. Garesse, J.G. de la Torre, B. Rizzuti

Human COA3 is an oligomeric highly flexible protein in solution
Biochemistry 55 (2016) 6209-6220.

16 E. Longo, F. Ciuchi, R. Guzzi, B. Rizzuti, R. Bartucci R
Resveratrol induces interdigitation in DPPC cell membrane model systems
Colloids and Surfaces B: Biointerfaces 148 (2016) 615–621.

B BOOK CHAPTERS

R. Bartucci
Spin-labeling EPR of lipid Membranes
In "Encyclopedia of Biophysics", G.C.K. Roberts (ed), Springer, Berlin-Heidelberg, vol 2, (2013)
2431-2439.

C PRESENTATIONS AT CONFERENCES

C.1 Oral presentations at international conferences

C. Labate, B. Zappone, R. Guzzi, M. P. De Santo, B. Rizzuti
Effects of the presence of metal ions on the aggregation of beta-lactoglobulin
ISMC 2013 – 3rd International Soft Matter Conference
September 15-19, 2013 – Roma

M. Pantusa, R. Bartucci, B. Rizzuti
Association of resveratrol to carrier proteins: a computational and experimental analysis
ISMC 2013 – 3rd International Soft Matter Conference
September 15-19, 2013 – Roma

S. Evoli, M. Pantusa, R. Guzzi, B. Rizzuti
Computational approaches for protein-ligand interaction studies
NanoPlasm 2014 – New frontiers in plasmonics and nano-optics
June 16-20, 2014 – Cetraro (CS)

R. Guzzi, B. Rizzuti, C. Labate, B. Zappone, M.P. De Santo
Modulation of protein nanofibril features by using metal ions
NanoPlasm 2014 – New frontiers in plasmonics and nano-optics
June 16-20, 2014 – Cetraro (CS)
J. L. Neira, M. Arruebo, J. Bintz, B. Rizzuti, T. Bonacci, S. Vega, A. Veláquez-Campoy, J. Iovanna, O. Abián
Development of an efficient protocol for screening FDA-approved small molecules able to inhibit the function of Nupr1, an Intrinsically Disordered Protein (IDP), to treat patients with a PDAC
1st Pancreatic Cancer Symposium
October 28-30, 2015 – Palais du Pharo – Marseille, Francia

C.2 Oral presentations at national conferences

S. Evoli, R. Guzzi, B. Rizzuti
Molecular dynamics and docking of fatty acids interacting with beta-lactoglobulin

FisMat 2013 – 1st Italian National Conference on Condensed Matter Physics
September 9-13, 2013 – Milano

S. Evoli, R. Guzzi, B. Rizzuti
A computational approach to investigate the molecular basis in fatty acid interactions with ß-lactoglobulin
SIF 2014 – 100th National Congress of SIF (Società Italiana di Fisica)
September 22-26, 2014 – Pisa

B. Rizzuti, S. Evoli, M. Pantusa, R. Guzzi
Molecular dynamics and docking of small ligands complexed with model transport proteins
SIBPA 2014 – 22nd National Conference of SIBPA (Italian Society for Pure ad Applied Biophysics)
September 23, 2014 – Palermo

B. Rizzuti
Bio and complex systems
IMIP kick-off meeting
March 12, 2015 – Lequile (LE)

B. Rizzuti, R. Guzzi
Computational methods for modeling host-ligand interactions: applications to pharmaceutical and nutraceutical molecules
Materials and technologies for healthcare and biodiagnostics at CNR-NANOTEC
September 11, 2015 – Bari

B. Rizzuti, S. Evoli, R. Guzzi, D. L. Mobley
Multiple binding modes of ibuprofen in human serum albumin identified by alchemical free energy calculations
FisMat 2015 – 2nd Italian National Conference on Condensed Matter Physics
September 29, 2015 – Palermo

R. Guzzi, R. Bartucci, M. Esmann, D. Marsh
Protein-Lipid Interface in Na,K-ATPase Membranes by pulsed EPR
FisMat 2015 – 2nd Italian National Conference on Condensed Matter Physics
September 29, 2015 – Palermo

C.3 Presentations at national conferences

D. Marsh, R. Bartucci, R. Guzzi, L. Sportelli
Librational fluctuations in protein glasses
FisMat 2013 – Italian National Conference on Condensed Matter Physics
September 9-13, 2013 – Milano

M. Pantusa, R. Bartucci, B. Rizzuti
Stabilizing effect of transport proteins on the trans-to-cis conversion of resveratrol
FisMat 2013 – Italian National Conference on Condensed Matter Physics
September 9-13, 2013 – Milano

A. Stirpe, M. Pantusa, R. Guzzi, L. Sportelli, R. Bartucci
Chain interdigitation in DPPC bilayers induced by HgCl2: evidences from continuous wave and pulsed EPR.
SIBPA 2014 – 22nd National Conference of SIBPA (Società Italiana di Biofisica Pura e Applicata)
September 21-24, 2014 – Palermo

M. Pantusa, A. Stirpe, L. Sportelli, R. Bartucci, R. Guzzi
Resveratrol modulates the early stage aggregation of human serum albumin
SIBPA 2014 – 22nd National Conference of SIBPA (Società Italiana di Biofisica Pura e Applicata)
September 21-24, 2014 – Palermo

R. Guzzi, B. Rizzuti, C. Labate, B. Zappone, M. P. De Santo
Thermal response in the formation of beta-lactoglobulin fibrils
SIBPA 2014 – 22nd National Conference of SIBPA (Società Italiana di Biofisica Pura e Applicata)
September 21-24, 2014 – Palermo

B. Rizzuti, B. Zappone, C. Labate, R. Guzzi, M.P. De Santo
Controlled self-assembly of beta-lactoglobulin fibrils by using metal ions
IMIP kick-off meeting
March 12-14, 2015– Lequile (LE)

S. Evoli, R. Guzzi, B. Rizzuti
Molecular docking and molecular dynamics simulations
IMIP kick-off meeting
March 12-14, 2015 – Lequile (LE)

A. Stirpe, R. Guzzi, L. Sportelli, A. Sanchez-Ferrer, J. Adamcik, R. Mezzenga
Glycation effects on the conformational properties and fibrillization of β-lactoglobulin
FisMat 2015 – 2nd Italian National Conference on Condensed Matter Physics
September 28 - October 02, 2015 – Palermo

E. Longo, B. Rizzuti, L. Sportelli, R. Bartucci
Resveratrol loaded in liposomes induces chain packing modification
FisMat 2015 – 2nd Italian National Conference on Condensed Matter Physics
September 28 - October 02, 2015 – Palermo

7. MOLECULAR PHYSICS – PHYSICS AND APPLICATIONS OF SOFT MATTER

Professors and Researchers

Barberi Riccardo
Bartolino Roberto
Caputo Roberto
Castriota Marco
Cazzanelli Enzo
Cipparrone Gabriella
De Luca Antonio
De Santo Maria Penelope
Golemme Attilio
Pagliusi Pasquale
Scaramuzza Nicola
Strangi Giuseppe
Versace Carlo
Umeton Cesare

CNR Personnel

Annesi Ferdinanda
Ciuchi Federica
Giocondo Michele
Mazzulla Alfredo
Pane Alfredo
Termine Roberto
Zappone Bruno

Collaborators

Luciano De Sio, Nelson Tabirian - *Beam Engineering for Advanced Measurements Company, 1300 Lee Rd, Orlando, FL 32810, USA*
Giulio Caracciolo, Daniela Pozzi - *Dipartimento di Medicina Molecolare, Sapienza Università di Roma, Viale Regina Elena 291, 00161, Roma*
Tiziana Placido, Roberto Comparelli, Maria Lucia Curri - *CNR-IPCF Istituto per i Processi Chimici e Fisici, Sez. Bari, c/o Dip. Chimica Via Orabona 4, 70126 - Bari, Italy*
Angela Agostiano - *Università degli Studi di Bari – Dip. Chimica, Via Orabona 4, 70126 - Bari, Italy - CNR-IPCF Istituto per i Processi Chimici e Fisici, Sez. Bari, c/o Dip. Chimica Via Orabona 4, 70126 - Bari, Italy*
Antonio Qualtieri - *ISN-CNR Piano Lago Mangone Cosenza*
Clementina Provenzano *(Postdoc fellow)*
Josue Raul Hernandez *(PhD, Postdoc fellow)*
Arianna Aprile *Postdoc fellow)*
Ulises Ruiz (*Postdoc fellow)*
Daria Lysenko *(PhD)*
Eugenia Lepera *(PhD)*
Tiziana Placido
Giovanni Palermo
Caterina Maria Tone
Vincenzo Caligiuri
Melissa Infusino

A. R. Rashed
Alessandro Veltri
Andreea Ionescu
Giuseppina Politano
Carlo Vena
Angela Fasanella
Luigia Pezzi
Ugo Cataldi

Nanoscience and biomedicine

Plasmonic photothermal therapy (PPTT) is a minimally-invasive oncological treatment strategy in which photon energy is selectively administered and converted into heat sufficient to induce cellular hyperthermia. To this end, plasmonic metallic nanoparticles (NPs) are a particular class of nanomaterials which possess the capability to localize light down to the nanoscale by exploiting a phenomenon called localized plasmon resonance (LPR). NPs have been used in therapeutics by triggering drug release or enhancing ablation of diseased tissues, while minimizing damage to healthy tissues. The breakthrough idea is based on the possibility to deliver NPs in the tumor site and by exploiting the efficient conversion of near infrared (NIR) light to heat opens up a new "drug-free" cancer therapy. To this purpose, we have studied the electrostatic interaction between positively charged gold nanorods (GNRs) and negatively charged, labeled, short DNA in terms of DNA concentration, ζ potential, hydrodynamic diameter and gel electrophoresis analysis. We have incubated complexes of DNA/GNRs, at different concentrations, with *HeLa* cells (an immortal cell line used in scientific research). By using the DNA as a localized fluorescent probe, we have evaluated the uptake capacity as well as the morphology of the cells by means of fluorescent and optical microscope, establishing the upper limit concentration for the cellular toxicity. Results represent a step-forward in the field of plasmonic gene therapy.

Gene delivery is the process of introducing foreign DNA, RNA into host cells as potential therapeutic strategies for various diseases by means of a nano-vehicle. In particular, the properties of an ideal non-viral vector are: low degradation, target specific cells avoiding immune response in the patient. One of the most promising alternative technologies for gene therapy is the use of NPs as delivery vehicles. The optical properties of NPs and their biocompatibility provide an efficient tool like non-viral vector for gene therapy. We have characterized the electrostatic interaction between GNRs and nucleic acids of different length by using analytical techniques, such as electrophoretic mobility assay, zeta-potential and scanning electron-microscopy. Both effective electrostatic charge and average size/shape can be easily controlled by carefully selecting the suitable GNRs/DNA molar ratio. In particular, the GNRs/DNA complexes also undergo through a charge inversion effect, differentiating negatively and positively charged conjugates. These distinctive features make them promising candidates for drug delivery and GT applications both in vitro and in vivo. The overall results are of wide interest and allow a deeper fundamental understanding of the interaction between charged plasmonic and biological materials and, at the same time, open-up the venue for realizing a new generation of tools for nanomedicine.

Chromonic liquid crystals:

Chromonics are a very interesting class of lyotropic liquid crystals (LLCs), which have become, over the last few years, an important research topic in several domains, like optical materials and devices in high technology, molecular electronics and biological sensing. Our work was mainly focused on:

- alignment, which is a difficult task and whose mechanisms are not fully understood,
- new chromonics materials in collaboration with chemistry department.

Chiral Optomechanics and photonics

Chirality is one of the most prominent and intriguing aspects of nature, from spiral galaxies down to aminoacids. Despite the wide range of living and non-living, natural and artificial chiral systems at different scales, the origin of chirality-induced phenomena is often puzzling.
We have recently developed chiral microparticles: polymeric spherical micropartilces result from light induced polymerization of cholesteric liquid crystal droplets. The method enables to create micro-particles with controlled internal chiral architectures and presents great flexibility providing several advantages connected to the acquired optical and photonics capabilities for the development of chiral colloidal systems and materials. Optomechanics and microphotonics investigations have been mainly performed.
We have performed an experimental and theoretical investigation of the simultaneous optical trapping and rotation of chiral microparticles. Due to the shell structure (Bragg dielectric resonator), the microparticles work as omnidirectional chiral mirrors yielding highly polarization-dependent optomechanical effects. The coupling of linear and angular momentum, mediated by the optical polarization and the microparticles chiral reflectance, allows for fine tuning of chirality-induced optical forces and torques. Such experiments gave an experimental evidence of the chiral resolution of linearly polarized and unpolarized light beams. Due to the interplay between linear and angular momentum exchange, basic manipulation tasks, as trapping, spinning or orbiting of micro-objects, can be performed even by light with zero helicity. The results might broaden the perspectives for development of miniaturized and cost-effective devices.

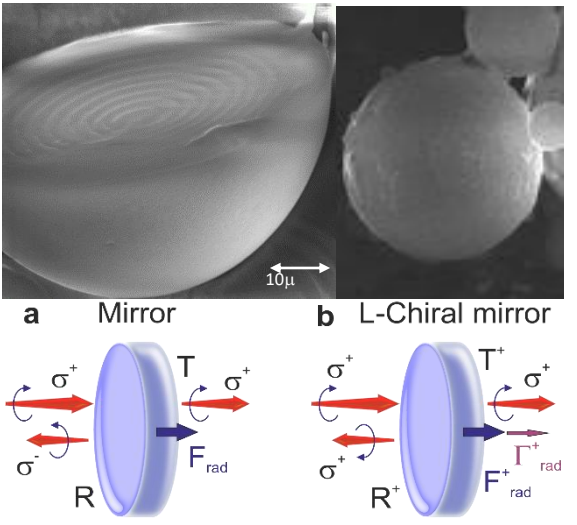

The dynamics in a dual-beam optical trap has been also investigated. Symmetric and asymmetric polarization configurations of dual-interfering beam traps have been investigated. Based on the polarization controlled asymmetric transmission of the particles, a tunable wash-board potential is created enabling the control of the trapping position along the beams axis. Asymmetric configurations display polarization controlled rotation of the trapped particles. Optical binding of rotating particles exhibits a complex dynamics.
The photonic properties of the cholesteric solid spherical microparticles have been also investigated. Omnidirectional lasing from the microparticles has been studied.

Topological defects designed in LC by surface patterning

Anisotropic fluids are a class of soft materials that offer wide possibilities for engineering a small scale laboratory; their physical properties can be manipulated on short length scale by appropriate confining conditions and external stimuli leading the systems across fascinating phenomena.
Arrays of topological defect lines are created in liquid crystal exploiting periodic arrangements of twisted domains with opposite handedness. The defect lines self-organize in a planar cell guided by a polarization holograms recorded in one aligning substrate that provides planar periodic alignment. 1D and 2D arrays of disclinations have been designed exploiting this approach. Then the arrays have been used as template to assemble and manipulate nanoparticles. The control of nanoparticle-loaded topological defects has been demonstrated by low power light and by an applied voltage.Full reconfigurability and time stability make this approach attractive for future developments and applications. Based on the obtained results, the topological defects and the electrically controlled convective have been combined to create a microfluidic platform for reconfigurable nanoparticles (NPs) patterning. The nanoscopic environments created by defects within liquid crystals have been used as linear nano-reservoirs of NPs. Afterwards, virtual channel flows that connect the linear reservoirs have been created by exploiting electro-convective rolls. The reported results reveal a new strategy for managing nanometric objects based on an unconventional microfluidic device characterized by switchable and contactless micro-channels.

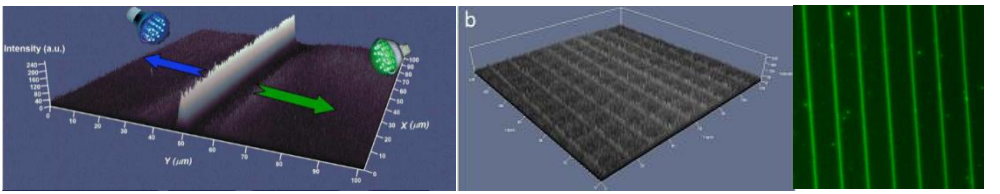

Vectorial holography: devices for light manipulations based on polarization holograms

- Generation of complex and vectorial beams

A highly efficient and flexible method to yield vector beams (VBs) with spatially variant amplitude, phase and polarization by means of combination of two polarization holograms (PHs) has been engineered. Left- and right-hand circularly polarized scalar beams, generated by the first hologram, are collinearly recombined by a second one to produce the vector beams. By taking advantage of the diffraction properties, the high efficiency, and the intrinsic achromaticity of the polarization holograms, the method aims to overcome the limitations related to stability and efficiency, making it attractive for applications.

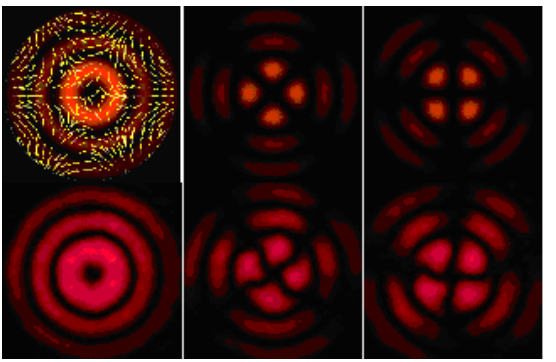

- Microlenses arrays.

The optical microsystems have become important tools for imaging, optofluidics and sensors applications. We have developed a versatile method to create microlens arrays (MAs) exploiting the spatial light modulator (SLM) assisted polarization holography, which enables an efficiency of diffraction up to 100%. Reconfigurable MAs with 90% total diffraction efficiency have been demonstrated exploiting liquid crystals cell where holograms work as photo-aligning substrates. The transparency of the liquid crystal on a wide range of wavelengths and the ability to tune appropriately its optical birefringence, through an external voltage, allowed us to create achromatic MAs with high efficiency.

Shaping supramolecular architectures in smart polymers

Light-controlled molecular alignment is a flexible and useful strategy introducing novelty in the fields of mechanics, self-organized structuring, mass transport, optics, and photonics and addressing the development of smart optical devices. Azobenzene-containing polymers are well-known photocontrollable materials with large and reversible photoinduced optical anisotropies. The vectorial holography applied to these materials enables peculiar optical devices whose properties strongly depend on the relative values of the photoinduced birefringences. Polarization holographic recording based on the interference of two orthogonal waves has been applied to a bifunctional amorphous polymer that, exceptionally, exhibits equal values of linear and circular birefringence. The peculiar photoresponse of the material coupled with the holographic technique demonstrates an optical device capable of decomposing the light into a set of orthogonally polarized linear components.

Molecular Recognition at Interfaces via Nonlinear Optical Spectroscopy

Inspired by Nature, supramolecular chemists synthesize biomimetic molecular receptors for chemical sensing that mimic the affinity and specificity of interactions between biomolecules, exploiting the concepts of shape and binding site complementarity. Achieving rapid and efficient specific molecular interaction often depends on immobilization of receptors to solid surfaces with appropriate surface density, preserving the functional conformation and optimizing the presentation of the binding fragments towards the target analyte. The accurate control over the molecular organization at the interfaces of a chemosensor, miming the biological structures to foster specific interactions, has the potential to push sensitivity, accuracy and speed of detection well beyond the present technology. Therefore, analytic techniques that can determine the absolute orientation and conformation of bio- and biomimetic molecules at the interfaces are of paramount relevance for providing a molecular-level understanding of the receptor-analyte interaction. Sum-frequency generation vibrational spectroscopy (SFG-VS) allows to achieve the conformational structure and orientation distribution of biomimetic and bio- molecules at interfaces, in the working environment for chemical and biochemical sensing. As a second-order nonlinear optical processes, SFG-VS has been proven to be a versatile tool for non-invasive probing of any interface accessible by light, with intrinsic surface specificity, chemical selectivity and sub-monolayer sensitivity.

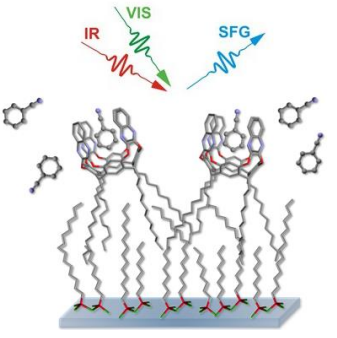

We have reported on the molecular architecture of a class of supramolecular receptors, namely Cavitands, on organosilane monolayers. These hybrid bilayers are of paramount importance for chemical and biochemical sensing, in that Cavitands have demonstrated high selectivity toward analytes of interest for environmental monitoring, drug detection and disease diagnosis. The analysis quantitatively assess orientation, conformation and relative surface density of Cavitand molecules transferred onto hydrophobic templates by Langmuir-Schaefer. We have then reported the first in-situ analytical investigation of the molecular recognition event at the solid-gas interface. In particular, we investigated the

complexation capability of surface-bound tetraquinoxaline Cavitands exposed to saturated vapors of benzonitrile and acetonitrile in air, resembling the real-world gas sensor operating conditions. The study allows to correlate the molecular architecture of the receptor-decorated substrate with the orientation of the complexed cognate analyte.

Thin Graphene Oxide Film

Thin film of graphene oxide and reduced graphene oxide are very promising materials for their electro-optical applications such as touch screens and flexible displays. Recently, by this method, we obtained thin films of graphene oxide (GO) and GO thermally reduced on glass substrates covered by a thin layer of titanium. The morphology and structural characteristics of these films were investigated by micro-Raman, X-ray and SEM reflectance by detecting thicknesses of some ten of nanometers and a discrete homogeneity of the material. In order to study its optical and electrical properties, variable angle ellipsometry and impedance analysis have been performed. Heat treatment strongly changes structural, electrical and optical properties because during the thermal process a number of orbital sp3 originally present in the GO is removed by improving its conductivity. Finally, the electrophoretic deposition provides thin films of GO characterized by a higher refractive index than the other deposition methods.

Turbulence and chaos in nematics

The effects of the order of the nematic mesophase on the transition DSM1 <- DSM2 were studied. The measurements were performed on films of a mixture of MBBA and 5CB at different concentrations of the two materials. The threshold electric field for the transition between the two turbulent states was measured in alternating regime at 70Hz. The addition of a small amount of 5CB to MBBA has the effect of reducing its dielectric anisotropy and disturbing its order as a result of the different form of molecules of the two composts and the different dielectric anisotropy, small and negative for MBBA and high and positive for 5CB. These considerations had led us to predict an increase in the threshold voltage with the 5CB concentration, on the contrary was experimentally observed an opposite behavior, which suggests that other factors have greater influence on threshold control, one of which could be the length of biaxial coherence, which is of the order of magnitude of defects.

High Charge Mobility Columnar Mesophases

In the field of photonic and optoelectronic device development, the researchers are currently investing efforts to replace the inorganic materials with the organic ones, as the latter introduce several advantages, being less expensive, lighter, more chemically and mechanically versatile and more eco-friendly. In any case, in spite of those advantages, the lack of crystalline order and the low polarizability typical of organic materials bring some disadvantages, such as the typical low charge mobility that is a key parameter for different organic devices, such as light-emitting diodes (OLEDs), organic field-effect transistors (OFETs) and organic photovoltaic devices (OPVs). Molecularly organized supramolecular materials are promising candidates to overcome this drawback, since several properties of functional materials, such as charge mobility, can be enhanced with a well-organized phase structure. Within this frame, the ability of liquid crystals to self-organize in functional architectures is frequently used. In particular, to increase charge mobility, the properties of columnar liquid crystals, where molecules spontaneously stack into columns to give one-dimensional structures of interacting systems, are often exploited. This organization induces a π-orbital overlap that allows a very efficient one-directional intracolumnar charge transfer, with the result of obtaining materials with high mobilities, comparable to that of amorphous silicon. Therefore, novel columnar liquid crystals based on innovative molecular and supramolecular architectures are studied. Particularly interesting is the study of discotic mesophases whit ambipolar electrical conductivity. One of the key parameters to obtain discotic liquid crystals with high mobility, is the achievement of a

macroscopic homogeneous alignment because if columns are not well aligned, grain boundaries effects prevent an efficient charge transfer and therefore high charge mobility.

Photovoltaics

The search for alternative energy sources is becoming a worldwide strategic problem, because of the rapid depletion of fossil fuels from one hand, and the need of eco-compatible solutions to face the global warming on the other hand. Sunlight is arguably the most abundant clean source of energy that is capable of enabling indefinite and sustainable economic growth, with minimum detrimental impact on the environment. Organic photovoltaics is one of the answers to such a quest, being potentially a low cost technology that can also be easily adapted into several different architectonic structures. However, more studies are necessary to obtain materials with efficiency and lifetime suitable for commercially exploitable devices. This objective can be pursued though a multidisciplinary approach, involving different material preparation and device configurations, photo- physical and electrical properties. In particular, we study:

- *Hybrid Perovskite Solar Cells*

Motivated by the recent results of hybrid organic/inorganic perovskite based solar cells, we aim at exploiting the peculiar properties of such materials. We study new preparation methods, new materials and the role that plasmonic materials (nanoparticles, hyperbolic metamaterials) can play to increase efficiency and the stability.

- *Bulk Heterojunction Solar Cells*

The well known architecture of this class of solar cells is exploited in order to test new materials and methods to boost the efficiency and increase the stability for commercial applications.

Electropolymerized polymers

Electropolymerization is a very simple method for the preparation of conducting polymers presenting several advantages, such as the absence of catalysts, the simultaneous formation and deposition of the polymers on a conductive substrate, an easy control of the film thickness, morphology and properties (i.e. doped/undoped states). Several conductive polymers can be prepared by electrochemical methods and, in this context, triphenylamine (TPA)-containing polymers are among the most widely studied, due to two intrinsic and useful features: the easy oxidability of the nitrogen center (makes the oxidative electropolymerization easier) and its ability to transport positive charges via radical-cation species (useful in several optoelectronic devices). Cyclometalated complexes containing the electropolymerizable TPA-fragment in their structure have been successfully synthesized and their photoconductive properties investigated. These polymeric organometallic thin films have shown a significant enhancement of photoconductivity when compared to their monomeric amorphous counterparts, mainly due to the improvement in photogeneration efficiency achieved after electropolymerization. These results are encouraging and confirm that electropolymerization of photoconductive cyclometalated complexes can actually represent a useful procedure for the preparation of thin films for optoelectronic applications, for example in electrochromic and photovoltaic devices.

Virtual unrolling and deciphering of Herculaneum papyri by X-ray phase-contrast tomography

A collection of more than 1800 carbonized papyri, discovered in the Roman ‘Villa dei Papiri’ at Herculaneum is the unique classical library survived from antiquity. These papyri were charred during 79 A.D. Vesuvius eruption, a circumstance which providentially preserved them until now. This magnificent collection contains an impressive amount of treatises by Greek philosophers and, especially, Philodemus of Gadara, an Epicurean thinker of 1st century BC. We read many portions of text hidden inside carbonized Herculaneum papyri using enhanced X-ray phase-contrast tomography non-destructive technique and a new set of numerical algorithms for ‘virtual-unrolling’. Our success lies in revealing the largest portion of Greek text ever detected so far

inside unopened scrolls, with unprecedented spatial resolution and contrast, all without damaging these precious historical manuscripts. Parts of text have been decoded and the 'voice' of the Epicurean philosopher Philodemus is brought back again after 2000 years from Herculaneum papyri.

Nanocomposite films by the insertion of graphene and other nanoparticles

New polymeric nanocomposite films containing graphene and Ag, Au or ZnO nanoparticles were synthesized,
and their morphological, thermal, surface and dielectric properties were studied. Graphene was obtained by the sonication method, which allows to obtain ''real'' graphene, without any chemical manipulation of graphite. This method preserves graphene lattice symmetry, which is responsible for its exceptional properties. The interaction between graphene and the other nanoparticles (NPs) confers to these polymeric films interesting characteristics, thus making them suitable for different applications. For example, the wetting property can be tuned by the insertion of nanofillers. Furthermore, the presence of these latter increases the dielectric strength of the polymer films. Polymeric nanocomposites were prepared by inserting graphene and/or Ag, Au and ZnO nanoparticles in a TEGDA (tetraethyleneglycol diacrylate) polymer matrix. The polymeric films were characterized in terms of their dielectric properties by electrochemical impedance spectroscopy. The impedance data were fitted by generalized relaxation functions in order to determine conductivity, dielectric response and molecular relaxation time of the nanocomposite films. In particular, a stretched exponential function, Kohlrausch-Williams-Watts function (KWW), was used to investigate polymer/graphene/metal nanocomposites.

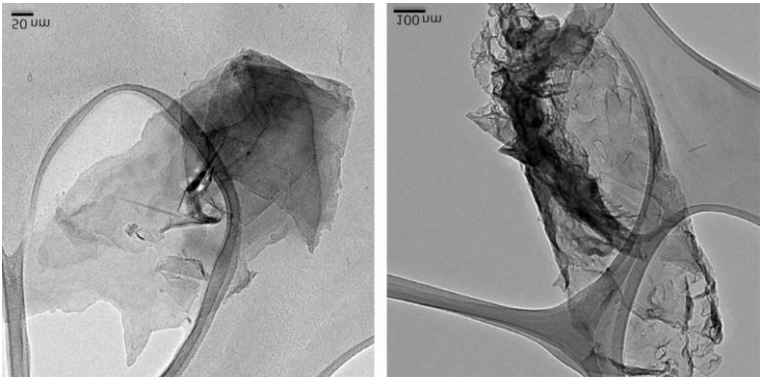

TEM images of TEGDA/graphene dispersion.

Plasma polymerized thin films

Polypyrrole (PPy) thin films were synthesized by plasma polymerization technique and investigated the influence of discharge power on microstructural, optical, surface wettability, and dielectric properties of grown films. As deposited PPy films were characterized by X-ray diffraction (XRD), Fourier transform Infrared spectroscopy (FTIR), Atomic force microscopy, UV-VIS spectroscopy and dielectric spectroscopy. The broad XRD peak present at 2u523.58 revealed the amorphous nature of grown PPy films. The FTIR spectra displayed characteristic peaks in the wavenumbers regions 3300–3400 cm21 and 1635–1700 cm21 and respective peaks intensities decreased slightly as a function of discharge powers. Significant modifications in surface morphology of the films were observed as a function of discharge powers and PPy films synthesized at higher discharge power of 50 W demonstrated characteristic surface morphology composed of characteristic vertical cone shaped clusters provided with rms roughness of 3.42 nm. The UV-VIS absorption spectra evidenced that the optical density values varied as a function of discharge power. The evaluated band gap energies

decreased with an increase of discharge power and found to be 2.53 eV for PPy films prepared at higher discharge power of 50 W. The surface wettability studies evidenced that as prepared PPy films were found to be hydrophilic in nature. The dielectric measurements were carried out for "ITO/polymer/ITO" structures in the frequency range 10 mHz to 100 kHz. As evidenced from dielectric spectroscopic measurements, PPy films synthesized at 50 W were demonstrated conductivity value of 6.0 3 10212 S/m.

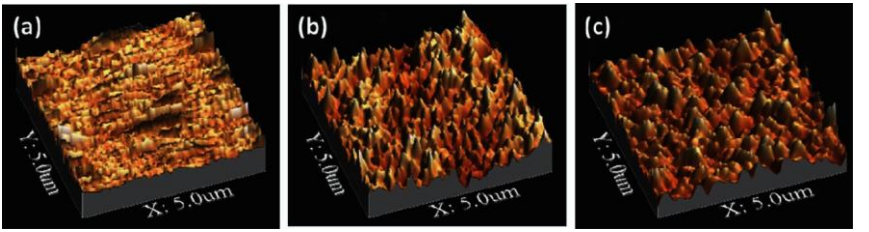

Atomic force micrographs of DC-discharge plasma polymerized PPy thin films prepared various discharge powers (a) 10 W, (b) 30 W, and (c)
50 W.

Blend based solid polymer electrolytes for sodium ion batteries

Polymer blend electrolytes based on Polyethylene oxide (PEO) and polyvinyl pyrrolidone (PVP), complexed with NaIO4 salt and Graphene oxide (GO) are investigated in the present report. The electrolytes are prepared by a facile solution cast technique. X-ray diffraction (XRD), Fourier transform infrared spectroscopy (FTIR), and scanning electron microscopy (SEM) are employed to study the influence of ion–polymer interactions on the micro structural properties of blend electrolytes. Measurements of electrical conductivity of the blend polymer complexes have been performed by using complex impedance spectroscopy in the frequency range 1 Hz - 1 MHz and within the temperature range 303 K – 343 K. A study on electrical conductivity properties of GO doped 'salt complexed electrolyte' systems is presented.

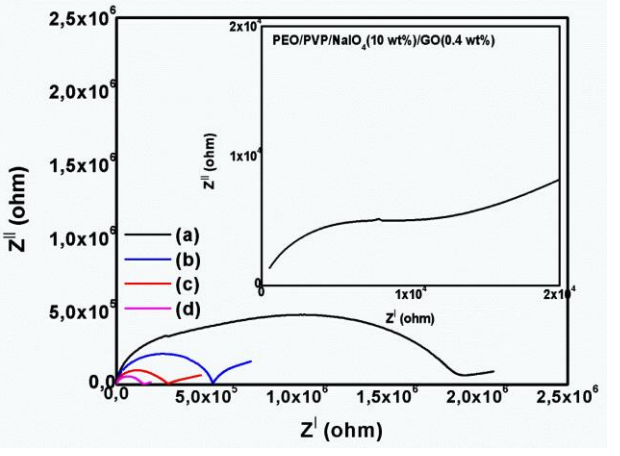

Nyquist plots at room temperature for NaIO4 salt complexed PEO/PVP blend electrolytes:
(a) PEO/PVP blend(b) PEO/PVP/NaIO4 (5 wt%), (c) PEO/PVP/NaIO4 (7.5wt%), (d) PEO/PVP/NaIO4(10 wt%).

Influence of thin layer of silver nanoparticles on optical and dielectric properties composite films

A thin interlayer of silver nanoparticles (Ag-NPs) is embedded in a matrix of poly(vinyl alcohol)(PVA) films, and its influence on the microstructural, optical, and dielectric properties of 'Ag/PVA' thin films is investigated. As evidenced from atomic force microscopy studies, size of the deposited Ag-NPs clusters and surface roughness of the films decreased with an increase of annealing temperature. Optical and structural properties of 'Ag/PVA' nanocomposites were studied using UV-Visible spectroscopy and Confocal Raman spectroscope. The PVA/Ag nanocomposite films demonstrated lower optical band gap values than pure PVA films and the estimated optical band values of 'Ag/PVA' nanocomposite films decreased from 3.66 eV to 3.57 eV with the increase of temperature from 20 °C to 200 °C, respectively. The multi-layered 'PVA/Ag-NPs/PVA' films (MLTs) were fabricated and studied their dielectric properties as a function of frequency. The presence of Ag-NPs inter layer shows significant influence on dielectric and conductivity properties of MLTs. At room temperature in comparison to pure PVA, MLTs exhibited three times higher dielectric permittivity value at 1 kHz and observed to increase 5 times with an increase in temperature to the higher value of 200 °C. The evaluated dc conductivity value of MLTs increased from −11.72 to −10.38 S/cm on a logarithmic scale with an increase in temperature from 20 °C to 200 °C, respectively.

Investigation and Applications of POLICRYPS Gratings

The acronym POLICRYPS indicates a nano/micro composite structure made of films of well aligned nematic liquid crystal (NLC) alternated to slices of almost pure polymer. Structures are fabricated by curing a homogeneous mixture of mesogenic material, monomer and a curing agent with UV radiation, under suitable physical and geometrical conditions. In particular, geometrical conditions determine (in the range 0.2 divided by 15 mu m) the spatial periodicity of the realized sample, which can be utilized for transmitting, diffracting or reflecting an impinging light beam, with negligible scattering losses. The spatial modulation of the refractive index (from polymer to NLC) can be switched ON and OFF both by applying an electric field of few V/mu m or, in some cases, by irradiating the sample with a light beam of suitable wavelength.

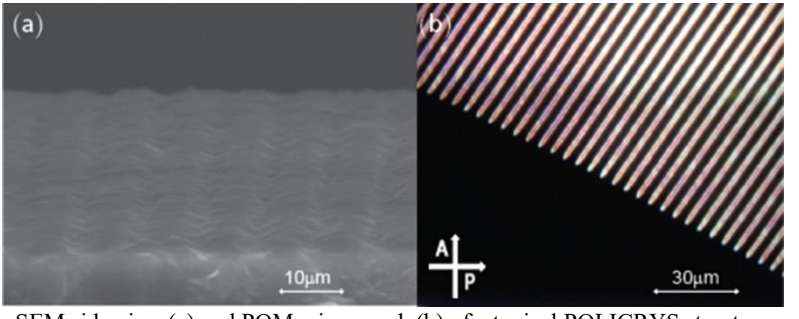

SEM side view (a) and POM micrograph (b) of a typical POLICRYS structure

The diffractive properties of the POLICRYPS structure has been characterized in terms of cell thickness, impinging probe angle and wavelength revealing a strong correlation between the diffraction efficiency and all above mentioned parameters. These results are very attractive for many applications such as switchable Bragg gratings for telecom devices, phase modulators, and displays. The electrical/optical tuneability is responsible for a series of distinctive characteristics of the optical effects produced by the structure, and determines the range of possible applications. In fact, in different geometries, the POLICRYPS can be exploited as a switchable holographic grating, a switchable optical phase modulator, a switchable beam splitter, a tuneable Bragg filter or it can be

exploited as an electro-optical edge filter in an optical interrogation system. In particular, we have realized and studied the following devices.

a) POLICRYPS based electro-switchable Bragg reflector

It is a switchable volume reflective element fabricated from a POLICRYPS structure by holographic photopolymerization at high temperature (70 °C) using a photosensitive/nematic liquid crystal prepolymer mixture. The submicron Bragg structure formed consists of periodic continuous polymeric walls separated by periodic LC channels. The phase separated NLC self-aligns in a homeotropic way between the polymer walls as indicated by polarizing optical microscopy analysis (Maltese cross). The resulting periodic grating structure results in a Bragg reflection notch upon illumination with white light due to the periodic variation in refractive index. Electro-optical experiments realized through in-plane electrodes and temperature experiments confirm that the multilayer structure acts as a Bragg mirror whose reflection efficiency can be controlled by either a small (~3V/μm) electric field or temperature variations.

b) Tuneable broadband optical filter based on soft-composite materials

It is a 'free space' diffractive optical filter based on a POLICRYPS periodic structure. Its polarization dependent diffractive properties have been exploited for realizing a diffractive, band-gap based, broadband optical filter. The sample is characterized in terms of its morphological, optical and electro-optical properties. We show that both electric fields and temperature variations can be exploited to tune the position of the diffractive band-gap of about 83 nm and 116 nm respectively.

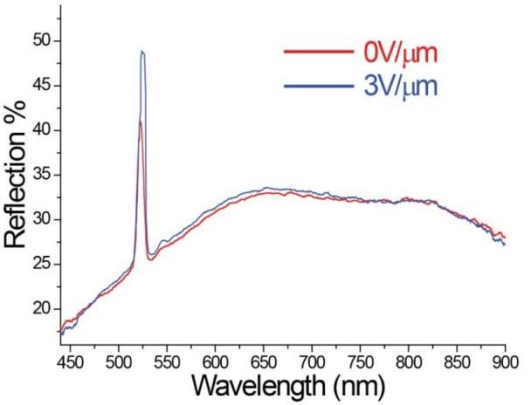

Reflection spectrum of the sample without (red curve) and with (blue curve) an applied electric field.

c) POLICRYPS diffraction gratings containing photo-responsive liquid crystal for nanosecond switching

The diffraction efficiency of POLICRYPS diffraction gratings containing photoresponsive LC is modulated using visible CW or pulsed radiation. Exposure of the periodic structure to green CW or pulsed excitation modulates both the spectral and amplitude transmission behavior of the grating structure. In particular, under the influence of single pulse excitation, the diffraction efficiency can be modulated from 87% to 17% in 4 ns with a spontaneous back relaxation time three orders of magnitude (microsecond) faster than the one observed for the same material conventionally aligned in standard glass cells. The ability to remotely and quickly change the diffraction properties of soft-composite periodic microstructures marks a breakthrough towards the realization of ultra-fast all-optical devices.

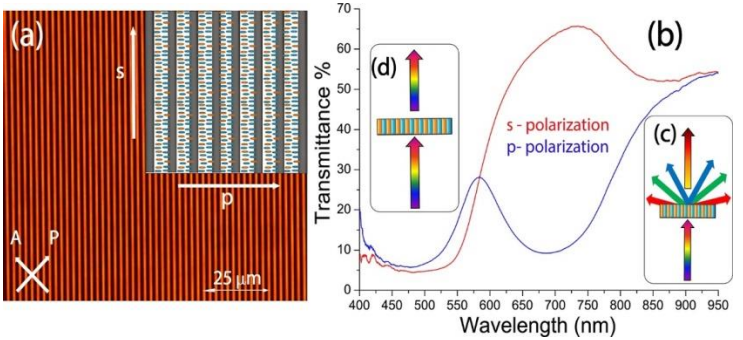

POM micrograph (a) and sketch (inset, where the orange and blue cigars represent the azo-dye and the NLC molecules, respectively) of the POLICRYPS structure. Spectral response (b) and schematic representation of the sample for impinging probe light p (c) and s (d) polarized. The two orthogonal impinging polarizations (p and s) are represented with the arrows in (a).

Realization and investigation of POLICRYPS structures exhibiting a polar geometry

We have realized a liquid crystal (LC)-based optical diffraction grating showing a polar symmetry of the director alignment. This has been obtained as a natural evolution of the POLICRYPS technique, which enables the realization of highly efficient, switchable, planar diffraction gratings. Performances exhibited in the Cartesian geometry are extended to the polar one by exploiting the spherical aberration produced by simple optical elements. This enables producing the required highly stable polar pattern that allows fabricating a circular optical diffraction grating. Results are promising for their possible application in fields in which a rotational structure of the optical beam is needed. In this framework, we have demonstrated that it is possible to exploit polar POLICRYPS diffractive structures to generate cylindrical vector beams. Local shaping of the polarization state of a light beam is appealing for a number of applications. This can be achieved by employing devices containing birefringent materials. Our polar POLICRYPS enables converting a uniformly circularly polarized beam into a cylindrical vector beam (CVB). We have characterized the resulting CVB profile and polarization for the cases of left and right circularly polarized incoming beams.

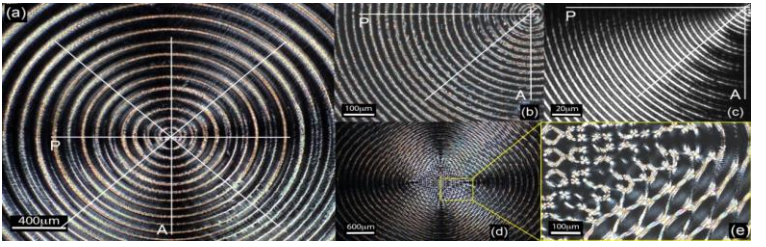

Micrographs (taken at the POM between crossed polarizers) of the morphology of a polar POLICRYPS. (a)-(c) circular POLICRYPS optical diffraction gratings with different number of rings and pitches; (d) circular POLICRYPS structures obtained by slightly misaligning the experimental set-up; (e) magnification of the central area of the structure of Fig. d.

It has been also demonstrated that it is possible to realize a spontaneous radial liquid crystals alignment on curved polymeric surfaces by imaging through a “Fresnel like” structure, which imparts an intensity profile onto a photosensitive mixture which subsequently forms periodic alternating curved polymeric and liquid crystal slices. Curved periodic microstructures are formed through the

controlled phase separation of the NLC and a polymerizing matrix comprising the LC. The phase separated concentric rings of NLC self-aligns in a radial alignment in between the polymer walls as indicated by polarizing optical microscopy analysis (Maltese cross). Electro-optical experiments confirm the possibility to control this alignment and the optical properties of the macroscopic structure by means of a quite low external voltage. The system exhibits high-quality and self-alignment of the NLC without the need of surface chemistry or functionalization.

POLICRYPS structure for Confinement and Alignment of Self-Organized Materials

An empty polymeric structure has been realized by combining a POLICRYPS and a selective microfluidic etching process. The distinctive features of the realized periodic microstructure enabled aligning several kinds of liquid crystal (LC) compounds, without the need of any kind of surface chemistry or functionalization. In particular, it has been possible to exploit light sensitive LCs for the fabrication of all-optical devices, cholesteric and ferroelectric LCs for ultrafast electro-optical switches, and a common LC for a two-dimensional periodic structure with high anisotropy. All-optical and electro-optical experiments, performed for investigating the samples in terms of switching voltages and response times, confirm good performances of the realized devices.

Light extraction in Photonic Quasi-crystals containing Liquid Crystals

We have realized an electro/all optical single mode optical filter by combining a functionalized gold Thue Morse Photonic Quasi Crystal (PQCs) and a Photoresponsive LC in a layer by layer geometry. A SEM analysis shows the high quality morphology of the structure before and after undergoing treatment with an alignment layer. It turns out that, starting from an unpolarized white light source trough a light extraction mechanism based on the diffraction of light, the high quality structure, combined with a uniformly aligned PLC, is able to give rise to a narrow (FWHM ≈9 nm) and linearly polarized single mode peak. Moreover, the spectral properties (switching and tuning) of the sample can be finely controlled by using both an external applied voltage or a suitable pump light source. The device has potential applications in the field of optical fibers and telecommunications.

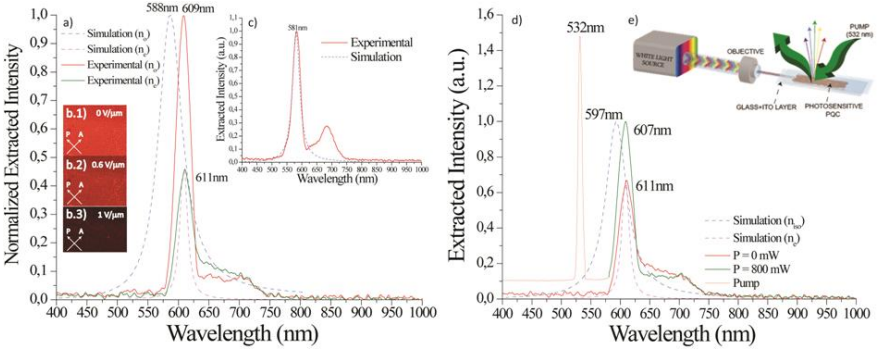

Emission spectra of the sample and its numerical simulations without (λpeak=611 nm) and with (experiment λpeak=609 nm, simulation λpeak=588 nm) the action of an external applied voltage. (b1, b2, b3) POM view of the sample while increasing the external applied voltage. c) emission spectrum (experiment and simulation) of the sample without the PLC layer. d) Emission spectra of the sample and its numerical simulations without (λpeak=610nm) and with (experiment λ=607 nm, simulation λ=597 nm) the presence of an external pump source. e) Optical setup used for the experimental characterization. POM view of the top-pump illuminated sample area.

It has been demonstrated that, by exploiting Metamaterials (MTMs) and PQCs, it is possible to realize man-made structures characterized by a selective EM response, which can be also controlled by

combining the distinctive properties of LCs. By finely controlling lattice parameters of a given photonic structure, it is possible to optimize its extraction characteristics at a precise wavelength, or minimize the extraction of undesired modes. In general, however, once a structure is realized, its extraction properties cannot be varied. To cross this problem, we have combined capabilities offered by both MTMs and PQCs with the reconfigurable properties of LCs; in this way, a completely new class of "reconfigurable metamaterials" (R-MTM) can be realized. We have reported on the realization and characterization of a switchable photonic device, working in the visible range, based on nanostructured photonic quasi-crystals, layered with an azodye-doped nematic LC (NLC). The experimental characterization shows that its filtering effect is remarkable with its extraction spectra which can be controlled by applying an external voltage or by means of a laser light. The vertical extraction of the light, by the coupling of the modes guided by the PQC slab to the free radiation via Bragg scattering, consists of an extremely narrow orange emission band at 621 nm with a full width at half-maximum (FWHM) of 8 nm. These results represent a breakthrough in the realization of innovative MTMs based active photonic devices such as tunable MTMs or reconfigurable lasers and active filters.

Active Plasmonic systems realized in soft elastomers

We have realized and characterized electro-responsive and pressure sensitive polydimethylsiloxane (PDMS) conductive photonic structures combined with the reconfigurable properties of short pitch cholesteric liquid crystals (aligned in Grandjean configuration). The sample has been realized by means of a layer by layer strategy. An indium tin oxide (ITO) layer has been sputtered on PDMS by utilizing thermal evaporation technique; an inter-diffusive scenario, leading to the embedding of the ITO layers within the PDMS matrix, makes the structure conductive and still morphologically homogeneous, even after mechanical stretching and deformation are applied to the sample. Then, the microstructure has been functionalized with an amorphous film of SiOx, infiltrated with an anisotropic and reconfigurable fluid (nematic liquid crystal, NLC). In this way, by combining ion-implantation process and surface chemistry functionalization, we have overcome the insulating properties of PDMS and induced long range organization of cholesteric liquid crystals, thus controlling both diffraction and selective Bragg reflection of light by means of external perturbations (electric field, pressure). We have characterized our devices in terms of morphological, optical and electro-optical properties.

Sample electro-optical and pressure dependent optical properties have been explored by applying a modulated electric field through the conducting PDMS and a uniform pressure on the top cover substrate. We have shown that both an electric field of a few V mu m(-1) and an external pressure of up to 128 kPa can tune the reflection band by about 100 nm.

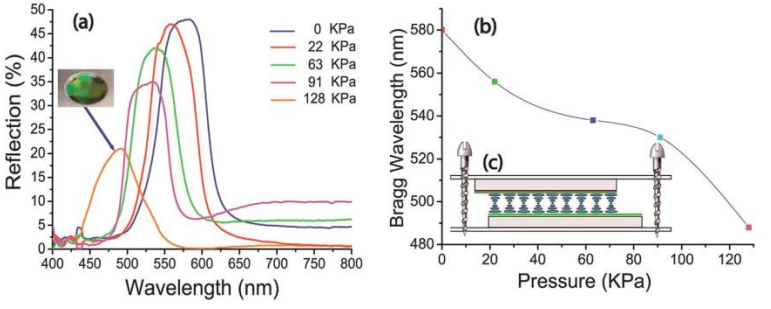

Spectral response (a) and band depth (b) of the sample for different values of the applied pressure

Growing gold nanoparticles on a flexible substrate. Plasmomechanis

A simple method has been presented to control and trigger the coupling between plasmonic particles using both a growing process of gold nanoparticles (GNPs) and a mechanical strain applied to the

elastomeric template where these GNPs are anchored. The large scale samples are prepared by first depositing and then further growing gold nanoparticles on a flexible PDMS tape. Upon stretching the tape the particles move further apart in the direction of the stretching and closer together in the direction perpendicular to it. The synergy between the controlled growth of GNPs and the mechanical strain, leads to a drastic shift of the plasmon band and a color change of the sample. Furthermore, the stretching by only a few percent of the amorphous and initially isotropic sample results in a strong polarization-dependent plasmon shift. At smaller gap sizes between neighboring particles, induced by stretching the PDMS tape, the plasmon shift strongly deviates from the behaviour expected considering the plasmon ruler equation. This shows that multipolar coupling effects significantly contribute to the observed shift. Overall, these results indicate that a macroscopic mechanical strain allows one to control the coupling and therefore the electromagnetic field at the nanoscale.

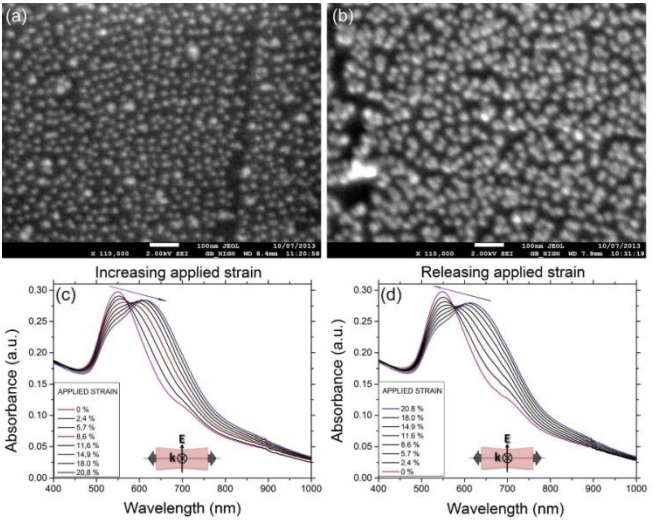

SEM micrographs of a gold nanoparticle coated PDMS substrate, taken (a) before and (b) after twelve growth cycles; (c) extinction spectra of the sample coated with gold nanoparticles (after twelve cycles of growth) acquired while increasing the applied strain from 0% to 20.8%. The sample was irradiated with t-polarized light (E field perpendicular to the stretching direction). (d) Extinction spectra acquired by releasing the strain applied to the same sample from 20.8% to 0%.

Plasmomechanics comes from the convergence between mechanics and plasmonics. We have investigated a topic whose technological aim is the development of plasmonic strain sensors. The idea is based on the ability to deduce Au nanoparticles (NPs) distance distributions from polarized optical extinction spectroscopy, which could thus give access to material strains. Variations of interparticle distances distributions can indeed lead to variations of plasmonic coupling and thus to material color change as shown experimentally and numerically for random Au NP assemblies deposited onto elastomer films.
We have carried out an experiment on a flexible polymeric substrate, coated with a monolayer of gold nanoparticles, which demonstrates how the combined effect of nanoparticle growth and stretching influences the average normalized gap between particles, thus modifying the extinction spectra of the sample. The study paves the way for the realization of a plasmonic strain sensor based on the plasmonic coupling of gold nanoparticles deposited onto elastomeric films: application of a

mechanical stretching induces a change of colour of the device and a fine control of the applied strain allows a continuous tuning of the colour.

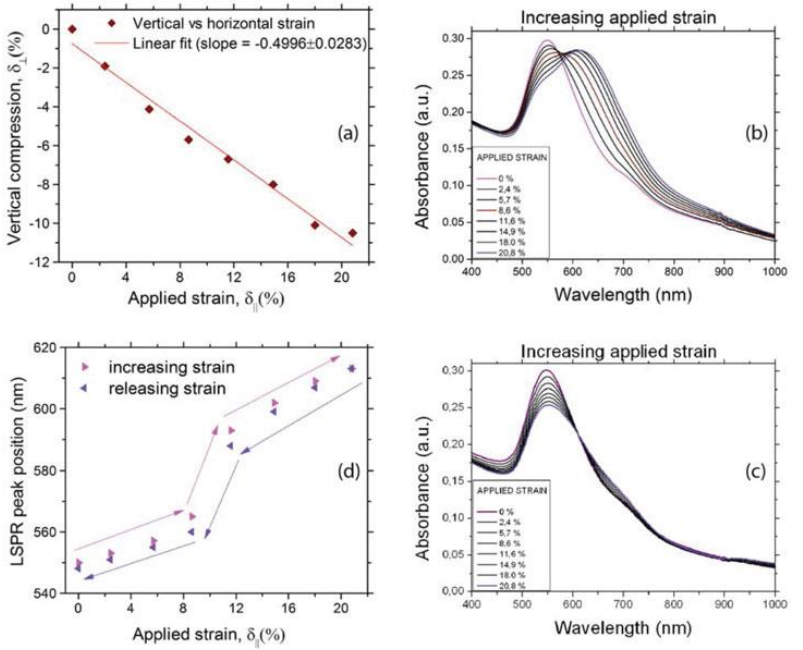

Measurement of the compression the sample undergoes in the direction perpendicular to the applied strain. A Poisson ratio of about 0.5 is confirmed for the PDMS substrate (a). Extinction spectra of the sample coated with gold nanoparticles (after twelve cycles of growth) acquired while increasing the applied strain from 0%to 20.8%; the sample has been irradiated with (b) light polarized perpendicularly to the stretching direction, and (c) light polarized parallel to the stretching direction. Spectral position of the resonance peak maxima as a function of the applied strain (d) during a straining-releasing cycle. A slight hysteresis is observed.

Liquid Crystals as an Active Medium: Novel Possibilities in Plasmonics

The peculiar properties of Liquid Crystals (LCs) foster new possibilities in plasmonics. The combination of the intrinsic tunability of LCs with the plasmonic properties of metallic nanoparticles (NPs) provides novel and intriguing features of systems commonly identified as active plasmonics. Being LCs, one of the media whose refractive index can be controlled through the application of external stimuli, they represent a convenient host for enabling plasmonic tunability. On the other hand, the localized plasmonic resonance, typical of NPs, can strongly influence and control the behavior of LCs. We have investigated several systems of NPs combined with LCs arranged in different configurations. The properties of the resulting systems suggest novel, intriguing outcomes in both fundamental and applied research.

a) Plasmonic Thermometer Based on Thermotropic Liquid Crystals

Investigation of the heat transport mechanism, from the heated MNPs to their surrounding medium, is fundamental for realizing applications in nanotechnology and thermal-based therapies, and a challenge is definitely represented by the possibility of measuring temperature variations at the surface of the MNPs undergoing optical illumination. In this framework, we have shown that an

ingenious combination of characteristics of short pitch liquid crystalline compounds and MNPs are effective to provide an advanced tool to monitor nanoscale temperature variations.

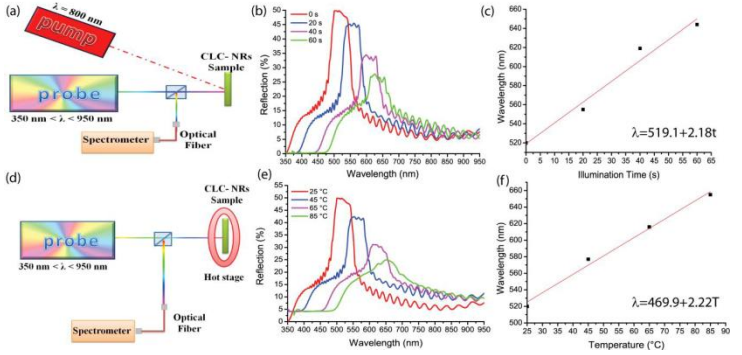

Pump-probe setup (a); Reflection response of the CLC-GNRs sample under optical pumping (b); Linear fit of the position of Bragg's wavelength versus illumination time (c); Thermal setup (d); Reflection response of the CLC-GNRs sample under the temperature variation effect (e); Linear fit of the position of Bragg's wavelength versus temperature (f).

b) Photo-thermal effects in gold nanoparticles dispersed in thermotropic nematic liquid crystals

The last few years have seen a growing interest in the ability of metallic nanoparticles (MNPs) to control temperature at the nanoscale. Under a suitable optical radiation, MNPs feature an enhanced light absorption/scattering, thus turning into an ideal nano-source of heat, remotely controllable by means of light. In this framework, we have modeled and characterized the photo-thermal effects observed in gold nanoparticles (GNPs) dispersed in thermotropic Liquid Crystals (LCs). Photo-induced temperature variations in GNPs dispersed in Nematic LCs (NLCs) have been studied by implementing an ad hoc theoretical model based on the thermal heating equation applied to an anisotropic medium. Theoretical predictions have been verified by performing photo-heating experiments on a sample containing a small percentage of GNPs dispersed in NLCs. Both theory and experiments represent an important achievement in understanding the physics of heat transfer at the nanoscale, with applications ranging from photonics to nanomedicine.

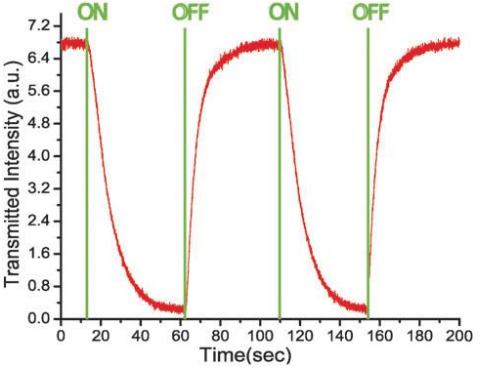

Switching behavior observed by using a periodic sequence of pump beam pulses. ON and OFF refer to the pump beam being allowed to impinge on the sample or not.

c) Nano-Localized Heating Source for Photonics and Plasmonics

We have reported on the realization and characterization of an innovative method for simultaneously achieving optical control of both the selective reflection of a CLC and the plasmonic resonance of GNRs. In particular, if surface chemistry functionalization is used for inducing planar alignment of the LC director in a glass cell, the obtained self-organization process of CLCs is able to effectively induce confinement and topological organization of GNRs along the sample structural defects. A photo-thermal effect, induced by the presence of a NIR selective plasmonic resonance, can be exploited for controlling the position of the selective reflection exhibited by the CLC configuration. Furthermore, the local heating induces a variation of the surrounding medium refractive index, with a consequent shift of the plasmonic resonance. This synergy between plasmonics and photonics can be profitably used for building up a method for detecting the temperature around NPs under optical illumination. In our opinion, the developed method opens up prospects for realizing, in the future, a nanomedicine tool, useful to avoid invasive treatments (e.g. hypothermic effects) on patients during therapy treatments.

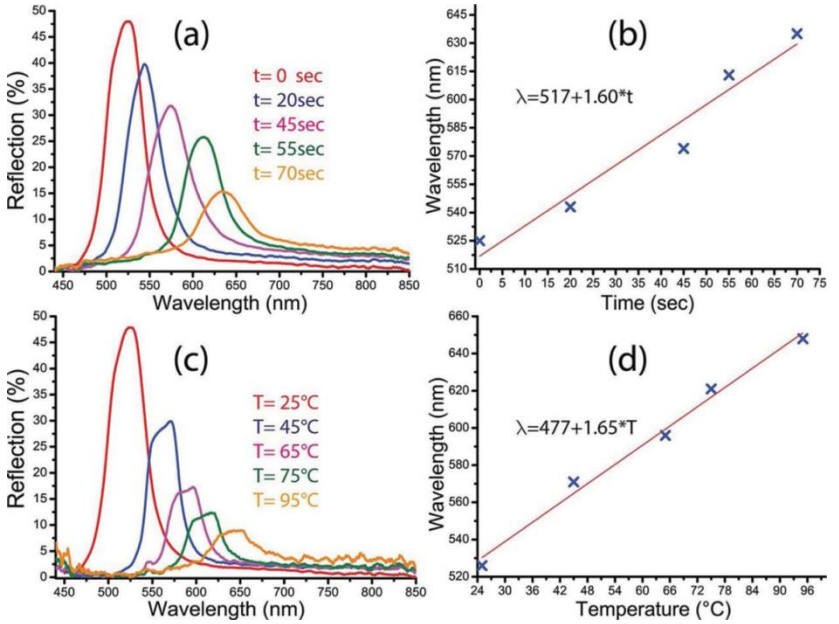

Reflection spectra of the sample for different values of illumination time (a) and temperature (c); linear fit of the position of the center of the reflection band versus illumination time (b) and temperature (d)

d) All-optical control of localized plasmonic resonance realized by photoalignment of LC

Large shifts in the plasmonic resonances of a thin film of gold nanorods (GNRs) are induced through the modulation of the local refractive index of the neighboring dielectric medium. This change is enabled through light-induced surface reorientation of a nematic liquid crystal in contact with a nanometer-thin photoalignment layer coating the GNR film. The presence of isolated and well distributed GNRs, both before and after the photoalignment layer deposition, is shown through atomic force and scanning electron microscopy. Exposure of the photoalignment layer to polarized light is shown to reorient aligned nematic liquid crystal molecules to an orthogonal direction, thereby changing the local refractive index of the medium in close proximity to the GNR film. This large

change in the local dielectric strength is shown to cause a broad red shift of the localized plasmonic longitudinal resonance and almost no shift in the local transverse resonance. The ability to remotely and quickly change the plasmonic properties of this GNR system marks a breakthrough towards the realization of all-optical plasmonic and photonic devices such as plasmonic colour filters.

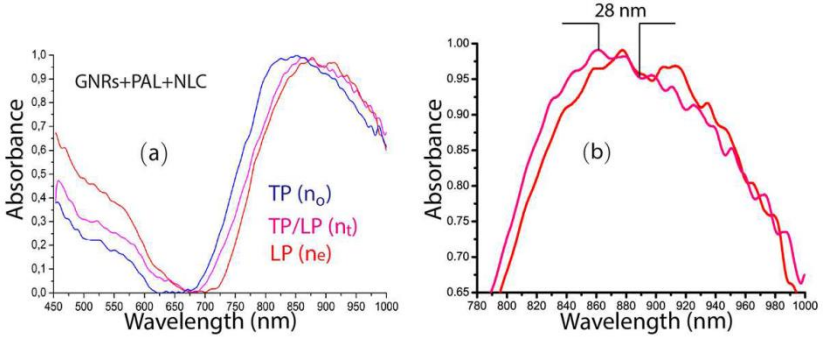

Spectral response of the sample (a) and high magnification of the effective tuning range (b) under optical illumination

e) Optical control of plasmonic heating effects using reversible photo-alignment of NLCs
We have demonstrated and characterized an optical control of the plasmonic heat delivered by a monolayer substrate of gold nanoparticles, obtained by modulating the effective refractive index of the neighboring dielectric medium. The effect, which exploits the dependence of the nematic liquid crystal (NLC) refractive index on the molecular director orientation, is realized by using a polarization dependent, light-induced molecular reorientation of a thin film of photo-alignment layer that the NLC is in contact with. For a suitable alignment, plasmonic pumping intensity values ranging from 0.25 W/cm(2) to 6.30 W/cm(2) can induce up to 17.4 degrees C temperature variations in time intervals of the order of seconds. The reversibility of the optically induced NLC molecular director orientation enables an active control of the plasmonic photo-induced heat. Published by AIP Publishing.

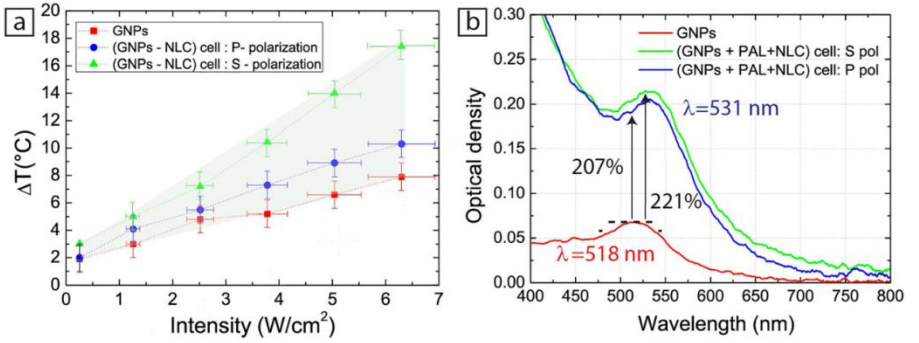

Temperature variations of the GNPs layer and of the GNPs-NLC cell for the two different director orientations of the NLC facing the substrate of GNPs (a). Spectral response of the substrate of GNPs surrounded by air (red curve) and of the GNPs-NLC cells in the case of P-polarized aligning blue light (blue curve) and S-polarize blue light (green curve) (b).

Soft Matter and nanoparticles for biological applications

a) Directed Organization of DNA Filaments in a Soft Matter Template

We have developed a noninvasive, all-optical, holographic technique for permanently aligning liquid crystalline DNA filaments in a microperiodic template realized in soft-composite (polymeric) materials. By combining optical intensity holography with a selective microfluidic etching process, a channeled microstructure has been realized which enables self-assembly of DNA. The striking chemico-physical properties of the structure immobilize the DNA filaments within the microchannels without the need of any kind of surface chemistry or functionalization. Polarized optical, confocal, and electronic microscopies have been used for characterizing the DNA geometry inside the microchannels in terms of birefringence, fluorescence, and nanoscale organization properties. In particular, observation of a far-field diffraction pattern confirms a periodic organization of the DNA filaments inside the polymeric template.

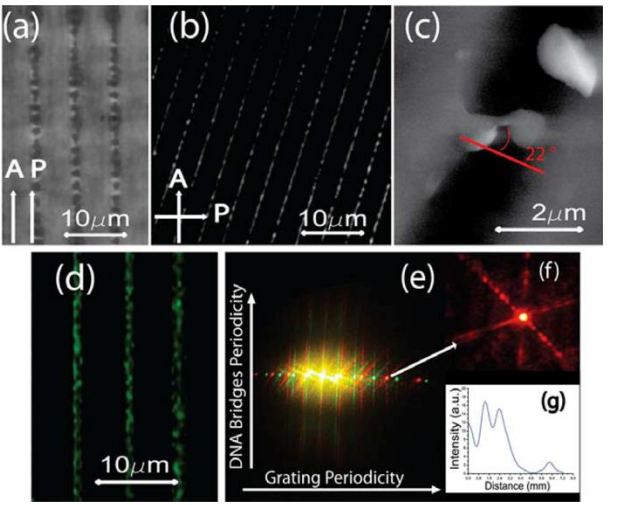

Optical micrograph (a), POM view (b), and ESEM picture of DNA bridge arrays (c) along with the confocal analysis image (d). Far-field 2-D diffraction pattern obtained by colaunching two laser beams of different color (e). High magnification of the “star-like” diffraction pattern (f). Intensity profile along one arm of the diffraction pattern (g).

b) Templating gold nanorods with liquid crystalline DNA

A liquid crystalline, negatively charged, whole-genome DNA is exploited to organize positively charged gold nanorods (GNRs) by means of electrostatic interaction. A mesoscopic alignment of the composite system along a preferred direction is obtained by casting a droplet of the DNA-nanorods solution onto an untreated glass substrate. Gel electrophoresis analysis enables evaluating the effective electric charge of the system, thus minimizing the DNA fragmentation. Polarized optical microscopy, combined with transmission and scanning electron microscopy, shows that, up to 20% in weight of GNR solution, the system exhibits both a long range order, induced by the liquid crystalline phase of the DNA, and a nanoscale organization, due to the DNA self-assembly. These evidences are confirmed by a polarized spectral analysis, which also points out that the optical properties of GNRs strongly depend on the polarization of the impinging probe light. The capability to organize plasmonic nanoparticles by means of DNA material represents a significant advance towards the realization of life science inspired optical materials.

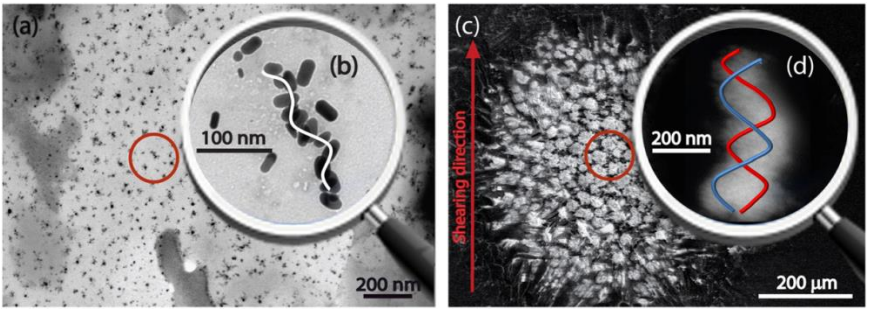

TEM (a) and ESEM (c) images of the sample along with their high magnification (b), (d), highlighting the 'helix like' organization (continue arrows) of GNRs wrapping the liquid crystalline DNA

c) Plasmonics Meets Biology through Optics

Plasmonic metallic nanoparticles (NPs) represent a relevant class of nanomaterials, which is able to achieve light localization down to nanoscale by exploiting a phenomenon called Localized Plasmon Resonance. In the last few years, NPs have been proposed to trigger DNA release or enhance ablation of diseased tissues, while minimizing damage to healthy tissues. In view of the therapeutic relevance of such plasmonic NPs; a detailed characterization of the electrostatic interaction between positively charged gold nanorods (GNRs) and a negatively charged whole-genome DNA solution is reported. The preparation of the hybrid biosystem has been investigated as a function of DNA concentration by means of ζ-potential; hydrodynamic diameter and gel electrophoresis analysis. The results have pointed out the specific conditions to achieve the most promising GNRs/DNA complex and its photo-thermal properties have been investigated. The overall study enables envisaging the possibility to combine plasmonic and biological materials, thus enabling design and development of an original non invasive all-optical methodology for monitoring photo-induced temperature variation with high sensitivity.

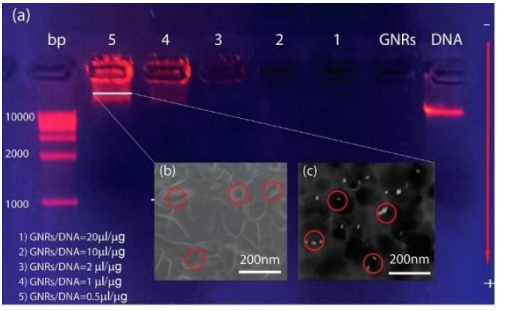

Gel electrophoresis (a) and environmental scanning electron microscope (ESEM) cross section of line 5 of agarose matrix before (without GNRs/DNA) (b) and after (with GNRs/DNA) electrophoretic run (c).

d) Photo-thermal effects in gold nanorods / DNA complexes

An ingenious combination of plasmonic nanomaterials and one of the most relevant biological systems, deoxyribonucleic acid (DNA) is achieved by bioconjugating gold nanorods (GNRs) with DNA via electrostatic interaction between positively charged gold nanorods (GNRs) and negatively charged short DNA. The obtained system is investigated as a function of DNA concentration by

means of gel electrophoresis, zeta-potential, DNA melting and morphological analysis. It turns out that the obtained bioconjugated systems present both effective electric charge and aggregate size that are particularly amenable for gene therapy and nanomedicine applications. Finally, the effect of the localized (photo-thermal heating) and delocalized temperature variation on the DNA melting by performing both light induced bio-transparent optical heating experiments and a thermographic analysis is investigated, demonstrating that the developed system can be exploited for monitoring nanoscale temperature variation under optical illumination with very high sensitivity.

Soft Matter exploitation for THz applications

a) Periodical Elements as Low-Cost Building Blocks for Tunable Terahertz Filters.

Periodical elements made by stacking thin layers of the cyclo-olefin polymer Zeonor, separated by spacers made of bi-adhesive tape, are used as building blocks for realizing tunable terahertz (THz) filters. The basic block is a Bragg reflector whose bandgap is controlled by changing the geometrical features of the periodical elements. By combining two of these Bragg building blocks, separated by a void defect cavity, a tunable bandpass filter is obtained. The thickness of the defect cavity is mechanically tuned by means of a translation stage. The resulting filters are mechanically stable and show both high transmittance and narrow linewidth, owing to the selected THz low-loss polymer.

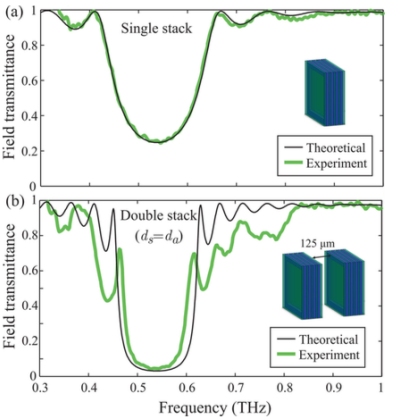

Measurement and reference simulations of the normalized electric field transmittance |Et/Eref| for (a) single 5-layer Zeonor stack and (b) double periodic stack by setting ds = da = 125 μm.

b) Flexible terahertz wire grid polarizer with high extinction ratio and low loss.

An aluminum-based terahertz (THz) wire grid polarizer is theoretically investigated and experimentally demonstrated on a subwavelength thin flexible and conformal foil of the cyclo-olefin Zeonor polymer. THz time-domain spectros- copy characterization, performed on both flat and curved configurations, reveals a high extinction ratio between 40 and 45 dB in the 0.3–1 THz range and in excess of 30 dB up to 2.5 THz. The insertion losses are lower than 1 dB and are almost exclusively due to moderate Fabry–Perot reflections, which vanish at targeted frequencies. The polarizer can be easily fabricated with low-cost techniques such as roll-to-roll and/or large-area electronics processes and promises to open the way for a new class of flexible and conformal THz devices.

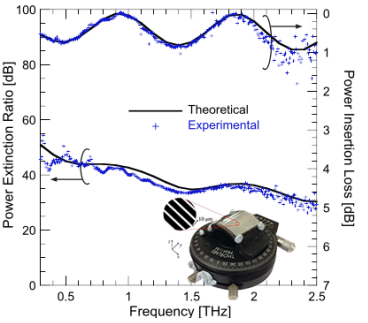

Comparison of experimental measurements and numerical results of the ER and IL for the THz wore grid polarizer with p 10μm and F=68% for normal incidence. The scattering of data at higher frequencies is due to the decreasing signal-to-noise ratio of the instrument. In the inset: Flexible THz polarizer on a curved mount, placed on a rotation stage for the THz-TDS experimental setup. The inset shows a micrograph of the fabricated WGP (p=10 μm and w=6.8 μm) under an optical microscope in transmission mode. The black parts are the Al stripes, while the transparent foil appears white.

Soft Matter application to hybrid systems

a)Two-color single hybrid plasmonic nano-emitters with real time switchable dominant emission wavelength

A two-color nanoemitter that enable the selection of the dominant emitting wavelength has been demonstrated by varying the polarization of excitation light. The nanoemitters were fabricated via surface plasmon-triggered two-photon polymerization. By using two polymerizable solutions with different quantum dots, emitters of different colors can be positioned selectively in different orientations in the close vicinity of the metal nanoparticles. The dominant emission wavelength of the metal/polymer anisotropic hybrid nanoemitter thus can be selected by altering the incident polarization.

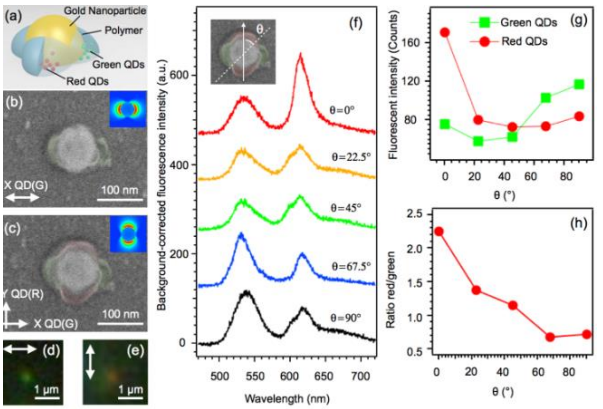

Nanodisk-based two color anisotropic nanoemitter: topographic and optical characterizations. (a) Schematic representation of the nanostructure. (b) SEM image of the Au nanodisk of d = 90 nm after the first exposure that positions green QDs along the X axis (plasmonic near-field intensity of dipole emission for polymerization is shown in the inset). (c) SEM image of the same nanodisk after the second exposure that traps red QDs along the Y axis (plasmonic near-field intensity of dipole

emission for second exposure is shown in the inset). For clarity, SEM images have been artificially colored according to the emission wavelengths of the trapped QDs. Far-field fluorescence image of the TCANE under illumination with (d) X axis polarization and (e) Y axis polarization. Double arrows represent the polarization of the excitation light. (f) Polarization-dependent fluorescence spectra from the TCANE. The polarizations of the excitation light (λexc= 405 nm) were at θ = 0° (red plot), 22.5° (orange), 45° (green plot), 67.5° (blue plot), and 90° (black plot) with respect to the Y axis. The inset defines the polarization angle θ. The dashed line represents the incident polarization direction. (g) Intensities of emission peaks of the green QDs (green square) and red QDs (red dot) as a function of polarization angle. (h) Ratio of intensity of red/green as a function of polarization. The excitation wavelength was set at λ exc = 405 nm for fluorescence images and spectra.

b) Enhanced adhesion of electron beam resist by grafted monolayer poly(methylmethacrylate-co-methacrylic acid) brush

In electron beam lithography, poor resist adhesion to a substrate may lead to resist structure detachment upon development. One popular method to promote resist adhesion is to modify the substrate surface. In this study, it is shown that a poly (methylmethacrylate-co-methacrylic acid) [P(MMA-co-MAA)] monolayer "brush" can be grafted onto a silicon substrate using thermal annealing that leads to chemical bonding of the P(MMA-co-MAA) copolymer to the hydroxyl group-terminated substrate, followed by acetic acid wash to remove the bulk, unbonded copolymer. The monolayer brush has a thickness of 12 nm. The authors show that it can greatly improve the adhesion of positive resist, the ZEP-520A, and negative resist polystyrene to bare silicon surfaces, which led to high resolution patterning without resist detachment upon development. The improvement was more dramatic when patterning dense sub-100 nm period grating structures. But the improvement was negligible for an aluminum substrate, because, even without the brush layer, resist adhesion to aluminum is found already to be strong enough to prevent resist structure peeling off. The current simple and low cost method could be very useful when resist adhesion to the substrate for a given developer is weak.

Surface analysis by X-ray tomography

Virtual unrolling and deciphering of Herculaneum papyri by X-ray phase-contrast tomography

A collection of more than 1800 carbonized papyri, discovered in the Roman 'Villa dei Papiri' at Herculaneum is the unique classical library survived from antiquity. These papyri were charred during 79 A.D. Vesuvius eruption, a circumstance which providentially preserved them until now. This magnificent collection contains an impressive amount of treatises by Greek philosophers and, especially, Philodemus of Gadara, an Epicurean thinker of 1st century BC. We read many portions of text hidden inside carbonized Herculaneum papyri using enhanced X-ray phase-contrast tomography non-destructive technique and a new set of numerical algorithms for 'virtual-unrolling'. Our success lies in revealing the largest portion of Greek text ever detected so far inside unopened scrolls, with unprecedented spatial resolution and contrast, all without damaging these precious historical manuscripts. Parts of text have been decoded and the 'voice' of the Epicurean philosopher Philodemus is brought back again after 2000 years from Herculaneum papyri.

Self-assembly of defects in LC films

Controlling the Self-Assembly of Periodic Defect Patterns in Smectic Liquid Crystal Films with Electric Fields,

Large-area periodic defect patterns are produced in smectic A liquid crystals confined between rigid plate electrodes that impose conflicting parallel and normal anchoring conditions, inducing the formation of topological defects. Highly oriented stripe patterns are created in samples thinner than 2 μm due to self-assembly of linear defect domains with period smaller than 4 μm, whereas hexagonal lattices of focal conic domains appear for thicker samples. The pattern type (1d/2d) and period can be controlled at the nematic–smectic phase transition by applying an electric field, which confines the

defect domains to a thin surface layer with thickness comparable to the nematic coherence length. The pattern morphology persists in the smectic phase even after varying the field or switching it off. Bistable, non-equilibrium patterns are stabilized by topological constraints of the smectic phase that hinder the rearrangement of defects in response to field variations.

REFERENCES

L. De Sio, G. Caracciolo, F. Annesi, T. Placido, D. Pozzi, R. Comparelli, A. Pane, M. L. Curri, A. Agostiano, R. Bartolino,
Plasmonics Meets Biology through Optics
Nanomaterials 2015, 5(2), 1022-1033.

L. De Sio, G. Caracciolo, T. Placido, D. Pozzi, R. Comparelli, F. Annesi, M. L. Curri, A. Agostiano, R. Bartolino *Applications of nanomaterials in modern medicine*
Rendiconti Lincei. Scienze Fisiche e Naturali 2015 (DOI: 10.1007/s12210-015-0400-y)

L. De Sio, F. Annesi, T. Placido, R. Comparelli, V. Bruno, A. Pane, G. Palermo, L. Curri, C. Umeton, R. Bartolino *Templating gold nanorods with liquid crystalline DNA*
J. Opt. 2015, 17, 025001

L. De Sio, G. Caracciolo, F. Annesi, T. Placido, D. Pozzi, R. Comparelli, A. Pane, M. L. Curri, A. Agostiano and R. Bartolino
Photo-thermal effects in gold nanorods/DNA complexes
Micro and Nano Syst Lett (2015) 3:8 DOI 10.1186/s40486-015-0025-z

C. M. Tone, M. P. De Santo, and F. Ciuchi
Alignment of Chromonic Liquid Crystals: A Difficult Task
Mol. Cryst. Liq. Cryst., Vol. 576: pp. 2–7, 2013

C.M., M.P. De Santo, F. Ciuchi
The role of surface energy in guanosine nucleotide alignment: an intriguing scenario
Colloids and Surfaces B: Biointerfaces 10.1016/j.colsurfb.2014.04.004 vol 119,99-105 (2014)

A. Crispini, D. Pucci, B. Sanz Mendiguchia, C.M. Tone, E. Ildyko Szerb, F. Ciuchi, M. Gao and M. Ghedini
Unconventionally shaped chromonic liquid crystals formed by novel silver(I) complexes
J. Mater. Chem. C, 2014, 2, 8780, DOI: 10.1039/C4TC01736F

R. Dhama, A. R. Rashed, V. Caligiuri, M. El. Kabbash, G. Strangi and A. De Luca,
Broadband optical transparency in plasmonic nanocomposite polymer films via exciton-plasmon energy transfer
Optics Express, 24, Issue 13 (2016)

M. El Kabbash, A. R. Rashed, K. V. Sreekanth, A. De Luca, M. Infusino and G. Strangi,
Plasmon-Exciton Resonant Energy Transfer: Across Scales Hybrid Systems
Journal of Nanomaterials, 2016, 4819040 (2016).

K.V. Sreekanth, Y. Alapan, M. ElKabbash, E. Ilker, M. Hinczewski, U. A. Gurkan, A. De Luca and G. Strangi,
Extreme sensitivity biosensing platform based on hyperbolic metamaterials
Nature Materials, 15, 621-627 (2016)

V. Caligiuri,, A. De Luca
Metal-semiconductor-oxide extreme hyperbolic metamaterials for selectable canalization wavelength
Journal of Physics D: Applied Physics, 49, 8 (2016)

V. Caligiuri, R. Dhama, K. V. Sreekanth, G. Strangi & A. De Luca
Dielectric singularity in hyperbolic metamaterials: the inversion point of coexisting anisotropies
Sci. Rep. Nature, 6, 20002 (2016)

G. Strangi, A. De Luca, R. Bartolino
From Life to Life: through new materials and plasmonics
Rendiconti Lincei, vol. 26, p. 127-128 (2015)

A. De Luca, R. Bartolino, M.A. Correa-Duarte, M.L. Curri, N.F. Steinmetz, G. Strangi
Gain-assisted plasmonic metamaterials: mimicking nature to go across scales
Rendiconti Lincei, vol. 26, p. 161-174 (2015)

A.R. Rashed, A. De Luca, R. Dhama, A. Hosseinzadeh, M. Infusino, M. El Kabbash, S. Ravaine, R. Bartolino and G. Strangi
Battling absorptive losses by plasmon–exciton coupling in multimeric nanostructures
RSC Adv., 5, 53245 (2015)

A. M. Wen, M. Infusino, A. De Luca, D. L. Kernan, A. E. Czapar, G. Strangi and N. F. Steinmetz,
Interface of Physics and Biology: Engineering Virus-Based Nanoparticles for Biophotonics
Bioconjugate Chem. 26 (1), pp 51–62 (2015)
K.V. Sreekanth, A. De Luca and G. Strangi
Excitation of volume plasmon polaritons in metal-dielectric metamaterials using 1D and 2D diffraction gratings
J. Opt. 16 - 105103 (8pp) (2014)

K.V. Sreekanth, K.H. Krishna, A. De Luca and G. Strangi
Large spontaneous emission rate enhancement in grating coupled hyperbolic metamaterials
Sci. Rep. Nature, 4 , 6340 (2014)

A. De Luca, A. Iazzolino, J.-B. Salmon, J. Leng, S. Ravaine, A. N. Grigorenko and G. Strangi,
Experimental evidence of exciton-plasmon coupling in densely packed dye doped core-shell nanoparticles obtained via microfluidic technique
J. of Appl. Phys. 116, 104303 (2014)

K.V. Sreekanth, A. De Luca and G. Strangi
Improved transmittance in metal-dielectric metamaterials using diffraction grating
App. Phys. Lett. 104, 171904 (2014)

M. Infusino, A. De Luca, A. Veltri, C. Vázquez-Vázquez, M. A. Correa-Duarte, R. Dhama and G. Strangi
Loss-Mitigated Collective Resonances in Gain-Assisted Plasmonic Mesocapsules
ACS Photonics, 1, 371-376 (2014)

A. De Luca, R. Dhama, A. R. Rashed, C. Coutant, S. Ravaine, P. Barois, M. Infusino and G. Strangi
Double strong exciton-plasmon coupling in gold nanoshells infiltrated with fluorophores
Appl. Phys. Lett., 104, 103103 (2014)

M. Infusino, A. De Luca, F. Ciuchi, A. Ionescu, N. Scaramuzza, G. Strangi
Optical and electrical characterization of a gold nanoparticle dispersion in a chiral liquid crystal matrix
J. Mater. Sci. 49, 1805–1811 (2014)

K.V. Sreekanth, A. De Luca, and G. Strangi
Experimental demonstration of surface and bulk plasmon polaritons in hypergratings
Sci. Rep. Nature 3, 3291 (2013) - DOI:10.1038/srep03291

L. De Sio, A. Veltri, R. Caputo, A. De Luca, G. Strangi, R. Bartolino and Cesare P. Umeton
POLICRYPS composite structures: realization, characterization and exploitation for electro-optical and all-optical applications
Liq. Cryst. Rev., 1, 2-9 (2013)

K. V. Sreekanth, A. De Luca and G. Strangi
Negative refraction in graphene-based hyperbolic metamaterials
Appl. Phys. Lett., 103, 023107 (2013)

A. De Luca, N. Depalo, E. Fanizza, M. Striccoli, M. L. Curri, M. Infusino, A. R. Rashed, M. La Deda, G. Strangi
Plasmon Mediated super-absorber flexible nanocomposites for metamaterials
Nanoscale, 5, 6097-6105 (2013)

M. Infusino, A. De Luca, F. Ciuchi, A. Ionescu, N. Scaramuzza, G. Strangi
Effects of gold nanoparticle dispersion in a chiral liquid crystal matrix
Mol. Cryst. Liq. Cryst., 572 (1) , 59-65 (2013)

A. Aprile, F. Ciuchi, R. Pinalli, E. Dalcanale and P. Pagliusi
Probing molecular recognition at the solid-gas interface by sum-frequency vibrational spectroscopy
Journal of Physical Chemistry Letters 7, 3022-3026 (2016)

O. Brzobohatý, R.J.Hernández, S.Simpson, A. Mazzulla, G.Cipparrone, bc, P. Zemánek
Chiral particles in the dual-beam optical trap
Optics Express, 24(23), 26382-26391 (2016).

C. Provenzano, A.Mazzulla, F. Chiaravalloti, B. Audia, G. Cipparrone
Topological defects and electro-convective flows in anisotropic fluids: A microfluidic platform for nano-objects tunable structuring
Applied Physics Letters, 109(7), 07190, (2016).

D. Kasyanyuk, P. Pagliusi, A. Mazzulla, S. Tmylko, V.Reshetnyak, Y. Reznikov, C. Provenzano, M. Giocondo, M. Vasnetsov, O. Yaroshchuk,G. Cipparrone
Manipulation of colloids by optical and electrical control of disclination lines in liquid crystals
Optofluidics, Microfluidics and Nanofluidics 3.1 (2016).

J. Hernandez, A. Mazzulla, C. Provenzano, P. Pagliusi, M. Viola, G. Cipparrone
Cholesteric solid spherical microparticles: Chiral optomechanics and microphotonics
Liquid Crystals Reviews, 4(1), 59-79 (2016).

D. Kasyanyuk, P. Pagliusi, A. Mazzulla, V.Reshetnyak, Y. Reznikov, C. Provenzano, M. Giocondo, M. Vasnetsov, O. Yaroshchuk,G. Cipparrone,
Light manipulation of nanoparticles in arrays of topological defects
Scientific Reports, 6, 20742, (2016).

M.G.Donato, A.Mazzulla, P. Pagliusi, A. Magazzù, R.J. Hernandez, C. Provenzano, P.G.Gucciardi, O.M. Maragò, G. Cipparrone
Light-induced rotations of chiral birefringent microparticles in optical tweezers
Scientific Reports, 6, 31977 (2016).

G.Pucci, D.Lysenko, C.Provenzano, Y. Reznikov, G. Cipparrone, R. Barberi
Patterns of electro-convection in planar-periodic nematic cells
Liquid Crystals, 43 (2), 26, 216-221 (2016).

D. E.Lucchetta, F. Simoni, R. J.Hernandez, A.Mazzulla, G. Cipparrone
Lasing from liquid crystal droplets generated in a microfluidic device
Progress in Electromagnetic Research Symposium (PIERS), 1007 . IEEE. (2016).

J. Hernandez, A. Mazzulla, C. Provenzano, P. Pagliusi, G. Cipparrone
Chiral resolution of spin angular momentum in linearly polarized and unpolarized light
Scientific Reports, 5 16926, DOI: 10.1038/srep16926 (2015).

D.E. Lucchetta, F. Simoni, P. Pagliusi, G.Cipparrone
Polymer stabilized Monodispersed Liquid Crystal Droplets: Microfluidics Generation and Optical Analysis
Optical Data Processing and Storage 1.1 (2015)

U. Ruiz, P. Pagliusi, C. Provenzano, E. Lepera, G.Cipparrone
Liquid crystal microlens arrays recorded by polarization holography
Applied Optics 54 (11) , pp. 3303-3307, (2015).

A. Aprile, P. Pagliusi, F. Ciuchi, R. Pinalli and E. Dalcanal
Probing cavitand-organosilane hybrid bilayers via sum frequency vibrational spectroscopy
Langmuir 30, 12843 (2014).

J. Reyes, C. Provenzano, P. Pagliusi, R.M. Tejedor, M. Pinol, L. Oriol
A bifunctional amorphous polymer exhibiting equal linear and circular photoinduced birefringences
Macromolecular Rapid Communications, 35, 1890-1895 (2014).

C. Provenzano, P. Pagliusi, G. Cipparrone, J. Royes, M. P iñol, L. Oriol
Polarization Holograms in a Bifunctional Amorphous Polymer Exhibiting Equal Values of Photoinduced Linear and Circular Birefringences
Journal of Physical Chemistry B, 118 (40), 11849–11854 (2014).

M.G. Donato, J. Hernandez, A. Mazzulla, C. Provenzano, R. Saija, R.Sayed, S. Vasi, A.Magazzu, P. Pagliusi, R. Bartolino, P.G. Gucciardi, O.M. Maragò, G. Cipparrone
Polarization dependent optomechanics mediated by chiral microresonators
Nature Communications, 5:3656 doi:10.1038/ncomms4656 (2014).
C. Provenzano, A. Mazzulla, P. Pagliusi, M. De Santo, G. Desiderio, I. Perrotta, G. Cipparrone
Self-organized internal architectures of chiral micro-particles
Applied Physics Letters Materials 2(2), 22103-22103 (2014).

M.G. Donato, J. Hernandez, A. Mazzulla, C. Provenzano, R. Saija, M.A. Iatì, A.Magazzu, P. Pagliusi, R. Bartolino, P.G. Gucciardi, O.M. Maragò, G. Cipparrone
Polarization dependent optical forces on chiral microresonators
Frontiers in Optics, Optical Society of America, FiO 2014 (2014).

R.J. Hernández, A. Mazzulla, A. Pane, K. Volke-Sepúlveda, G. Cipparrone
Attractive-repulsive dynamics on light-responsive chiral microparticles induced by polarized tweezers
Lab on Chip, 13, 459-467 (2013).

U. Ruiz, P. Pagliusi, C. Provenzano, K. Volke-Sepúlveda, G.Cipparrone
Polarization holograms allow highly efficient generation of complex light beams
Optics Express 21 (6) , pp. 7505-7510 (2013).

U. Ruiz, P. Pagliusi, C. Provenzano, G. Cipparrone
Highly efficient generation of vector beams through polarization holograms
Applied Physics Letters 102 (16) , art. no. 161104 (2013).

A. Mazzulla, G. Cipparrone, R.J. Hernandez, A. Pane, R. Bartolino
Self-organized chiral microspheres
Molecular Crystals and Liquid Crystals 576 (1) , pp. 15-22, (2013).

D. Lysenko , P. Pagliusi , C. Provenzano , Y. Reznikov , K.Slyusarenko , G. Cipparrone,
Periodic defects lines in liquid crystal cell guided by polarization holograms at an aligning surface
Applied Physics Letters ,103, art. N. 151913 (2013).

G.Politano, C.Versace, C.Vena, M.Castriota, A.Fasanella, F.Ciuchi, E.Cazzanelli
Physical investigation of electrophoretically deposited graphene oxide and reduced graphene oxide thin film
Journal of Applied Physics, 120 (2016) 195307

G.Pucci, F.Carbone, C.Vena, G.Lombardo, C.Versace, R.Barberi
DSM1-DSM2 transition threshold in turbulent" nematic mictures
Molecular Crystal and Liquid Crystals, 614 (2015) 100,105

C.Vena, R.Massarelli, F.Carbone, C.Versace
An approach to a model disordered birefringent medium for light depolarization applied to a liquid crystal device Journal of Optics 16 (2014) 065705

C.Vena, C.Versace, R.Bartolino
Stokes parameter analysis of light that is temporally and spatially depolarized
Europhysics Letters 101(2013) Article Number: 24003

Ruiz, Constanza; Pandey, Upendra K.; Termine, Roberto; Garcia-Frutos, Eva M.; Lopez-Espejo, Guzman; Ponce Ortiz, Rocio; Huang, Wei; Marks, Tobin J.; Facchetti, Antonio; Ruiz Delgado, M. Carmen; Golemme, Attilio; Gómez-Lor, Berta
Mobility versus Alignment of a Semiconducting pi-Extended Discotic Liquid-Crystalline Triindole
ACS Applied Materials & Interfaces, 8, 26964-26971 (2016).

Feringan, Beatriz; Romero, Pilar; Serrano, Jose Luis; Folcia, Cesar L; Etxebarria, Jesus; Ortega, Josu; Termine, Roberto; Golemme, Attilio; Gimenez, Raquel; Sierra, Teresa

H-Bonded Donor-Acceptor Units Segregated in Coaxial Columnar Assemblies: Toward High Mobility Ambipolar Organic Semiconductors
Journal of the American Chemical Society, 138, 12511-8 (2016).

Ionescu, Andreea; Lento, Raffaella; Mastropietro, Teresa F.; Aiello, Iolinda ; Termine, Roberto; Golemme, Attilio; Ghedini, Mauro; Bellec, Nathalie; Pini, Elena; Rimoldi, Isabella; Godbert, Nicolas
Electropolymerized Highly Photoconductive Thin Films of Cyclopalladated and Cycloplatinated Complexes
ACS Applied Materials & Interfaces, 7, 4019-4028 (2015).

Ismael Gracia, Beatriz Fering_n, Josè Luis Serrano, Roberto Termine, Attilio Golemme, Ana Omenat, and Joaquìn Barberà
Functional Carbazole Liquid-Crystal Block Codendrimers with Optical and Electronic Properties
Chemistry - a European Journal, 21, 1359-1369 (2015).

Bucos, Madalina ;Sierra, Teresa; Golemme, Attilio; Termine, Roberto; Barbera, Joaquin; Gimenez, Raquel ; Luis Serrano, Jose ; Romero, Pilar; Marcos, Mercedes
Multifunctional Supramolecular Dendrimers with an s-Triazine Ring as the Central Core: Liquid Crystalline, Fluorescence and Photoconductive Properties
Chemistry - a European Journal, 20, 10027-10037 (2014).

Angiolini, Luigi; Benelli, Tiziana; Giorgini, Loris; Golemme, Attilio; Mazzocchetti, Laura; Termine, Roberto
Effect of a chiral substituent on the photochromic and photoconductive properties of a methacrylic polymer bearing side chain azocarbazole moieties
Dyes and Pigments, 102, 53-62, (2014).

Benito-Hernandez, Angela; Pandey, Upendra K.; Cavero, Emma; Termine, Roberto; Garcia-Frutos, Eva M.; Serrano, Jose L.; Golemme, Attilio; Gomez-Lor, Berta
High Hole Mobility in Triindole-Based Columnar phases: Removing the Bottleneck of Homogeneous Macroscopic Orientation
Chemistry of Material, 25, 117-121 (2013).

Sassi, Mauro; Crippa, Maurizio; Ruffo, Riccardo; Turrisi, Riccardo; Drees, Martin; Pandey, Upendra K.; Termine, Roberto; Golemme, Attilio; Facchetti, Antonio; Beverina, Luca
Open circuit voltage tuning through molecular design in hydrazone end capped donors for bulk heterojunction solar cells
Journal of Materials Chemistry A, 1, 2631-2638 (2013).

Castelar, Susana; Barbera, Joaquin; Marcos, Mercedes; Romero, Pilar; Serrano, Jose-Luis; Golemme, Attilio; Termine, Roberto
Supramolecular dendrimers based on the self-assembly of carbazole-derived dendrons and triazine rings: liquid crystal, photophysical and electrochemical properties
Journal of Materials Chemistry C, 1, 7321-7332 (2013).

Roberto Termine and Attilio Golemme, *"Photorefractive Smectic Mesophases",* In "Photorefractive Organic Materials and Applications", P. A. Blanche editor, ISBN 978-3-319-29334-9, pag 187-222, Elsevier 2016.

Bukreeva, I.; Mittone, A.; Bravin, A.; Festa, G.; Alessandrelli, M.; Coan, P.; Formoso, V.; Agostino, R.G.; Giocondo, M); Ciiuchi, F.; Fratini, M.; Massimi, L.; Lamarra, A.; Andreani, C.; Bartolino, R.;

Gigli, G.; Ranocchia, G.; Cedola, A.
Virtual unrolling and deciphering of Herculaneum papyri by X-ray phase-contrast tomography
SCIENTIFIC REPORTS Volume: 6 Article Number: 27227 DOI: 10.1038/srep27227 Published: JUN 6 2016
Corrigendum: SCIENTIFIC REPORTS Volume: 6 Article Number: 30364 DOI: 10.1038/srep30364 Published: SEP 9 2016

Palermo, G.; De Sio L.; Placido, T.; Comparelli, R. ; Curri, M.L. ; Bartolino R.; Umeton, C.
Plasmonic Thermometer Based on Thermotropic Liquid Crystals
MOLECULAR CRYSTALS AND LIQUID CRYSTALS Volume: 614 Issue: 1 Pages: 93-99 DOI: 10.1080/15421406.2015.1050279 Published: JUN 13 2015

Gryn, I.; Lacaze, E. Bartolino, R.; Zappone, B.
Controlling the Self-Assembly of Periodic Defect Patterns in Smectic Liquid Crystal Films with Electric Fields ADVANCED FUNCTIONAL MATERIALS Volume: 25 Issue: 1 Pages: 142-149 DOI: 10.1002/adfm.201402875 Published: JAN 7 2015

De Sio, L.; Placido, T.; Serak, S.; Comparelli, R.; Tamborra, M. ; Tabiryan, N; Curri, M.L.; Bartolino R.; Umeton, C.; Bunning, T.
Nano-Localized Heating Source for Photonics and Plasmonics
ADVANCED OPTICAL MATERIALS Volume: 1 Issue: 12 Pages: 899-904 DOI: 10.1002/adom.201300275 Published: DEC 2013

De Sio, L.; D'Aquila, P. ; Brunelli, E.; Strangi, G.; Bellizzi, D.; Passarino, G.; Umeton, C.; Bartolino R.
Directed Organization of DNA Filaments in a Soft Matter Template
LANGMUIR Volume: 29 Issue: 10 Pages: 3398-3403 DOI: 10.1021/la3035787 Published: MAR 12 2013

De Sio, L.; Ferjani, S.; Strangi, G.; Umeton, C.; Bartolino R.
Soft Periodic Microstructures Containing Liquid Crystals
JOURNAL OF PHYSICAL CHEMISTRY B Volume: 117 Issue: 4 Pages: 1176-1185 DOI: 10.1021/jp311027p Published: JAN 31 2013

Y. G. Marinov, G. B. Hadjichristov, A. G. Petrov, S. Marino, C. Versace, N. Scaramuzz
Electro-optical response of PDLC single layers of large nematic droplets oriented by rubbed Teflon nanolayers JOURNAL OF APPLIED PHYSICS 113, 064301 (2013)

M. Infusino, A. De Luca, F. Ciuchi, A. Ionescu, N. Scaramuzza & G. Strangi
Effects of Gold Nanoparticle Dispersion in a Chiral Liquid Crystal Matrix
MOLECULAR CRYSTALS AND LIQUID CRYSTALS 572 (1), March 2013, pages 59-65

P. A. Santoro, E. K. Lenzi, L. R. Evangelista, F. Ciuchi, A. Mazzulla, N. Scaramuzza
Anomalous Diffusion Effects on the Electrical Impedance Response of Liquid-Crystalline Systems
MOLECULAR CRYSTALS AND LIQUID CRYSTALS 576, 2013, pages 23-31

Yordan G. Marinov, Georgi B. Hadjichristov, Alexander G. Petrov, Salvatore Marino, Carlo Versace, Nicola Scaramuzza
Selective amplitude-frequency electro-optical modulation by polymer-dispersed liquid crystal films aligned by Teflon nanolayers
COMPTES RENDUS DE L'ACAD´EMIE BULGARE DES SCIENCES 66(6), 2013, 819-826

G.B. Hadjichristov, I.G. Marinov, A.G. Petrov, S. Marino, C. Versace, N. Scaramuzza
Single-Layered Microscale PDLC Films for Electro-Optical Modulation of Laser Radiation
Bulg. J. Phys. 40 (2013) 301–306

Melissa Infusino, Antonio De Luca, Federica Ciuchi, Andrei Ionescu, Nicola Scaramuzza, Giuseppe Strangi
Optical and electrical characterization of a gold nanoparticle dispersion in a chiral liquid crystal matrix
J. MATER. SCI., February 2014, Volume 49, Issue 4, pp 1805-1811.

Francesco Vita, Katia Sparnacci, Guido Panzarasa, Immacolata F. Placentino, Salvatore Marino, Nicola Scaramuzza, Giuseppe Portale, Emanuela Di Cola, Claudio Ferrero‖ Sofia I. Torgova, Giancarlo Galli, Michele Laus, and Oriano Francescangeli
Evidence of Cybotactic Order in the Nematic Phase of a Main-Chain Liquid Crystal Polymer with Bent-Core Repeat Unit
ACS Macro Lett., 2014, 3, 91−95

V. Alzari, V. Sanna, S. Biccai, T. Caruso, A. Politano, N. Scaramuzza, M. Sechi, D. Nuvoli, R. Sanna, A. Mariani *Tailoring the physical properties of nanocomposite films by the insertion of graphene and other nanoparticles* COMPOSITES PART B: ENGINEERING, 2014, 60, 29–35

Georgi B. Hadjichristov, Yordan G. Marinov, Alexander G. Petrov, Emanuela Bruno, Lucia Marino and Nicola Scaramuzza
Electro-optically responsive composites of gold nanospheres in 5CB liquid crystal under direct current and alternating current joint action
JOURNAL OF APPLIED PHYSICS 115, 083107-1-083107-14 (2014)

L. Marino, S. Marino, D. Wang , E. Bruno and N. Scaramuzza
Nonvolatile memory effects in an orthoconic smectic liquid crystal mixture doped with polymer-capped gold nanoparticles
SOFT MATTER – ADVANCED ARTICLE, 2014, 10, 3842

Lucia Marino, Andrei Th. Ionescu, Daniela Pucci, Salvatore Marino, Emanuela Bruno, and Nicola Scaramuzza
Use of dielectric spectroscopy for evidencing subphases in an antiferroelectric liquid Crystal
JOURNAL OF APPLIED PHYSICS 116, 114101 (2014);

Georgi B. Hadjichristov, Yordan G. Marinov, Alexander G. Petrov, Emanuela Bruno, Lucia Marino & Nicola Scaramuzza
Electro-Optics of Nematic/Gold Nanoparticles Composites: The Effect from Dopants
MOLECULAR CRYSTALS AND LIQUID CRYSTALS Volume 610, Issue 1, March 2015, pages 135-148

F. Carbone, A. Mazzulla, F. Ciuchi and N. Scaramuzza
Dielectric relaxation in non-polar nematic liquid crystal devices
EUR. PHYS. J. PLUS (2015) 130: 151 DOI 10.1140/epjp/i2015-15151-0

Valeria Alzari, Daniele Nuvoli, Vanna Sanna, Tommaso Caruso, Salvatore Marino, and Nicola Scaramuzza
Study of polymeric nanocomposites prepared by inserting graphene and / or Ag, Au and ZnO nanoparticles in a TEGDA polymer matrix, by means of the use of dielectric spectroscopy

AIP ADVANCES 6, 035005 (2016)

G B Hadjichristov, Y G Marinov, A G Petrov, L Marino and N Scaramuzza
Dielectric and electrical characterization of 5CB nematic liquid crystal doped with silver nanoparticles
JOURNAL OF PHYSICS: Conference Series 682 (2016) 012015

H.K. Koduru, L. Marino, V. Janardhanam, N. Scaramuzza
Influence of Thin layer of Silver nanoparticles on Optical and Dielectric Properties of Poly(vinyl alcohol) Composite films
SURFACES AND INTERFACES http://dx.doi.org/10.1016/j.surfin.2016.09.008

Hari Krishna Koduru, Lucia Marino, Janardhanam Vallivedu, Chel-Jong Choi, Nicola Scaramuzza
Microstructural, wetting, and dielectric properties of plasma polymerized polypyrrole thin films
J. APPL. POLYM. SCI. 133(38) 2016, 43982 (1 of 10)

H K Koduru, M T Iliev, K K Kondamareddy, D Karashanova, T Vlakhov, X Z Zhao, N Scaramuzza
Investigations on Poly (ethylene oxide) (PEO) – blend based solid polymer electrolytes for sodium ion batteries JOURNAL OF PHYSICS: Conference Series 764 (2016) 012006

Palermo G, Cataldi U, De Sio L, Burgi T, Tabiryan N, Umeton C
Optical control of plasmonic heating effects using reversible photo-alignment of nematic liquid crystals
APPLIED PHYSICS LETTERS, 109, 191906, DOI: 10.1063/1.4967377, (2016)

Pezzi L, De Sio L, Palermo G, Veltri A, Placido T, Curri ML, Tabiryan N, Umeton C
Nematic liquid crystals used to control photo-thermal effects in gold nanoparticles
EMERGING LIQUID CRYSTAL TECHNOLOGIES XI, Edited by Chien LC, Broer DJ, Kikuchi H, Tabiryan N, Book Series: Proceedings of SPIE, 9769, UNSP 97690C, DOI: 10.1117/12.2216201 (2016)

Ferraro A, Zografopoulos D. C, Caputo R, Beccherelli R
Periodical Elements as Low-Cost Building Blocks for Tunable Terahertz Filters
Ieee Photonics Technology Letters, 28, 2459 (2016)

Ferraro, A.; Zografopoulos, D. C.; Missori, M.; Peccianti, M.; Caputo, R.; Beccherelli, R.
Flexible terahertz wire grid polarizer with high extinction ratio and low loss
Optics Letters, 41, 2009 (2016)

Palermo G, De Sio L, Umeton C, Flexible
Structures Based on a Short Pitch Cholesteric Liquid Crystals
MOLECULAR CRYSTALS AND LIQUID CRYSTALS, vol. 619, p. 35-41, ISSN: 1542-1406, doi: 10.1080/15421406.2015.1087275 (2015)

Rippa M, Bobeico E, Umeton, C, Petti L
Tunable Bragg extraction of light in photonic quasi crystals: dispersed liquid crystalline metamaterials
LIQUID CRYSTALS XIX, Book Series: Proceedings of SPIE Edited by Khoo, IC, 9565, 956516, DOI: 10.1117/12.2190362 (2015)

Pezzi L, De Sio L, Veltri A, Placido T, Palermo G, Comparelli R, Curri M L, Agostiano A, Tabiryan N, Umeton C, *Photo-thermal effects in gold nanoparticles dispersed in thermotropic nematic liquid crystals*
PHYSICAL CHEMISTRY CHEMICAL PHYSICS, vol. 17, p. 20281-20287, ISSN: 1463-9076, doi: 10.1039/c5cp01377a (2015)

Caputo R, Cataldi U, Buergi T, Umeton C
Plasmomechanics: A Colour-Changing Device Based on the Plasmonic Coupling of Gold Nanoparticles.
MOLECULAR CRYSTALS AND LIQUID CRYSTALS, vol. 614, p. 20-29, ISSN: 1542-1406, doi: 10.1080/15421406.2015.1049897 (2015)

Alj, D, Paladugu, S, Volpe, G, Caputo, R, Umeton C
Polar POLICRYPS diffractive structures generate cylindrical vector beams
APPLIED PHYSICS LETTERS, vol. 107, ISSN: 0003-6951, doi: 10.1063/1.4935605 (2015)

H. M Atkuri, E. Sok Ping Leong, J. Hwang, G. Palermo, G. Si, J. M. Wong, L. C. Chien, J. Ma, K. Zhou, Y. J. Liu and L. De Sio
Developing novel liquid crystal technologies for display and photonic applications
Displays 36, 21 (2015)

L. De Sio, T. Placido, R. Comparelli, L. Curri, M. Striccoli, N. Tabiryan, T. Bunning
Next-generation thermo-plasmonic technologies and plasmonic nanoparticles in optoelectronics
Progress in Quantum Electronics, 41, 23 (2015)

R. Caputo, P. Palermo, M. Infusino, L. De Sio
Liquid Crystals as an Active Medium: Novel Possibilities in Plasmonics
Nanospectroscopy, 1, 2300 (2015)

L. De Sio, N. Tabiryan, T. Bunning
POLICRYPS based electro-switchable Bragg reflector
Optics Express, 23, 32696 (2015)

Maurer, T.; Marae-Djouda, J.; Cataldi, U.; Gontier, A.; Montay, G.; Madi, Y.; Panicaud, B.; Macias, D.; Adam, P. M.; Leveque, G.; Burgi, T.; Caputo, R.
The beginnings of plasmomechanics: towards plasmonic strain sensors
Frontiers of Materials Science, 9, 170 (2015)

Viscomi, F. N.; Dey, R. K.; Caputo, R.; Cui, B.
Enhanced adhesion of electron beam resist by grafted monolayer poly(methylmethacrylate-co-methacrylic acid) brush. Journal of Vacuum Science & Technology B, 33, (2015)

Zhou, X.; Wenger, J.; Viscomi, F.; Le Cunff, L.; BÈal, J.; Kochtcheev, S.; Yang, X.; Wiederrecht, G. P.; Colas Des Francs, G.; Bisht, A. S., Jradi S, Caputo R, Demir, Schaller RD, Plain J, Vial A, Sun XW, Bachelot R,
Two-color single hybrid plasmonic nano-emitters with real time switchable dominant emission wavelength
Nano letters, 15, 13 (2015)

Caligiuri V, De Sio L, Petti L, Capasso R, Rippa M, Maglione M G, Tabiryan N, Umeton C,

Electro-/All-Optical Light Extraction in Gold Photonic Quasi-crystals Layered with Photosensitive Liquid Crystals
ADVANCED OPTICAL MATERIALS, vol. 2, p. 950-955, ISSN: 2195-1071, doi: 10.1002/adom.201400203 (2014)

Alj D, Caputo R, Umeton C
From Cartesian to polar: a new POLICRYPS geometry for realizing circular optical diffraction gratings
OPTICS LETTERS, vol. 39, p. 6201-6204, ISSN: 0146-9592, doi: 10.1364/OL.39.006201 (2014)

Cataldi U, Caputo R, Kurylyak Y, Klein G, Chekini M, Umeton C, Buergi T,
Growing gold nanoparticles on a flexible substrate to enable simple mechanical control of their plasmonic coupling
JOURNAL OF MATERIALS CHEMISTRY. C, vol. 2, p. 7927-7933, ISSN: 2050-7526, doi: 10.1039/c4tc01607f (2014)

De Sio L, Caligiuri V, Umeton C
Tuneable broadband optical filter based on soft-composite materials
JOURNAL OF OPTICS, vol. 16, ISSN: 2040-8978, doi: 10.1088/2040-8978/16/6/065703 (2014)

L. De Sio and N. Tabiryan
Polymer liquid crystal/polymer composite systems containing self-aligning liquid crystals
J. Polym. Sci., Part B: Polym. Phys., 52, 158 (2014)

L. De Sio, S. Serak, N. Tabiryan, T. Bunning
Nanosecond switching of photo-responsive liquid crystal diffraction gratings
J. Mater. Chem. C, 2, 3532 (2014)

L. De Sio, N. Tabiryan, T. Bunning
Spontaneous radial liquid crystals alignment on curved polymeric surfaces
Applied Physics Letters, 104, 221112 (2014)

De Sio Luciano, Umeton C, Placido Tiziana, Tamborra Michela, Comparelli Roberto, Serak Svetlana, Tabiryan Nelson, Klein Gerard, Cunningham Alastair, Buergi Thomas, Bunning Timothy
Breakthrough in all-optical plasmonics and photonics
ABSTRACTS OF PAPERS - AMERICAN CHEMICAL SOCIETY, vol. 245, ISSN: 0065-7727 (2013)

De Sio Luciano, Tabiryan Nelson, Bunning Timothy, Kimball Brian R., Umeton C
Dynamic Photonic Materials Based on Liquid Crystals
PROGRESS IN OPTICS, vol. 58, p. 1-64, ISSN: 0079-6638, doi: 10.1016/B978-0-444-62644-8.00001-7 (2013)

Romito Marilisa, De Sio Luciano, Vasdekis Andreas E., Umeton C
Optofluidic Microstructures Containing Liquid Crystals
MOLECULAR CRYSTALS AND LIQUID CRYSTALS, vol. 576, p. 135-140, ISSN: 1542-1406, doi: 10.1080/15421406.2013.789716 (2013)

Palermo, G, De Sio, L, Caputo, R, Umeton C, Bartolino, R
Liquid crystals order in polymeric microchannels

In: Liquid Crystalline Polymers. vol. 2, p. 1-14, ISBN: 978-331920270-9, doi: 10.1007/978-3-319-20270-9_1 (2015)

Pezzi, L, Palermo, G, Umeton C
Plasmonics: A theoretical background
In: Active Plasmonic Nanomaterials . vol. 1, p. 1-32, ISBN: 978-981461301-9 (2015).

ORGANIZATION OF WORKSHOPS AND CONFERENCES

11th Mediterranean Workshop and Topical Meeting "Novel Optical Materials and Applications", Cetraro (Italy), 10-15 Giugno 2013, Chairman: Cesare Umeton

"From Life to Life through new materials and plasmonics",
Roma, Accademia dei Lincei, 23 Giugno 2014, Chairman: Roberto Bartolino

12th Mediterranean Workshop and Topical Meeting "Novel Optical Materials and Applications", Cetraro (Italy), 7-13 Giugno 2015, Chairman: Cesare Umeton

"I papiri di Ercolano tra scienza e filosofia"
Roma, Accademia dei Lincei, 25 ottobre 2016, Chairman: Roberto Bartolino

EDITORSHIPS

R. Bartolino: RENDICONTI LINCEI-SCIENZE FISICHE E NATURALI AUG 2015
Volume 26 volume special, atti del convegno " From Life to Life through new materials and plasmonics "

CONTRIBUTIONS TO INTERNATIONAL CONFERENCES

P. Pagliusi, A. Aprile, E. Dalcanale,
"Probing receptor architectures and molecular recognition at interfaces by sum-frequency vibrational spectroscopy"
Materials 2016 Italian National Conference on Materials Science and Technology, Aci Castello – Catania (Italy), Dec. 12-16, 2016

Cipparrone G., Hernandez R. J., Mazzulla A., Provenzano C., Pagliusi P., Bartolino R.,
"Chiral Optomechanics" (Invited)
102° Congresso Nazionale della Società Italiana di Fisica, Padova (Italy), Sept. 26-30, 2016

A. Mazzulla, P. Pagliusi, C. Provenzano, D. Kasyanyuk, Yu. Reznikov, M. Giocondo, G. Cipparrone,
"Self-assembling and manipulation of nanoparticles in topological defects" (Invited)
8th Japanese-Italian Liquid Crystal Workshop JILCW 2016, Kyoto (Japan), July 5-7, 2016

D. Kasyanyuk, C. Provenzano, A. Mazzulla, P. Pagliusi, Yu. Reznikov, G. Cipparrone,
"Manipulation of nanoparticles in topological defects"
3rd Italian-Brazilian Workshop on Liquid Crystals and 12th National Conference of SICL, Portonovo (Italy), June 20-23, 2016

A.Aprile, E. Dalcanale, P. Pagliusi
"Nonlinear optical probing of molecular architectures and host-guest complexation at the interfaces"

Cost Action MP1205 “Advances in Optofluidics: Integration of Optical Control and Photonics with Microfluidics”, MC and WG Meeting, Center for Nano Science and Technology of IIT@PoliMi (Italy), Oct. 19-20, 2015.

R. J. Hernandez, A. Mazzulla, P. Pagliusi, C. Provenzano, M. G. Donato, O. Maragò, D. Kasyanyuk, Yu. Reznikov, G. Cipparrone,
“Chiral optofluidics” (Invited)
FisMat2015, Palermo (Italy) Sept. 28 – Oct. 2, 2015

R. J. Hernandez, A. Mazzulla, P. Pagliusi, C. Provenzano, M.G. Donato, O. Marago, D. Kasyanyuk, Yu. Reznikov, G. Cipparrone,
“Chiral optofluidics” (Invited)
36th PIERS Progress In Electromagnetics Research Symposium 2015, Prague (Czech Republic), July 6-9, 2015

A.Aprile, E. Dalcanale, P. Pagliusi,
“Nonlinear optical probing of receptor architectures and molecular recognition at the solid-air interface for chemical sensing”
12th Mediterranean Workshop and Topical Meeting "Novel Optical Materials and Applications" NOMA 2015, Cetraro (Italy), Jun. 7-13, 2015

A.Aprile, E. Dalcanale, P. Pagliusi,
“Probing supramolecular receptor architectures at the solid-air interface”
International Workshop on Sum Frequency Spectroscopy, Wiesbaden Naurod (Germany), March. 30 – Apr. 1, 2015

M. G. Donato, J. Hernandez, A. Mazzulla, C. Provenzano, R. Saija, M.A. Iati, A. Magazzù, P. Pagliusi,, R. Bartolino, P. G. Gucciardi, O. M. Maragò and G. Cipparrone,
“Polarization dependent optical trapping of chiral microresonators”
10th International Conference Series on Laser-light and Interaction with Particles, Marseille (France), Aug. 25-29, 2014

A. Mazzulla, C. Provenzano, P. Pagliusi, G. Cipparrone,
“Circular dichroism spectrometer based on a diffractive liquid crystal cell” (Invited)
Workshop Norte-Paranaese de Fluidos Complexos, Maringà (Brazil), Oct. 8, 2013

General Meeting, Cetraro (IT), Jun. 10-15, 2013
“Chiral Self-assembled solid microparticles”
“Shaping supramolecular chirality in smart polymers with 2D Polarization Light Patterns”

Ferdinanda Annesi, Alfredo Pane, Luciano De Sio, Giulio Caracciolo, Tiziana Placido, Daniela Pozzi, Roberto Comparelli, Maria Lucia Curri, Angela Agostiano, Nelson Tabirian, Roberto Bartolino
“PLASMONICS MEETS BIOLOGY”
Kick off meeting IMIP - Lecce - 12-14 Marzo 2015

Alfredo Pane, Ferdinanda Annesi, Luciano De Sio, Giulio Caracciolo, Tiziana Placido, Daniela Pozzi, Roberto Comparelli, Maria Lucia Curri, Lorenzo Florese, Angela Agostiano, Nelson Tabirian, Roberto Bartolino. “PLASMONICS MEETS BIOLOGY”
NOMA 2015 Novel Optical Materials and Applications - Cetraro - Italy, June 2015

F. Annesi, A. Qualtieri, A. Pane, L. Florese, L. De Sio, G. Caracciolo, T. Placido, D. Pozzi, R. Comparelli, M. L. Curri, A.Agostiniano, Roberto Bartolino
"Targeting cancer cells with fluorescently labeled gold nanorods/dna complexes"
International Conference on Plasmonics and NanoOptics - Cetraro (CS) - Italy - 13 - 17 June 2016

A. Golemme, U. K. Pandey, R. Termine, E. Bruno, M. P. De Santo
"Surface Rubbing: a Simple and Effective Method for Enhancing the Efficiency of organic Photovoltaic Devices"
IX Convegno Nazionale INSTM, Bari, June 30 – July 3, 2013

L. Angiolini, T. Benelli, L. Giorgini, L. Mazzocchetti, A. Golemme, R. Termine
"A Novel Multicomponent Polymer Containing Side-Chain Optically Active Azocarbazole Moieties"
European Polymer Congress, Pisa, 16-21 Giugno 2013

A. Golemme, R. Termine, U. K. Pandey, E. Bruno, M. P. De Santo
"Surface Charging by Rubbing and its Effect on the Efficiency of Organic BHJ Cells"
Hybrid and Organic Photovoltaics HOPV14, Losanna (CH), 11-14 Maggio 2014

R. Lento, S. V. Siprova, A. Ionescu, R. Termine, N. A. Kudriaskov, A. V. Nezhdanov, A. I. Mashin, A. Golemme, N. Godbert
"Electropolymerized Highly Photoconductive Thin Films of Cyclometallated Complexes"
XIX International symposium on Nanophysics and Nanoelectronics,10-14 March 2015, Nizhny Novgorod, Russia.

S. Siprova, J. T.-W. Wang, A. Golemme, H. J. Snaith
"Combined vapour/solution deposition of perovskite thin-films for efficient solar cells"
International Conference on Hybrid and Organic Photovoltaics HOPV 2015, Rome, May 10-13, 2015.

A. Ionescu, R. Lento, R. Termine, M. Ghedini, A. Golemme, N. Godbert
"Electropolymerized near-IR electrochromic and highly photoconductive thin films of cyclometallated complexes"
X Convegno Nazionale INSTM, Favignana (TP, Italy) June 28 – July 1, 2015.

R. Lento, V. Caligiuri, R. Termine, A. De Luca, A. Golemme
"Efficiency enhancement of solar cells via organo/metallic hyberbolic metastructures"
Hybrid and Organic PhotoVoltaics HOPV 2016, Swansea (UK), June 28 – July 1, 2016.

R. Lento, V. Caligiuri, R. Termine, A. De Luca, A. Golemme
"Towards Plasmonic MetaMaterials Structures for Efficiency Enhancement of Solar Cells"
II International Workshop Nanoplasm 2016: "New Frontiers In Plasmonics And Nano-Optics", Cetraro (Italy), June 13-17, 2016

F. Vita, M. Laus, N. Scaramuzza, E. Scharrer, E. T. Samulski, O. Francescangeli
"Unconventional Properties in Bent-Core Nematics Exhibiting Room Temperature Cybotactic Order"
25th International Liquid Crystal Conference Dublin (Ireland) 2014, 29th June - 4th July

Yordan G. Marinov, Georgi B. Hadjichristov, Alexander G. Petrov, Emanuela Bruno, Lucia Marino, Nicola Scaramuzza
"Electro-optics of nematic/gold nanoparticles composites: the effect from dopants"
25th International Liquid Crystal Conference. Dublin (Ireland) 2014, 29th June - 4th July

Hari Krishna Koduru and Nicola Scaramuzza
“Investigations on Structural, Optical and Dielectric properties of Cold Plasma Polymerized Polypyrrole Thin films for Soft Matter Applications”
INERA Conference – Light in Nanoscience and Nanotechnology. Hissar (Bulgaria) 2015, October 20-22

G. B. Hadjichristov, Y. G. Marinov, A. G. Petrov, L. Marino and N. Scaramuzza “Electrical and Electro-Optical Characterization of 5CB Nematic Liquid Crystal Doped with Silver Nanoparticles”
INERA Conference – Light in Nanoscience and Nanotechnology. Hissar (Bulgaria) 2015, October 20-22

Hari Krishna Koduru, M. Iliev, T. Vlakhov, N. Scaramuzza “Investigations on Poly (ethylene oxide) (PEO) – blend based solid polymer electrolytes for sodium batteries” INERA CONFERENCE (organized in the frame of the FP7 Project REGPOT 316309) – Vapor Phase Technologies for Metal Oxide and Carbon Nanostructures July 6 –8, 2016 Velingrad, Bulgaria

Y. G. Marinov, M. P. Marinov, G. B. Hadjichristov, S. K. Prasad, L. Marino,N. Scaramuzza
“Dielectric study of azo-doped aerosil/7CB filled nematic upon UV light” INERA Workshop - Membrane and Liquid Crystal Nanostructures (MELINA) September 4 – 5, 2016 Varna, Bulgaria –

Hari Krishna Koduru, M. Iliev, Y. Marinov, D. Karashanova, N. Scaramuzza
“Synergetic effect of TiO2 nanofillers and NaIO4 additives on conductivity and dielectric properties of PEO/PVP nanocomposite electrolytes for electrochemical cell applications”

INERA Workshop - Membrane and Liquid Crystal Nanostructures (MELINA) September 4 – 5, 2016 Varna, Bulgaria

PROJECTS

COST Action MP1205, ADVANCES IN OPTOFLUIDICS: INTEGRATION OF OPTICAL CONTROL AND PHOTONICS WITH MICROFLUIDICS, Chair Gabriella Cipparrone.
Progetto di Grande Rilevanza Italia-Messico 2011-2013: Strategie di manipolazione ottica della materia soffice mediante pinze olografiche con gradiente di polarizzazione.
“EXECUTIVE PROGRAMME FOR SCIENTIFIC AND TECHNOLOGICAL CO-OPERATION BETWEEN THE ITALIAN REPUBLIC AND ROMANIA FOR THE YEARS 2013-2014: Ordered Soft Materials: Electrical, optical and dielectric spectroscopy characterization

FP7-REGPOT-2012-2013-1 project “Research and Innovation Capacity Strengthening of ISSP-BAS in Multifunctional Nanostructures” (Acronym INERA)

Project ”Proof of Concept Network” (PoCN) del Consorzio per l'AREA di Ricerca Scientifica e Tecnologica di Trieste, “Nanocompositi basati su materiali morbidi (soft matter) ottenuti mediante la polimerizzazione al plasma freddo”, 2015

8. NUCLEAR AND SUBNUCLEAR PHYSICS

8.1 ATLAS EXPERIMENT AT THE LHC PROTON-PROTON COLLIDER (Geneva – Switzerland)

Physicists: V.M.M Cairo
M. Del Gaudio
A. Mastroberardino
A. Milazzo
A. Policicchio
D. Salvatore
M. Schioppa
G. Susinno

Technicians: V. Romano, P. Turco

International collaboration

Nature has given us more than one elementary particle (6 leptons, 6 quarks and the carriers of the four fundamental interactions), whose masses range in a wide interval of values from the mass-less photon to the top quark mass, M_t=170 GeV/c^2. The mechanism that determines the particle masses is still unknown and many experiments with particle accelerator have been undertaken to give an insight into it and explain the mass origin.
In 1964 Peter Higgs first proposed a clever solution to this puzzle: an undetectable field, similar to the electromagnetic one, permeates the whole space. As particles move in space they travel through this field, and interaction with this field allows them to acquire their masses. This is similar to the action of viscous forces felt by particles moving through any thick liquid: the stronger the interaction of the particles with the field, the bigger the mass they seem to have. We know from quantum theory that fields have particles associated with them, so a Higgs boson should be associated to the Higgs field. Up to now no one has ever observed the Higgs boson in an experiment to confirm the theory. Finding this particle would give an insight into why particles have certain mass, and help to develop subsequent physics. The technical problem is that we do not know the mass of the Higgs boson itself, which makes it more difficult to identify. Physicists have to look for it by systematically searching a range of mass within which it is predicted to exist. The yet unexplored range is accessible using the Large Hadron Collider (LHC).
On 4 July 2012 the ATLAS and CMS Collaborations jointly announced the independent discovery of a previously unknown neutral boson, compatible with the Higgs Boson, with a mass in the range 125-127 GeV/c^2. The latest ATLAS publication (Phys. Lett. B716 (2012) 1-29) reports a discovery significance of 1 in 588 million chance of being due to random background effects and a mass value of 126.0 ± 0.4 (stat) ± 0.4 (sys) GeV/c^2 . The new particle appears to be fully compatible with the production and decay properties of the Standard Model Higgs Boson.
This collider provides 10 times higher center of mass energy and 100 times higher p-p collision rates than Tevatron collider and is fully operational since November 2009. This opens up a new frontier of physics and the LHC experiments, ATLAS, CMS, ALICE and LHCb, are ready to explore this great potential.
ATLAS is a general-purpose experiment. Designed to see a wide range of particles and phenomena produced in LHC collisions, it involves approximately 2500 physicists and engineers from some 35 countries. These scientists use the data collected from the complex detectors to search for new phenomena, including the Higgs boson, super-symmetry and extra dimensions. They also measure the properties of previously-discovered quarks and bosons with unprecedented precision, and are on the

lookout for completely new, unpredicted phenomena. The basic design concept to achieve these goals includes three detector systems (fig. 3):

11. the *inner tracker***,** with semiconductor pixel and strip detectors for very high accuracy measurements of the charged particle trajectories, followed by straw tube detectors giving independent electron identification. The tracker is confined to a cylinder 6.8 m long and with a radius of 1.1 m in a 2 T magnetic field, provided by a superconductive solenoid;
12. the *calorimeter***,** with an inner cylinder in highly granular liquid argon technology with Pb absorber, followed at large radius by an iron-tile scintillator calorimeter providing good resolution in a very cost-effective manner;
13. the high precision standalone *muon spectrometer*. Its conceptual layout is based on the magnetic deflection of muon track in a system of three large superconducting air-core toroid magnets instrumented with separate-function trigger and high-precision tracking chambers.

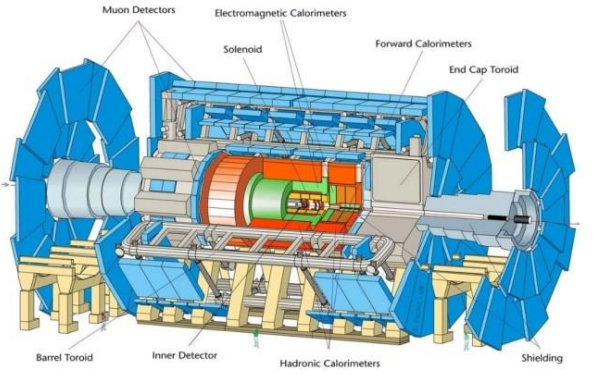

Fig. 3 Overview of the ATLAS detector.

The researchers of the experimental high energy physics (HEP) group of UNICAL have been strongly involved in various aspects of the design, construction, installation and test of the muon spectrometer since 1994. During this period the contribution from many undergraduate, graduate and PhD students and postdoc researchers has been substantial to this end.

From 2013 up to now the Unical HEP group gave a major contribution to the following ATLAS activities:

14. **Maintenance and improvement task force** of the muon precision chambers at CERN. This group of expert physicists take care of the whole detector performance, overlooking the functionality of gas, readout, alignment, data control, high and low-voltage systems.

15. **Development and maintenance of the Gnam package**, the low-level data acquisition software for the ATLAS sub-detector online monitoring. This tool has been developed since 2004 for the combined test beam of a slice of the ATLAS Muon Spectrometer. It was highly appreciated and widely used during the installation and commissioning phase of the spectrometer and has been inserted into the official Trigger and Data Acquisition software of the ATLAS experiment. At the moment most of the ATLAS sub-detectors use Gnam online histograms to evaluate the quality of acquired data. In fact it is capable to promptly spot if sub-detectors are not working properly. It decodes the raw data coming from sub-detectors and shows the relevant quantities through histograms. As an example, it reveals dead or noisy channels, which may affect the data taking itself and subsequent reconstruction and pattern recognition processes.

16. **Study of the W and Z bosons production**. This study constitutes an important part of the ATLAS physics program at the LHC. The measurement of the their large production cross sections, that are known at the next-to-next-to-leading order (NNLO) in QCD, will allow to perform stringent tests of the predictions of the Standard Model and to study the properties of the gauge bosons in a hitherto unexplored kinematics region. After the re-start of the LHC in June 2015 and with the increasing amount of data taken during the year, the production cross sections of the W and Z bosons were measured with proton–proton collision data corresponding to an integrated luminosity of 81 pb^{-1}, collected at the centre-of-mass energy of 13 TeV. The delivered peak instantaneous luminosity was $L = 1.7 \times 10^{33}$ cm^{-1} s^{-1} and the mean number of pp interactions per bunch crossing (hard scattering and pile-up events) was $<\mu> = 19$. The systematic uncertainty arising from the pile-up modeling as well as from the multi-jet background is the largest systematics in the measurement of the W-boson production cross-section. Within this study, the group gave a major contribution to both measurements. Since the beginning of 2016, we are involved in the W-boson produced measurement in association with b-jets, which is based on the full 2015-2016 data set corresponding roughly to 40 fb^{-1}. The cross section of this process at the centre of mass energy of 13 TeV is almost twice as big as the cross section at 7 TeV, but the top-quark production cross section, which represents one of the main background sources, is four times larger. In this search our studies had the crucial role of minimizing the top-background contribution. In addition, thanks to the expertise acquired in our extensive participation to the ATLAS Inner Detector Group activities, we were responsible of a challenging simulation-based method to calibrate the light-flavour jets which are mis-tagged as b-jets, usually evaluated by means of data-driven techniques. The simulation-based approach consists in evaluating the systematics on tracks (impact parameter resolution, material uncertainties, etc…), by means of the modified track collection in the b-tagging algorithms. The results of these studies are now part of the recommended benchmark values to be applied as scale factors in any analysis which uses light-flavour jets.

17. **ID Tracking and Material Studies**. The ATLAS experiment was consolidated and improved in the period 2013-2014, during the first long shutdown of the LHC, to meet the increasingly challenging experimental conditions. A fourth pixel layer, the Insertable B-Layer, was installed in the Inner Detector together with a new thinner beam pipe, at a radius of 33 mm. The Pixel Services, located between the Pixel and SCT detectors, were also modified. The tracking algorithms needed to be updated accordingly and this was one of the main important tasks in the context of the ATLAS software: the track reconstruction performance and the optimization procedures of analysis programs and strategies needed to be carefully studied. We improved the algorithm to track particles in the upgraded ATLAS Inner Detector with a leading contribution to the implementation of a more robust reconstruction of low-momentum tracks (down to a transverse momentum of 100 MeV) with respect to Run 1. The LHC resumed operations in June 2015 for what would become a very successful RUN 2. The 151 μb-1 of data collected at 13 TeV with a particular configuration of the accelerator (low beam currents and reduced focusing to give a mean number of interactions per bunch crossing of 0.005) were used to study the Inner Detector Tracking Performance and Material Distribution as well as to measure Charged-Particle Multiplicities (or Minimum Bias Events). The performance of the ATLAS track reconstruction algorithm was checked in data and compared to Monte Carlo simulations, as extensively described in. The material distribution in the revised ID has been thoroughly studied, which led to an improvement of the geometry model description in the detector simulation programs as well as to a significant reduction of the systematic uncertainty on the estimate of the track reconstruction efficiency, which constitutes the main ingredient of the Charged-Particle Multiplicity measurements. The material distribution in the forward pseudorapidity region of the Run 2 ATLAS Inner Detector was studied in detail with the Track-Extension Efficiency method, which

measures the stopping rate of charged hadrons in the material between the Pixel and the SCT detectors. For the first time in ATLAS, this measurement and the related uncertainties were explicitly expressed in terms of nuclear interaction lengths by using a complex calibration procedure. It was found that in the Inner Detector geometry model used as a baseline in the 2015 ATLAS simulation, up to (3.69±0.86)% of nuclear interaction lengths were missing in some pseudorapidity regions. This corresponds to roughly 10% of the pixel services material in the same region. These studies, conducted by Drs. Valentina Cairo, were published and are a reference for the subject along with other two methods used to perform studies of the central pixel region, namely secondary vertices from Hadronic Interactions and Photon Conversions.

18. **Soft QCD.** The main aim of collecting minimum bias data at 13 TeV was the analysis of Charged-Particle distributions. Studies were performed for three different fiducial phase spaces, which include the usual ATLAS acceptance, by requiring events with at least one charged-particle with $|\eta| < 2.5$ and $p_T > 500$ MeV together with a measurement performed in the low transverse momentum regime by requiring events with at least two charged-particles with $|\eta| < 2.5$ and $pT > 100$ MeV and an additional measurement performed in a phase space common to the ATLAS, CMS and ALICE experiments, in which events with at least 1 charged-particle with $|\eta| < 0.8$ and $pT > 500$ MeV are selected. It must be stressed that the low-p_T phase space is always very challenging owing to the effect of multiple scattering which dominates that regime and due to the imprecise knowledge of the material distribution in the Inner Detector which constitutes the main source of systematic uncertainty. The methodology used in the 13 TeV analyses is similar to that used at lower centre-of-mass energies in ATLAS. The events collected correspond to minimum-bias datasets based on inelastic pp interactions. The data were recorded during special fills with low beam currents and reduced focusing to give a mean number of interactions per bunch crossing below 0.005. This procedure guarantees that the contribution from pile-up in these analyses is negligible. The measurements use tracks from primary charged-particles, corrected for detector effects to the particle level, and presented as inclusive distributions in a fiducial phase space region. Four quantities are measured, such as $\frac{1}{N_{evt}} \cdot \frac{dN_{ch}}{d\eta}$; $\frac{1}{N_{evt}} \cdot \frac{1}{2\pi p_T} \cdot \frac{d^2N_{ch}}{d\eta dp_T}$ and $\frac{1}{N_{evt}} \cdot \frac{dN_{ev}}{dn_{ch}}$ as well as the mean $p_T < p_T >$ of all primary charged-particles versus n_{ch} is the number of primary charged-particles in an event, N_{ev} is the number of events with $n_{ch} > 1$, and N_{ch} is the total number of primary charged-particles in the data sample. A data-driven correction to the simulation-based tracking efficiency in the pseudorapidity distribution of charged-particles with $p_T > 500$ MeV was derived by using the results of the Track-Extension Efficiency. This allowed for a reduction of the systematic uncertainties to the Charged-Particle Multiplicity measurement by more than 50% with respect to earlier analyses in the corresponding phase space. In addition, differently than in previous analyses, strange baryons were removed from the definition of primary charged-particles because of the low reconstruction efficiency of their decay products and owing to large variations in the predicted rates, which would lead to a significant model dependence of the results presented here. To have a measurement, which is as much model independent as possible, is of utmost importance in order to allow Monte Carlo developers to focus on unbiased parameters to be used in the tuning process. The mean number of primary charged-particles in the central region is computed by averaging over $|\eta| < 0.2$ to be 2.874 ± 0.001 (stat)±0.033 (syst). This measurement is then corrected for the contribution from strange baryons and compared to previous measurements at different centre-of-mass energy values together with the MC predictions, which show clear differences with respect to the measured distributions. These results have been already used by the ATLAS Collaboration in order to produce a new tune of the Pythia 8 Monte Carlo Event Generator, referred to as Pythia 8 - A3.

1. **Searches for Long-Lived Neutral Particles (LLNP).** LLNPs arise in several theories, including SUSY, Hidden Sector models, Inelastic Dark Matter models, etc., explaining the open questions in modern particle physics. Particularly interesting are the models predicting the Higgs boson decaying to a new sector of particles which finally produce displaced vertices or lepton-jets. Even if the observation of the new boson at the LHC is compatible with the expected production and decay of the Standard Model Higgs boson at the 125 GeV mass, room is still available for non-SM decays. Testing the SM Higgs hypothesis is thus of utmost importance. To this end two effects may be considered: (i) additional resonances which arise in an extended Higgs sector found in many extensions of the SM, or (ii) rare exotics decays of the Higgs boson acting as a portal to new physics sectors at the O(100GeV) scale. The searches for LLNP decays in the LHC collisions cover both of the above described aspects, deriving constraints on additional Higgs-like bosons, as well as placing bounds on the branching ratio of the discovered 125 GeV resonance into a new physics sector. Particles with long decay paths and many particle decay final states represent a challenge both for the trigger and for the reconstruction capabilities of the ATLAS apparatus. A big effort has started in 2008 and it is still continuing to adapt the ATLAS detector to searches, not accounted at the moment of its design, exploring the detector capabilities beyond the range where it was originally designed to work. Our group is responsible of the maintenance (after the development) of the signature-based triggers for the selection of events with displaced vertices and lepton-jets, otherwise rejected because of a trigger system originally designed to select objects originating at the pp interaction point. These triggers have been central to the searches in the Run1 8 TeV LHC data for evidence of a Higgs boson decaying to a pair of displaced vertices or lepton-jets. No evidence for signals have been found and limits on the cross section for this kind of signal are set as a function of the long-lived particle lifetime. A lepton-jet Monte Carlo generator has been developed in order to determine the efficiency to reconstruct lepton-jets as a function of kinematic variables (p_T, eta and phi) and provided the results in a form useful to other analyses. The results of the lepton-jet search based on the full 13 TeV statistics collected during 2015 and 2016 are expected for the summer 2017 conferences. The new analysis will be extended to include a search for a mono lepton-jet object with interpretation in Inelastic Dark Matter, Drell-Yan and W/Z associated lepton-jet production models for which a detailed description and understanding of the SM background is required. An ATLAS note presented the first 13 TeV Run2 result based on 3.4/fb at the ICHEP 2016 conference in Chicago. The research group has the direct responsibility on this analysis. In these three years the group has produced interesting published results: "Search for long-lived neutral particles decaying into lepton jets in proton–proton collisions at $\sqrt{s}$ = 13 TeV with the ATLAS detector", G. Aad et al. [ATLAS Collaboration], ATLAS-CONF-2016-042 "Search for long-lived neutral particles decaying into lepton jets in proton-proton collisions at $\sqrt{s}$ = 8 TeV with the ATLAS detector", G. Aad et al. [ATLAS Collabo- ration], JHEP 1411 (2014) 088.

19. **Measurement of b-quark production cross section**. The measurement of jets containing a b-hadron (b-jets) produced in proton–proton collisions at the Large Hadron Collider provides an important test of perturbative quantum chromodynamics (pQCD). Calculations of the b-quark production cross section have been performed at next-to-leading order of alpha_s (NLO) in pQCD. These calculations can be combined with different parton-shower and hadronisation models to generate simulated events, which can be compared to data. Measurements performed previously by ATLAS, CMS and TeVatron collaborations agree with NLO predictions for well-separated b-jets, although b-jets with large transverse momenta in the central regions are not well described by simulations. Some results also agree with the NLO predictions; though small deviations are present at large transverse momenta in events with a b-jet and light-flavour jet (jet generated by a light quark). The CMS measurement found that in the phase-space region of small angular separation between the b-jets, there are substantial differences between data and NLO predictions, and among the NLO predictions themselves. At the ATLAS experiment, cross

sections for bb-pair production have been measured using the 2010 dataset, focusing on the case where the b-jets were the leading and sub-leading jets in the event (flavour creation - FCR) and thus suppressing higher-order production mechanisms (flavour excitation – FEX and gluon splitting - GSP). This measurement, based on 2011 dataset, aims to extend the previous measurement of bb-production to a larger kinematic range and to include all event topologies. Differential cross-sections are measured as a function of the angle between the jets, the dijet mass, momentum, boost and rapidity.

20. **Phase 1 Muon Spectrometer upgrade**. In order to cope with the increased hit rate of up to 15kHz/cm^2 in the innermost station of the muon endcap spectrometer, the currently used precision detectors will be replaced by resistive strip Micromegas. In the New Small Wheel the detectors will be arranged in pairs of trapezoidal shaped quadruplets. Each Micromegas quadruplet is made of 5 panels with aluminium honeycomb core sandwiched by printed circuit boards and 4 micro-meshes, for a total of 4 detection layers. To achieve 15% transverse momentum resolution for 1 TeV muons, each active plane has to achieve a spatial resolution better than 100um and challenging construction accuracy with an alignment of the readout elements (300um wide strip) at the level of 30um along the precision coordinate and 80um orthogonally to the plane. The Cosenza group has the responsibility of the completion of the drift panels of the SM1 modules. Moreover the Cosenza group has developed the procedure and the tooling for the planarity of the drift panel measurement, for the gas tightness of the panels and for the gas mixture distribution for the cosmic ray test stand and for the beam test area at CERN and it is contributing to the quality control of the Printed Circuit Boards. Furthermore, the group worked on the integration and development of the offline simulation programs, including also validation and physics simulation activities, for the ATLAS New Small Wheel. The aim of this work was the implementation of the latest chamber layout (based on Micro Mesh Gas Structure, MicroMeGaS, and small Thin Gap Chambers, sTGC, technologies), which implied a different geometry to be described in simulation. These new features needed to be validated and complementary validation procedures have been studied in order to check the results. An algorithm for a daily automatic validation (Run Time Tester, RTT) of the New Small Wheel has been implemented as well.

8. **Trigger system.** The LHC is designed with a maximum bunch crossing rate of 40 MHz. The ATLAS trigger system consists of a hardware Level-1 and a software-based high level trigger that reduces the bunch-crossing rate to an average recording rate of a 200-400 Hz, based on the distinctive final states of the physics processes to be studied in pp collisions. The first hardware trigger level receives its inputs from the Calorimeter, Muon and additional forward detectors and provides a decision with a latency of less than 2.5 μs and it reduces the rate to a maximum of 75 kHz. When an event is accepted by Level-1, data from each detector is transferred to the high level software trigger. Offline-like algorithms for identifying candidate objects including tracking, calorimeter clustering algorithms and muon reconstruction, reduce the rate to 200-400 Hz with an average processing time of ∼4 s/event. A high-performance trigger is essential to guarantee a high discovery potential of the LHC. Several activities are carried out within the ATLAS trigger group and some of these are still continuing. They are summarized in the list below.
    a. The development and the maintenance of the trigger algorithms for the selection of events with displaced vertices and tracks. In particular, a set of three trigger algorithms has been designed to select displaced objets otherwise rejected because of a trigger system originally designed to select objets originating at the pp interaction point. By 2010 such dedicated triggers were included in the ATLAS trigger menu. The design and the performance of these triggers are described in ATL-PHYS-PUB-2009-082 and JINST 8 (2013) P07015.
    b. Optimization, development and maintenance of the high level trigger algorithms for the selection of events with close-by muons and displaced muons using only information from the muon spectrometer (2011-present). Such triggers are mainly used for the selection of events

with the production of clusters of collimated muons from the decay of new light particles (dark photons), possibly long-lived, and for exotics analyses as the τ decay to three muons. I am also in charge of the evaluation of the systematic uncertainty of the trigger efficiency using Tag&Probe method based on J/Ψ → μμ and Z → μμ decays. A description of such triggers and of the method for systematic evaluation can be found in e.g. JHEP 1411 (2014) 088 and Eur. Phys. J. C75 (2015) 120.

c. Co-responsibility of the high level muon trigger validation (2009-present). The objective of the trigger validation is to ensure that the trigger software runs as expected and produces the expected results. In particular the monitoring of the trigger performance is realized using a Tag&Probe method based on J/Ψ → μμ and Z → μμ data and Monte Carlo simulations. The performance of the muon trigger system are described in e.g. Eur. Phys. J. C75 (2015) 120 and Eur. Phys. J. C72 (2012) 1849.
d. Central trigger validation shifts (2009-present). The aim of the central validation is to ensure that the trigger part of a ATLAS software release is fully functional; if a package fails, the shifter has to identify the problem and to notify the developer via a bug tracker. It is requested to have a good knowledge of the ATLAS trigger software and of the status of the trigger system development.

8.2 HYDE: Hybrid Detectors for neutrons, INFN CSN5 project

Physicists: A. Mastroberardino
A. Policicchio
D. Salvatore
M. Schioppa

The HYDE project, financed by INFN CSN5 for the years 2012-2014, involves the groups of Legnaro, Trento and Cosenza. The Cosenza Unit joined the Collaboration in 2013. The aim of this experiment was the development of a hybrid compact neutron detector, by coupling a 3D silicon detector with a recently produced polysiloxane based scintillator, deposited into the 3D detector cavities. This system combines the detection of neutron reaction products, by means of the 3D sensor system, with the detection of the light produced by the polysiloxanic scintillator by means of a photodetector. The Cosenza Unit was responsible of the Geant4 simulation of the detector response to thermal and fast neutrons. In particular, geometry optimization studies were performed and determined the adjustment of the size of the cavities and the gap in between them, so as to maximize the neutron detection efficiency.

8.3 ATLAS Inner Tracker (ITk) Project AT THE LHC PROTON-PROTON COLLIDER (Geneva – Switzerland)

Physicists: A. Mastroberardino
A. Policicchio
D. Salvatore
M. Schioppa

Over the next decade the Large Hadron Collider at CERN will undergo a series of upgrades, increasing both the energy and the luminosity, culminating in the Phase-II upgrade that will deliver an unprecedented instantaneous luminosity of 5×10^{34} cm^{-1} s^{-1} at an energy of 14 TeV. This will present a unique opportunity to substantially extend the mass reach in searches for many signatures of new physics, in several cases well into the multi-TeV region, and to significantly extend the study of

the properties of the Higgs boson. The ATLAS detector will be extensively changed to meet the challenges of this upgrade. In particular, the current Inner Tracker will need to be replaced with a new all silicon Inner Tracker (ITK) to maintain tracking performance in the high occupancy environment and to cope with the increase of approximately a factor of ten in the total radiation fluence. An intense R&D program started in 2008 and is currently underway at CERN to develop the new sensor technologies meeting this challenge. The Cosenza group is involved in the study and development of a new generation of micro- machined sensors, the 3D silicon sensors, developed by Fondazione Bruno Kessler (Trento, Italy), with electrodes etched inside the silicon bulk rather than on the wafer's surface. This peculiar geometrical structure makes such sensors extremely radiation hard and interesting candidates for the highly exposed Pixel Detector levels in the LHC upgrades. 3D silicon sensors populate 25% of the total sensing area of the Insertable B-Layer (IBL), a fourth pixel layer added to the present ATLAS Pixel Detector at CERN, during the long shut down of the LHC in 2013, to improve the primary vertex reconstruction for the phase I runs. The IBL served as a technological advance towards the upgrade of the Pixel Detector in high luminosity runs. Within the IBL project, the group participated in the development of the online monitoring software for sensor performance tests.

8.4 ACTIVE: ATLAS and CMS Towards InnoVative pixEls, INFN-CSN5 call

Physicists: A. Mastroberardino (Local Coordinator)
A. Policicchio
D. Salvatore
M. Schioppa

ACTIVE (Atlas and Cms Towards InnovatiVe pixEls) is a joint proposal, established in 2015, for R&D activities on several core technologies for future pixel detectors. The aim is to push the technology another step forward, to fulfil the requirements of the two main experiments in the LHC phase-II upgrade (High Luminosity LHC, HL-LHC). In 2015 part of the proposal plan was redirected into the "ATLAS Pixel R&D for HL-LHC", one of the **most challenging and intensive R&D programs** aiming to meet the challenges of a 5-fold increase in collision rate foreseen for the phase II.

The proponents of the ACTIVE project have world leading expertise in the above technologies and are in partnership with two Italian firms (FBK and Selex), which have been developing for many years sensors (planar and 3D) and bump-bonding packaging with indium (developed jointly with INFN for the present ATLAS Pixel detector). The proponents also include most of the INFN institutes that have already expressed interest in the new ATLAS and CMS Phase-II trackers. This exploits the strong links between INFN researchers and international colleagues in the two experiments and fosters the synergy between the ATLAS and CMS INFN groups. The Cosenza group is among the proponents and is involved in the 3D silicon detector optimization and qualification studies for extreme radiation hardness. The ACTIVE research program is conducted in strong synergy with the AIDA-2020 project (Advanced European Infrastructures for Detectors at Accelerators), funded by the European Union's Horizon 2020 research and innovation programme **"Integrating and opening existing national and regional research infrastructures of European interest".** The AIDA-2020 project brings together the leading European infrastructures in detector development and a number of academic institutes, thus assembling the necessary expertise for the ambitious programme of work. In total, 19 countries and CERN are involved in this programme, which follows closely the priorities of the European Strategy for Particle Physics. AIDA-2020 is leading to enhanced coordination within the European detector community, leveraging EU and national resources. The project is exploring novel detector technologies and providing the particle physics community with world-class infrastructure for detector development, benefiting thousands of researchers participating in future particle physics projects, and contributing to maintaining Europe's leadership of the field.

8.5 MATHUSLA: MAssive Timing Hodoscope for Ultra Stable neutraL pArticles

Physicists: A. Policicchio, M. Schioppa
International collaboration

Lifetime is a free parameter in the models predicting long-lived neutral particles (LLNP). The only upper limit comes from the Nucleosynthesis after Big Bang (BBN): $c\tau < \sim 10^{7-8}$ m: decays of LLNP during and after BBN would have changed the variables related to BBN itself. Given the not optimal design of the LHC detectors to searches for particles with long life, the upper limit in lifetime reachable after the High Luminosity LHC phase (assuming an integrated luminosity of ~ 3 ab^{-1}) is ~ 10^3 m. LLNP with $c\tau$ near to the BBN limit would escape undetected from LHC detectors. The MAssive Timing Hodoscope for Ultra Stable neutraL pArticles (MATHUSLA) collaboration, born in 2016, is working to propose a new low-cost detector to explore the lifetime frontier. A 200 m^2 surface, 20 m height detector to be installed at the ground level over the ATLAS or the CMS detector (10% geometrical acceptance for e.g. LLNP coming from the rare decay of the Higgs boson (BR(H → LLNPs) = 10%)) with only top and bottom surfaces instrumented with a tracking system, would allow to observe tens of LLNPs decaying in the detector volume with lifetime at the BBN limit in ~ 3 ab^{-1}. The idea is to explore the possibility of using Resistive Plate Chambers (RPC) and segmented scintillators to build such a large surface detector: RPCs planes for tracking and vertex reconstruction; scintillator planes for redundant background rejection and timing. The cost is estimated to be order of magnitude lower with respect to proposed dedicated experiments and the detector could be ready for High Luminosity LHC phase. Detailed simulation studies and tests have started with the purpose to understand background sources and optimise detector geometry and space/time resolution. The first test, using a small 2.5 × 2.5 m^2 unit detector to be installed in the ATLAS hangar at Point 1, is planned for summer 2017.

The group is contributing to setting-up a Geant4 simulation of the test detector to optimize the geometry and to carry out Monte Carlo studies of the cosmic background using the CORSIKA air shower generator interfaced with Geant4.

8.6 KLOE-2 EXPERIMENT AT DAFNE E-E+ COLLIDER (National Laboratory of Frascati)

Physicists: M. Schioppa
Technician: P. Turco

International collaboration

The DAFNE collider accelerates stores electrons and positrons of 510MeV energy each to produce PHI-mesons via the reaction e^+e^- -> gamma* -> PHI. This meson is made of strange – anti-strange quarks, has 1020 MeV/c^2 mass and has the quantum numbers of the photon: $J^{PC} = 1^{--}$. It decays at rest and the final state contains mainly charged and neutral kaon pairs (branching ratio BR=49.5% and BR=34.3% respectively), RHO-PI and PI+PI-PI0 (BR=15.5%), ETA-GAMMA (BR=1.3%), ETA'-GAMMA (BR=0.00012). The neutral kaon pairs are produced in a well-defined quantum and kinematical state with negative charge parity. The kaons are monochromatic (the momentum is 127MeV/c for charged kaons and 110MeV/c for the neutral one) and are emitted back to back to be detected in an almost background free environment. With the integrated luminosity of 2.5fb-1 (2001-2006) the collider has produced 10^10 PHI-mesons and than about 10^10 kaon pairs.

The KLOE apparatus is a general purpose detector designed to study all kinds of kaon, PHI, RHO, ETA and ETA' decays emphasising tests of discrete symmetries (CP-, CPT-, T-invariance) and measurements of hadronic cross sections and tests of chiral perturbation theory.

The detector is composed of an Inner Tracker (four layers of triple GEM), close to the interaction point, surrounded by a huge (4m diameter, 4m long), transparent drift chamber with 55000 stereo wires, in 0.5 Tesla magnetic field produced by a super-conductive solenoid, in helium based gas mixture. The tracking chambers are surrounded by a lead-scintillating fibre calorimeter, $15X_0$ thick, 98% solid angle coverage with a resolution of 54ps/SQRT(E)+140ps (E in GeV) in time and 5.7%/SQRT(E) in energy.

During 2008 the INFN has approved the KLOE-2 proposal at the improved DAFNE luminosity performance. The data taking campaign (5-10fb-1) started on spring 2011.

The contribution to KLOE-2 project of the UNICAL's researcher has been focused on CCALT LYSO calorimeter performance studies using GEANT4 simulations, QCALT tile calorimeter tests with UV pulsed LED on photodiodes, tiles and fibres, cylindrical GEM inner tracker detector construction and test and the study of light boson weekly coupled with standard matter using initial state radiation events.

8.7 AIR SHOWER OBSERVATORY WITH EEE PROJECT DETECTORS ARRAY

Physicists: M. Schioppa
PhD: A. Milazzo, L. Garritano, F. Lento
Technician: P. Turco
International collaboration

The cosmic ray observation has considerably contributed to the better understanding of the laws that govern the Universe. At the same time it has also left many open questions, i.e. the origin, the acceleration mechanism and the elementary composition of the Cosmic Rays, that can be coped only with ground based experimental apparatus. In fact they represent the only experiments able to detect CR coming from galactic and extra-galactic exotic astrophysical sources and directly from the Big Bang. Indeed these particles have energy greater than 100TeV (UHE) and interact with the nuclei of the atmosphere generating extensive air showers (EASs) detectable at the ground surface. During the last 30 years the ground-based apparatus have reached goals unattainable with the other techniques to explore the Universe. For example it has put in evidence a very large number of gamma-sources from our galaxy and from other galaxy, it has demonstrated the existence of very complex gamma sources, and it has discovered extra-galactic gamma source at distance never explored previously.

The researchers of UNICAL physics department participate to the Extrem Energy Events national project. In particular the group has the responsibility of the muon telescopes of the Calabria Region that consist of two muon telescopes and four schools waiting for new installations. At present the network is formed of 50 muon telescopes distributed throughout the entire Italian territory. Each telescope consists of three multigap resistive plate chambers (MRPC). The muon telescopes are housed in high schools. Students and teachers contribute to their construction, commissioning and maintenance. This peculiarity is a big plus for the experiment, which combines the scientific relevance of its objectives with effective outreach activities.

The experiment started to take coordinated data in a pilot run in the fall of 2014 and up to now it collected 40 bilions of "good tracks". The data from the schools are transmitted to the INFN/CNAF data center, where they are immediately reconstructed and stored. The current analysis refers to km-scale coincidences, the variation with time of the muon cosmic flux on astrophysical phenomena like Forbush decrease, upward flux of particle, search for anisotropies in the muon angular distribution, etc.

A. PUBLICATIONS ON SCIENTIFIC JOURNALS
A.1 Publications on international journals
A.1.1 Publications on international journals printed in 2013-2016

40. Anastasi A. et al., KLOE-2 Collaboration,
Measurement of the running of the fine structure constant below 1 GeV with the KLOE Detector
Physics Letter B, online 13 December (2016). arXiv:1609.06631 [hep-ex]

41. Anastasi A. et al., KLOE-2 Collaboration,
Limit on the production of a new vector boson in $e^+e^- \to U\gamma$, $U \to \pi^+\pi^-$ with the KLOE experiment
Physics Letter B757 (2016) 356-361. arXiv:1603.06086 [hep-ex]

42. Abbrescia M. et al., EEE Project,
A study of upward going particles with the Extreme Energy Events telescopes
Nucl.Instrum.Meth. A816 (2016) 142-148.

43. Anastasi A. et al., KLOE-2 Collaboration,
Precise measurement of $\eta \to \pi^+\pi^-\pi^0$ the Dalitz plot distribution with the KLOE detector
JHEP 1605 (2016) 019. arXiv:1601.06985 [hep-ex]

44. Anastasi A. et al., KLOE-2 Collaboration,
Measurement of the $\phi \to e^+e^-\pi^0$ transition form factor with the KLOE detector
Phys.Lett. B757 (2016) 362-367. arXiv:1601.06565 [hep-ex]

45. Abbrescia M. et al., EEE Project,
Looking at the sub-TeV sky with cosmic muons detected in the EEE MRPC telescopes
Eur.Phys.J.Plus 130 (2015) n.9,187.

46. Anastasi A. et al., KLOE-2 Collaboration,
Limit on the production of a new vector boson in $e^+e^- \to U\gamma$, $U \to e^+e^-$ with the KLOE experiment
Physics Letter B750 (2015) 363-367. arXiv:1509.00740 [hep-ex]

47. Anastasi A. et al., KLOE-2 Collaboration,
Search for dark Higgsstrahlung in $e^+e^- \to \mu^+\mu^-$ and missing energy events with the KLOE experiment
Physics Letter B747 (2015) 365-372. arXiv:1501.06795 [hep-ex]

48. Anastasi A. et al., KLOE-2 Collaboration,
Study of the Dalitz decay $\phi \to \eta e^+e^-$ with the KLOE detector
Physics Letter B742 (2015) 1-6. arXiv:1409.4582 [hep-ex]

49. Anastasi A. et al., KLOE-2 Collaboration,
Measurement of the absolute branching ratio of the $K \to \pi^+\pi^-\pi^0 + (\gamma)$ decay with the KLOE detector
Physics Letter B738 (2014) 128-133. arXiv:1407.2028 [hep-ex]

50. Anastasi A. et al., KLOE-2 Collaboration,

Search for light vector boson production in $e^+e^- \to \mu^+\mu^-\gamma$ interactions with the KLOE experiment
Physics Letter B736 (2014) 459-464. arXiv:1404.7772 [hep-ex]

51. Anastasi A. et al., KLOE-2 Collaboration,
Test of CPT and Lorentz symmetry in entangled neutral kaons with the KLOE experiment
Physics Letter B730 (2014) 115-118.

52. Anastasi A. et al., KLOE-2 Collaboration,
A new limit on the CP violating decay $K_S \to 3\pi^0$ with the KLOE experiment
Physics Letter B723 (2013) 54-60. arXiv:1301.7623 [hep-ex]

53. Anastasi A. et al., KLOE-2 Collaboration,
Precision measurement of $\sigma(e^+e^- \to \pi^+\pi^-\gamma)$ / $\sigma(e^+e^- \to \mu^+\mu^-\gamma)$ and determination of the $\pi^+\pi^-$ contribution to the muon anomaly with the KLOE detector
Physics Letter B720 (2013) 336-343. arXiv:1212.4524 [hep-ex]

54. Anastasi A. et al., KLOE-2 Collaboration,
Measurement of η meson production in $\gamma\gamma$ interactions and $\Gamma(\eta \to \gamma\gamma)$ with the KLOE detector
JHEP 1301 (2013) 119. arXiv:1211.1845 [hep-ex]

55. Anastasi A. et al., KLOE-2 Collaboration,
Limit on the production of a light vector gauge boson in phi meson decay with the KLOE detector
Phys.Lett. B720 (2013) 111-115. arXiv:1210.3927 [hep-ex]

56. Anastasi A. et al., KLOE-2 Collaboration,
Measurement of $\Gamma(\eta \to \pi^+\pi^-\gamma)$ / $\Gamma(\eta \to \pi^+\pi^-\pi^0)$ with the KLOE detector
Phys.Lett. B718 (2013) 910-914. arXiv:1209.4611 [hep-ex]

18. Aad G. et al., ATLAS collaboration,
Charged-particle distributions in $\sqrt{s}$ = 13 TeV pp interactions measured with the ATLAS detector at the LHC,
Physics Letters B, Volume 758, 10 July 2016, Pages 67–88,
DOI: 10.1016/j.physletb.2016.04.050

19. Aad G. et al., ATLAS collaboration,
Measurement of W± and Z-boson production cross sections in pp collisions at $\sqrt{s}$ = 13 TeV with the ATLAS detector,
Physics Letters B, Volume 759, 10 August 2016, Pages 601–621,
DOI: 10.1016/j.physletb.2016.06.023

20. Aad G. et al., ATLAS collaboration,
Charged-particle distributions at low transverse momentum in $\sqrt{s}$ = 13 TeV pp interactions measured with the ATLAS detector at the LHC,
Eur. Phys. J. C 76 (2016) 502,
DOI: 10.1140/epjc/s10052-016-4335-y

21. Aad G. et al., ATLAS Collaboration,

Measurement of the bb dijet cross section in pp collisions at 7 TeV with the ATLAS detector
Eur. Phys. J. C 76 (2016) 670.

22. Aad G. et al., ATLAS Collaboration,
Combined Measurement of the Higgs Boson Mass in pp Collisions at root s=7 and 8 TeV with the ATLAS and CMS Experiments,
Physical Review Letters 114 (2015) 191803.

23. Aad G. et al., ATLAS Collaboration,
Search for pair-produced long-lived neutral particles decaying to jets in the ATLAS hadronic calorimeter in pp collisions at 8 TeV,
Physics Letters B 743 (2015) 15-34.

24. Aad G. et al., ATLAS Collaboration,
Jet energy measurement with the ATLAS detector in proton-proton collisions at root s=7 TeV, Eur. Phys. J. C 73 (2013) 2304.

25. Aad G. et al., ATLAS Collaboration,
Search for long-lived neutral particles decaying into lepton jets in proton--proton collisions at √s = 13 TeV with the ATLAS detector,
ATLAS-CONF-2016-042

26. Aad G. et al., ATLAS Collaboration,
Search for pair-produced long-lived neutral particles decaying in the ATLAS hadronic calorimeter in pp collisions at √s 8 TeV,
Phys. Lett. B 743 (2015) 15-34

27. Aad G. et al., ATLAS Collaboration,
*Search for long-lived, weakly interacting particles that decay to displaced hadronic jets in proton-proton collisions at √s = 8 TeV with the ATLAS detecto*r,
Phys. Rev. D 92 (2015) no.1, 012010

28. Aad G. et al., ATLAS Collaboration,
Performance of the ATLAS muon trigger in pp collisions at √s = 8 TeV,
Eur. Phys. J. C75 (2015) 120

29. Aad G. et al., ATLAS Collaboration,
Searches for heavy long-lived charged particles with the ATLAS detector in proton-proton collisions at √s = 8 TeV,
JHEP 1501 (2015) 068

30. Aad G. et al., ATLAS Collaboration,
Search for long-lived neutral particles decaying into lepton jets in proton-proton collisions at √s= 8 TeV with the ATLAS detector,
JHEP 1411 (2014) 088

31. Aad G. et al., ATLAS Collaboration,
Standalone vertex finding in the ATLAS muon spectrometer,
JINST 9 P02001 (2014)

32. Aad G. et al., ATLAS Collaboration,

Searches for heavy long-lived sleptons and R-hadrons with the ATLAS detector in pp collisions at √s = 7 TeV,
Phys. Lett. B 720 (2013) 277-308

33. Aad G. et al., ATLAS Collaboration,
Search for displaced muonic lepton jets from light Higgs boson decay in proton-proton collisions at √s = 7 TeV with the ATLAS detector, Phys. Lett. B 721, 32 (2013)

34. Aad G. et al., ATLAS Collaboration,
Triggers for displaced decays of long-lived neutral particles in the ATLAS detector, JINST 8 (2013) P07015

B. PUBLICATIONS ON CONFERENCE PROCEEDINGS

B.1 Publications on international conference proceedings in 2013-2016

1. Schioppa M.,
Boosted objects and jet substructure at the LHC
IFIC Valencia, 23rd-27th of July 2012 – ArXiv:1311.2708 [hep-ex]
Eur. Phys.J C74 (2014) 3, 2792

2. Schioppa M.,
BSM Higgs searches with the ATLAS experiment
Cracow EPIPHANY Conference on the Physics in the LHC Run2, Acta Physica Polonica B Vol. 47 No. 6 – June 2016, 1565
3. Schioppa M.,
Search for long-lived neutral particles decaying into lepton-jets in 20.3 fb-1 proton-proton collisions at sqrt(s)=8 TeV with the ATLAS detector
EPJ Web of Conferences 126, 05011 (2016)

4. Schioppa M.,
BSM searches (SUSY and Exotic) from ATLAS
7th High Energy Physics International Conference, September 17-22, 2015, Antananarivo, Madacascar, SLAC eConf C150917

5. A. Policicchio,
Search for Long-Lived particles at ATLAS,
Prepared for IFAE 2013, Cagliari, Italy (2013), Nuovo Cim. C 037, no. 01, 38 (2014)

6. D. Del Re and A. Policicchio,
Search for new physics with Long-Lived particles at the LHC,
Prepared for LHCpp 2013, Genova, Italy (2013), PoS LHCPP2013, 012 (2013)

7. A. Policicchio,
Search for exotics long-lived neutral particles with ATLAS at the LHC,
Prepared for EPS HEP 2013, Stockholm, Sweden (2013); PoS EPS-HEP2013, 132 (2013)

8. A. Policicchio,
BSM searches in ATLAS,
prepared for Corfu Summer Institute 2014 "School and Workshops on Elementary Particle Physics and Gravity, Corfu, Greece (2014); PoS COR- FU2014, 063 (2015)

9. A. Policicchio,
Searches for highly ionizing particles in ATLAS and CMS,
prepared for EPS- HEP 2015, Vienna, Austria (2015); PoS EPS-HEP2015, 149 (2015)

10. A. Policicchio,
Search for long-lived neutral particles decaying into "lepton-jets" with the ATLAS detector in proton-proton collision data at (s) = 13 TeV,
prepared for ICHEP 2016, Chicago, USA (2016), PoS ICHEP 2016, 1149 (2016)

11. V.M.M. Cairo, R. de Oliveira R, P. Fonte, S. Franchino, V. Peskov, P. Picchi P, F. Pietropaolo,
Demonstration of new possibilities of multilayer technology on resistive microstrip/microdot detectors,
JOURNAL OF INSTRUMENTATION, vol. 9, ISSN: 1748-0221, doi: 10.1088/1748-0221/9/11/C11022

12. V.M.M. Cairo,
Improvements to ATLAS track reconstruction for Run II,
Nuclear Instruments and Methods in Physics Research Section A: Accelerators, Spectrometers, Detectors and Associated Equipment, Nucl.Instrum.Meth. A824 (2016) 6-8

13. V.M.M Cairo.
Measurements of charged-particle distributions with the ATLAS detector
Proceedings of Low-x Meeting 2016, https://arxiv.org/abs/1610.06231

14. V.M.M. Cairo, A. Dell'Acqua,
Stato degli studi per la realizzazione di un Futuro Collider Circolare adronico (FCC-hh) al CERN di Ginevra.
Società Italiana di Fisica, 100° CONGRESSO NAZIONALE. ISBN: 978-88-7438-088-6, Pisa, Italy, September 2014

15. V.M.M. Cairo, A. Dell'Acqua,
New Small Wheel per l'upgrade di ATLAS: simulazione del layout, trigger e ricostruzione
Società Italiana di Fisica, 100° CONGRESSO NAZIONALE. p. 230, ISBN: 978-88-7438-088-6, Pisa, Italy, September 2014

16. V.M.M. Cairo,
Minimum bias at √s = 13 TeV: Tracking and material distribution studies in ATLAS,
Colloquia IFAE 2015, IL NUOVO CIMENTO 39 C (2016) 205 DOI 10.1393/ncc/i2016-16205-2, Rome, Italy, April 2015

17. Salvatore D,
Search for Long-Lived particles and Lepton-Jets with the ATLAS detector, LHCP 2013, 13-17 May 2013, Barcelona (Spain).

18. Salvatore D,
Searches for Long-Lived Neutral Particles decaying to jets in ATLAS, EPS-HEP 2015, Vienna, 22-29, July, 2015.

19. Del Gaudio M.,
Quality tests for SM1 MicroMegas detector module, IFAE 2015, Rome, Italy 2015, Nuovo Cim. C39 (2016) no.1, 255

D. INVITED PRESENTATIONS

D1. Invited presentations at international conferences in 2013-2016

1. A. Policicchio,"Search for non-prompt leptonjets in ATLAS", Invited Collider Cross-Talk, CERN Theory Division, Geneve, Switzerland (2015).
.

E. PRESENTATIONS AT CONFERENCES

E1. Presentations at international conferences in 2013-2016

1. Schioppa M. on behalf of the ATLAS Collaboration,
BSM Higgs searches with the ATLAS experiment
22th Cracow EPIPHANY Conference on the Physics in the LHC Run2, Cracow, Poland, 7-9 January 2016.

2. Schioppa M. on behalf of the ATLAS Collaboration,
Search for long-lived neutral particles decaying into lepton-jets in 20.3 fb-1 proton-proton collisions at sqrt(s)=8 TeV with the ATLAS detector
4th ICFNP 2015, 23-30 August 2015, Crete (Gr).

3. Schioppa M. on behalf of the ATLAS Collaboration,
BSM searches (SUSY and Exotic) from ATLAS
7th High Energy Physics International Conference, September 17-22, 2015, Antananarivo, Madagascar.

4. Mastroberardino A. on behalf of the ATLAS Collaboration,
Searches for Long-Lived particles in Hidden Valley scenarios with the ATLAS detector at the LHC, 23rd International Conference on Supersymmetry and Unification of Fundamental Interactions, Lake Tahoe (California), 2015, August 23-29
5. Mastroberardino. on behalf of the ATLAS Collaboration,
Overview of SUSY Physics at Atlas
8th High Energy Physics International Conference, October 2016, Antananarivo, Madagascar.

6. A. Policicchio on behalf of the ATLAS Collaboration,
Search for exotics long-lived neutral particles with ATLAS at the LHC,
EPS HEP 2013, Stockholm, Sweden (2013).

7. A. Policicchio on behalf of the ATLAS Collaboration,
BSM searches in ATLAS,
CORFU2014 - Summer School and Workshop on the Standard Model and Beyond, Corfu, Greece (2014).

8. A. Policicchio on behalf of the ATLAS Collaboration,
Leptonjets, long-lived-particles and exotics Higgs,

ATLAS Physics Workshop - Ready for Run2, Aix-les-Bains, France (2014).

9. A. Policicchio on behalf of the ATLAS Collaboration,
Searches for highly ionizing particles in ATLAS and CMS,
EPS-HEP 2015, Vienna, Austria (2015).

10. A. Policicchio on behalf of the ATLAS Collaboration,
Search for long-lived neutral particles decaying into "lepton-jets" with the ATLAS detector in proton-proton collision data at $\sqrt{s}$ *= 13 TeV*,
ICHEP 2016, Chicago, USA (2016).

11. A. Policicchio on behalf of the ATLAS Collaboration,
Searches for non-prompt lepton-jets,
UEH 2016, Searching for Exotic Hidden Signatures with ATLAS in LHC Run2: Workshop on the Detection of Dark Sector Signals, Cosenza, Italy (2016).

12. V.M.M. Cairo on behalf of the ATLAS Collaboration,
Improvements to ATLAS Track Reconstruction for RUN-II,
Pisa Meeting on Advanced Detectors – May 2015 (Isola D'Elba, Italy)

13. V.M.M. Cairo on behalf of the ATLAS Collaboration,
Results on Minimum Bias Interactions, Underlying Events and Particles Production from ATLAS,
QCD@LHC - September 2015 (UK)

14. V.M.M. Cairo on behalf of the ATLAS Collaboration,
Charged-particle multiplicities at 13 TeV with ATLAS at the LHC,
Lake Louise Winter Institute – February 2016 (Canada)

15. V.M.M. Cairo on behalf of the ATLAS Collaboration,
Measurements of the charged-particle distributions with the ATLAS detector,
Low-x Meeting – June 2016 (Hungary)

16. V.M.M. Cairo on behalf of the ATLAS Collaboration,
Monte Carlo tuning for Multiple Parton Interactions from the ATLAS data,
MPI@LHC – December 2016 (Mexico)

17. Salvatore D. on behalf of the ATLAS Collaboration,
Search for Long-Lived Particle decays in the Hadronic Calorimeter,
ATLAS Long-Lived Particle searches: current status and plans for Run II workshop, Rome2, 3rd-5th December 2013.

19. Salvatore D. on behalf of the ATLAS Collaboration,
Search for Long-Lived particles and Lepton-Jets with the ATLAS detector,
LHCP 2013, 13-17 May 2013, Barcelona (Spain).

20. Salvatore D. on behalf of the ATLAS Collaboration,
Searches for Long-Lived Neutral Particles decaying to jets in ATLAS,
EPS-HEP 2015, Vienna, 22-29, July, 2015.

21. Salvatore D. on behalf of the ATLAS and CMS Collaborations,
Searches for exotic long-lived particles with displaced signatures at the LHC,

LHCP 2015, 31 August – 5 September 2015, St. Petersburg (Russia).

22. Del Gaudio M. on behalf of the ATLAS Collaboration, "*The INFN MM Module-0 Prototype for the Muon Spectrometer Upgrade of the ATLAS Experiment",* IEEE Nuclear Science Symposium, Strasbourg, France (2016)

E1. Presentations at national conferences in 2013-2016

1. A. Policicchio,
   Search for Long-Lived particles at ATLAS,
   Incontri di Fisica delle Alte Energie (IFAE) 2013, Cagliari, Italy (2013).

2. A. Policicchio,
   Search for new physics with Long-Lived particles at the LHC,
   LHCpp 2013, Genova, Italy (2013).

3. V.M.M. Cairo,
   New Small Wheel per l'upgrade di ATLAS: simulazione del layout, trigger e ricostruzione,
   100° Congresso Nazionale della Società Italiana di Fisica, Pisa, Italy, September 2014

4. A. Policicchio*,*
   Search for non-prompt leptonjets,
   X ATLAS Italia workshop on physics and upgrade, Milano, Italy 10-12 February 2015.

5. V.M.M. Cairo,
   Early RUN-II Standard Model Analyses,
   X ATLAS Italia Workshop on Physics and Upgrade, Milan, Italy 10-12 February 2015

6. V.M.M. Cairo,
   Minimum Bias at √s = 13 TeV: Tracking and Material Distribution Studies with the ATLAS Inner Detector,
   Incontri di Fisica delle Alte Energie (IFAE) 2015, Università di Roma Tor Vergata, 8-10 April 2015

7. A. Policicchio,
   Search for non-prompt leptonjets in ATLAS,
   101° Congresso Nazionale della Società di Fisica, Rome, Italy, 21-25 September 2015.

8. Schioppa M.,
   Ricerca di particelle neutre a lunga vita media che decadono in getti di leptoni con l'esperimento ATLAS all'acceleratore protone-protone LHC di Ginevra all'energia nel centro di massa di 13 TeV
   102° Congresso Nazionale della Società Italiana di Fisica, Padue, Italy, September 26-30, 2016.
9. Salvatore D.
   Ricerca di particelle a lunga vita media in ATLAS: algoritmi di selezione (Search for Long-lived particles in ATLAS: selection algorithms),
   XCIX Congresso Nazionale SIF, Trieste, 23 - 27 September 2013.

10. Salvatore D.,
   Search for Long-Lived Particles with the ATLAS detector,

ATLAS Italia Meeting, Bologna, 14-16 January 2014.

11. Salvatore D.,
Ricerca di particelle neutre a lunga vita media all'esperimento ATLAS (Search for neutral long-lived particles with the ATLAS experiment),
101° Congresso Nazionale SIF, Roma, 21-25 September, 2015.
12. Salvatore D.,
Searches for long-lived particles with displaced signatures with the ATLAS detector: results from Run 1 and plans for Run 2,
XI ATLAS Italia Workshop, Cosenza, 4-6 November 2015.

13. Salvatore D.,
Searches for long-lived particles with displaced signatures with the ATLAS detector: status and plans,
XII ATLAS Italia Workshop, Napoli, 23-23 November 2016.
14. Del Gaudio M.,
Quality control e Quality assurance per la costruzione e l'assemblaggio dei rivelatori MicroMegas, (talk),
Congresso Nazionale della Società Italiana di Fisica, Rome, Italy (2015)

15. Del Gaudio M.,
*Test di qualità delle camere MicroMegas***,**
IFAE 2015 , Rome, Italy (2016)

16. Del Gaudio M.,
Ricerca di particelle neutre a lunga vita media decadute in coppie collimate μ/e/π con l'esperimento ATLAS nelle collisioni p-p a 13 TeV,
IFAE 2016, Genova, Italy, (2016)

9. QUANTUM PHYSICS OF MATTER AND MATERIALS

Professors and Researcher	Giovanni Falcone Daniela Pacilè Marco Papagno Francesco Plastina Pierfrancesco Riccardi Antonio Sindona
Postdoc fellows	Salvatore Lorenzo (July 2015, June 2016) Tony J. G. Apollaro (2013-2014) Francesco Francica (2014 - 2015) Claudia Giallombardo (2014 - 2015) Mario Gravina (2014 - 2015) Michele Pisarra (2014 - 2015)
PhD students	Gianluca Francica (2014-2016) Jacopo Settino (since 2016) Ilenia Grimaldi (since 2016) Cristian Isaac Vacacela Gomez (2013-2016)

Collaborators W. M. Silkin, M. J. Pitarke (*University of the Basque Country, SPAIN*)
F. J. García de Abajo (*ICFO Barcelona, SPAIN*)
S. Bellucci (*Laboratori Nazionali di Frascati, Italy*)
M. Palummo, O. Pulci, G. Stafanucci (*Università di Roma Torvergata, Italy*)
C.A. Dukes (*University of Virginia, USA*)
C. Carbone (*Istituto di Struttura della Materia-CNR Trieste, Italy*)
I. Vobornik *(Istituto Officina dei Metriali- Trieste, Italy)*
M. Grioni, H. Brune (*Ecole Polytechnique Fédérale de Lausanne*)
G. Costantini *(University of Warwick)*
M. G. Betti *(Università Sapienza, Roma)*
V. de Renzi *(Università degli studi di Modena e Reggio Emilia, Italy)*
E. V. Chulkov *(Saint Petersburg State University, Russia)*
F. Ciccarello, G. M. Palma (*Università di Palermo, Italy*)
N. Lo Gullo (*Università di Milano, Italy*)
J. Goold (*ICTP, Trieste, Italy*).
S. Maniscalco, J. Piilo, A. Karlsson *(University of Turku, FI)*
M. Paternostro, R. McCloskey, C. Di Franco, G. De Chiara, L. Mazzola, S. Campbell (*Queen's University, Belfast, UK*)
Th. Busch (*Okinawa Institute of Science and Technology, JP*)
A. Cuccoli *(Università di Firenze, Italy)*
R. Vaia, P. Verrucchi *(ISC-CNR, Firenze, Italy)*
L. Banchi (*ISI Foundation, Torino*)
L. Caputi, N. Ligato, A. Cupollillo (*UNICAL*)
M. G. A. Paris (*Università di Milano*),
R. Zambrini, F. Galve, G. Giorgi (*IFISC, Palma de Mallorca*)
S. Paganelli (*Università dell'Aquila, Italy*)
A. Alecce, L. Dell'Anna (*Università di Padova, Italy*)

Research subjects:

9.1 Experimental investigation of Graphene-related materials, displaying Dirac-like structures
9.2 Many Electron Phenomena in Low-Dimensional and Nanostructured Systems
9.3 Local perturbations and orthogonality catastrophe in fermion systems
9.4 Decoherence and Memory effects
9.5 Non-equilibrium thermodynamics and Irreversibility
9.6 Quantum Information and Quantum Correlations
9.7 Outreach activities

Introduction

The "Quantum physics of matter and material" group is a team comprising both theorists and experimentalists working in various areas of condensed matter physics. In the period 2013-2016, we have been working on a very broad set of subjects, ranging from the experimental and theoretical

studies of Carbon-based materials, to the characterzation of information flow in magnetic spin systems, a subject of interest in the context of quantum information and communication theory. We have been interested in general theoretical issues, such as the description of the irreversible behavior of a non-adiabatically driven critical system, as well as in more application-oriented investigations, such as the study of graphene-ferromagnetic interfaces. Despite the apparent diversity of subjects, our research themes are much more interrelated than it appears by looking at the list above. We aim at investigating both equilibrium and out-of-equilibrium many-body physics, with a particular emphasys on the physics of matter and materials. Our work is highly multidisciplinary, as it involves Quantum and Condensed Matter Physics, Statistical Mechanics, Quantum Information and Open Quantum System Theory. The main unifying theme of many of our research activities is the investigation of the response of condensed matter systems to various form of external perturbations. To this end, we employ either photons, electrons or ions as probes to perform various kind of spectroscopic analysis, and, from the theoretical side, both numerical and analytic techniques. Part of our efforts has been devoted to outreach activities, in particular in collaboration with high schools.

9.1 Experimental investigation of Graphene-related materials, displaying Dirac-like structures

Our expertise, developed over the past ten years and supported by international collaborations, is spread on several topics, mostly concerning innovative materials. Among them, graphene and topological insulators.

Graphene is the mother system of all the carbon-based materials. It is made out of a single planar sheet of carbon atoms (sp^2 bonded) located along the corner of an hexagon. From an electronic point of view, graphene is an exciting novel material. Its peculiar properties derive mainly by the presence of Dirac quasiparticles, e.g. quasiparticles with a linear E vs k dispersion and by a zero density-of-states at the Fermi level. These features give rise to a series of fascinating effects, as very-high electronic mobilities, which render graphene suitable for nanoelectronic devices and nanometre gas sensors. The physics of graphene is particularly interesting also from a fundamental point of view, as it marks the failure of the Fermi liquid picture in the description of the Dirac quasiparticles.
In this context, we have extensively studied the electronic properties of graphene grown by chemical vapor deposition (CVD) on several transition metal surfaces, by means of angle-resolved photoemission spectroscopy (ARPES) and scanning tunneling microscopy (STM) measurements. These studies showed how to tailor graphene electronic properties by means of perturbing periodic potentials, how to synthesize graphene flakes with different structural and electronic properties, and how to growth artificially lattice mismatched graphene/metal interface. These results represent a fundamental step toward the engineering needed for graphene-based electronic circuits. Also, the intercalation of foreign metallic and ferromagnetic atoms not only act as spacers, but also influence the hybridization between the metal electronic orbitals and graphene states. Another interesting aspect of graphene is its use in the field of carbon-based nano-electronics. However, in order to access the potential of graphene in spintronic devices, its ability to mediate magnetic exchange interactions has to be assessed. By performing the advanced investigation techniques X-ray magnetic circular dichroism (XMCD), scanning tunneling microscopy (STM), and density functional theory (DFT), along with international co-workers, we have showed that Co/G/Ni junctions display a significant G-mediated exchange coupling between Co atoms and Ni(111). These latter findings are important for the utilization of graphene as a spacer layer in magnetic heterostructures and spintronic devices, as well as to understand the complex interaction between graphene and magnetic impurities.

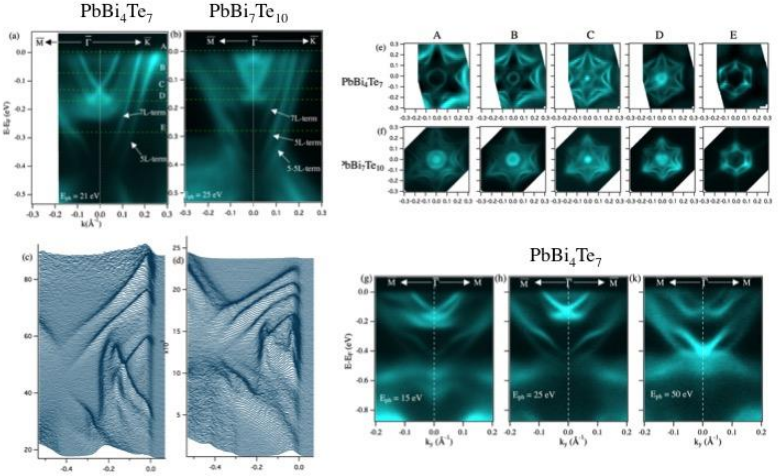

Figure 9.1: Experimental electronic band structure of (a) $PbBi_4Te_7$ and (b) $PbBi_6Te_{10}$ along the K^-–$\bar{\Gamma}$–M^- direction along with the corresponding energy distribution curves in (c) and (d), respectively. Constant energy surfaces of (e) $PbBi_4Te_7$ and (f) $PbBi_6Te_{10}$. Experimental electronic band structure of $PbBi_4Te_7$ along the M^-–$\bar{\Gamma}$–M^- direction collected at (g) 15 eV, (h) 25 eV, and (k) 50 eV photons energy. From Ref. [10], and M. Papagno *et al.,* in preparation.

The latest wonder in condensed- matter physics is the family of substances called topological insulators (TI). As with graphene, the discovery of TIs has generated an enormous amount of fundamental interest as well as speculation over the possibility of new devices. The key feature that determines all relevant properties of a material is its band structure, that is, the relationship between its electrons energies and their momenta. The stability of this linear band structure against local magnetic perturbations which break time-reversal symmetry, is a prerequisite for the realization of spintronic devices based on TI material. An interesting aspect of topological insulators is the possibility to engineer the electronic band structure by synthesizing new systems by alternating binary or ternary quintuple-layer (QL) or septuple-layer (SL) structured compounds. The surface terminations of these new systems support Dirac states that, as a consequence of the complicated bulk band inversion, differ in Dirac point energy, band dispersion, and spatial charge density localization. We have recently examined the electronic band structure of $PbBi_4Te_7$ and $PbBi_6Te_{10}$ by ARPES measurements, see Fig. 9.1, accompanied by STM measurements, and accurate DFT calculations. STM measurements confirm distinct cleavage planes at the surface in agreement with the atomic structure of $PbBi_4Te_7$ and $PbBi_6Te_{10}$ compounds. High-resolution ARPES measurements provide evidence of the coexistence of multiple Dirac topological surface states at the zone-center, displaying distinct electronic band dispersion, constant energy contours, and Dirac point energies. These results (see [10], and M. Papagno *et al.,* in preparation) shed light on the diversity of topological surface states and may pave a way for the application of the topological insulator to the real spintronic devices.

9.2 Many Electron Phenomena in Low-Dimensional and Nanostructured Systems

A large part of our activity in the last few years has been devoted to the experimental and theoretical characterization of genuinely many-body phenomena, arising from the interaction between charged and/or neutral particles in condensed matter. In particular, we have investigated the interaction of slow ions and electrons with solid surfaces and nanostructured materials, inducing electronic excitations, charge transfer and electron and ion emissions, which are modified to some extent by sputtering. Besides the implications in the development of spectroscopic tools for the characterization of new materials, this research has technological applications in plasma display, in the study of discharge phenomena and He microscopy.

The theoretical description of these many-body proecsses has undergone remarkable developments along with the increased computational power and capacity for data management, which have made numerical calculations practical for real systems. With the raise of low-dimensional quantum materials, be them in the form of graphene-based lattices or beyond-graphene nanostructures, some of the excited-state properties, collective modes, and non-equilibrium dynamical features of such systems have become more and more controllable by experiments and accessible to theoretical modeling.

The research activities of our group have been devised to focus on the role of collective excitations, non-adiabatic events, and critical phenomena in low-dimensional nanostructured materials, along various complementary research lines.

9.2.1 Highly excited states of graphite and graphene/transition metal interfaces

We analyzed some experimental energy distributions of secondary electrons emitted by highly oriented pyrolytic graphite (HOPG) and graphene (G) grown on the (111) surface of nickel, obtaining information on the dispersions of the unoccupied electronic bands of the systems, along specific high symmetry directions of the first Brilluoin zone.

These observations were supported by a density functional theory (DFT) study, based on a plane-wave pseudo-potential method and the local density approximation.

The analysis was used to assign spectroscopic features observed in secondary electron emission experiments either to the graphene sheet or to the nickel substrate, providing a first evidence of highly excited states peculiar to the two-dimensional nature of graphene. Finally, we proposed a combined theoretical and experimental method to examine the graphene-substrate interaction between the carbon and nickel states.

9.2.2 Plasmon modes in graphene, graphene nanoribbons, bilayer graphene, and silicene

We used time-dependent (TD) density functional theory (DFT)- within the linear response formalism and the random phase approximation- to explore the dielectric properties of graphene, silicone, bilayer graphene, and graphene nanoribbon arrays with zigzag and armchair shaped edges.

In extrinsic graphene, we predicted the occurrence of an acoustic plasmon, in addition to the conventional two-dimensional plasmon. The origin of this novel mode stems from the anisotropy in the graphene band structure near the Dirac point, where the valence and conduction bands have a conical behavior, being populated by massless Dirac fermions.

The above mentioned anisotropy, lying outside the Dirac-cone approximation, allows for the coexistence of virtually massless carriers moving with two distinct Fermi velocities.

In buckled silicene the same two-dimensional and acoustic modes were detected, together with an additional effect due to sp2-sp3 hybridization effects, which are absent in unbuckled graphene.

In bilayer graphene, the existence of a double Dirac-cone structure allowed us to define various extrinsic plasmon modes and to analyze them with reference to the design of novel nanodevices.

Finally, we found out that semiconducting (armchair) nanoribbons are characterized by an intraband plasmon and an interband plasmon, whose fascinating interplay is extremely responsive to either injection of charge carriers or increase in electronic temperature. These oscillations share some

common trends with recent nanoinfrared imaging of confined edge and surface plasmon modes detected in graphene nanoribbons of 100–500 nm width (Z. Fei et al, Nano Lett. 15, 4973 2015)

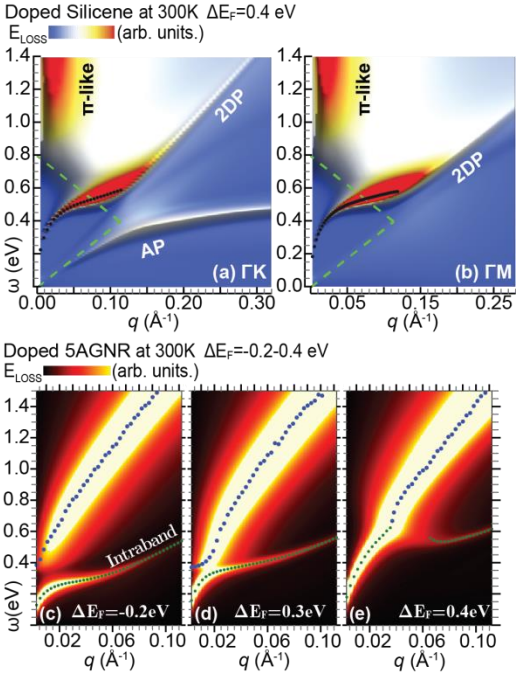

Figure 9.2: Plasmon spectrum of graphene nanoribbon arrays with armchair shaped edges (a)-(c) and buckled silicene (d)-(e), as computed from TDDFT; in panels (a)-(c) the arrays, having widths of the order of ~0.7 nm, show two distinct intraband and interband modes, which can be tuned by changing the doping concentration, i.e., shifting the Fermi energy of the systems by ΔE_F (see Ref. [10]); in (d)-(e) the silicene sample is shown to be characterized by two distinct plasmon modes (2DP,AP), originated by distinct type of massless Dirac fermions (see C. Vacacela Gomez et al, accepted by Phys. Rev. B)

9.2.3 Dynamic core hole screening in fullerene molecules and carbon nanotubes

We inspected the role of core-hole electron excitations in fullerene molecules and cylindric conducting carbon nanotubes. We used density functional theory (DFT) with minimal, split-valence, and triply-split-valence basis sets plus the generalized gradient approximation for exchange and correlation (dictated by the PBE and B3LYP functionals).

We performed finite-size computations, and simulated the sudden creation of a core state by replacing a 1s electron pair, localized at a central site of the structures, with the effective pseudo-potentials of both neutral and ionized atomic carbon.

We applied the Fermi golden rule, including the ground state of the neutral systems and the excited states of the ionized systems, with some corrections due lifetime and finite-temperature effects to compute the many-electron response of the nano-objects. We found the simulated DFT spectrum of the fullerene molecule to be in good agreement with some x-ray photoemission

experiments on thick C-60 films, reproducing the low energy satellites at excitation energies below 4 eV within a peak position error of ca. 0.3 eV. The experimental line-shapes from bundles of single walled carbon nanotubes (SWCNTs) and highly oriented pyrolytic graphite (HOPG) were also correctly reproduced.

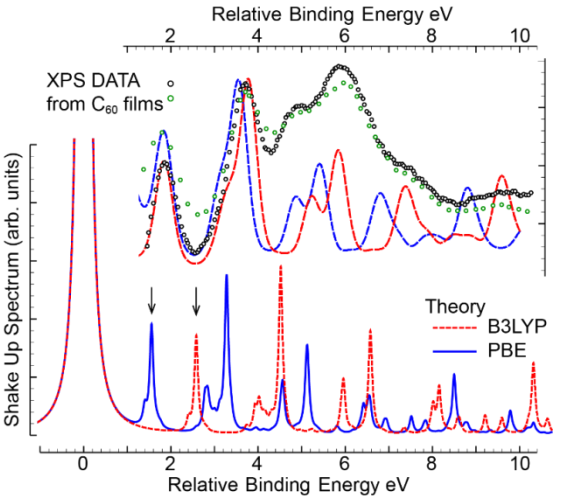

Figure 9.3: Shake up spectrum of a C_{60} fullerene molecule, as computed from DFT with two differentexchange-correlation functionals (PBE, B3LYP), compared with x-ray photoemission data from C_{60} films. See Ref. [23].

9.3 Local perturbations and orthogonality catastrophe in fermion systems

Another theoretical research line developed in the past years, strongly connected with both that reported the previous section, and with that of Sec. 9.4, has concerned the investigation of the orthogonality catastrophe dynamically induced in fermion systems by the dispersive coupling with a local impurity, which can also play the role of a probe of the response of the fermions if one is able to monitor its dynamics. A striking connection, indeed, exists between the decohering dynamics of the probe, generated by the interaction with the fermion environent, and the description of the re-adjustment (or shake-up) of the Fermi gas induced by the switching on of the probe-gas interaction. From the formal point of view, the decoherence factor entering the open dynamics of the probe coincides with the so called vacuum persistence amplitude, describing the dynamic shake-up process in the gas, which reacts to the local disturbance produced by the probe. The fact that the persistence amplitude ultimately decays to zero is the essence of the Anderson's orthogonality catastrophe: despite the fact that only a small, local perturbation is applied, the final state of the gas is orthogonal to the initial one due to the singular behavior (at very low temperatures) induced by the presence of an edge structure in the statistical Fermi-Dirac distribution. As a result, the coupling with the probe can be thought, from the point of view of the Fermi gas, as a not-slow-enough thermodynamic transformation, bringing the system out of its initial thermal equilibrium state. In this thermodynamic context, see also Sec. 9.5, the persistence amplitude can be shown to coincide with the characteristic function of the distribution of the work performed during the transformation. Its knowledge, thus, gives access to a series of physical quantities of well defined thermodynamic meaning, such as the irreversible entropy production. Finally, in a more information-theory oriented treatment, the modulus square of the persistence amplitude is equal to the Loschmidt echo function, whose knowledge enables the characterization of the memory effects in the probe dynamics.

9.3.1 *Orthogonality Catastrophe in a trapped ultra-cold Fermi gas*

That of a local quench of a Fermi gas, giving rise to the Fermi edge singularity and the Anderson orthogonality catastrophe, is an analytically tractable out of equilibrium problem in condensed matter. It describes the generic physics that occurs when a localized scattering potential is suddenly introduced in a Fermi sea leading to a brutal disturbance of its quantum state. We proposed that the effect can be efficiently simulated in a controlled manner using ultra-cold fermions trapped in an harmonic potential, so as to mimic solid-state-like situations, with the advantage of the great flexibility of the cold atoms platforms. For such a case, in particular, we studied the response of a degenerate Fermi gas by performing a diagrammatic many-body calculation that uses the linked cluster expansion in order to obtain the Green's function for the impurity. In time domain, this gives the so called vacuum persistence amplitude, while, in the frequency domain, the same quantity gives the spectrum of the single-particle excitations generated in the gas. We also analyzed the quench problem from a thermodynamic perspective, using the fullstatistics of the so called work distribution. The statistics of work have been shown to provide an accurate insight into the fundamental physics of the process.

Similar trends have been detecetd in the sudden response of the valence electrons of low dimensional nanostructured materials (e.g., fullerene molecules) to an x-ray pulse, which gives more suggestive insights into the generality of the treatment.

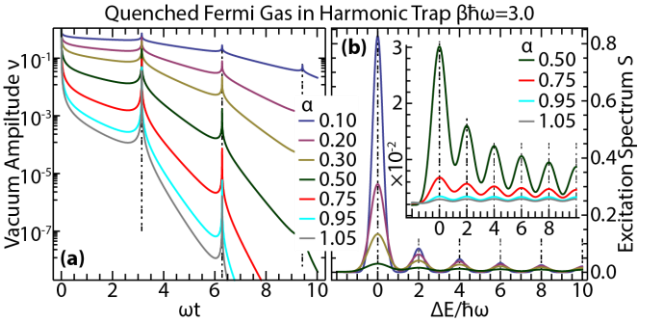

Figure 9.4 Sudden response (a) and excitation spectrum (b) of a gas of ultra-cold atoms, trapped into a harmonic potential of characteristic frequency ω and probed by a sudden, δ-like perturbation, which produces critical behavior of the many fermion system, associated to the critical exponent α. See Ref.[33] and [38].

9.3.2 *Local Perturbation in spin chains*

We considered the generation and propagation of local perturbations in the Ising model in transverse field in response to the presence of a local field defect (or an impurity spin) at one edge. The magnetic impurity gives a twofold effect: 1) the topological (Kitaev) Majorana mode in the ferromagnetic phase gets distorted; 2) a localized eigenmode appears, which itself becomes a zero mode within a one-dimensional subregion of the otherwise trivial topological phase.

As a consequence, the phase diagram in presence of the defect becomes much richer, due to the presence of either one or two of these localized modes. The localized character of these fermionic excitation is shown to i) enable a characterization of the Ising phase transition through a local-only measurement performed on the edge spin, and ii) strongly affect the propagation of quasi-particles emitted after the sudden removal of the defect, so that the dynamics of the local magnetization shows clear deviations from a ballistic behavior in presence of the Majorana fermions. In other words, the defect can serve as a probe of the spin system. Indeed, its population inversion, which is proportional

to the local transverse magnetization, gives a direct way to detect the phase of the whole spin chain despite the fact that the probe resides on the edge of the chain, while the phase is essentially a bulk property. Furthermore, when tuning the level spacing of the probe, the resulting disturbance propagation through the spin system shows a clear signature of the presence of the Majorana mode, enabling its detection. This is due to the fact that once the local quench is performed, quasiparticles are "emitted" from a finite region around the defect and are able to propagate throughout the system, unless they get pinned there because of the excitation of the Majorana mode.

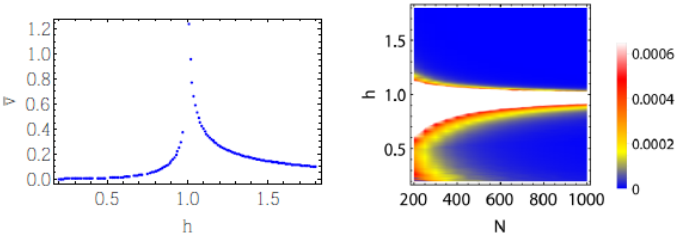

Figure 9.5: Left: Average asymptotic speed of the magnetization wave propagating in the Ising chain with N = 800 sites. Right: Scaling with the system size N and with the external field h of the amplitude of the long time oscillations displayed by the propagation speed v(t) around the average. In the white region the limiting speed is not well defined because of the persistence of its oscillations, due to the excitation of the Majorana mode. See Ref. [11] for more details

9.4 Decoherence and Memory effects

We developed a research line concerning the dynamics of open quantum systems undergoing non-Markovian evolution evolution. The study of memory effects, which can substantially modify the time evolution of an open system outside the Markovian regime, has become an intense field of activity in the last few years. In particular, we investigated the interplay between forgetful and memory-keeping evolution enforced on a quantum system by a spin environment whose elements are, in turn, connected to individual bosonic baths. Contrarily to the expectation that any non-Markovian effect would be buried by the forgetful mechanism induced by the spin-bath coupling, we actually showed that a full Markovian-to-non-Markovian transition of the system's dynamics takes place, which is controllable through accessible parameters such as the energy mismatch between the system and the spin environment.

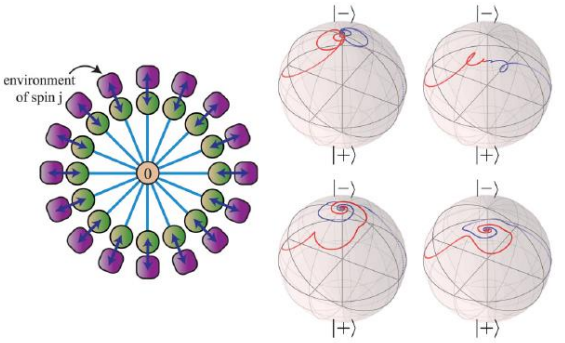

Figure 9.6 (Left) Skecth of a system in which the central spin 0 interacts with *N* peripheral spins, each affected by its own local environment. (Right) Evolution of two x-eigenstates of the central spin, for a star with $N = 4$ peripheral sites. The Bloch spheres in the first (second) column correspond

to an isotropic (anisotropic) spin-spin coupling. The top (bottom) row is for the resonant (off-resonant) case. In the isotropic cases, the final state of spin 0 is pure and resides on the surface of the sphere. For more details, see Ref. [44].

In a similar setting, we have established a connection among Loschmidt echo, non-Markovianity and Orthogonality Catastrophe (see Sec. 9.3), and studied a specific model in which decoherence occurs in a trapped fermion environment, which helps in highlighting such a link. We have also introduced a new geometric tool for the quantitative characterization of the departure from Markovianity of a given dynamical process, which is linked to the change of the volume of the set of physical states that are dynamically accessible to the open system during its evolution.

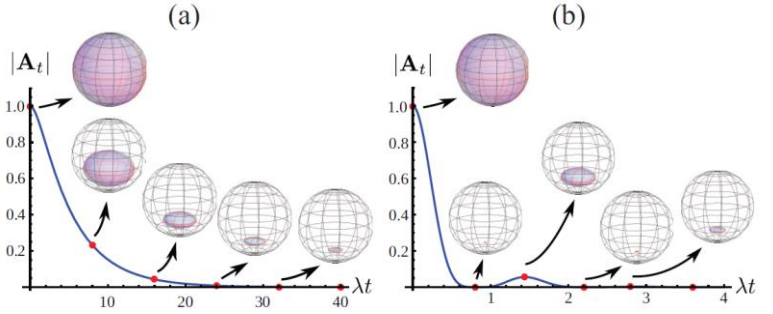

Figure 9.7 Time evolution of the determinant of the map for a generic Markovian (a) and non-Markovian dynamics (b). Quantitatively, the curves correspond to the spontaneous emission of a two-level system in a resonant leaky cavity with a Lorentzian spectral density of width λ.Panel (a) shows the Markovian case occurring in the bad cavity limit (with a coupling strenght much smaller than the cavity line width); while, panel (b) shows a non-Markovian evolution in the good cavity limit, where the determinant display a non- monotonic behavior. We also picture the set of accessible states (which is this case is the Bloch sphere), whose volume changes in time according to the behavior of the determinant. Taken from Ref. [40].

In general terms, non-Markovianity can be associated to a non-monotonous information flow: a system monotonously relaxing towards its equilibrium state will show no memory effects, as a unidirectional information flow occurs in this case, from the system towards its environment. Memory effects, on the other hand, will lead to an information back-flow towards the system. The latter can be modified, to some extent, if external actions are applied to the system, such as a coupling with some auxiliary sub-systems, or the switching of a further, coherent, transition channel.

9.5 Quantum Information and Quantum Correlations

Spin lattice models, originally employed to study magnetic insulator system and with the aim of exploring subtle statistical mechanics effects, such as cooperativity and universality, in the simplest possible scenarios, have attracted a renewd interest in the quantum information context. Spin ½ on a lattice, indeed, can be understood as quantum bits, locally addressable by magnetic field and correlated to their neighboring partners because of the exchange interaction.Quantum information can be encoded in the spin state, and magnetic interaction can be used to process this information or to communicate it towards a spin-qubit residing at a different site. In such a framework, the spin system can be seen as a quantum channel, a data bus that enables a high fidelity transfer of information from one site to another. We have investigated various schemes to control and guide this information transfer and have explored the role of quantum correlations both as a part of the information to be

transferred, and as a diagnostic tool to quantify the effectiveness of the control strategy or of the synchronization between distant qubits.

9.5.1 Quantum Correlations in spin systems

A primitive operation in a qubit register is the on demand decoupling of connected sites. We have explored the feasibility of such an operation, performed through the introduction of an impurity in an otherwise homogeneous spin system. Two-point magnetic correlations functions, Classical Correlations and Quantum Discord shared by spins residing on the two sides of the impurity have been shown to decay to zero even for a relatively modest values of the impurity strength. Such figures of merit certify the effective cutting of the spin connection.

Quantum correlations, on the other hand, can be used to reveal a connection established between distant spins by the action of an intermediary channel that is able to enforce their synchronization. In particular, the synchronization is shown not to be witnessed by the entanglement, but rather by quantum discord, whose generation by unitary operations has also been investigated in details. For two-qubit unitary evolutions, in particular, we have introduced a quantifier of the ability to produce discord, that we dubbed "discording power", which is shown to be optimized by a class of operations that include the square root of the SWAP.

Quantum correlations in general and discord in particular are also "naturally" contained in the ground state of interacting many-body systems. Specifically, for systems undergoing a phase transition, quantum correlations are known to re-arrange at the critical point, thus signalling the occurrence of the transition and, often, dysplang a critical, scaling behavior for finite size systems. In this context, we performed an extensive study of the properties of global quantum correlations in finite-size one-dimensional quantum spin models at finite temperature.

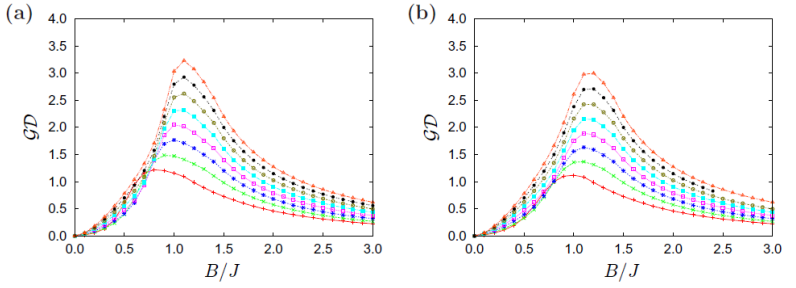

Figure 9.8: Global Discord for Ising rings containing from 3 to 10 spins at non-zero temperature: (a) $KT = 0.05\ J$ and (b) $KT = 0.1\ J$ (where J is the amplitude of the exchange coupling). For increasing temperatures, the maximum values of the curves decrease, while, in any case, the global discord is null at zero field. Taken from Ref. [42].

By adopting the recently introduced *global discord*, we were able to show that critical points can be neatly detected even for many-body systems that are not in their ground state.We considered the transverse Ising model, the cluster-Ising model where three-body couplings compete with an Ising-like interaction, and the nearest-neighbor XX Hamiltonian in transverse magnetic field. These models are canonical examples showing the sensitivity of global quantum discord close to criticality. For the Ising model, we found a universal scaling of global discord with the critical exponents pertaining to the Ising universality class.

9.5.2 Quantum Communication

We have proposed and characterized various information transfer protocols to be performed in one-dimensional spin chains, designed to work as information channels connecting sending a

receiving stages. In particular, we have analyzed single qubit states as well as entanglement transfer, which can be performed with a very high quality and on short time scales, provided some local magnetic field is applied near the sender and receiver sites. We have also analyzed the performance of two- and many-qubit state transfer between fixed senders and receivers and information routing as well, in which the targeted receiver site to be reached can be decided by applying properly designed magnetic barriers along the channel.

Figure 9.9: Sketch of the scheme for a 2 qubit state transfer, depicting the sender and receiver blocks coupled by a quantum channel to which they are coupled by weak links. For the analysis of various schemes analogous to this one, see Ref. [20] and [22].

9.6 Non-equilibrium thermodynamics and Irreversibility

In collaboration with researchers in Palma de Mallorca and Padova, we discussed the thermodynamics of closed quantum systems driven out of equilibrium by a change in a control parameter and undergoing a unitary process. We compared the work actually done on the system with the one that would be performed along ideal adiabatic and isothermal transformations. The comparison with the latter leads to the introduction of irreversible work, while that with the former leads to the introduction of inner friction, which quantifies the amount of non-adiabatic work. These two quantities can be treated on an equal footing, as both of them can be linked with the heat exchanged in thermalization processes and both can be expressed as relative entropies. Furthermore, we showed that a specific fluctuation relation for the entropy production associated with the inner friction exists, which allows the latter to be written in terms of its cumulants.
Moreover, we have investigated the concepts of inner friction, non-adiabaticity and energy dissipation an exactly solvable physical model of a thermal quantum engine, where the working substance consists of an ensemble of misaligned spins interacting with a magnetic field and performing the Otto cycle. The effect of static disorder under a finite-time cycle gives a new perspective of the concept of inner friction under realistic settings, as we have been able to relate the efficiency and power of this engine to the amount of friction due to spin misalignment (disorder) and to the temperature difference between the heat baths. Finally, we have proposed an alternative experimental implementation of the cycle, where the spin is encoded in the polarization degree of freedom of single photons.

9.7 Outreach activities

The group has devoted a substantial part ot its activity to science popularization, educational entertainment and outreach activities on a local scale, in particular within primary and high schools of the region. We have been involved in the editorial staff and as the host of the weekly radio broadcast “The Sound of Science”, collaborated with the “Città dei Ragazzi” in Cosenza to put forward summer educational activities, and coordinated many school activities with nearby high schools. Among all our outreach actions, the more relevant are the following:

- **Liceo delle Tecnologie Fisiche e dei Materiali**

This is an experimental proposal for high School teaching that has started in September 2016 at Liceo scientifico “E. Fermi”, Cosenza. It is based on the idea of allowing highschool students to attend special laboratory sessions dedicated to physics and material science, and is run as a collaboration between Liceo “E. Fermi” and the Physics dpt. at UNICAL. The experimental activities are based on those put forward for the “Progetti Lauree Scientifiche”, which included Lab. projects performed in various schools in Calabria in the past years. The underlying motivation is that of steering the

educational programs of the Liceo towards the scientific and technological market by including additional classes that aims at improving abilities in the Key Enabling Technologies (KET) defined by the EU commission; namely, nanotechnology, advanced materials, photonics, biotechnology micro- and nano-electronics.

- **Training course for high-school physics teachers**
  "La didattica della fisica nelle nuove indicazioni ministeriali"

The training course, attended by matematics and physics teachers has addresses mainly modern physics subjects that are now included in the fifth year programs according to the new ministerial indications. In particular, the course, held at Liceo Scientifico "E. Fermi", has included 20 hours dedicated to the teaching strategies to convey basic aspects of quantum mechanics to high-school students.

- **"Quando la Scienza si poteva immaginare"**

This is the title of a science popularization book by prof. G. Falcone, dedicated to the description of scientific thinking and language, published by Aracne ed. in 2015. It recounts the story of scientific developments with an emphasis on the creation of new scientific language and ideas that occurred before the scientific revolutions of XX century and that paved the way to relativity and quantum mechanics.

A. PUBLICATIONS ON SCIENTIFIC JOURNALS

A.1 Publications on international journals

A.1.1 Publications on international journals printed in the period 2013-2016

1. P. Riccardi, "The beauty of outreach", Science **354**, 674 (2016).

2. P. Riccardi, A. Sindona, C. A. Dukes, "Evidence for charge exchange effects in electronic excitations in Al by slow singly charged He ions", Nucl. Inst. Meth. In Phys. Res. B **382**, 7 (2016).

3. P. Riccardi, A. Sindona, C. A. Dukes, "Double electron excitation in He ions interacting with an aluminum surface°, Phys. Rev. A **93,** 042710 (2016).

4. M. Pisarra, A. Sindona, M. Gravina, V. M. Silkin, J. M. Pitarke, "Dielectric screening and plasmon resonances in bilayer graphene", Phys. Rev. B **93**, 035440 (2016).

5. C. Vacacela Gomez, M. Pisarra, M. Gravina, J. M. Pitarke, A. Sindona, "Plasmon modes of graphene nanoribbons with periodic planar arrangements", Phys. Rev. Lett. **117**, 116801 (2016).

6. P. M. Sheverdyaeva, R. Requist, P. Moras, S. K. Mahatha, M. Papagno, L. Ferrari, E. Tosatti, and C. Carbone, "Energy-momentum mapping of d-derived Au(111) states in a thin film", Phys. Rev. B **93**, 035113 (2016).

7. Q. Dubout, F. Calleja, G. Sclauzero, M. Etzkorn, A. Lehnert, L. Claude, M. Papagno, F. D. Natterer, F. Patthey, S Rusponi, A. Pasquarello and H. Brune, "Giant apparent lattice distortions in STM images of corrugated sp2-hybridised monolayers", New J. Phys. **18**, 103027 (2016);

8. A. Barla, V. Bellini, S. Rusponi, P. Ferriani, M. Pivetta, F. Donati, F. Patthey, L. Persichetti, S. K Mahatha, M. Papagno, C. Piamonteze, S. Fichtner, S. Heinze, P. Gambardella, H.

Brune, C. Carbone, “Complex Magnetic Exchange Coupling between Co Nanostructures and Ni (111) across Epitaxial Graphene”, ACS NANO **10**, 1101 (2016).

9. C. Carbone, P. Moras, P. M. Sheverdyaeva, D. Pacilè, M. Papagno, L. Ferrari, D. Topwal, E. Vescovo, G. Bihlmayer, F. Freimuth, Y. Mokrousov, and S. Blugel, “Asymmetric band gaps in a Rashba film system”, Phys. Rev. B **93**, 125409 (2016).

10. M. Papagno, S.V. Eremeev, J. Fujii, Z. S. Aliev, M. B. Babanly, S. Kr. Mahatha, I. Vobornik, N. T. Mamedov, D. Pacilè and E. V. Chulkov, “Multiple Coexisting Dirac Surface States in Three- Dimensional Topological Insulator PbBi6Te10”, ACS NANO **10,** 3518 (2016).

11. G. Francica, T. J. G. Apollaro, N. Lo Gullo, F. Plastina, “Local Quench, Majorana Zero Modes, and Disturbance Propagation in the Ising chain”, Phys. Rev. B **94**, 245103 (2016).

12. A. Karlsson, F. Francica, J. Piilo, F. Plastina, “Quantum Zeno effect and non-Markovianity in a three-level system”, Sc. Rep. **6**, 39061 (2016).

13. S. Lorenzo, F. Ciccarello, G. M. Palma, “Class of exact memory-kernel master equations”, Phys. Rev. A **93**, 052111 (2016).

14. S. Lorenzo, R. McCloskey, F. Ciccarello, M. Paternostro, G. M. Palma, “Landauer's Principle in Multipartite Open Quantum System Dynamics”, Phys. Rev. Lett. **115**, 120403 (2015).

15. P. Moras, P.M. Sheverdyaeva, D. Pacile', C. Carbone, “Spectroscopic signatures of an ordered array of independent Ag heptamers”, J. Phys.: Condens. Matter **27**, 305502 (2015).

16. A Crepaldi, R. R. Zhan, S. Moser, P. M. Sheverdyaeva, C. Carbone, M. Papagno, P. Moras, A.Baraldi and M. Grioni, “Interplay between electronic and structural properties in the Pb/Ag(1 0 0) interface”, *J.Phys.: Condens. Matter* **27,** 455502 (2015).

17. P. Moras, G. Bihlmayer, P. M. Sheverdyaeva, S. K. Mahatha, M. Papagno, J. Sanchez-Barriga, O. Rader, L. Novinec, S. Gardonio, and C. Carbone, “Magnetization-dependent Rashba splitting of quantum well states at the Co/W interface”, Phys. Rev. B **91**, 195410 (2015).

18. D. Mencarelli, S. Bellucci, A. Sindona, L. Pierantoni, “Spatial dispersion effects upon local excitation of extrinsic plasmons in a graphene micro-disk”, J. Phys. D. Applied Physics **48**, 465104 (2015).

19. P. Riccardi, A. Sindona, C. A. Dukes, “Electron emission and electronic stopping in the interaction of slow helium ions with aluminum”, Phys. Rev. B **92**, 045425 (2015).

20. T. J. G. Apollaro, S. Lorenzo, A. Sindona, S. Paganelli, G. Giorgi, F. Plastina, “Manyqubit quantum state transfer via spin chains”, Physica Scripta T **165**, 014036 (2015).

21. A. Alecce, F. Galve, N. Lo Gullo, L. Dell’Anna, F. Plastina, R. Zambrini, “Quantum Otto cycle with inner friction: finite time and disorder effects”, New J. Phys. **17**, 075007 (2015).

22. S. Lorenzo, T. J. G. Apollaro, S. Paganelli, G. M. Palma, F. Plastina, “Transfer of arbitrary

two qubit states via a spin chain", Phys. Rev. A **91**, 042321 (2015).

23. A. Sindona, M. Pisarra, M. Gravina, C. Vacacela Gómez, P. Riccardi, G. Falcone, F. Plastina, "Statistics of Work and Orthogonality Catastrophe in discrete level systems: an application to fullerene molecules and ultracold trapped Fermi gases", Beilstein J. Nanotechnol. **6**, 755 (2015).

24. D. Pacilè, S. Lisi, I. Di Bernardo, M. Papagno, L. Ferrari, M. Pisarra, M. Caputo, S. K. Mahatha, P. M. Sheverdyaeva, P. Moras, P. Lacovig, S. Lizzit, A.Baraldi, M. G. Betti, C. Carbone, "Electronic structure of graphene/Co interfaces", Phys. Rev. B **90**, 195446 (2014).

25. M. Pisarra, D. Pacilè, P. Moras, P. M. Sheverdyaeva, A. Sindona, M. Papagno, C. Carbone, "Electronic structure of epitaxial graphene grown on stepped Pt(997)", Phys. Rev. B **89**, 195438 (2014).

26. E. Cappellutti, L. Benfatto, M. Papagno, D. Pacilè, P. M. Sheverdyaeva, P. Moras, "Massless Dirac cones in graphene: Experiments and theory", Ann. der Phys. **526**, 387 (2014).

27. L. Massimi, S. Lisi, D. Pacilè, C. Mariani, M. G. Betti, "Interaction of iron phthalocyanine with the graphene/Ni(111) system", Beilstein J. Nanotech.**5**, 308 (2014).

28. M. Pisarra, P. Riccardi, A. Sindona, A. Cupolillo, N. Ligato, C. Giallombardo, L. Caputi, "Probing graphene interfaces with secondary electrons", Carbon **77**, 796 (2014).

29. N. Ligato N, A. Cupolillo, A. Sindona, P. Riccardi, M. Pisarra, L. Caputi, "A comparative study of the plasmonic properties of graphene on lattice-matched and lattice-mismatched Ni surfaces", Surf. Science **626**, 40 (2014).

30. M. Pisarra, A. Sindona, P. Riccardi, V. M. Silkin, J. M. Pitarke, "Acoustic plasmons in extrinsic free- standing graphene", New J. Phys. **16**, 083003 (2014).

31. F. Plastina, A. Alecce, T. J. G. Apollaro, G. Falcone, G. Francica, F. Galve, N. Lo Gullo, R. Zambrini, "Irreversible work and inner friction in quantum thermodynamic processes", Phys. Rev. Lett. **113**, 260601 (2014).

32. T. J. G. Apollaro, S. Lorenzo, C. Di Franco, F. Plastina, M. Paternostro, "Competition between memory- keeping and memory-erasing decoherence channels", Phys. Rev. A **90**, 012310 (2014).

33. A. Sindona, N. Lo Gullo, J. Goold, F. Plastina, "Statistics of the work distribution for a quenched Fermi gas", New J. Phys. **16**, 045013 (2014).

34. M. Papagno, P. Moras, P. M. Sheverdyaeva, J. Doppler, A. Garhofer, F. Mittendorfer, J. Redinger, C. Carbone, "Hybridization of graphene and a Ag monolayer supported on Re(0001)", Phys. Rev. B **88,** 235430 (2013).

35. D. Pacilé, P. Leicht, M. Papagno, P. M. Sheverdyaeva, P. Moras, C. Carbone, K. Krausert, L. Zielke, M. Fonin, Y. S. Dedkov, F. Mittendorfer, J. Doppler, A. Garhofer, J.

Redinger, “Artificially Lattice Mismatched Graphene/Metal Interface: Graphene/Ni/Ir(111)”, Phys. Rev. B **87,** 035420 (2013).

36. T. J. G. Apollaro, F. Plastina, L. Banchi, A. Cuccoli, R. Vaia, P. Verrucchi, M. Paternostro, “Effective cutting of a quantum spin chain by bond impurities”, Phys. Rev. A **88**, 052336 (2013).

37. G. L. Giorgi, F. Plastina, G. Francica, R. Zambrini, “Spontaneous synchronization and quantum correlation dynamics of open spin systems”, Phys. Rev. A **88**, 042115 (2013).

38. A. Sindona, J. Goold, N. Lo Gullo, S. Lorenzo, F. Plastina, “Orthogonality catastrophe and decoherence in a trapped-Fermion environment”, Phys. Rev. Lett. **111**, 165303 (2013).

39. F. Plastina, A. Sindona, J. Goold, N. Lo Gullo, S. Lorenzo, “Decoherence in a fermion environment: Non- Markovianity and Orthogonality Catastrophe”, Open Sys. & Information Dyn. **20**, 1340005 (2013).

40. S. Lorenzo, F. Plastina, M. Paternostro, “Geometrical characterization of non-Markovianity”, Phys. Rev. A (R) **88**, 020102 (2013).

41. S. Paganelli, S. Lorenzo, T. J. G. Apollaro, F. Plastina, G. L. Giorgi, “Routing quantum information in spin chains”, Phys. Rev. A **87**, 062309 (2013).

42. S. Campbell, L. Mazzola, G. De Chiara, T. J. G. Apollaro, F. Plastina, Th. Busch, M. Paternostro, “Global quantum correlations in finite-size quantum spin chains”, New J. Phys. **15**, 043033 (2013).

43. S. Lorenzo, T. J. G. Apollaro, A. Sindona, F. Plastina, “Quantum-state transfer via resonant tunneling through local-field-induced barriers”, Phys. Rev. A **87**, 042313 (2013).

44. S. Lorenzo, F. Plastina, M. Paternostro “Tuning non-Markovianity by spin-dynamics control”, Phys. Rev. A **87**, 022317 (2013).

45. A. Sindona, M. Pisarra, F. Naccarato, P. Riccardi, F. Plastina, A. Cupolillo, N. Ligato, L. S. Caputi, G. Falcone, “Core hole effects in fullerene molecules and small-diameter conducting nanotubes: a density functional theory study”, J. Phys.: Condens. Matter **25**, 115301 (2013).

46. T. J. G. Apollaro, S. Lorenzo, F. Plastina, “Transport of Quantum Correlations across a spin chain”, Int. J. Mod. Phys. B **27**, 1345305 (2013).

47. F. Galve, F. Plastina, M. G. A. Paris, R. Zambrini, “Discording power of quantum evolutions”, Phys. Rev. Lett. **110**, 010501 (2013).

48. P Riccardi, M Pisarra, A Sindona, A Cupolillo, N Ligato, LS Caputi, “High Energy Excited States of Graphene Adsorbed on Ni(111), Nanosc. & Nanotech. Lett. **5**, 1191 (2013).

49. P. Riccardi, A. Sindona, C. A. Dukes, “Local charge exchange of He+ ions at Aluminum surfaces”, Phys. Lett. A **381**, 1174 (2013).

50. A. Sindona, F. Naccarato, M. Pisarra, P. Riccardi, G. Falcone, “Dynamic core hole screening in small- diameter conducting carbon nanotubes: a cluster density functional study”, THIN SOLID FILMS **543**, 41 (2013).

A.1.2 Publications on international journals accepted in 2016

1. G. Avvisati, S. Lisi, P. Gargiani, A. Della Pia, O. De Luca, D. Pacilé, C. Cardoso, D. Varsano, D. Prezzi, A. Ferretti, and M. G. Betti, “ FePc Adsorption on the Moiré Superstructure of Graphene Intercalated with a Cobalt Layer”, accepted by J. Phys. Chem. (2016).

2. I. Grimaldi, M. Papagno, L. Ferrari, P.M. Sheverdyaeva, S.K. Mahatha, D. Pacilé, C. Carbone, “Magnetic decoupling of ferromagnetic metals through a graphene spacer”, accepted by Journal of Magnetism and Magnetic Materials (2016).

3. J. Settino, N. Lo Gullo, A. Sindona, J. Goold, F. Plastina, “Signatures of the single particle mobility edge in the ground state properties of Free Fermion and Tonks-Girardeau gases in a bichromatic potential”, accepted by Phys. Rev. A.

4. G. Francica, J. Goold, F. Plastina, M. Paternostro, “Daemonic Ergotropy: Enhanced Work Extraction from Quantum Correlations”, accepted by Nature pj Quantum Information.

5. C. Vacacela Gomez, M. Pisarra, M. Gravina, P. Riccardi, and A. Sindona, “Plasmon properties and hybridization effects in silicone”, accepted by Phys. Rev. B.

B. PUBLICATIONS ON CONFERENCE PROCEEDINGS

B.1 Publications on international conference proceedings in the period 2013-2016

1. C. Vacacela Gomez, M. Pisarra, M. Gravina, S. Bellucci, A. Sindona, “ Ab initio modelling of dielectric screening and plasmon resonances in extrinsic silicone”, IEE CONFERENCE PUBLICATION, p. 63-66, ISSN: 0537-9989, doi: 10.1109/RTSI.2016.7740557, 2016;

2. L. Pierantoni, D. Mencarelli, A. Sindona, S. Bellucci, “Comparison of rigorous vs approximate methods for accurate calculation of 2D-materials band structures and applications to THz nanoelectronics”, IEE CONFERENCE PUBLICATION, p. 1-3, ISSN: 0537-9989, doi: 10.1109/MWSYM.2015.7167142, 2015;

3. S. Bellucci, A. Sindona, D. Mencarelli, L. Pierantoni, “Electromagnetic characterization of graphene and graphene nanoribbons via ab-initio permittivity simulations”, IEE CONFERENCE PUBLICATION, p. 926-929, ISSN: 0537-9989, doi: 10.1109/ICEAA.2015.7297251, 2015

4. L. Pierantoni, D. Mencarelli, A. Sindona, M. Gravina, M. Pisarra, C. Vacacela Gomez, S. Bellucci, “Innovative full wave modeling of plasmon propagation in graphene by dielectric permittivity simulations based on density functional

theory”, IEE CONFERENCE PUBLICATION, p. 1-3, ISSN: 0537-9989, doi: 10.1109/MWSYM.2015.7167130, 2015;

5. L. Pierantoni, D. Mencarelli, A. Sindona, M. Gravina, M. Pisarra, L. Spurio, S. Bellucci, “Advanced techniques for the band structure-quantum transport modeling in graphene and 2D-materials beyond graphene”, PROCEEDINGS OF THE IEEE CONFERENCE ON NANOTECHNOLOGY, p. 624-627, ISSN: 1944-9399, doi: 10.1109/NANO.2014.6968186, 2014

6. L. Pierantoni, D. Mencarelli, M. Bozzi, R. Moro, A. Sindona, L. Spurio, S. Bellucci, “Full-wave techniques for the electromagnetic-quantum transport modeling in nano-devices”, IEE CONFERENCE PUBLICATION, p. 11-16, ISSN: 0537-9989, doi: 10.1109/SMICND.2014.6966379, 2014.

C. BOOK CHAPTERS

1. A Sindona, M. Pisarra, D. Mencarelli, L. Pierantoni, S. Bellucci, “Plasmon modes in extrinsic graphene: ab initio simulations vs semi-classical models”. In: “Fundamental And Applied Electromagnetics”, NATO SCIENCE FOR PEACE AND SECURITY SERIES. B, PHYSICS AND BIOPHYSICS, editors: A. Maffucci and S.Maksimenko, SPRINGER VERLAG GMBH, ISBN: 9401774889, ISSN: 1874-6500, doi: 10.1007/978-94-017-7478-9, 2016.

2. S. Bellucci, D. Mencarelli, A. Sindona, L. Pierantoni, “Excitation of surface-waves at terahertz frequencies on a suspended graphene sheet”, in “Nanoscale excitations in emergent materials”, editors: A. Marcelli, C. Balasubramanian, published by Superstripes Onlus, ISBN: 9788866830450, 2015.

D. INVITED PRESENTATIONS

D1. Invited presentations at international conferences in the period 2013-2016

1. A. Sindona, "Plasmon Modes of Graphene NanoRibbons with Periodic Planar Arrangement: Ab
   Initio stratagies on Small-Size Arrays, Experimental Observations and possible apllications to
   Nanoelectronics", invited talk at "NANOSCIENCE & NANOTECHNOLOGY 2016", September 30 2015, Frascati, Italy.

2. F. Plastina, “Signatures of mobility edge for fermions and bosons in a bichromatic lattice”, invited talk at the conference “Taming Quantum Noise-TQN 2016”, September 9, 2016, Mazara del Vallo (TP), Italy;

3. F. Plastina, “Dynamics of the Driven Dicke Model: Time Dependent Mean Field and Quantum Fluctuations”, invited talk at the conference “PIERS 2016”, August 9, 2016, Shanghai, China;

4. A. Sindona: "Time Dependent Density Functional approach to Optical Plasmon modes in Graphene", invited talk at "NANOSCIENCE & NANOTECHNOLOGY 2015", September 30 2015, Frascati, Italy.

5. F. Plastina, “Geometrical Aspects of non-markovianity”, invited talk at the conference “Non-Markovian Quantum Dynamics”, August 25 2015, Cortona (AR), Italy

6. F. Plastina, “Non-adiabaticity and irreversible entropy production”, invited talk at “PIERS 2015”, July 7 2015, Prague, Czech Republic;

7. A. Sindona, "Work distribution and Dynamic Core-Hole screening in carbon based nanostructures: a Quantum Thermodynamic Model at the NanoScale", invited talk at "Nanostructures and Nanomaterials Self Assembly 2014”, July 08 2014, Marseille, France.

8. A. Sindona, "Work distribution, Dynamic Core Hole Screening, and Dielectric Properties of
Nanocarbon Materials: Statistical Field Theory Approaches and Experimental Measurements of the
Anderson Orthogonality Catastrophe in Fullerene Films", "NANOSCIENCE & NANOTECHNOLOGY 2014" October 06 2014, Frascati, Italy.

9. F. Plastina, “Generation of quantum correlations in spin systems", invited talk at the 23th International Laser physics workshop “LPHYS'14”, July 16 2014, Sofia, Bulgaria;

10. F. Plastina, “Geometrical description of non-Markovianity", invited talk gven at “Twin workshop on complex quantum systems", May 28 2013, Wick, UK;

11. A. Sindona, "Anderson Orthogonality Catastrophe in Nanostructured Systems: Statistical Field Theory Approaches and Experimental Observations", invited talk at "NANOSCIENCE & NANOTECHNOLOGY 2013", September 30 2013, Frascati, Italy.

D2. Invited presentations at national conferences in the period 2013-2016

1. F. Plastina, “Non-adiabaticity and irreversible entropy production”, invited talk at “FISMAT2015” October 2 2015, Palermo, Italy;

2. F. Plastina, “Decoherence in a Fermion environment: non-Markovianity and Fermi edge singularity", invited talk given at ``IQIS 2013”, 6th Italian Quantum Information Science Conference, 25 September 2013, Como, Italy

E. PRESENTATIONS AT CONFERENCES

E1. Presentations at international conferences in the period 2013-2016

1. F. Plastina, “Local Quench and Probing in the Ising chain", at the First QuProQS Meeting, March 9 2016, Milano, Italy

2. F. Plastina, “Non-adiabaticity and irreversible entropy production”, talk given at the ``2nd Quantum thermodynamics Conference", April 20 2015, Palma de Mallorca, Spain

3. F. Plastina, “Irreversible work and inner friction in quantum thermodynamic processes”, talk given at the conference “Quantum thermodynamics”, August 19 2014, Belfast, UK

4. M. Papagno: “Novel mismatched graphene-ferromagnetic interfaces”, talk given at FisMat 2013, September 9, 2013, Milano, Italy

5. D. Pacilè, “Graphene-ferromagnet interfaces”, talk given at The European Workshop on Epitaxial Graphene and 2D Materials, June 15, 2014, Primonsten, Croatia

6. D. Pacilè, “Shielding effect of graphene within ferromagnetic metals”, talk given at FisMat2015, September 28, 2015, Palermo, Italy

7. P. Riccardi, “Electron promotion effects in the interaction of slow ions with Al surface” talk given at the Conference “Inelastic Ion Surface collisions – IISC 21”, October 20 2015, San Sebastian, Spain.

F. INTERNATIONAL AND NATIONAL PROJECTS

1. FIRB Futuro in Ricerca 2010 “PlasmoGraph: Plasmons and terahertz device in graphene”, Grant N. RBFR10M5BT, Principal investigators: Marco Polini (NEST, CNR Pisa) and Daniela Pacilè (UNICAL) Grant budget: 754180 €, Time span: March 2012-March 2015.

2. FET PROACTIVE-Quantum Simulation project QUPROCS - Quantum Information Probes for Complex Systems, Grant Agreement 641277, Time span: 2015-2018 (Local Principal investigator F. Plastina, the group is included in the Italian node based in Milan).

3. COST Action MP1209, “Thermodynamics in the quantum regime”, Time span: 2013 – 2017 (Local coordinator: F. Plastina).

4. NEMESYS - INFN Specific Initiative 2017-2020, National Coordinator A. Sindona.

5. SEMS - INFN Specific Initiative 2013-2016, Local Coordinator A. Sindona.

6. Project “CoDe – Correlazioni e Decoerenza”, funded within the POR Calabria – FSE 2007/2013, Asse IV “Capitale Umano”, Piano Regionale per le Risorse Umane – Piano d’Azione 2011/2013 - Obiettivo Operativo M.2 Intervento D.3, ARUE programme, Scientific Responsible: F. Plastina

7. Project “PESCI – Processi di Eccitazione elettronica e Scambio di Carica in Interazioni ioni-superfici”, funded within the POR Calabria – FSE 2007/2013, Asse IV “Capitale Umano”, Piano Regionale per le Risorse Umane – Piano d’Azione 2011/2013 - Obiettivo Operativo M.2 Intervento D.3, ARUE programme, Scientific Responsible: P. Riccardi

8. Project “PENC – Processi Elettronici in Nanotubi di Carbonio”, funded within the POR Calabria – FSE 2007/2013, Asse IV “Capitale Umano”, Piano Regionale per le Risorse Umane – Piano d’Azione 2011/2013 - Obiettivo Operativo M.2 Intervento D.3, ARUE programme, Scientific Responsible: A. Sindona

9. Project “SISMIC – SImulazioni e Spettroscopie elettroniche di Materiali Innovativi a base di Carbonio”, funded within the POR Calabria – FSE 2007/2013, Asse IV “Capitale Umano”, Piano Regionale per le Risorse Umane – Piano d’Azione 2011/2013 - Obiettivo Operativo M.2 Intervento D.3, ARUE programme, Scientific Responsible: G. Falcone.

10. SURFACE ELECTRON SPECTROSCOPY (SPES)

Professors and Researchers	Elio Colavita Raffaele Giuseppe Agostino Vincenzo Formoso Tommaso Caruso
Postdoc fellows	Alfonso Policicchio Sara Stelitano Francesco Demetrio Minuto Raffaele Filosa Valentino Pingitore Tania Rugiero
PhD students	José Francisco Brito del Pino Oreste De Luca Giuseppe Scionti
EOMAT Fellowships and collaborators	Giuseppe Conte Victor Lazzaroli Giuseppe Demofonti
Technicians	Giovanni Desiderio (Nanotec/CNR) Vito Fabio Eugenio Li Preti
Collaborators	Valeria Alzari, Alberto Mariani, *Dip. di Chimica e Farmacia, Univ. di Sassari (I)* Teresa J. Bandosz *The City College of New York, CUNY (USA)* Alberto Bravin, *ESRF synchrotron (F)* Carlo Spartaco Casari, Andrea Li Bassi, *Dip. di Energia, Politecnico di Milano (I)* Alessia Cedola, Federica Ciuchi, *CNR Nanotec – Roma - Rende (CS) (I)* Giovanni Costantini *Department of Chemistry – University of Warwick (UK)* Dimitris Gournis, *Dep. of Materials Science & Engineering, Un. of Ioannina (GR)* Michael Hirscher *Max Planck Institute for Intelligent Systems - Stuttgart, (D)* Mirosław Kwiatkowski, *AGH University of Science and Technology, Krakow (PL)* Daniela Pacilé, Marco Papagno. E. Cazzanelli, M. Castriota, N. Scaramuzza, M. De Santo, *Dipartimento di Fisica – Università della Calabria* Petra Rudolf, *Zernike Institute for Advanced Materials, Un. of Groningen, (NL)* A. Taliano Grasso, *Dipartimento di Studi Umanistici – Università della Calabria*

Lorenzo Ulivi, Milva Celli, Daniele Colognesi, *ISC-CNR - Sesto Fiorentino (FI), IT*
Franco Zanini, *Elettra Sincrotrone Trieste, Trieste (I)*
M. Migliori, G. Giordano, D. Vuono, A. Aloise, *DIATIC – Università della Calabria*

Introduction

The activities of the Surface Science group in the 2013-2016 period underwent to an important evolution: a series of new initiatives were put in place starting from both the knowledge developed by investigating the surface properties and the skills acquired by developing new spectroscopic tools. Beside to the traditional **electronic spectroscopies**, the interest of the group was focused to the **spectro-microscopic characterization of nanostructured materials** in the field of the **energy conversion and storage**.

A series of research project allowed to establish new branches of the SPES laboratory together with the participation to joint research initiatives as the DeltaH laboratory and the **PON Materia** laboratories (**STAR_Lab** and Advanced Spectroscopy and Microscopy Lab - **LSAM**).

A strong effort was placed into the realization of **new laboratory equipment** in order to pave the way to a deeper investigation of the molecule-to-surface interaction processes as the adsorption of energy carrier gases in ultramicroporous materials and the electronic properties of dye molecular layers on active substrates.

After the realization of the microtomographic experimental station **µTomo** at the STAR light source, a new series of activities was started in the **Cultural Heritage** field by applying the SPES tools to investigate the hidden features of archaeological matters and decipher the traces that they bring us from the past.

Since 2000, SPES group continues its strong interaction with **DeltaE**, a research spin-off company working in the prototypal instruments development field.

Research subjects:

10.1. SPECTROSCOPIC AND MICROSCOPIC STUDIES OF CARBON AND METAL-OXIDE NANOSTRUCURES.

10.1.1. Synchrotron studies of dye molecules on nanostructured anatase

The chemical and physical characterization of an organic-inorganic interface is a key issue for the effective understanding of the charge transfer mechanism between a photoexcited molecule and a substrate. Beside the studies on ordered molecular overlayers on crystalline surfaces it is nowadays important to address more complex interfaces i.e. nanostructured films functionalized by a dye. These systems are in fact more and more used in photovoltaic and dye-sensitized or hybrid solar cell applications.

The adsorption of Zn-tetraphenylporphyrin (ZnTPP) on nanoporous hierarchically organized anatase TiO2 structures and the properties of the corresponding hybrid interface were studied by synchrotron radiation experiments.

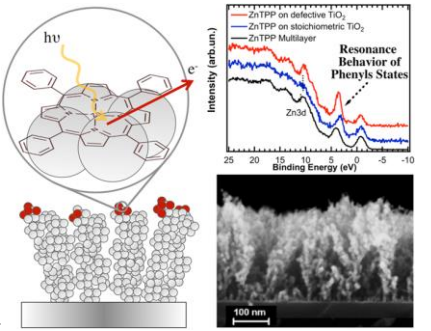

The molecular structure, electronic properties, and bonding with nanostructured TiO2 surfaces were analyzed by photoemission (XPS and UPS) and X-ray absorption spectroscopy (XAS). The charge transfer at the interface was investigated by means of valence band resonant

photoemission experiments (ResPES) at the C K-edge. We could show that the charge-transfer dynamics between the photoexcited ZnTPP and TiO2 is strongly influenced by the presence of defects on the TiO2 surface. On a stoichiometric anatase nanostructure, ZnTPP bonding occurs primarily via carbon atoms belonging to the molecular phenyl rings, and this creates a preferential channel for the charge transfer. This phenomenon is reduced in the case of defective TiO2 surface, where ZnTPP interacts mainly through the molecule macrocycle. Our results represent a surface science study of the dye molecule behavior on a nanoporous TiO2 photoanode relevant to **dye-sensitized or hybrid solar cell applications**, and they show the importance of the surface oxidation state for the charge-transfer process.

These studies were accomplished in a collaboration effort with the Elettra-Sincrotrone Trieste and the Center for Nano Engineered Materials and Surfaces, Politecnico di Milano.

10.1.2. Polymeric nanocomposite films containing graphene and Ag, Au or ZnO nanoparticles

Composites materials are regularly addressed in research and technological processes in order to improve their behavior or to identify novel properties, by exploiting synergic effects. As a matter of fact, the mixing of polymers and nanoparticles is interesting for engineering flexible composites that exhibit advantageous properties.

Polymeric nanocomposite films containing graphene and Ag, Au or ZnO nanoparticles were synthesized, and their morphological, thermal, surface and dielectric properties were studied. Graphene was obtained by the sonication method, and the interaction between graphene and the other nanoparticles (NPs) confers to these polymeric films interesting characteristics.

The results indicated that the nanoparticles were dispersed homogeneously within the polymer matrix of PTEGDA. It was found that the presence of both graphene and nanoparticles influences the film surface properties. In particular, the wettability and conductivity increases when the nanoparticles are added to the PTEGDA/graphene composites, thus paving the way for advanced applications.

These studies were accomplished in collaboration with the Dipartimento di Chimica e Farmacia, Università degli Studi di Sassari.

10.1.3. Self-assembling dye molecular layer

In recent years, the study of self-assembled monolayers (SAMs) of organic molecules on various substrates has assumed an important role in surface physics. These systems are very attractive, and the reasons of interest concern the synthesis of various advanced functional materials and devices through molecular manipulation, as well as the determination of their structures and physical and chemical properties.

The formation of a 2-dimensional self-assembled monolayer on a solid surface depends on several factors, among which the intermolecular interactions and the molecule-substrate interactions play an important role. Assemblies of molecular architectures, such as porphyrins, phthalocyanines and carboxylic acid compounds, can be studied on graphene and metal surfaces, in order to produce artificial molecular configurations. Several systems, including metal-organic and organic molecule/graphene interfaces, are investigated by microscopic (Atomic Force Microscopy - AFM and Scanning Tunneling Microscope – STM at LSAM laboratory of the Materia_lab cluster and at the Department of Chemistry, University of Warwick (UK)) and spectroscopic (X-Ray Photoemission Spectroscopy – XPS at Elettra Synchrotron) techniques.

Among the investigated systems, the iron-phthalocyanine (FePc) deposition on highly artificially corrugated graphene (Co intercalation) surface represented an interesting

topic. The preferential adsorption regions of the FePc molecules on the graphene Moiré superstructure and the interaction of the central Fe ion with the underlying Co were investigated. In this particular system, upon molecular adsorption, the distance of C atoms from the Co template mainly drives the strength of the molecules-substrate interaction, thereby allowing for locally different electronic properties within the corrugated interface.

Another focus of the SPES group research activity is the metal-organic interface between zinc(II) tetraphenylporphyrin (ZnTPP) molecules and Au(111) surface. Monolayer self-assembly was studied (see Figure 1 and 2), with a particular emphasis on the ZnTPP/Au(111) interaction. Moreover, mono- to bilayer transition was investigated (see Figure 3).

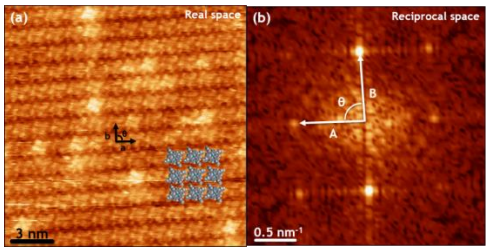

Figure 1. (a) 18x18nm2 STM acquisition of ZnTPP monolayer on Au(111) and (b) FFT analysis of (a) image. Tunneling parameters: U=0.9V, I=0.1nA. Unit cell parameters are: a=(13.9±0.1)Å, b=(13.6±0.3)Å, θ=89°±1°.

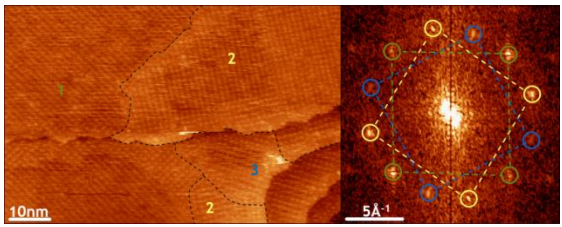

Figure 2. left: STM acquisition of three rotational domains of ZnTPP molecules on Au(111) surface; right: FFT analysis of left image. Tunneling parameters: U=1.2 V, I=0.1 nA. Each domain is rotated of about 30°± 2° relative to one another.

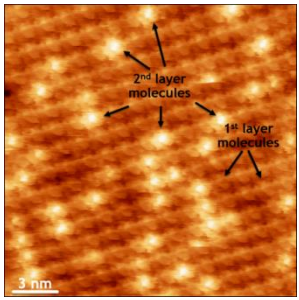

Figure 3. 20x20nm2 STM acquisition of ZnTPP molecules on Au(111). Tunneling parameters: U=1V, I=0.1nA. The darker spots represents 1st layer molecules, while the brighter spots are the 2nd layer molecules.

10.2.ENERGY-RELATED MATERIALS

10.2.1. Hydrogen storage

A possible method to increase the H_2 density is store it in solids via physisorption; thanks to weak interaction forces between the solid and the H_2 molecule, a dense H_2 layer it's created in proximity of the solid surface. The higher the surface the higher is the amount of H_2 physisorbed. For this reason the best materials suitable for hydrogen storage are porous materials exhibiting high surface area (SSA) as activated carbon, zeolites, silicas, MOF, COF, PNO, PMO etc.

Our aim is to understand the base mechanisms that regulate the adsorption of H_2 on different material's surface. The research activity is divided in three main areas: H_2 adsorption characterization, material synthesis, material characterization.

Molecular hydrogen adsorption characterization of different porous material is performed in our laboratories by mean of volumetric apparatus Sievert's like (PcT). H_2 adsorption storage capacity is evaluable up to 80 bar at different temperature, from 77 K up to 350 K. Standard routine measurements are performed by mean of commercial PcT while for advanced full customizable measurements we developed our prototypal Sievert's apparatus.

Materials engineering is the key to achieve hydrogen storage performance satisfying real application requirements. Our group is involved in this activity directly synthetizing porous material, like activated carbon form the pyrolysis of organic-based compound in controlled environment, either collaborating to develop new porous material with specific structural proprieties, like zeolite, carbon zeolite-like materials, nano- and meso-porous organosilicas.

Great importance and care is deserved to the material characterization since it is the link between the H_2 storage characterization and the material engineering activities. Analyzing the materials by mean of different techniques (Raman, XRD, XPS/UPS, XRF, STM, AFM, Porosimetry) we are able to find out which are material's structural proprieties affecting positively the storage performance. Successively, by using a feedback on the synthesis process, these performances are enhanced and developed in order to synthetize materials with improved storage performances.

10.2.2. Nanostructured materials for methane storage

Since 2007, the SPES group started working on porous systems for gas separation and storage in collaboration with European research center and Universities. In particular, a strong partnership has been established with the Universities of Ioannina and Crete (Greece), the National Research Council (ITM-CNR and CNR Nanotech) (Italy) and the Landi Renzo SpA company (Italy). Part of the research activities carried out from the group is focused on new kind of materials for application in the field of methane storage. In particular, the researcher developed a homemade apparatus in order to implemented a synthesis method, already discussed in literature, for the synthesis of High Specific Surface Area Activated Carbon (HSAC). The idea was to synthesize light and sponge like materials able to adsorb in reversible way as much methane as possible. At the same time, our Greek collaborators developed Periodic Mesoporous Organosilicas materials trying to optimizing structural properties. It is known, in fact, the dependence of the gas storage capacity on the specific surface area and porosity of the sample.

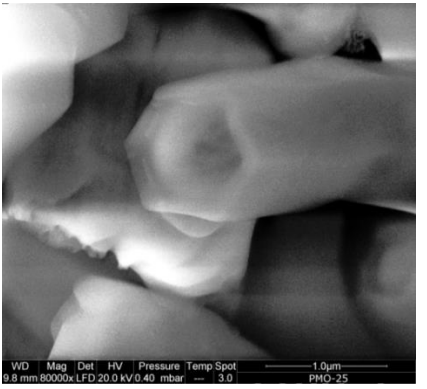

Scanning Electron Microscopy images of Periodic Mesoporous Organosilicas, an effective adsorbent for CH_4.

The characterization has been performed in collaboration with the Department Environmental Engineering and Land and Chemical Engineering - University of Calabria. The methane adsorption properties of the different samples were evaluated at room temperature (298K) and pressure up to 3.5 MPa using a new optimized volumetric apparatus f-PcT (fast Pressure-concentration-Temperature) for accurate and reliable gas adsorption measurements. The apparata was developed in collaboration with **DeltaE srl** (CNR Spin-off). A comprehensive characterization of different nano/mesostructured samples was carried out by means of helium picnometry for the skeletal density evaluation, by the Brunauer-Emmett-Teller (BET) method for the measurement of the surface area, by Scanning Electron Microscopy (SEM) and X-ray diffraction (XRD) for topography and long-range order estimation, respectively. Comparison with data available in the literature shows a good agreement in terms of maximum methane uptake on similar materials and an enhanced performance for the reversible adsorption at very low pressure. The probed HSAC samples, in fact, show both higher methane storage values for pressure up to 1.5 MPa and totally reversible methane uptake up to many cycles. These results represent the starting point for a real and efficient alternative method to the natural gas storage for static and/or automotive applications.

10.2.3. Organic nanostructures for CO2 capture and storage

In the last years, the CO_2 capture technologies are under study and development due to the necessity to decrease its environmental effects. For this reason, the SPES group focused part of its research activity to study CO_2 adsorption and capture into porous materials. This represented an opportunity to start new collaborations among which those with the Department of Chemical Engineering - City College of New York (USA) and the Faculty of Energy and Fuels - AGH University of Science and Technology (Poland). This partnership leads to analysis of MOF-based system and GO-based nanoporous carbon for the comprehension of the phenomena related to the CO_2 reversible adsorption. In the last cases, the adsorbents used have complex surfaces from the viewpoints of their porosity and chemistry. The addition of graphite oxide to the carbon and oxidation of the nanoporous carbon and its composite further modifies the surface,

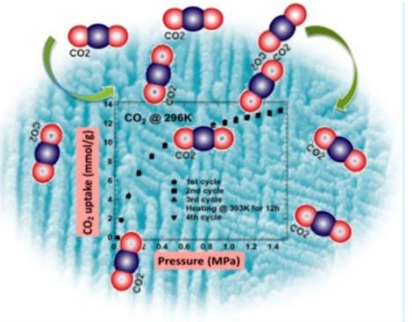

which has a visible effect on the thermodynamics of CO_2 interactions with these surfaces but also on the extent of its adsorption. Even though the volume of small pores is a main parameter governing the extent of the adsorption process, surface chemistry was found as important for the energetics of adsorption and for the clustering patterns the CO_2 molecules in the pore system. The results suggest that it is rather not the total number of polar groups, that has a marked impact on the adsorption mechanisms but it is their specific surface chemistry. It is possible that CO_2, upon being adsorbed, oxidizes sulfoxides and sulfones further modifying the surface features from the viewpoints of both, chemistry and texture.

Measurements performed on the MOF-based sample, in particular its composites with GO and aminated GO show a typical physical absorption mechanism with notable increase of the maximum storage capacity increasing the urea content together with specific thermal treatment. Using *f*-PcT apparata study and the characterization of the carbon dioxide adsorption properties on the different were carried out. Furthermore, the evaluation of maximum storage capacity, reversibility and sample recovery studies were performed to estimate the performances of each analyzed sample; calculation of the enthalpy of adsorption were obtained with the use of specific models.

Other preliminary and useful results on CO_2 capture were obtained on carbon nanotubes produced by CVD (Department Environmental Engineering and Land and Chemical Engineering – University of Calabria). Carbon nanotubes were analyzed through scanning electron microscopy (SEM), Raman spectroscopy and thermal gravimetric/differential analysis (TGA/DTA) measurements by the several tools present in our Department. A deeper analysis on the adsorption/desorption capacity was performed with the volumetric apparatus. The obtained results represent the starting point for the development of new carbon based materials using cheap and classical synthesis method.

10.3.RESEARCH PROJECTS

10.3.1. The PON MATERIA project

10.3.1.1. Advanced spectroscopy and microscopy laboratory (LSAM) at Materia_Lab

The SPES group is involved in the PON Materia project since its beginning on 2012. STAR-Lab and Materia-Lab have been founded after the MaTeRiA-project "Materials, Technology and Advanced Search" (PONa3_00370) as part of the “Sistema Tecnologico Materia” of the University of Calabria.
The Laboratory of Spectroscopy for Advanced Materials (LSAM) is a part of the Materia-Lab, a cluster of five laboratories in close collaboration with the STAR-Lab activities. LSAM delivers services on the spectro-microscopic haracterization of surfaces by means of a UHV apparatus equipped with an Advanced AFM/STM tool: a variable temperature Scanning Probe Microscope for AFM and STM operation (Specs - SPM Aarhus 150 with KolibriSensor™) in ultra-high vacuum (UHV) conditions.

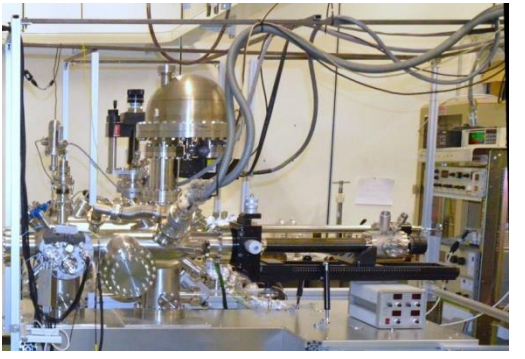

This is an indispensable tool for the surfaces physics since it allows to investigate the surface of both conductive

and insulators materials on an atomic scale. In particular, it allows to study both the electronic structure and the morphology of innovative materials as well as the dynamics of the chemical-physical processes occurring on surfaces that have a crucial role in catalysis, in the thin films growth and in sensor technology. In fact, it allows to depict the real space maps at the atomic level of phenomena such as diffusion, reaction, nucleation and growth on surfaces. Furthermore, a series of nanometer-resolved spectroscopies can be performed for the energy-resolved mapping of the electronic density.

The new system has been completely redesigned and previous available parts have been integrated with the new equipment. In particular, apart from the AFM/STM head, the system is equipped with an ion gun, a quick insertion system of the samples, a manipulator coolable liquid nitrogen and heated to 800 ° C with five degrees of freedom and a new pumping system.

The LSAM laboratory is in straight collaboration with three Physics laboratories (SPES lab., Laboratory of Raman Spectroscopy, Laboratory of Molecular Biophysics) providing to researchers and companies integrated and complementary information on the composition, structure, chemical and physical properties of materials (organic, inorganic, biological) resolved at the micro and nanometer scale.

10.3.1.2. STAR_Lab

All modern medical X-ray imaging devices are based on the attenuation through photoelectric absorption of the X-rays penetrating the specimen to be imaged. However, for soft matter with little absorption, this provides poor contrast. This issue in soft tissue can be overcome with phase-contrast imaging. Several imaging techniques have been developed based on the phase shift of X-ray waves owing to refraction. An X-ray source for X-ray phase-contrast imaging must fulfill two requirements: the source must have some degree of spatial and temporal coherence, and the beam must be large enough to cover a reasonable field of view. The best results for high-resolution and high-sensitivity phase-contrast applications are obtained on brilliant and narrow band-pass X-ray sources. Third-generation synchrotron radiation sources certainly offer the necessary beam quality and brilliance, but they are far too costly and they are incompatible with a clinical or cultural heritage environment. The newly developped Compact Light Sources (CLS) are able to combine the compactness of the instrument with a beam of high intensity, high quality and tuneable in energy. The STAR (Southern European Thomson source for Applied Research) CLS source fulfils both requirements mentioned above, and thus is a promising source for X-ray phase-contrast imaging applications. The small size of the intersection point gives a highly coherent cone beam with a few milliradiant angular divergence and a few per cent energy spread. The beam divergence of the STAR is much larger than at normal synchrotrons. This is an advantage in imaging, as a larger field of view can be obtained at shorter source-to-sample distances. Compact Light Source, like STAR, in combination with

grating-based X-ray phase-contrast imaging has the potential to yield images of a quality previously only obtained at large-scale synchrotron radiation facilities.

Our Thomson Back-Scattering (TBS) source is based on the head-on interaction of a high-energy electron beam with a high power laser pulse. The interaction, which takes place in a region with diameter of the order of 10 micron, gives rise to an x-ray beam in the multi-keV range, traveling in the same direction of the electron beam, with the majority of photons concentrated in a narrow cone few mrads wide, with a degree of monochromaticity of few percent. Since the small interaction zone the photon beam generated has high coherence, angular divergence of a few milliradians and an energy spread of a few percent.

The characteristics of the radiation produced (coherence, monochromaticity, tunability and energy range) make the STAR source the ideal tool to bridge the gap among the great facilities and the X-ray tubes used in hospitals and in industry and for use the latest technological innovations in the field of imaging methods phase contrast.

The STAR facility site at Univ. of Calabria campus, in Rende (CS, Italy) is under commissioning in an ad-hoc designed building. The STAR LINAC is composed by: one S-band 1.6 Cell RF Gun (Cu photocathode) based on a new design. It represents one of the first Gun, of this type, able to reach 100Hz of repetition rate. The Gun is followed by a solenoid, a 1.8m drift and one S-band SLAC-type 3 m long Traveling Wave (TW) accelerating cavity. The solenoid and the TW cavity, placed in the peculiar position where the beam is still space charge dominated, perform the emittance correction. This scheme, used by server labs, has been mainly studied and tested at the SPARC lab. [6-7]. Downstream the accelerating cavity is foreseen a long drift ad hoc to host an additional TW cavity (S-band SLAC type). The addiction cavity can be installed without any difficulty and will permit a fast upgrade, rising the final energy from 60 MeV up to 90-105 MeV (limit given by the RF power available). All the beam line has been studied, simulated and careful optimized, to host the log drift, to fully com- pensate the emittance and to minimize the energy-spread. Beam parameters and plots have been already presented in the reference [8]. The good beam quality at the linac exit, $\varepsilon_{n,x,y} = 0.9\mu m, \frac{\Delta\gamma}{\gamma} = 0.2\%,$ for the quite high bunch charge of Qb = 500 pC, permits to pass through the dog- leg and to reach the Interaction Point (IP) with a very narrow final spot of 15 µm (or smaller) on the both planes.The relevant expected source parameters of STAR are:

	Phase 1	*Phase 2*
Energy (keV)	7-120	7-240
Flux (ph/s)	$5*10^9$	$5*10^{12}$
Source size	10 µm	10 µm
Cone aperture	6 mrad	3 mrad
Bandwidth	<5%	<2%
Pulse length	<5 ps	<5 ps

In various fields of applications such as biomedical science, cultural heritage preservation and material science researches, sources like STAR should provide an easy working environment and the methods currently used at synchrotrons could be largely developed in a lab-size environment as hospitals, labs, or museums.

10.3.1.3. µTomo beamline

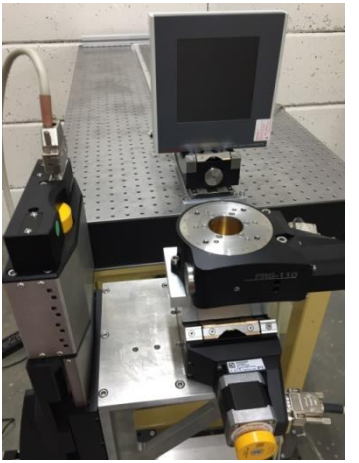

µTomo experimental station was designed to exploit the hard X-ray beams produced by STAR for advanced X-ray micro-tomographic investigations. Standard X-ray tomography is based on absorption and it is a well-known tool for imaging the internal structure of thick objects with hard X-rays. For low-absorption materials (like Carbon-based objects) small attenuation in the sample produces low contrast in the images. Thus standard absorption tomography is an inappropriate technique to discriminate details of similar densities in distinguishing, for example, carbon fibre-based papyrus foil from carbon-based ink used in writing on the papyrus. In the latter case, as shown in this study, a better contrast was achieved by imaging the phase modulation induced by the object in a coherent or partially coherent beam. Several experimental approaches exist for detecting X-ray phase contrast. A simple yet effective phase-contrast method for hard X-rays is based on in-line imaging after free-space propagation.

The microtomography station installed at STAR-Lab will operate in two possible configurations:

a. In-line using the TBS source. In this case, we will have a experimental set-up that will make us competitive and at the same time complementary with major third-generation facilities (ESRF, Elettra). The experimental station of X-ray micro-computed tomography (micro-CT) use the radiation produced by the STAR source. The STAR linear accelerator produces a beam of electrons of high brilliance which is used to generate X-rays through the Thomson backscattering process.

   The synchrotron radiation source of the third generation (ESRF, Elettra, ...) have high beam quality and high brilliance but they are too expensive and incompatible with the clinical environment structures.

   Instead, the compact radiation sources (type STAR) not only have the right technical features (a certain degree of spatial and temporal coherence, a field large enough view that you can study large samples, high resolution and high sensitivity) but given the relatively low cost and small size of STAR makes it feasible to install it in hospitals, museum and laboratories.

   The µTomo station exploits the characteristics of coherence, monochromatic and energy tunability of the STAR X-ray source. In particular:

   1) The coherence of the X beam makes possible the phase contrast images (PHC);

2) The tunability in the X-ray energy allows acquiring resolved maps chemically impossible with conventional light sources and makes much more effective the quantitative analysis of densities;

3) The energy range extension allows you to go beyond the limits obtained with synchrotron sources (see Elettra) or get the same performance with low costs minor (see ESRF).

b. Off-line using a classical microfucus X-ray source. In this case, if and when the STAR source were to be involved in other experiments, it is possible however do tomography measurements in phase contrast even if with alower resolution, even if the measurement time increases.

The application of tomography phase contrast X-ray is the subject of a growing interest due to the potential of this innovative technique in various biomedical fields and beyond, where high resolution, high contrast, low doses of radiation and fast data acquisition are required.

10.3.1.4. Microtomigrafic studies in the Cultural Heritage field

1. Virtual unrolling and deciphering of Herculaneum papyri by X-ray phase-contrast tomography

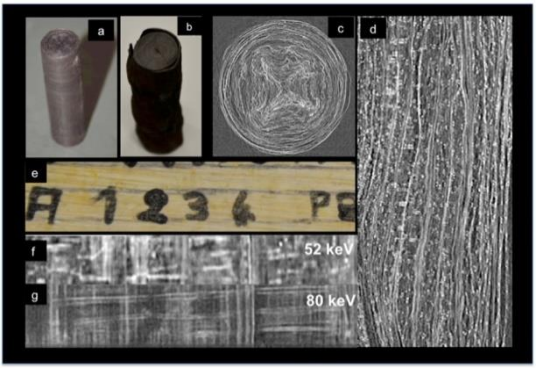

Modern papyrus roll. a, before and b, after carbonization; c, axial and d, longitudinal view of the 3D tomographic reconstruction of the internal part of the carbonized papyrus roll; e, text of the papyrus written using ink mixed with Pb; f, virtually unrolled text of the carbonized papyrus in absorption and g, phase contrast.

Sequences of letters revealed in the PHerc. 375 papyrus rolls through the 'virtual-unrolling' technique. Deciphered text: [□□□]

Hundreds of papyrus scrolls, buried in Herculaneum by Vesuvius eruption in 79AD and belonging to the only ancient library in our possession, are preserved in Naples National Library. The crucial task today is to read the text written inside them without having to unroll them mechanically.

In this framework, we joined to a multidisciplinary team of CNR/NANOTEC and CNR/ILIESI to provide complementary expertise and tackle this hard and fascinating problem.

We verified the difficulty of the task by examining in a pilot test at ID17 some phantoms prepared by us following the literature findings on the ink composition (gum Arabic, carbon and water) and the temperature of carbonization of the Herculaneum rolls. On a modern sheet of papyrus we writed same words with carbon ink, we rolled and, finally, we burned in controlled atmosphere in absence of oxygen. The test experiment on the phantoms allowed identifying the more suitable incident energies, the most promising phase contrast technique and experimental conditions, as well as the most efficient algorithms to process the data.

Stimulated by encouraging preliminary results on phantoms at ID17, we used *X-ray phase contrast tomography* (XPCT) to investigate Herculaneum papyrus rolls and fragments to enable the analysis of individual overlapping layers.

We demonstrated that XPCT combined with advanced algorithms for data analysis and with other complementary techniques, is well suited for i) classifying and replacing overlapping papyrus layers, ii) reading underlying layers, iii) potentially reading words written inside rolled-up papyrus rolls.
We were able to read the fragments and part of the scrolls of Herculaneum papyri.

2. Microtomographic studies as a tool in the identification of a new ceramic class: The metal-imitating pottery as grave goods among Brettians and Lucanians

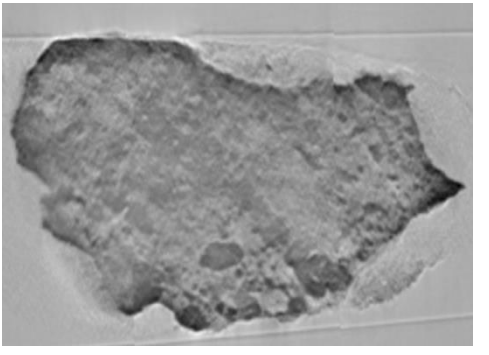

The synchrotron-based microtomography allowed us to reveal the details of the metal layer as well as those of the interfacial region. The high-resolution results obtained by an accurate use of the data treatment algorithms clearly indicate that the silver-imitating pottery was obtained by covering the surface of the objects with a tin alloy layer whose thickness, internal structure and ceramic/metal interface varied slightly for all the sampled artefacts. On the basis of the outcomes, the main characteristics of the production technique are recovered and a clear assessment on the peculiar manufacture is outlined in comparison with the metal-imitating pottery produced in different sites.

10.3.2. The PON EOMAT Project

The impact that hydrogen technology could have on our day life is enormous. As the steam technology produced the industrial revolution, hydrogen can be the key to reinvent our society. The transition from oil to hydrogen economy be deeply transform the world economy, politic and relations between counties.

Hydrogen is the ideal energy vector because of its gravimetric energy density of 39,4 kWh/Kg, however since H2 volumetric energy density is very low (0,003 kWh/L) at normal condition (NTP), it is not suitable for mobile applications.

The main challenge for the technological development of a Hydrogen-based economy concerns the storage of this gas in a useful and safe way. Currently, several approaches are pursued for the H_2-storage: compression in high-pressure tanks; cryogenic liquefaction; chemical storage in solid materials and the physical adsorption in porous materials. Although all the storage methods have benefits, no approach meets all requirements in terms of efficiency, size, weight, cost and safety. The EOMAT project is placed in this framework: in collaboration with industrial partners, Centro Sviluppo Materiali SpA and Ingegneria del Sistemi SpA, the project is aimed to the development, testing and validation of innovative materials and components for gas storage, in particular hydrogen.

In order to maximize the research goals, a new equipped area, called DeltaH, was realized in the Arcavacata campus area by the SPES team and the CSM one.

DeltaH is a new facility of the Matelios District, a consortium among several private companies and research and academic institutions, dedicated to the study and development of advanced materials and technologies for the implementation of systems of energy production from renewable sources. The research activities and services of the DeltaH laboratory are devoted to the development, testing and validation of materials for the H2 storage, transportation and distribution.

The concerned areas are the development, testing and validation of:

- full-scale tanks for the containment of strongly compressed hydrogen (up to 1000 bar) for stationary and mobile applications;
- materials and components for the distribution of hydrogen;
- materials for the hydrogen storage.

Expressly designed test devices that will expand the possible characterization of traditional and innovative materials compose the facility's equipment. DeltaH is equipped with a prototypal apparatus allowing the adsorption/desorption tests on kg-scale amounts of sorbent materials at pressures up to 250 bar and controlled temperatures ranging in a wide range (RT ± 40 K). A second prototypal instrument is devoted to tensile and fatigue tests of metal samples exposed to very high H2 pressures (up to 1000 Bar).

References

1. D. Vuono, E. Catizzone, A. Aloise, A. Policicchio, R.G. Agostino, M. Migliori, G. Giordano
Modelling of adsorption of textile dyes over multi-walled carbon nanotubes: Equilibrium and kinetic
Chinese Journal of Chemical Engineering, (2016) DOI: 10.1016/j.cjche.2016.10.021 (Available online)

2. Bukreeva, I., Mittone, A., Bravin, A., Festa, G., Alessandrelli, M., Coan, P., Formoso, V., Agostino, R.G., Giocondo, M., Ciuchi, F., Fratini, M., Massimi, L., Lamarra, A., Andreani, C., Bartolino, R., Gigli, G., Ranocchia, G., Cedola, A.
Virtual unrolling and deciphering of Herculaneum papyri by X-ray phase-contrast tomography.
Scientific Reports, 6, pg 27227 (2016) DOI: 10.1038/srep27227

Corrigendum: Virtual unrolling and deciphering of Herculaneum papyri by X-ray phase-contrast tomography.
Scientific Reports 6, pg 30364 (2016) DOI: 10.1038/srep30364

3. Agostino, R.G., Donato, S., Caruso, T., Colavita, E., Zanini, F., D'Alessio, A., Pisarra, D., Taliano Grasso, A.
Microtomographic studies as a tool in the identification of a new ceramic class: The metal-imitating pottery as grave goods among Brettians and Lucanians
Microchemical Journal, 126, pp. 138-148 (2016)

4. Kalantzopoulos, G.N., Policicchio, A., Maccallini, E., Krkljus, I., Ciuchi, F., Hirscher, M., Agostino, R.G., Golemme, G.
Resistance to the transport of H_2 through the external surface of as-made and modified silicalite-1 (MFI)
Microporous and Mesoporous Materials, 220, pp. 290-297 (2016)

5. Kalantzopoulos, G.N., Antoniou, M.K., Enotiadis, A., Dimos, K., Maccallini, E., Policicchio, A., Colavita, E., Agostino, R.G.
Enhanced hydrogen and methane storage of hybrid mesoporous organosilicas
Journal of Materials Chemistry A, 4 (23), pp. 9275-9285 (2016)

6. Policicchio, A., Filosa, R., Abate, S., Desiderio, G., Colavita, E.
Activated carbon and metal organic framework as adsorbent for low-pressure methane storage applications: an overview
Journal of Porous Materials, pp. 1-18 (2016) DOI: 10.1007/s10934-016-0330-9

7. Kwiatkowski, M., Policicchio, A., Seredych, M., Bandosz, T.J.
Evaluation of CO2 interactions with S-doped nanoporous carbon and its composites with a reduced GO: Effect of surface features on an apparent physical adsorption mechanism
Carbon, 98, pp. 250-258 (2016)

8. Simari, C., Potsi, G., Policicchio, A., Perrotta, I., Nicotera, I.
Clay-Carbon Nanotubes Hybrid Materials for Nanocomposite Membranes: Advantages of Branched Structure for Proton Transport under Low Humidity Conditions in PEMFCs
Journal of Physical Chemistry C, 120 (5), pp. 2574-2584 (2016)

9. Alzari, V., Nuvoli, D., Sanna, V., Caruso, T., Marino, S., Scaramuzza, N.
Study of polymeric nanocomposites prepared by inserting graphene and / or Ag, Au and ZnO nanoparticles in a TEGDA polymer matrix, by means of the use of dielectric spectroscopy
AIP Advances, 6 (3), art. no. 035005 (2016)

10. Castellarin-Cudia, C., Caruso, T., Maccallini, E., Li Bassi, A., Carrozzo, P., De Luca, O., Goldoni, A., Lyamayev, V., Prince, K.C., Bondino, F., Magnano, E., Agostino, R.G., Casari, C.S.

Chemical bonds and charge-transfer dynamics of a dye-hierarchical-TiO2 hybrid interface
Journal of Physical Chemistry C, 119 (16), pp. 8671-8680 (2015)

11. Minuto, F.D., Policicchio, A., Aloise, A., Agostino, R.G.
Liquid-like hydrogen in the micropores of commercial activated carbons
International Journal of Hydrogen Energy, 40 (42), pp. 14562-14572 (2015)

12. Policicchio, A., Vuono, D., Rugiero, T., De Luca, P., Nagy, J.B.
Study of MWCNTs adsorption performances in gas processes
Journal of CO2 Utilization, 10, pp. 30-39 (2015)

13. Antoniou, M.K., Diamanti, E.K., Enotiadis, A., Policicchio, A., Dimos, K., Ciuchi, F., Maccallini, E., Gournis, D., Agostino, R.G.
Methane storage in zeolite-like carbon materials
Microporous and Mesoporous Materials, 188, pp. 16-22 (2014)

14. Alzari, V., Sanna, V., Biccai, S., Caruso, T., Politano, A., Scaramuzza, N., Sechi, M., Nuvoli, D., Sanna, R., Mariani, A.
Tailoring the physical properties of nanocomposite films by the insertion of graphene and other nanoparticles
Composites Part B: Engineering, 60, pp. 29-35 (2014)

15. Caruso, T., Castriota, M., Policicchio, A., Fasanella, A., De Santo, M.P., Ciuchi, F., Desiderio, G., La Rosa, S., Rudolf, P., Agostino, R.G., Cazzanelli, E.
Thermally induced evolution of sol-gel grown WO3 films on ITO/glass substrates
Applied Surface Science, 297, pp. 195-204 (2014)

16. Kalantzopoulos, G.N., Enotiadis, A., Maccallini, E., Antoniou, M., Dimos, K., Policicchio, A., Klontzas, E., Tylianakis, E., Binas, V., Trikalitis, P.N., Agostino, R.G., Gournis, D., Froudakis, G.E.
Hydrogen storage in ordered and disordered phenylene-bridged mesoporous organosilicas
International Journal of Hydrogen Energy, 39 (5), pp. 2104-2114 (2014)

17. Policicchio, A., Zhao, Y., Zhong, Q., Agostino, R.G., Bandosz, T.J.
Cu-BTC/aminated graphite oxide composites as high-efficiency Co2 capture media
ACS Applied Materials and Interfaces, 6 (1), pp. 101-108 (2014)

18. Policicchio, A., Maccallini, E., Kalantzopoulos, G.N., Cataldi, U., Abate, S., Desiderio, G., Agostino, R.G.
Volumetric apparatus for hydrogen adsorption and diffusion measurements: Sources of systematic error and impact of their experimental resolutions
Review of Scientific Instruments, 84 (10), art. no. 103907 (2013)

19. Policicchio, A., Maccallini, E., Agostino, R.G., Ciuchi, F., Aloise, A., Giordano, G.
Higher methane storage at low pressure and room temperature in new easily scalable large-scale production activated carbon for static and vehicular applications
Fuel, 104, pp. 813-821 (2013)
20. Cazzanelli, E., Caruso, T., Castriota, M., Marino, A.R., Politano, A., Chiarello, G., Giarola, M., Mariotto, G.
Spectroscopic characterization of graphene films grown on Pt(111) surface by chemical vapor deposition of ethylene

Journal of Raman Spectroscopy, 44 (10), pp. 1393-1397 (2013)

21. Cirillo, G., Caruso, T., Hampel, S., Haase, D., Puoci, F., Ritschel, M., Leonhardt, A., Curcio, M., Iemma, F., Khavrus, V., Grobosch, M., Picci, N.
Novel carbon nanotube composites by grafting reaction with water-compatible redox initiator system
Colloid and Polymer Science, 291 (3), pp. 699-708 (2013)

22. Politano, A., Campi, D., Formoso, V., Chiarello, G.
Evidence of confinement of the π plasmon in periodically rippled graphene on Ru (0001).
Physical Chemistry Chemical Physics, 15(27), 11356-11361 (2013).

23. Politano, A., Formoso, V., Chiarello, G.
Evidence of composite plasmon–phonon modes in the electronic response of epitaxial graphene.
Journal of Physics: Condensed Matter, 25(34), 345303 (2013).

24. Politano, A., Formoso, V., Chiarello, G.
Collective electronic excitations in thin Ag films on Ni (111).
Plasmonics, 8(4), 1683-1690 (2013).

25. Politano, A., Formoso, V., & Chiarello, G.
Interplay between single-particle and plasmonic excitations in the electronic response of thin Ag films.
Journal of Physics: Condensed Matter, 25(30), 305001 (2013).

Conference proceedings

26. A Bacci, I Drebot, L Serafini, V Torri, Infn / Milan, M Rossetti Petrillo, Conti, D Alesini, M Bellaveglia, F Bisesto, B Buonomo, G Di Pirro, A Esposito, F Iungo, J J Beltrano, G Borgese, G Di Raddo, A Gallo, A Ghigo, L Pellegrino, A Stella, C Vac-Carezza, A Cianchi, R G Agostino, R Barberi, M Ghedini, F Martire, C Pace, G Dauria, A Fabris, M Marazzi:
Status of the STAR Project.
IPAC 2016; 01/2016

27. A. Bacci, D. Palmer, L. Serafini, V. Torri, V. Petrillo, P. Tomassini, Ezio Puppin, D. Alesini, M. P. Anania, M. Bellaveglia, F. Bisesto, G. Di Pirro, A. Esposito, M. Ferrario, A. Gallo, G. Gatti, A. Ghigo, B. Spataro, C. Vaccarezza, F. Villa, A. Cianchi, R. G. Agostino, G. Borgese, M. Ghedini, F. Martire, C. Pace, T. Levato, G. Dauria, A. Fabris, M. Marazzi:
The STAR project.
5th International Particle Accelerator Conference (IPAC), Dresden, Germany; 06/2014

28. Antonino D'Alessandro, Raffaele Giuseppe Agostino, Lorenzo Festa, Anna Gervasi, Ignazio Guerra, Dennis T. Palmer, Luca Serafini:
Spatial correlation analysis of seismic noise for STAR X-ray infrastructure design.
EGU General Assembly 2014, Vienna Austria; 04/2014
In press

29. Elio Colavita, Francesco Pecora, Matteo Scornajenghi,
Considerazioni e Meditazioni su alcuni argomenti di Struttura della Materia,
Luigi Pellegrini Editore, ISBN:9788868223748

30. D. Vuono, E. Catizzone, A. Aloise, A. Policicchio, R.G. Agostino, M. Migliori, G. Giordano
Study of Adsorption Behavior of Multi-Walled Carbon Nanotubes towards Dyes Applied in Textile Applications
Advanced Science Letters (In Press).

31. Simari, C., Baglio, V., Lo Vecchio, C. A. S. Aricò, R.G. Agostino, L. Coppola, C. Oliviero Rossi, I. Nicotera,
Reduced methanol crossover and enhanced proton transport in nanocomposite membranes based on clay−CNTs hybrid materials for direct methanol fuel cells,
Ionics (2017). doi:10.1007/s11581-017-2059-0

11. SURFACE NANOSCIENCE

Professors and Researchers	Lorenzo Salvatore Caputi Anna Cupolillo
Postdoc fellows	Nadia Ligato
PhD students	Denia Marlenis Cid Perez Diana Carolina Coello Fiallos Gabriela Viaviana Tubon Usca Salih M. Osman
Collaborators	Donatella Barca (*Dip. di Scienze della Terra - UNICAL*). Marco Alfano *(Dip. Ingegneria Meccanica, Università della Calabria)* Silvia Scalese *(CNR – Catania, Italy)* Melvin Arias *(Instituto Tecnologico de Santo Domingo)* Giuseppe Nicotra (*CNR-IMM, Catania*) Gaetano Granozzi (*University of Padova*) Sihem Jaziri (*Université de Carthage, Tunisia*) Songül Duman (*Atatürk University, Erzurum,Turkey*) Ziya Aliev (*ANAS, Baku, Azerbaijan*) Davide Campi (*EPFL, Lausanne, Switzerland*) Olimpia Arias de Fuentes *(IMRE, La Habana, Cuba)* Ernesto Pelaez *(Insituto de Quimica, Universidad de la Habana, Cuba)* Adalgisa Tavolaro *(Istituto per la Tecnologia delle Membrane (ITM) – CNR UNICAL)* Leonardo Pagnotta *(DIMEG UNICAL)* Dennis Cazar Ramirez *(Escuela Superior Politecnica de Chimborazo (ESPOCH) Riobamba, Ecuador)*

Introduction

The discovery of 2D materials has started a new era of materials science. New materials, atomically thin and mechanically, thermally and electronically stable, with a large variety of electronic properties are available and they can be assembled in ultrathin flexible devices. Angle-resolved Electron Energy Loss Spectroscopy (AREELS) is mainly used to obtain information about the valence band structure and the momentum-space-dependence of collective excitations in well-ordered thin films. Electron emission, excited by photons or monochromatized electrons, follows the conservation laws of energy and momentum parallel to the surface. This means that the parallel component of the wave vector of either the valence electrons or the excited plasmons can be obtained together with the energy. In particular, we are focusing on two-dimensional (2D) plasmons, whose charge fluctuations are strongly localized at a monolayer. We addressed our research on the fabrication and study of graphene overlayers epitaxially grown on metallic surfaces and successfully intercalated with atoms, in order to improve the comprehension of the graphene-substrate interaction. Likewise we have studied electronic properties and plasmon excitations in two-dimensional semiconductors such as indium selenide single crystal and a monolayer of silicon atoms epitaxially grown on Ag(111). Graphene-based nanomaterials were also synthesized by top-down strategies, using the arc discharge technique in water between carbon electrodes. Polyhedral carbon nano-onions were obtained and studied by TEM and Raman.

The research activity of the group is oriented in four closely related directions, which are briefly described in the following sections:

1. Substrate-dependent plasmonic properties of supported graphene
2. Intercalation of atoms and molecules in graphene/metals
3. Electronic properties and plasmon excitations in two-dimensional materials beyond graphene
4. Synthesis and characterization of graphene and related materials

11.1. SUBSTRATE-DEPENDENT PLASMONIC PROPERTIES OF SUPPORTED GRAPHENE

The plasmonic properties of graphene (GR) interfaced with substrates of different nature (oxides, semiconductors or metals) are mandatory for technological applications. GR–metal contacts are unavoidable components of each GR-based device. Therefore, the investigation of the nature and dispersion of plasmon modes at GR/metal interfaces is a critical step toward engineering plasmonic applications of GR.

The synthesis of graphene was obtained successfully on a large number of transition metal (TM) surfaces including Ni, Ru, Ir, Cu and Pt. In some cases the strong hybridization of the d-orbitals of the transition metal substrate with the π electronic states of the graphene layer modifies the intrinsic band structure of the graphene sheet and induces a charge transfer between epitaxial graphene and the metal substrates. As regards the degree of interfacial hybridization between graphene π and transition metal d states, a different behavior has been found for surfaces belonging to different groups of TMs. The lattice matched interface between graphene and Ni(111) is among the most extensively studied graphene/metal systems. Ni(111) has a lattice parameter similar to that of graphene (2.47 Å vs 2.46 Å), which makes it an ideal candidate for epitaxial growth of excellent graphene layers in nearly perfect register with the substrate. The electronic structure of graphene on Ni(111) surface was investigated by means of several spectroscopic methods. These works showed that the strong hybridization of the valence band states of graphene with the substrate d states leads to a considerable interaction between C and Ni atoms, resulting in a substantial modification of graphene's electronic structure. We have investigated plasmonic excitations at the graphene/ Ni(110) surface in order to compare the dispersion curve obtained in this system with that measured for graphene/Ni(111). The aim of this study is to explore the modifications of the collective electronic properties caused by a different matching between the epitaxial graphene and the Ni surfaces. We have evaluated how a worse lattice matching can affect the bond between graphene and the Ni(110) substrate, although the Ni belongs to the group of 3d transition metals for which the interaction with graphene is strong. Our analysis of the degree of interaction between graphene and Ni substrates with different crystalline structure correlates well with photoemission measurements of a graphite monolayer adsorbed on different Ni surfaces. In this work the authors demonstrate how graphite π-band energy depends on crystallographic Ni faces, the larger the number of substrate atoms that are in contact with the adsorbate, the stronger the interaction between substrate atoms and the graphite coating. In particular, according to our results, a weaker interaction has been found for
graphene/Ni(110) with respect to graphene/Ni(111). The interband plasmon dispersion for graphene on Ni(110) clearly
shows a $\sqrt{q_{\parallel}}$ behavior, which, as it happens for graphene on Ni(111), is indicative of a two-dimensional charge density associated to the hybridization between graphene π orbitals and nickel 3d electrons. The graphene/Ni(110) dispersion curve is quasi-rigidly downshifted, which means that the oscillating charge density is lower with respect to the graphene/Ni(111) case. This behavior can be attributed to a weaker hybridization between graphene π orbitals and Ni 3d electrons, due to the complete mismatch between graphene and Ni(110) as compared to the perfect matching between graphene and Ni(111).

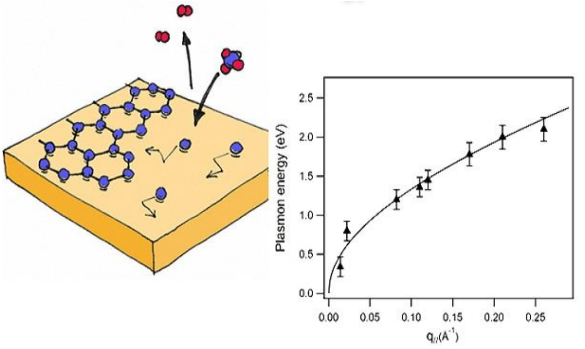

.

11.2. INTERCALATION OF GRAPHENE FILMS ON METALS WITH ATOMS AND MOLECULES

The tendency of atomic species to intercalate at the graphene/metal interface is an efficient method to insulate graphene
from its substrate. This behavior can be finalized to perform chemical reactions of materials underneath graphene sheet and it may be used to engineer its properties. Previous works exploited the modifications of the electronic structure of the valence band and of the phonon spectra caused by different metal atoms intercalation. They demonstrated how this intercalation takes the system closer to ideal freestanding graphene, with the ‘‘stiffening’’ of the phonon modes, and with the recovery of the π band linearity at Dirac points. Therefore, one would expect that the influence of intercalated atoms on the electronic structure of the epitaxial graphene would reflect itself in the collective electronic properties of the intercalated system with respect to freestanding or weakly interacting graphene. To address this issue, we have studied the process of intercalation of atomic species underneath a graphite monolayer formed on Ni(111) in order to investigate modifications of the collective electronic properties caused by intercalation. Angle-resolved electron-energy-loss spectroscopy has been used to study the momentum space- dependent behavior of π plasmon on epitaxial graphene on Ni(111) and on the same system intercalated by atoms of cesium or oxygen. The dispersion curves were found to be significantly different: a square-root behavior of the plasmon mode is observed in epitaxial graphene, allowing us to conclude that the fluctuating charge density is strictly two dimensional; a linear π plasmon dispersion is observed in the same system intercalated by atoms; the combine between the linearity of dispersion curve with the π band linearity at Dirac points shows how alkali metal atoms makes graphene to be quasi-free with the recovery of the typical Dirac cones observed in free standing flakes.

Moreover, the intercalation of oxygen atoms allowed us, in some condition, to obtain graphene-insulating system, essential for a new generation of electronic devices. As a result of intercalation process, Electron Energy Loss Spectra reveal the presence of NiO islands underneath epitaxial graphitic layer and a dramatic change in the character of the energy dispersion curve of the graphene π plasmon.
Taking advantage of the detailed study of the ultra-thin Ni-oxide formation at high temperature we have developed a method for the intercalation of a single layer of graphene on Ni with oxygen atoms. A partial oxidation of the substrate was inferred from the comparison between the electronic properties of the intercalated system and those measured for the single layer of NiO. As a result of oxygen intercalation, the plasmon dispersion of epitaxial graphene on Ni(111) changed drastically from a square-root behavior to a linear dependence. We assumed this trend as an evidence of a transition from an interacting to a quasi non-interacting regime. Oxygen atoms intercalation at the

strong interacting graphene/Ni(111) interface allowed us to develop an alternative free-transfer method able to exploit the full potential of graphene at the macroscopic level, without altering its structure. Particularly, we demonstrated that non-metal intercalation represents a successful approach to control the interface interaction and obtain graphene layer on an insulating material.
In relation to electronic properties, for the first time we also demonstrated that graphene collective excitations can be tailored by intercalation of atomic species. Currently, plasmon excitations in metallic structures are a subject of nanoplasmonics, a field which has emerged at the confluence of optics and condensed matter physics. However, perspective of graphene for nanoplasmonics is largely unexplored since plasmon modes of graphene flakes have not been addressed so far. As our results indicate, a great amount of control over plasmon properties in the epitaxial graphene makes it a promising material for applications.

11.3. SYNTHESIS AND CHARACTERIZATION OF POLYHEDRAL CARBON NANO-ONIONS

In the last 30 years, an increasing attention has been devoted to the study of closed-shell carbon nanostructures. The triggering facts in this regard were the discovery in 1980 of graphitic onions in amorphous carbon films prepared by vacuum deposition and, especially, the report in 1992 regarding quasi-spherical nano-onions obtained by electron irradiation of graphitic particles. These nano-materials, thanks to their very particular shapes forming different kinds of carbon cages, can be considered as a sort of multi-wall fullerenes having particular properties. These properties make them very promising materials for practical applications in electronic, biomedical, catalytic, and wastewater treatment fields. As a matter of fact, the importance of polyhedral carbon onions (PCO) has been increasing in the last years. They are the kind of material obtained in several experimental methods of preparation of nano-onions, as for example, the one based on a submerged arc discharge of graphite electrodes in water. We have used such technique to obtain PCO, which have been successively studied by TEM and Raman spectroscopy. The fine structure of the Raman spectra of PCO presents several features that allows distinguish them from other carbon nanostructures, especially from spherical nano-onions. In particular, we have found that in these materials the G band is composed of two or three peaks, which correspond to different contributions from the curved zones and from the plane zones of the polyhedron. We also found that the 2D band is basically composed of two or four peaks, with the former corresponding to PCOs with graphitic turbostratic walls, while the latter comes from particles with walls formed by ordered graphite. We have also reported the existence of cases with more complex fine structure of the 2D band, as well as the presence of a very defined and sharp peak in the zone of (1400–1450) cm^{-1}, which is absent in the Raman spectra of the spherical nano-onions.

11.4. ELECTRONIC PROPERTIES AND PLASMON EXCITATIONS IN TWO-DIMENSIONAL MATERIALS BEYOND GRAPHENE

A recent surge of interest in two dimensional (2D) crystals beyond graphene, is justified given their newly found remarkable properties that establish them as a distinct class of materials with unique technological potential. Four requisites are crucial for a suitable use of 2D materials in nanotechnology: (*i*) high mobility of charge carriers; (*ii*) the possibility to achieve highly crystalline samples via mechanical/liquid exfoliation; (*iii*) ambient stability; (*iv*) high flexibility together with a sufficiently high fracture toughness. Two-dimensional (2D) van der Waals semiconductors combining finite band gaps and flexibility, are emerging in recent years as the most promising materials for nanoelectronics. Furthermore, the presence of a band gap, absent in graphene, is crucial for achieving a high ON/OFF ratio in nanodevices. Particular attention is paid to the materials containing a III group metal (Al, Ga, In or Tl) and chalcogen (VI group element). Due to their interesting optical properties, III–VI materials are considered as promising candidates for many technological

applications and have shown their potential in optoelectronic and photo-electrochemical domains. A good trade-off between graphene and TMDCs is represented by a novel class of atomically thin 2D elemental materials: silicene, germanene, and phosphorene. Silicene and germanene, two dimensional allotropes of silicon and germanium, possess predicted electron transport properties similar to graphene, as well as the advantage of compatibility with existing silicon-based technology. Additionally, the inversion symmetry breaking imparted by the buckled lattice structure of both materials may be taken advantage of through the application of an external electrical field perpendicular to the plane for highly controllable band gap tunability.
Recently, our group has investigated plasmonic excitations at the surface of Silicene on Ag(111).
Silicene, one single layer of silicon atoms packed in a honeycomb structure, has been predicted to be a new two-dimensional (2D) Dirac-fermion material. The electrons in silicene behave as massless charge carriers that can exhibit transport at ultra-fast velocity, due to the linear energy-momentum dispersion relation at the Dirac point. Strong spin-orbital coupling makes silicene a promising candidate material for the quantum spin Hall effect (QSHE), and, as said above, it is compatible with current Si-based device technologies. To date, epitaxial growth is the only method that can produce silicene on certain metal substrates. The electronic structure of such epitaxial silicene is therefore significantly modified by a strong coupling with the substrate, which may annihilate silicene's Dirac-fermion characteristics.
We have studied the electronic structure of the clean Ag(111) and silicene/Ag(111) system by angle-resolved electron-energy-loss spectroscopy. The aim of this work was to investigate by electron-energy-loss spectroscopy (EELS) the collective electronic properties of the silicene/Ag(111) system. In fact, the study of the plasmon dispersion curves may be decisive to understand the effects due to the silicene-substrate interaction and to determine how this interaction can influence the behavior of Dirac fermions in the silicene/Ag(111) system. Different phases for silicon deposited onto Ag(111) have been observed as a function of substrate temperature during Si deposition and deposition time.
Our EEL measurements have revealed the existence of an interband plasmon excitations as a result of silicene/ Ag(111) hybridization. The interface states responsible of such excitation are the consequence of a strong interaction with the substrate and the charge density associated to these states does not preserve characteristic properties of two-dimensional systems confirming that the distinctive Dirac cones of ideal freestanding silicene fade out as a result of the hybridization with Ag bands. Therefore, our data indicate that silicene on Ag(111) does not preserve the freestanding electronic properties of the two-dimensional honeycomb lattice, in contrast to graphene on noble metals, where the interactions with the substrate can be considered almost negligible. For all these reasons, the silicene seems to be a less promising material for applications even with respect to the strongly interacting graphene/Ni(111). Moreover, the reactivity of silicene and germanene mean that they are more challenging to fabricate than graphene. Both materials bond easily with other materials and may oxidize rapidly in air, therefore they are fabricated using techniques such as epitaxial growth under ultra-high vacuum.
The next goal would be to find a material which can be obtained via mechanical exfoliation, with not zero energy gap and high electrons mobility and also chemically inert with respect to the external environment. In this respect, InSe seems a more promising material.
InSe is a typical member of layered materials from the III–VI group, which is composed by vertically stacked Se–In–In–Se layers with relatively weak van der Waals interactions.
Recently, many works reported the superb performance of InSe-based optoelectronic devices.
However, contrarily to III–V and II–VI semiconductors, indium selenide is not in the main stream of semiconductor literature. To devise broadband photodetectors and, moreover, to assess the suitability of this material for plasmonics, a detailed knowledge of the electronic band structure and of the dielectric response to electromagnetic fields is mandatory.
We have studied the electronic properties of indium selenide by means of a combination of spectroscopic tools and DFT. The loss function, probed by EELS, shows the direct free exciton and several dispersionless features, all ascribed to resonances originated from interband transitions, which

predominate over plasmonic modes. We observe that damped resonances arising from interband transitions predominate over fully coherent plasmonic excitations in the dielectric response. Moreover, we have identified the interband transitions by comparing the EELS spectra with symmetry-projected density of states (DOS).
In addition, we find that exposure to ambient atmosphere introduces a *p*-type doping by 130 meV, i.e. a rigid shift in the VB. However, the band structure is stable in ambient conditions without the emergence of oxygen- or water-induced adsorbate bands. Ambient stability is crucial in the prospect of InSe-based nanoelectronics and optoelectronics.

A. PUBLICATIONS ON SCIENTIFIC JOURNALS

A.1 Publications on international journals

A.1.1 Publications on international journals printed in 2013-2016

1. Cupolillo A., Ligato N.,Caputi L. S.
Low energy two-dimensional plasmon in epitaxial graphene on Ni (111)
Surface Science, **608**, 88-91 (2013).

2. Cupolillo A., Ligato N.,Caputi L. S.
Plasmon dispersion in quasi-freestanding graphene on Ni(111)
Applied Physics Letters, **102**, 111609-111604 (2013).

3. Ligato N., Cupolillo A.,Caputi L. S.
Study of the intercalation of graphene on Ni(111) with Cs atoms: Towards the quasi-free graphene
Thin Solid Films, **543**, 59-62 (2013).

4. Riccardi P., Pisarra M., Sindona A., Cupolillo A., Ligato N.,Caputi L. S.
High energy excited states of graphene adsorbed on Ni(111)
Nanoscience and Nanotechnology Letters, **5**, 1191-1194 (2013).

5. Sindona A., Pisarra M., Naccarato F., Riccardi P., Plastina F., Cupolillo A., Ligato N., Caputi L. S.,Falcone G.
Core-hole effects in fullerene molecules and small-diameter conducting nanotubes: A density functional theory study
Journal of Physics: Condensed Matter, **25**, 115301 (2013).

6. Ligato N., Cupolillo A., Sindona A., Riccardi P., Pisarra M.,Caputi L. S.
A comparative study of the plasmonic properties of graphene on lattice-matched and lattice-mismatched Ni surfaces
Surface Science, **626**, 40-43 (2014).

7. Pisarra M., Riccardi P., Sindona A., Cupolillo A., Ligato N., Giallombardo C.,Caputi L. S.
Probing graphene interfaces with secondary electrons
Carbon, **77**, 796-802 (2014).

8. Codorniu Pujals D., Arias de Fuentes O., Desdín García L. F., Cazzanelli E.,Caputi L. S.
Raman spectroscopy of polyhedral carbon nano-onions
Applied Physics A: Materials Science and Processing, **120**, 1339-1345 (2015).

9. Cupolillo A., Politano A., Ligato N., Cid D., Chiarello G.,Caputi L. S.
Substrate-dependent plasmonic properties of supported graphene

Surface Science, **634**, 76–80 (2015).

10. Nicotra G., Mio A. M., Cupolillo A., Hu J., Wei J., Mao Z., Deretzis I., Politano A.,Spinella C.
STEM and EELS Investigation on Black Phosphorus at Atomic Resolution
Microscopy and Microanalysis, **21**, 427-428 (2015).

11. Politano A., Chiarello G.,Cupolillo A.
Toward a novel theoretical approach for determining the nature of electronic excitations in quasi-two-dimensional systems
New Journal of Physics, **17**, 081002 (2015).

12. Cupolillo A., Ligato N., Osman S. M.,Caputi L. S.
Carbon K-edge electron-energy-loss near-edge structure in the reflection mode on graphene/Ni(111)
Applied Physics Letters, **109**, 161603 (2016).

13. Lamuta C., Campi D., Cupolillo A., Aliev Z. S., Babanly M. B., Chulkov E. V., Politano A.,Pagnotta L.
Mechanical properties of Bi_2Te_3 topological insulator investigated by density functional theory and nanoindentation
Scripta Materialia, **121**, 50-55 (2016).

14. Lamuta C., Cupolillo A., Politano A., Aliev Z. S., Babanly M. B., Chulkov E. V., Alfano M.,Pagnotta L.
Nanoindentation of single-crystal Bi_2Te_3 topological insulators grown with the Bridgman–Stockbarger method
physica status solidi (b), **253**, 1082–1086 (2016).

15. Lamuta C., Cupolillo A., Politano A., Aliev Z. S., Babanly M. B., Chulkov E. V.,Pagnotta L.
Indentation fracture toughness of single-crystal Bi_2Te_3 topological insulator
Nano Research, **9**, 1032-1042 (2016).

16. Ligato N., Caputi L. S.,Cupolillo A.
Oxygen intercalation at the graphene/Ni(111) interface: Evidences of non-metal islands underneath graphene layer
Carbon, **100**, 258-264 (2016).

17. Politano A., Cattelan M., Boukhvalov D. W., Campi D., Cupolillo A., Agnoli S., Apostol N. G., Lacovig P., Lizzit S., Farías D., Chiarello G., Granozzi G.,Larciprete R.
Unveiling the Mechanisms Leading to H_2 Production Promoted by Water Decomposition on Epitaxial Graphene at Room Temperature
ACS Nano, **10**, 4543–4549 (2016).

18. Politano A., Cupolillo A., Di Profio G., Arafat H., Chiarello G.,Curcio E.
When plasmonics meets membrane technology
Journal of Physics: Condensed Matter, **28**, 363003 (2016).

19. Tubon Usca G., Hernandez-Ambato J., Pace C., Caputi L. S.,Tavolaro A.

Liquid-phase exfoliated graphene self-assembled films: Low-frequency noise and thermal-electric characterization
Applied Surface Science, **380**, 268-273 (2016).

A.1.2 Publications on international journals accepted in 2016

1. Politano A., Argurio P., Di Profio G., Sanna V., Cupolillo A., Chakaraborthy S., Arafat H. A., Curcio E.,
Photothermal membrane distillation for seawater desalination
Advanced Materials, **29**, 1603504 (2017).

2. Politano A., Campi D., Cattelan M., Ben Amara I., Jaziri S., Mazzotti A., Barinov A., Gürbulak B., Duman S., Agnoli S., Caputi L. S., Granozzi G., Cupolillo A.,
Indium selenide: an insight on electronic band structure and surface excitations
Scientific Reports, accepted (2017).

B PUBLICATIONS ON CONFERENCE PROCEEDINGS

B.1 Publications on international conference proceedings in 2013-2016

1. Fiallos D. C., Gómez C. V., Usca G. T., Pérez D. C., Tavolaro P., Martino G., Caputi L. S.,Tavolaro A. *Removal of acridine orange from water by graphene oxide*
in AIP Conference Proceedings 1646, 38 (2015).

2. Longo F., Nicoletti L., Florio G., Vetrano M., Bruno L.,Caputi L. S.
Inside virtual: A new app for interactive and intelligent cultural heritage fruition
in 27th European Modeling and Simulation Symposium, EMSS 2015, p.471 (2015), ISBN: 978-1-5108-1376-2.

3. Usca G. T., Gómez C. V., Fiallos D. C., Tavolaro P., Martino G., Caputi L. S.,Tavolaro A.
Preparation of graphene oxide as biomaterials for drug adsorption
in AIP Conference Proceedings 1646, 79 (2015).

C. PARTICIPATION TO INTERNATIONAL AND NATIONAL PROJECTS

5. COST Action CA1507 MultiCOMP **"**Multi-Functional Nano-Carbon Composite Materials".
6. COST Action MP1306 "Modern Tools for Spectroscopy on Advanced Materials: a European Modelling Platform"

12. THEORETICAL PHYSICS OF FUNDAMENTAL INTERACTIONS AND APPLICATIONS

Professors and Researchers

Domenico Giuliano (Researcher)
Alessandro Papa (Associate Professor)
Marco Rossi (Researcher)

Postdoc fellows

Francesco Caporale
Gabriele Infusino

PhD students

Francesco Giovanni Celiberto *(XXIX cycle)*
Giacinto Ciappetta (*XXV cycle*)
Francesca Cuteri *(XXVIII cycle)*
Rosa Giuliano *(XXXII cycle)*
Beatrice Murdaca (*XXV cycle*)
Andrea Nava *(XXVIII cycle)*
Amedeo Perri (*XXVI cycle*)

Contract lecturers

Roberto Fiore

Collaborators

I. Affleck **(***University of British Columbia, Vancouver, Canada)*
B. Alles *(INFN-Pisa, Italy)*
A. Belitsky *(Arizona State University, Phoenix)*
A. Bonini *(Università di Bologna & INFN-Bologna, Italy)*
O. Borisenko (*Bogolyubov Institute for Theoretical Physics, Kiev, Ukraine)*
A. Brunetti *(Heinrich Heine Universität, Düsseldorf, Germany)*
G. Campagnano *(Università "Federico II", Napoli, Italy)*
P. Cea *(Università di Bari & INFN-Bari, Italy)*
G. Chachamis *(Universidad de Valencia and IFT Univ. Autonoma Madrid, Spain)*
V. Chelnokov (*Bogolyubov Institute for Theoretical Physics, Kiev, Ukraine)*
A. Cirillo *(Università di Perugia & INFN-Perugia, Italy)*
G. Cortese *(Universidad de Zaragoza)*
L. Cosmai *(INFN-Bari, Italy)*
C. Czaban *(Goethe Institute, Frankfurt, Germany)*
R. Egger *(H. Heine Universität, Düsseldorf, Germany)*
E. Eriksson *(H. Heine Universität, Düsseldorf, Germany)*
V.S. Fadin *(Budker Institute for Nuclear Physics, Novosibirsk, Russia)*
S. Fazio *(Brookhaven National Laboratory)*
D. Fioravanti *(Università di Bologna & INFN-Bologna, Italy)*
M. Giordano *(ATOMKI, Debrecen, Hungary)*
D. Gordo Gomez *(IFT Univ. Autonoma Madrid, Spain)*
A.V. Grabovsky *(Budker Institute for Nuclear Physics, Novosibirsk, Russia)*
M. Gravina *(Cyprus University)*
M. Hentschinski *(Brookhaven Labs, Brookhaven, USA)*
D.Yu. Ivanov *(Sobolev Institute of Mathematics, Novosibirsk, Russia)*
L.L. Jenkovszky *(Bogolyubov Institute for Theoretical Physics, Kiev, Ukraine)*

V. Kushnir (*Bogolyubov Institute for Theoretical Physics, Kiev, Ukraine)*
A.A. Lavorini *(Università della Calabria, Italy)*
V. Libov *(DESY-Hamburg, Germany)*
L.N. Lipatov *(St. Petersburg State University, Russia)*
P. Lucignano *(CNR Napoli, Italy)*
M. Machado *(Univ. Federal Rio Grande do Sul, Porto Alegre)*
J.D. Madrigal *(IFT Univ. Autonoma Madrid, Spain)*
M. Mancini *(Università di Perugia & INFN-Perugia, Italy)*
C. Mora *(Ecole Normale Supérieure, Paris, France)*
N.N. Nikolaev *(Landau Inst., Chernogolovka, Russia)*
O. Philipsen *(Goethe Institute, Frankfurt, Germany)*
G. Pinke *(Goethe Institute, Frankfurt, Germany)*
S. Piscaglia *(Tokyo Institute of Technology, Tokyo)*
D. Rossini *(Scuola Normale Superiore, Pisa, Italy)*
A. Sabio Vera *(IFT Univ. Autonoma Madrid, Spain)*
C. Salas *(IFT Univ. Autonoma Madrid, Spain)*
A. Salii (*Bogolyubov Institute for Theoretical Physics, Kiev, Ukraine)*
P. Sasorov *(Institute of Theoretical and Experimental Physics (ITEP), Moscow, Russia)*
A. Sciarra *(Goethe Institute, Frankfurt, Germany)*
P. Sodano *(INFN-Perugia, Italy & International Institute of Physics, Natal, Brasil)*
I. Surzhikov (*Bogolyubov Institute for Theoretical Physics, Kiev, Ukraine)*
A. Tagliacozzo *(Università "Federico II", Napoli, Italy)*
C. Torrero *(Università di Parma & INFN-Parma, Italy)*
A. Trombettoni *(SISSA-Trieste, Italy)*
V. Zoller *(Institute of Theoretical and Experimental Physics (ITEP), Moscow, Russia)*

Introduction

The research activity is developed along the following main lines

1) Junctions of topological superconductors and Luttinger liquids (D. Giuliano)
2) Effective theories of quantum spin chains and of junctions of quantum spin chains (D. Giuliano)
3) QCD and hadron phenomenology (A. Papa)
4) Lattice gauge theories and spin models (A. Papa)
5) Integrability in the N=4 Super-Yang-Mills (SYM) theory (M. Rossi)

12.1. JUNCTIONS OF TOPOLOGICAL SUPERCONDUCTORS AND LUTTINGER LIQUIDS

12.1.1 Junctions between topological superconductors and quantum wires

It has been shown that the phase diagram of the junction between a 2-channel interacting wire, regarded as a Luttinger liquid, and a topological superconductor, hosting a Majorana fermion at its endpoint, contains a novel phase, corresponding to a finite-coupling fixed point. This has been investigated and characterized by deriving both at the dc conductance tensor of the junction and at the boundary entropy of the system. In particular, the results concerning the boundary entropy at the fixed points of the phase diagram appear to be in perfect agreement with Affleck-Ludwig's "g theorem" for boundary interaction Hamiltonians.

A junction between a topological superconductor quantum wire and a normal wire has also proposed as a device to observe the "Majorana screening length", the analog of the Kondo screening length in this specific system, which can be observed in as a crossover in the current shape versus the system size a dc Josephson current measurement.

12.1.2 Josephson current in long quantum wires

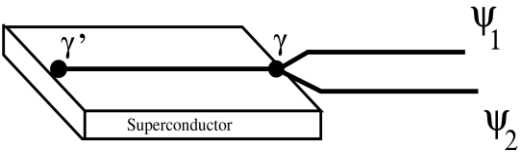

It has been shown that, in a long single-channel, as well as multi-channel, SNS-junction, at low temperatures, the contribution to the dc Josephson current flowing across a quantum wire between two superconducting leads at fixed difference, typically obtained by summing contributions from sub-gap Andreev bound states, as well as from continuum states propagating within the superconducting leads, add up, so that the current can be entirely expressed in terms of single-particle normal- and Andreev reflection amplitudes at the Fermi level at both SN interfaces. The derivation applies to a generic number of channels in the normal region and/or in the superconducting leads, without assumptions about scattering processes at the SN interfaces: if the channels within the central region have the same dispersion relation, it leads to simple analytical formulas for the current at low temperatures; if the channels within the central region have different dispersion relations, it allows for expressing the current in terms of a simple integral involving only scattering amplitudes at the Fermi level.

12.2. EFFECTIVE THEORIES OF QUANTUM SPIN CHAINS AND OF JUNCTIONS OF QUANTUM SPIN CHAINS

12.2.1 Quantum spin chains

Using a similarity Hamiltonian renormalization procedure, an effective spin-1/2 representation of the Bose-Hubbard model at half-integer filling and at a finite on-site interaction energy U has been derived, in terms of a Luttinger liquid Hamiltonian with renormalized coupling and anisotropy parameters. This allowed for providing analytical estimates of the correlation functions of the Bose-Hubbard model and compare the analytical results with those based on DMRG numerical simulations, showing an excellent agreement up to 10% between the output of analytical and numerical computations, even for relatively small values of U.

12.2.2 Junctions of spin chains

A Y-junction of anisotropic critical quantum XY spin chains has been shown to host a version of the topological Kondo effect, whose number of channels depends on the chain parameters, as well as on the boundary couplings at the junction. The system evolves from an effective four-channel topological Kondo effect for a junction of XX-chains with symmetric boundary couplings into a two-channel one at a junction of three quantum critical Ising chains. Using a renormalization group approach, the flow of the boundary couplings has been determined and, accordingly, the Kondo temperature has been estimated. It has also been shown that a junction of three off-critical quantum Ising chains can be regarded as a quantum spin chain realization of the two-channel spin-1/2 overscreened Kondo effect with two superconducting leads. In particular, as long as the Kondo

temperature is larger than the superconducting gap, the equivalent Kondo model flows towards the 2 channel Kondo fixed point. This, besides its the theoretical interest, is of importance for potential applications to a number of context, including the analysis of the quantum entanglement properties of a Kondo system.

12.3. QCD AND HADRON PHENOMENOLOGY

12.3.1 Perturbative QCD in the high-energy limit

The unprecedented energies and luminosities reached at the Large Hadron Collider (LHC) allow to investigate strong interaction in regimes so far unexplored. An important class of processes which can be studied at the LHC are the so called "semihard processes", characterized by a strong hierachy of scales: the squared center-of-mass energy is much larger that the hard scale typical of the process which, in its turn, is much larger that the typical hadronic mass. A successful theoretical description of these processes would provide with a stringent test of the theory of strong interactions, the Quantum ChromoDynamycs (QCD) in the high-energy regime. The most suitable theoretical framework to study semihard processes is the Balitsky-Fadin-Kuraev-Lipatov (BFKL) approach, which represents a consistent procedure to resum to all orders of perturbation theory the leading and subleading logarithms of the center-of-mass energy of a given process. During the period 2013-2016, our research group has contributed both to the understanding of some general, formal properties of the BFKL approach and to its application to the LHC phenomenology.
The former line of investigation, carried out in collaboration with the Budker Institute of Nuclear Physics in Novosibirsk, included the extension of the BFKL approach to the N=4 supersymmetric Yang-Mills (SYM) theory, the study within this theory of some symmetry properties (such as Möbius invariance), and its consistency with the Bern-Dixon-Smirnov (BDS) ansatz for some amplitudes with gluon external lines.

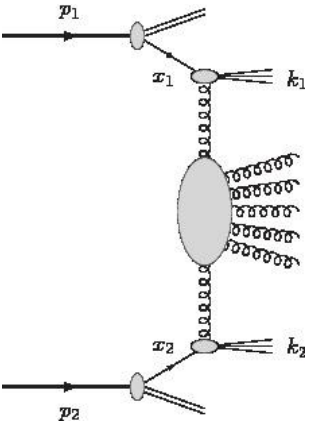

Figure 1: Schematic representation of the Mueller-Navelet jet production process

The latter research line, carried out in collaboration with the Sobolev Institute of Mathematics in Novosibirsk and the Instituto de Fisica Teorica of the Universidad Autonoma in Madrid, included the production of a wealth of theoretical predictions for observables relevant to the some partially exclusive processes under current investigation at, or within the reach of, the LHC: the inclusive production of two jets widely separated in rapidity (Mueller-Navelet jets), the inclusive production of two identified hadron separated in rapidity (dihadrons), the inclusive three-jet and four-jet production at the LHC.

12.3.2 Hadron Phenomenology

There is a vast class of hadronic processes which lie beyond or at the border of the application regime

of perturbative QCD. These include the deeply-virtual-Compton scattering (DVCS) off protons, the exclusive diffractive production of vector mesons in the deep-inelastic electron-proton scattering and vector meson production in ultraperipheral collisions at the LHC. For such processes, the modelization of physical amplitudes according to the Regge theory still represents a powerful investigation tool. Our research group has produced several predictions for quantities related with these processes, which successfully compare with experimental data.

12.4. LATTICE GAUGE THEORIES AND SPIN MODELS

12.4.1 QCD confinement

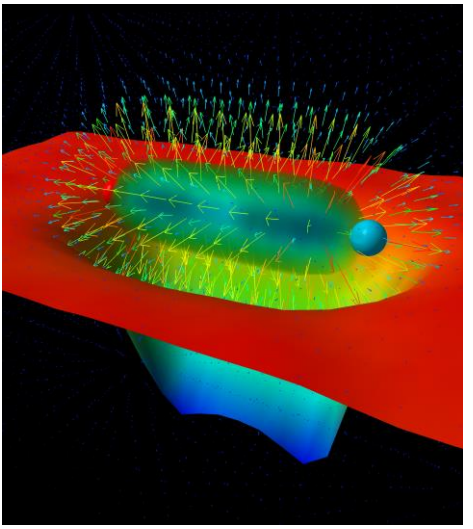

Figure 2: Schematic view of a flux tube (from "Visualizations of Quantum Chromodynamics", http://www.physics.adelaide.edu.au/theory/staff /leinweber/VisualQCD/Nobel/)

The problem of hadron confinement within a Yang-Mills theory, such as the pure gauge SU(3) theory or gluodynamics, is one of the "Millennium problems" (see http://www.claymath.org/millennium-problems/yang–mills-and-mass). While there is a wealth of numerical evidences, based on Monte Carlo lattice simulations, that a confining potential sets in between a static quark-antiquark pair, growing linear with the distance for large enough distances, with the color field lines distributed along the axis connecting the quarks in stringlike or tubelike structures, the underlying mechanism of confinement is still unknown. In the mid-seventies a scenario was proposed by t't-Hooft and Mandelstam, based on the hypothesis of the vacuum as a "dual superconductor": the condensation of color magnetic monopoles in the vacuum would play the same role as the condensation of Cooper pairs in a standard superconductor. The key assumption of the dual superconductor model is to understand the "flux tube" between a static quark-antiquark as the dual counterpart of an Abrikosov tube inside an ordinary superconductor.
This scenario leads to predictions about the shape and structure of the flux tube which can be carefully tested in lattice Monte Carlo simulations. Our group, in collaboration with the group of Bari, has thoroughly investigated the properties of flux tubes, including their shape and the dependence on the distance between the sources and on the temperature, both in the pure gauge SU(3) theory and in true QCD. The result obtained can contribute to understand the dynamics of confinement in strong interactions.

12.4.2 Lattice QCD at finite baryon density

The property of strong interactions to be confining is expected to be lost at high enough temperatures and baryon densities. Predicted in the mid-seventies by N. Cabibbo e G. Parisi, a "deconfined" state

of matter, is experimentally searched for in relativistic collisions of heavy ions, while, on the theory side, it must derive from principles within the theory of strong interactions, the QCD.

Understanding the phase diagram of QCD in the temperature – baryon density plane if of the utmost importance, due to the implications in cosmology, in the phenomenology of relativistic collisions of heavy ions and in the astrophysics of compact objects. Perturbation theory is helpful only in the two extreme regimes of high temperature - low baryon density and low temperature – high baryon density; the other first-principle approach, namely the discretization of QCD on a space-time lattice and its numerical simulation on computers by Monte Carlo techniques is severely limited by the so called "sign problem" which restricts its domain of applicability to the region where the baryon chemical potential is smaller or of the same order of the temperature (in units of the Boltzmann constant). All remaining regions of the QCD phase diagram can be understood only within effective models.

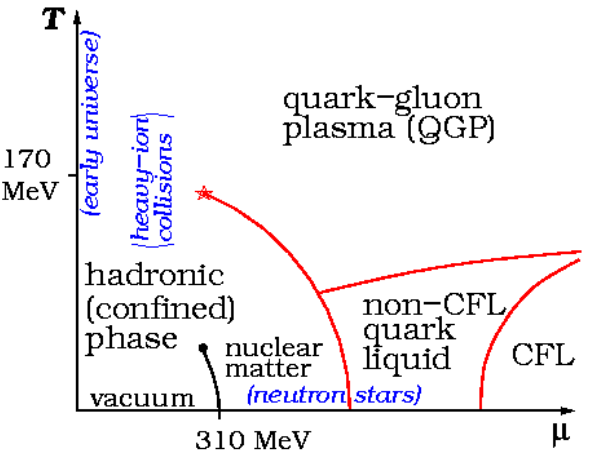

Figure 3: Current understanding of the QCD phase diagram on the temperature - quark chemical potential plane (from Wikipedia)

Within the lattice approach, our group, in collaboration with the Bari group, has contributed to the determination of the QCD critical line on the temperature – baryon density plane, by means of massive Monte Carlo simulations of a public code implemented by the MILC collaboration, suitably modified to include a nonzero imaginary baryon chemical potential. The extension to real chemical potentials was carried out by analytic continuation. Simulations were performed on space-time lattices of various sizes, to keep under control the finite-size effects and to be able to take the extrapolation to the continuum limit. The resulting shape of the critical line nicely agrees with the "freeze-out" curve determined experimentally in heavy-ion collision experiments.

12.4.3 Other gauge theories and spin models

The dynamics of confinement and deconfinement and the existence of non-trivial topological structures is not an exclusive prerogative of QCD, but can be found and studied also low-dimension theories, both based on gauge and spin degrees on freedom.
Our group, in collaboration with the Bogolyubov Institure for Theoretical Physics in Kiev, has carried out an extensive study of the Berezinski-Kosterlitz-Thouless (BKT) transition in many gauge theories and spin models, Abelian and non-Abelian, at zero and non-zero temperature, looking for possible distinctive features with respect to its paradigmatic manifestation in the two-dimensional XY model. Such transition belongs to the class of "topological transitions", whose relevance has been recognized with the 2016 Nobel Prize in Physics.

12.5. INTEGRABILITY IN THE N=4 SYM THEORY

At present the most advanced and profound form of description of physical phenomena is based on quantum / statistical field theories (which reveal and unify understanding of very disparate processes). The fundamental objects of these theories are the quantum / statistical fields, i.e. local operators or local statistical fields; in this context, the greatest success has been achieved so far by quantum electrodynamics (QED). Other important examples are the quantum chromodynamics (QCD) of strong interactions and the standard model of electroweak interactions. In general, it is impossible to find exact solutions of these theories, such as the spectrum of observables or the probability of diffusion processes. Then, to extract predictions, the more used tool is the 'perturbative' expansion in a small parameter, the coupling constant. However, this is only an approximation, which highlights how important it is to find ideas for possible non-perturbative calculations. Some years ago research from different groups (including Minahan, Zarembo, Beisert, Staudacher) found that for supersymmetric gauge theories in 3+1 dimensions, such as the theory N = 2, N = 4 SYM and N=6 Chern-Simons, in many respects similar to QCD, accurate predictions can be made thanks to their deep equivalence to integrable systems in 1 + 1 dimensions: for example with regard to the spectrum of the local fields or for what concerns computations of probability of scattering processes. In particular, progress on computations of scattering amplitudes was possible thanks to their remarkable equivalence to fundamental non-local operators, the so-called Wilson loops. Research of M. Rossi and his collaborators (Bonini, Fioravanti, Piscaglia, Belitsky) belongs to this framework and focuses in particular on applications of the following techniques coming from integrable models, the Bethe Ansatz, the Thermodynamic Bethe Ansatz, the Non-linear Integral Equation, T and Q system functional relations, towards exact (i.e. non perturbative) computations of quantities in quantum field theories with supersymmetry. Recent results on these subjects can be found in the papers reported in the bibliography, whose content we are now going to discuss.

In the paper 'On the scattering on the GKP vacuum' we converted the Asymptotic Bethe Ansatz equations of N = 4 SYM into non-linear integral equations, finding two dimensional scattering amplitudes of excitations on top of the GKP vacuum. We proved that our set-up is powerful for the understanding and computation of the whole S-matrix. Eventually, we showed that all the amplitudes depend on the fundamental scalar-scalar one. The construction of all the scattering factors was preparatory for the results reported in the paper 'Asymptotic Bethe Ansatz on the GKP vacuum as a defect spin chain: scattering, particles and minimal area Wilson loops'. We found that the resulting model on the GKP vacuum is an integrable spin chain of length R = 2 ln s (s = spin) with particle rapidities as inhomogeneities, two (purely transmitting) defects and SU(4) (residual R-)symmetry. The non-trivial dynamics of N = 4 SYM appears in elaborated dressing factors of the 2D two-particle scattering factors, all depending on the 'fundamental' one between two scalar excitations. From scattering factors we determined bound states. In particular, we studied the strong coupling limit, in the non-perturbative, perturbative and giant hole regimes. Eventually, from these scattering data we constructed the 4D pentagon transition amplitudes (perturbative regime). In this manner, we detail the multi-particle contributions (flux tube) to the MHV gluon scattering amplitudes/Wilson loops (OPE or BSV series) and re-sum them to the Thermodynamic Bubble Ansatz. In the subsequent paper 'Strong Wilson polygons from the lodge of free and bound mesons' we studied the appearance, between the excitations over the GKP quantum vacuum, of a new particle at strong coupling, formed by one fermion and one anti-fermion. We found that this two-dimensional meson shows up, along with its infinite tower of bound states, while analysing the fermionic contributions to the Operator Product Expansion (collinear regime) of the Wilson null polygon loop. Moreover, its existence turns out to be a powerful idea in re-summing all the contributions (at large coupling) for a general n-gon ($n \geq 6$) to a Thermodynamic Bethe Ansatz, which is proven to be equivalent to the known one and suggests new structures for a special Y-system. Finally, in the paper 'The contribution of scalars to N = 4 SYM amplitudes' we analysed the contribution of 2n scalars to the Operator Product Expansion

series for MHV gluon scattering amplitudes/polygonal Wilson loops in planar N = 4 SYM. Hence, we summed up on 2n for large 't Hooft coupling λ: the logarithm of the amplitude is proportional to √λ, thus competing, unexpectedly, with the famous classical contribution (analysed in the previous papers). We gave explicit expressions for the first terms at large λ in case of two and four scalars. For finalising this analysis, we find profitable an explicit computation of the 2n-scalar term at any coupling by means of Young tableaux, paralleling, under certain aspects, the Nekrasov-Okounkov expressions for N = 2 SYM prepotential.
On a slight different track is the content of the paper 'Reciprocity and self-tuning relations without wrapping'. Here, we considered scalar Wilson operators of N = 4 SYM at high spin, s, and generic twist in the multi-color limit. We showed that the corresponding (non)linear integral equations (originating from the asymptotic Bethe Ansatz equations) respect certain 'reciprocity' and functional 'self-tuning' relations up to all terms in powers of 1/(s ln s) at any fixed 't Hooft coupling λ. Of course, this relation entails straightforwardly the well-known (homonymous) relations for the anomalous dimension at the same order in s. On this basis we gave some evidence that wrapping corrections should enter the non-linear integral equation and anomalous dimension expansions at the next order $((\ln s)/ s)^2$, at fixed 't Hooft coupling.

A. PUBLICATIONS ON SCIENTIFIC JOURNALS

A.1 Publications on scientific journals in 2013

1. D. Giuliano, I. Affleck,
   "*The Josephson current through a long quantum wire"*,
   Journal of Statistical Mechanics: Theory and Experiment, vol. P02034, p. 1-25 (2013).

2. I. Affleck, D. Giuliano,
   "*Topological superconductor - Luttinger liquid junctions"*,
   Journal of Statistical Mechanics: Theory and Experiment, vol. P06011, p. 1-53 (2013).

3. D. Giuliano, D. Rossini, P. Sodano, A. Trombettoni,
   "*XXZ spin-1/2 representation of a finite-U Bose-Hubbard chain at half-integer filling"*,
   Physical Review B, vol. 87, p. 035104 (2013).

4. D. Giuliano, P. Sodano,
   "*Realization of a two-channel Kondo model with Josephson junction networks"*,
   Europhysics Letters, vol. 103, p. 57006 (2013).

5. O. Borisenko, V. Chelnokov, G. Cortese, M. Gravina, A. Papa, I, Surzhikov,
   "*Phase structure of 3D Z(N) lattice gauge theories at finite temperature*",
   Nuclear Physics B, vol. 870, Issue 1, p. 159 (2013).

6. V.S. Fadin, R. Fiore, L.N. Lipatov, A. Papa,
   "*Möbius invariant BFKL equation for the adjoint representation in N=4 SUSY*",
   Nuclear Physics B, vol. 874, Issue 1, p. 230 (2013).

7. F. Caporale, D. I. Ivanov, B. Murdaca, A. Papa,
   "*Mueller–Navelet small-cone jets at LHC in next-to-leading BFKL*",
   Nuclear Physics B, vol. 877, Issue 1, p. 63 (2013).

8. F. Caporale, B. Murdaca, A. Sabio Vera, C. Salas,
"Scale choice and collinear contributions to Mueller-Navelet jets at LHC energies",
Nuclear Physics B, vol. 875, Issue 1, p. 134 (2013).

9. F. Caporale, G. Chachamis, J.D. Madrigal, B. Murdaca, A Sabio Vera,
"A study of the diffusion pattern in N = 4 SYM at high energies",
Physics Letters B, vol. 724 p. 127 (2013).

10. R. Fiore, P.V. Sasorov, V.R. Zoller,
"*Non-linear BFKL dynamics: Color screening vs. gluon fusion*",
JETP Letters, vol. 96, Issue 11, p. 687 (2013).

11. S. Fazio, R. Fiore, A. Lavorini, L. Jenkovszky, A. Salii,
"***Reggeometry of Deeply Virtual Compton Scattering and Exclusive Vector Meson Production at HERA*",** *Acta Physica Polonica B, vol. 44, no. 6, p. 1333 (2013).*

A.2 Publications on scientific journals in 2014

1. D. Giuliano, I. Affleck,
*"**dc Josephson current in a long multichannel quantum wire**"*,
Physical Review B, vol. 90, p. 045133 (2014).

2. I. Affleck, D. Giuliano,
"***Screening Clouds and Majorana Fermions**"*,
*Journal of Statistical Physics, v*ol. 157, p. 666-691 (2014).

3. V. Parente, G. Campagnano, D. Giuliano, A. Tagliacozzo, and F. Guinea,
"*Topological Defects in Topological Insulators and Bound States at Topological Superconductor Vortices"*,
Materials, vol. 7, p. 1652-1686 (2014).

4. E. Eriksson, A. Nava, C. Mora, and R. Egger,
"***Tunneling spectroscopy of Majorana-Kondo devices*",**
Physical Review B, *v*ol. 90, p. 245417 (2014).

5. B. Alles, M. Giordano, and A. Papa,
"***Behavior near theta = pi of the mass gap in the two-dimensional O(3) nonlinear sigma model*",**
Physical Review B, *v*ol. 90, p. 184421 (2014).

6. O. Borisenko, V. Chelnokov, G. Cortese, M. Gravina, and A. Papa,
"***Critical behavior of 3D Z(N) lattice gauge theories at zero temperature*",**
Nuclear Physics B, vol. 879, p. 80-97 (2014).

7. P. Cea, L. Cosmai, and A. Papa,
"*Critical line of 2+1 flavor QCD*",
Physical Review D, vol. 89, p. 074512 (2014).

8. P. Cea, L. Cosmai, F. Cuteri, and A. Papa,
"Flux tubes in the SU(3) vacuum: London penetration depth and coherence length",
Physical Review D, vol. 89, p. 094505 **(2014).**

9. O. Borisenko, V. Chelnokov, M. Gravina, and A. Papa,
"*Phase structure of 3D Z(N) lattice gauge theories at finite temperature: Large-N and continuum limits*", Nuclear Physics B, vol. 888, p. 52-64 (2014).

10. R. Fiore, N.N. Nikolaev, and V. Zoller,
"*Color Screening, Absorption, and σ^{pp}_{tot} at LHC*",
JETP Letters, vol. 99, p. 363-367 (2014).

11. V.S. Fadin and R. Fiore,
"Impact factors for Reggeon-gluon transition in N=4 SYM with large number of colours",
Physics Letters B, vol. 734, p. 86-91 (2014).

12. D.Yu Ivanov, B. Murdaca, and A. Papa,
"*The gamma*gamma* total cross section in next-to-leading order BFKL and LEP2 data*",
Journal of High Energy Physics, *vol. 1410, p. 58 (2014).*

13. F. Caporale, D.Yu. Ivanov, B. Murdaca, A. Papa,
"Mueller-Navelet jets in next-to-leading order BFKL: theory versus experiment",
European Physical Journal C, vol. 74, no. 10, p. 3084 (2014); Erratum ibid., vol. 75, no. 11, p. 535 (2015).

14. M. Hentschinski, M. J. D. Martinez, B. Murdaca, and A. Sabio Vera,
"*The gluon-induced Mueller-Tang jet impact factor at next-to-leading order*",
*Nuclear Physics B, v*ol. 889, p. 549-579 (2014).

15. M. Hentschinski, M. J. D. Martinez, B. Murdaca, and A. Sabio Vera,
"*The quark induced Mueller-Tang jet impact factor at next-to-leading order*",
*Nuclear Physics B, v***ol. 887, p. 309-337 (2014).**

16. M. Hentschinski, J.D. Madrigal Martinez, B. Murdaca, A. Sabio Vera,
"The next-to-leading order vertex for a forward jet plus a rapidity gap at high energies",
Physics Letters B, vol. 735, p. 168 (2014).

17. S. Fazio, R. Fiore, L. Jenkovszky, and A. Salii,
"*Unifying "soft" and "hard" diffractive exclusive vector meson production and deeply virtual Compton scattering*",
Physical Review D, vol. 90, p. 016007 (2014).

18. D. Fioravanti, S. Piscaglia, M. Rossi,
"*On the scattering on the GKP vacuum*",
Physics Letters B, vol. 728, p. 288 (2014).

A.3 Publications on scientific journals in 2015

1. D. Giuliano, A. Nava,
*"**Dual fermionic variables and renormalization group approach to junctions of strongly interacting quantum wires**"*,
Physical Review B, vol. 92, p. 125138 (2015).

2. G. Campagnano, P. Lucignano, D. Giuliano, A. Tagliacozzo,

"***Spin-orbit coupling and anomalous Josephson effect in nanowires****"*,
Journal of Physics – Condensed Matter, vol. 27, Issue 20, p. 205301 (2015).

3. O. Borisenko, V. Chelnokov, M. Gravina, A. Papa,
"***Deconfinement and universality in the 3D U(1) lattice gauge theory at finite temperature: study in the dual formulation",***
Journal of High Energy Physics, vol. 1509, p. 62 (2015).

4. F. Caporale, D. Yu Ivanov, B. Murdaca, A. Papa,
"***Brodsky-Lepage-Mackenzie optimal renormalization scale setting for semihard processes",***
Physical Review D, vol. 91, Issue 11, p. 114009 (2015).

5. V.S. Fadin, R. Fiore,
"***Discontinuities of BFKL amplitudes and the BDS ansatz",***
Nuclear Physics B, vol. **901, p. 115 (2015).**

6. **F.G. Celiberto, D.Yu Ivanov, B. Murdaca, A. Papa,**
"*Mueller-Navelet jets at LHC: BFKL versus high-energy DGLAP*",
European Physical Journal C, vol. **75, Issue 6, p. 292 (2015).**

7. **R. Fiore, L. Jenkovsky, V. Libov, M. V. T. Machado,**
"*Vector meson production in ultra-peripheral collisions at the LHC",*
Theoretical and Mathematical Physics, vol. 182, Issue 1, p. 141 (2015).

8. D. Fioravanti, S. Piscaglia, M. Rossi,
"*Asymptotic Bethe Ansatz on the GKP vacuum as a defect spin chain: scattering, particles and minimal area Wilson loops''*,
Nuclear Physics B, vol. 898, p. 301 (2015).

9. D. Fioravanti, G. Infusino, M.Rossi,
"*Reciprocity and self-tuning relations without wrapping"*,
Advances in High Energy Physics, vol. 2015, p. 762481 (2015).

A.4 Publications on scientific journals in 2016

1. G. Campagnano, P. Lucignano, D. Giuliano,
"*Chirality and Current-Current Correlation in Fractional Quantum Hall Systems*",
Physical Review B, vol. 93, p. 075441 (2016).

2. D. Giuliano, P. Sodano, A. Tagliacozzo, A. Trombettoni,
"*From four- to two-channel Kondo effect in junctions of XY spin chains*",
Nuclear Physics B, vol. **909, p. 135 (2016).**

3. D. Giuliano, G. Campagnano, A. Tagliacozzo,
"*Junction of three off-critical quantum Ising chains and two-channel Kondo effect in a superconductor*", European Physical Journal B, vol. 89, p. 251 (2016).

4. A. Nava, R. Giuliano, G. Campagnano, D. Giuliano,
"*Transfer matrix approach to the persistent current in quantum rings: Application to hybrid normal-superconducting rings*",
Physical Review B, vol. 94, p. 205125 (2016).

5. D. Massarotti, B. Jouault, V. Rouco, G. Campagnano, D. Giuliano, P. Lucignano, D. Stornaiuolo, G. P. Pepe, F. Lombardi, F. Tafuri, A. Tagliacozzo,
"*Hysteretic Critical State in Coplanar Josephson Junction with Monolayer Graphene Barrier*",
Journal of Superconductivity and Novel Magnetism, vol. 30, Issue 1, p. 5 (2017) [On line 2016].

6. P. Cea, L. Cosmai, A. Papa,
"Critical line in (2+1)-flavor QCD: Towards the continuum limit",
Physical Review D, vol. 93, p. 014507 (2016).

7. P. Cea, L. Cosmai, F. Cuteri, A. Papa,
"Flux tubes at finite temperature",
Journal of High Energy Physics, vol. 1606, p. 33 (2016).

8. O. Borisenko, V. Chelnokov, F. Cuteri, A. Papa,
"BKT phase transitions in two-dimensional non-Abelian spin models",
Physical Review E, vol. 94, p. 012108 (2016).

9. V.S. Fadin and R. Fiore,
"On Hermitian separability of the next-to-leading order BFKL kernel for the adjoint representation of the gauge group in the planar N=4 SYM",
European Physical Journal C, vol. 76, no. 5, p. 230 (2016).

10. R. Fiore, B. Mudaca, A. Papa et al. [LHC Forward Physics Working Group Collaboration],
"LHC Forward Physics",
Journal of Physics G, vol. 43, p. 110201 (2016).

11. F.G. Celiberto, D.Yu. Ivanov, B. Murdaca, A. Papa,
"Mueller-Navelet jets at 13 TeV LHC: dependence on dynamic constraints in the central rapidity region",
European Physical Journal C, vol. 76, p. 224 (2016).

12. F.G. Celiberto, D.Yu. Ivanov, B. Murdaca, A. Papa,
"High energy resummation in dihadron production at the LHC",
Physical Review D, vol. 94, p. 034013 (2016).

13. F. Caporale, F.G. Celiberto, G. Chachamis, D. Gordo Gomez and A. Sabio Vera,
"BFKL Azimuthal Imprints in Inclusive Three-jet Production at 7 and 13 TeV",
Nuclear Physics B, vol. 910, p. 374 (2016).

14. F. Caporale, G. Chachamis, B. Murdaca and A. Sabio Vera,
"Balitsky-Fadin-Kuraev-Lipatov Predictions for Inclusive Three Jet Production at the LHC",
Physical Review Letters, vol. 116, no. 1, p. 012001 (2016).

15 F. Caporale, F.G. Celiberto, G. Chachamis, and A. Sabio Vera,
"Multi-Regge kinematics and azimuthal angle observables for inclusive four-jet production",
European Physical Journal C, vol. 75, p. 165 (2016)

16. R. Fiore, L. Jenkovszky and R. Schicker,
"Resonance production in Pomeron–Pomeron collisions at the LHC",
European Physical Jourmal C, vol. 76, no. 1, p. 38 (2016).

17. A. Bonini, D. Fioravanti, S. Piscaglia, M. Rossi,
"*Strong Wilson polygons from the lodge of free and bound mesons''*,
Journal of High Energy Physics, vol. 1604, 029 (2016).

B. PUBLICATIONS ON CONFERENCE PROCEEDINGS

B.1 Publications on conference proceedings in 2013

1. O. Borisenko, V. Kushnir, B. Alles, A. Papa and C. Torrero,
"*2D O(3) sigma model with a theta-term: construction of a positive Boltzmann weight",*
Proceedings of the International School-Seminar "New Physics and Quantum Chromodynamics at External Conditions", Dnipropetrovsk, Ukraine, May 22-24, 2013, pp. 90-93.
http://ff.dsu.dp.ua/theorph/npqcd-2013/npqcd-2013_en.htm.

2. C. Torrero, O. Borisenko, V. Kushnir, B. Alles and A. Papa,
"*A new approach to the two-dimensional sigma-model with a topological charge",*
Proceedings of Science [Lattice 2013] 338.

3. O. Borisenko, V. Chelnokov, G. Cortese, M. Gravina, A. Papa and I. Surzhikov,
"*Phase transitions in the three-dimensional Z(N) models",*
Proceedings of Science [Lattice 2013] 347.

4. O. Borisenko, V. Chelnokov, G. Cortese, M. Gravina, A. Papa and I. Surzhikov,
"*Critical properties of 3D Z(N) lattice gauge theories at finite temperature",*
Proceedings of Science [Lattice 2013] 463.

5. P. Cea, L. Cosmai, F. Cuteri, A. Papa,
"*Flux tubes and coherence length in the SU(3) vacuum",*
Proceedings of Science [Lattice 2013] 468.

6. F. Caporale, D.Yu. Ivanov, B. Murdaca, A. Papa, A. Perri,
"*NLO forward jet vertex",*
AIP Conference Proceedings, vol. 1523, p. 282 (2013).

7. D.Yu. Ivanov, A. Papa,
"*Inclusive production of a pair of identified, rapidity-separated hadrons in proton collisions",*
AIP Conference Proceedings, vol. 1523, p. 286 (2013).

8. F. Caporale, D.Yu. Ivanov, B. Murdaca, A. Papa,
"*Mueller-Navelet jets in high-energy hadron collisions",*
AIP Conference Proceedings, vol. 1523, p. 290 (2013).

9. R. Fiore, P.V. Sasorov, V.R. Zoller,
"*BFKL, BK and the infrared*",
AIP Conference Proceedings, vol. 1523, p. 324 (2013).

B.2 Publications on conference proceedings in 2014

1. P. Cea, L. Cosmai and A. Papa,

"Curvature of the QCD critical line with 2+1 HISQ fermions",
Proceedings of Science [Lattice 2014] 171.

2. P. Cea, L. Cosmai, F. Cuteri, and A. Papa,
"*London penetration depth and coherence length of SU(3) vacuum flux tubes*",
Proceedings of Science [Lattice 2014] 350.

3. A. Papa and M. Gravina,
"*Critical behavior and continuum scaling of 3D Z(N) lattice gauge theory***",**
Proceedings of Science [Lattice 2014] 311.

B.3 Publications on conference proceedings in 2015

1. F. Caporale, D.Yu. Ivanov, B. Murdaca and A. Papa,
"*Semihard processes with BLM renormalization scale setting",*
AIP Conference Proceedings, vol. 1654, p. 070001 (2015).

2. D.Yu. Ivanov, B. Murdaca and A. Papa,
"*The γ*γ* total cross section in NLA BFKL",*
AIP Conference Proceedings, vol. 1654, p. 070007 (2015).

3. M. Hentschinski, J.D. Madrigal Martinez, B. Murdaca and A. Sabio Vera,
"NLO Vertex for a Forward Jet plus a Rapidity Gap at High Energies",
AIP Conference Proceedings, vol. 1654, 070013 (2015).

4. **R. Fiore, L. Jenkovsky, V. Libov, M.V.T. Machado, A. Salii,**
"*Vector meson production in ultra-peripheral collisions at the LHC",*
AIP Conference Proceedings, vol. 1654, p. 090002 (2015).

5. F.G. Celiberto, D.Yu. Ivanov, B. Murdaca, A. Papa,
"***Mueller–Navelet Jets at the LHC: Discriminating BFKL from DGLAP by Asymmetric Cuts",***
Acta Physics Polonica B (Proc. Suppl.), vol. 8, p. 935 (2015).

6. P. Cea, L. Cosmai and A. Papa,
*"**Curvature of the pseudocritical line in (2+1)-flavor QCD with HISQ fermions",***
Proceedings of Science [Lattice 2015] 143.

7. P. Cea, L. Cosmai, F. Cuteri and A. Papa,
"***Anatomy of SU(3) flux tubes at finite temperature",***
Proceedings of Science [Lattice 2015] 322.

B.4 Publications on conference proceedings in 2016

1. P. Cea, L. Cosmai, F. Cuteri, A. Papa
"*Flux tubes in QCD with (2+1) HISQ fermions",*
Proceedings of Science [LATTICE2016] 344.

2. F.G. Celiberto,
"*BFKL phenomenology: resummation of high-energy logs in semi-hard processes at LHC*",
Frascati Phys. Ser. 63 (2016) 43.

3. F.G. Celiberto, D.Yu. Ivanov, B. Murdaca and A. Papa,
   "BFKL effects and central rapidity dependence in Mueller-Navelet jet production at 13 TeV LHC,"
   Proceedings of Science [DIS 2016] 176.

4. F. Caporale, F.G. Celiberto, G. Chachamis, A. Sabio Vera,
   "*Inclusive four-jet production: a study of Multi-Regge kinematics and BFKL observables"*,
   Proceedings of Science [DIS 2016] 177.

5. G. Chachamis, F. Caporale, F.G. Celiberto, D. Gordo Gomez, A. Sabio Vera,
   "*Inclusive three jet production at the LHC for 7 and 13 TeV collision energies"*,
   Proceedings of Science [DIS 2016] 178.

6. F.G. Celiberto, L.L. Jenkovszky, V. Myronenko,
   "*Saturation effects in low-x DIS structure functions and related hadronic total cross sections"*,
   EPJ Web Conf. 125, 040012 (2016).

7. F. Caporale, G. Chachamis, B. Murdaca and A. Sabio Vera,
   "Inclusive three jet production at the LHC as a new BFKL probe",
   Proceedings of the 7th International Workshop on Multiple Partonic Interactions at the LHC (MPI@LHC 2015): Miramare, Trieste, Italy, November 23-27, 2015, DESY-PROC-2016-01, p. 167-170.

8. R. Fiore, L. Jenkovszky, R. Schicker,
   "*Central diffractive resonance production at the LHC",*
   EPJ Web Conf. 120, 02006 (2016).

9. R. Schicker, R. Fiore, L.Jenkovszky,
   "Resonance production in Pomeron-Pomeron collisions at the LHC",
   Proceedings of Science [DIS 2016] 184.

C EDITORSHIP OF CONFERENCE PROCEEDINGS

C.1 Editorship of conference proceedings in 2013

1. *M. Capua, R. Fiore, A. Papa, A. Sabio Vera and E. Tassi,*
   "Proceedings of the 7th Workshop on Diffraction in High-Energy Physics",
   AIP Conference Proceedings, vol. 1523 (2013).

C.2 Editorship of conference proceedings in 2015

1. M. Capua, R. Fiore, K. Kumericki, A. Papa, E. Tassi, G.P. Vacca,
   "Proceedings of the 8th Workshop on Diffraction in High-Energy Physics",
   AIP Conference Proceedings, vol. 1654 (2015)

D PRESENTATIONS AT SCHOOL AND CONFERENCES

D.1 Presentations at schools and conferences in 2013

1. B. Murdaca,
   "Mueller-Navelet small-cone jets",

talk given at “Low-x Physics”, Weizmann Institute of Science - Rehovot & Eilat (Israel), May 30 - June 4, 2013.

2. A. Papa,
   “The QCD phase diagram from the method of analytic continuation”,
   invited talk given at the IV Workshop on Fermions and Extended Objects on the Lattice, Benasque, Spain, June 16 – 22, 2013.

3. B. Murdaca,
   “Mueller-Navelet small-cone jets”,
   talk given at “Forward Physics at the LHC”, Reggio Calabria (Italy), July 15 -18, 2013.

4. F. Cuteri,
   “Flux tubes and coherence length in the SU(3) vacuum”,
   presented at the 31st International Symposium on Lattice Field Theory, Mainz, Germany, July 29 - August 3, 2013.

5. A. Papa,
   “Critical properties of 3D Z(N) lattice gauge theories at finite temperature”,
   presented at the 31st International Symposium on Lattice Field Theory, Mainz, Germany, 29 July 2013 - 3 August 2013.

6. D. Giuliano,
   “Frustration effects and phase diagram of topological superconductor-Luttinger liquid junctions”,
   talk given at the conference Nano&Nano 2013, Frascati, September 30 – October 4, 2013.

D.2 Presentations at schools and conferences in 2014

1. D. Giuliano,
   “*Realization of a two - channel kondo model with Josephson junction networks*”,
   talk given at the conference Nano&Nano 2014, Frascati, October 6 – 7, 2014.

2. D. Giuliano,
   “*Topological Superconductor-Luttinger Liquid junction*”,
   talk given at the conference New frontiers for Majorana fermions: from condensed to dark matter, Frascati, May 5 – 6, 2014.

3. F. Cuteri,
   “*Flux tubes in the SU(3) vacuum: London penetration depth and coherence length*”,
   talk given at the XXXIV Convegno Nazionale di Fisica Teorica, Cortona, May 28 – 31, 2014.

4. F. Cuteri,
   “*London penetration depth and coherence length of SU(3) vacuum flux tubes*”,
   talk given at the 32nd International Symposium on Lattice Field Theory, New York, June 23 – 28, 2014.

5. A. Papa,
   “***Critical behavior and continuum scaling of 3D Z(N) lattice gauge theories",***
   presented at the 32nd International Symposium on Lattice Field Theory, New York, June 23 – 28, 2014.

6. A. Papa,
   "Calculation of impact factors relevant for QCD processes in MRK & QMRK",
   invited talk at the Workshop "Scattering Amplitudes and Multi-Regge Limit", Madrid (Spain), February 10 - 14, 2014.

7. B. Murdaca,
   "*Mueller Navelet jets*",
   talk given at the conference LHC Working Group on Forward Physics and Diffraction, Trento, April 14 – 18, 2014.

8. B. Murdaca,
   "*Mueller-Navelet jets at LHC*",
   talk given at the Baikal summer JINR-ISU school 2014, Bol'shie Koty – Irkutsk, Russia, July 5 – 12, 2014.

9. B. Murdaca,
   "*Semihard processes with BLM renormalization scale setting",*
   talk given at the Workshop "Diffraction 2014", Primošten, Croatia, September 10 – 16, 2014.

D.3 Presentations at schools and conferences in 2015

1. D. Giuliano,
   "*Fermionic renormalization group approach to junctions of strongly interacting quantum wires*",
   invited talk given at the conference "Trieste Mini Meeting in Statistical Field Theory", SISSA - Trieste, October 9 – 10, 2015.

2. F. Cuteri,
   "*Anatomy of SU(3) flux tubes at finite temperature*",
   talk given at the 33rd nternational Symposium on Lattice Field Theory, Kobe, Japan, July 14 – 18, 2015.

3. A. Papa,
   "*Curvature of the pseudocritical line in (2+1)-flavor QCD",*
   talk given at the *"*XVI Workshop on Statistical Mechanics and non-perturbative Field Theory", Bari, December 9 - 11, 2015.

4. A. Papa,
   "Semihard processes and BFKL",
   invited talk at the First Italian Workshop on Hadron Physics and Non-Perturbative QCD, "NPQCD 2015", Cortona, April 22, 2015.

5. B. Murdaca,
   "*BFKL vs DGLAP in Mueller-Navelet jets at LHC*",
   talk given at the "LHC Working Group on Forward Physics and Diffraction", Madrid, Spain, April 21 – 25, 2015.

6. F.G. Celiberto,
   "*Mueller-Navelet jets at LHC: discriminating BFKL from DGLAP by asymmetric cuts* ",
   talk given at the "16th conference on Elastic and Diffractive Scattering (EDS 15)", Borgo, Corse, France, June 29 – July 4, /2015.
7. A. Papa,

"Semihard processes and BFKL resummation",
invited lecture at the International School "Diffractive and electromagnetic processes at high energies", Bad Honnef (Germany), August 17 - 21, 2015.

8. F.G. Celiberto,
"BFKL resummation effects in di-hadron production at LHC",
talk given at the "Low-x Meeting 2015", Sandomierz (Poland), September 1 – 5, 2015.

D.4 Presentations at schools and conferences in 2016

1. F.G. Celiberto,
"BFKL effects and central rapidity dependence in Mueller-Navelet jet production at 13 TeV LHC",
talk given at the Workshop "DIS 2016", DESY Hamburg (Germany), April 11 – 15, 2016.

2. F.G. Celiberto,
"Inclusive four-jet production: a study of Multi-Regge kinematics and BFKL observables",
talk given at the Workshop "DIS 2016", DESY Hamburg (Germany), April 11 – 15, 2016.

3. F.G. Celiberto,
"BFKL phenomenology: resummation of high-energy logs in semi-hard processes at LHC",
talk given at the 5th Young Researchers Workshop: "Physics Challenges in the LHC Era", Laboratori Nazionali di Frascati, May 9 and 12, 2016.

4. F.G. Celiberto,
"High-energy effects in multi-jet production at LHC",
talk given at the "Low-x Meeting 2016", Károly Róbert Főiskola, Gyöngyös (Hungary), June 6 –11, 2016.

5. *F.G. Celiberto,*
"Dihadron Production at LHC: BFKL Predictions for Cross Sections and Azimuthal Correlations",
talk given at Workshop "Diffraction 2016", Acireale, September 2 – 8, 2016.

6. *F.G. Celiberto,*
"Inclusive three- and four-jet production in multi-Regge kinematics at the LHC",
talk given at Workshop "Diffraction 2016", Acireale, September 2 – 8, 2016.

7. *F.G. Celiberto,*
"BFKL phenomenology: from Mueller–Navelet jets to multi-jet production",
talk given at the Workshop "QCD at LHC: forward physics and UPC collisions of heavy ions", ECT, Villazzano Villa Tambosi, Trento, September 26 – 30, 2016.*

E. ORGANIZATIONAL ACTIVITY

E.1 Organizational activity in 2014

1. R. Fiore and A. Papa *et al*.,
   Organization of "Diffraction 2014", International Workshop on Diffraction in High-Energy Physics, Primošten, Croatia, September 10 – 16, 2014

E.3 Organizational activity in 2016

1. R. Fiore, A. Papa and M. Rossi *et al.,*
   Organization of "Diffraction 2016", International Workshop on Diffraction in High-Energy Physics, Acireale, Italy, September 2 – 8, 2016.